An analysis of the interaction between the front and rear axles of a four-wheel-drive tractor, and its contribution to power delivery efficiency.

By

Ianto John Guy

MEng(Hons) Off Road Vehicle Design
Harper Adams University College

BA(Hons) Lighting Design
Rose Bruford College

Thesis submitted to Harper Adams University College for the award of the Degree of Doctor of Philosophy

Harper Adams University College, Newport, Shropshire, TF10 8NB, United Kingdom

Declaration

I declare that this thesis has been composed entirely by myself and has not been submitted or accepted in any previous application for a degree. The work, of which it is a record, has been carried out by myself. Quotations have been distinguished by quotation marks and sources of information have been specifically acknowledged.

Ianto John Guy

Abstract

The aim of this project was to assess the effect of lead ratio, the speed of the front axle relative to the rear, of a front-wheel-assist agricultural tractor, on the power delivery efficiency of the machine.

This project sought to measure, in real-time, the power generated by the engine of a 67kW (90hp) front-wheel-assist agricultural tractor, the output power of that tractor at the drawbar and the power flowing through the front and rear axles of the tractor.

The tractor was instrumented using three ABB Torductor-S non-contact torque sensors, non-contact shaft and wheel speed sensors, drawbar loadcell and microwave ground speed sensor, to accurately map the flow of power from the engine, via the axles, to the drawbar.

The experiments conducted involved operating the tractor at a fixed throttle and gear setting, while drawing a progressively increasing rolling load. The tractor was operated at wheel slips between 0 and 50%. Testing was conducted at Harper Adams University College on a heavy clay soil, a light sandy soil and tarmac.

Experimentation showed that the optimum lead ratio, in terms of power output, drawbar pull and efficiency changed depending on soil conditions.

Power flow to the front and rear axles exhibited distinctly different characteristics, with the power flowing to the front axle remaining almost constant throughout the drawbar power range, while the power transmitted by the rear axle had a direct linear relationship to drawbar power. The mechanism by which power delivery efficiency varied was different on the two soils tested; on the clay soil higher power delivery efficiency was associated with a reduction in wheel slip and engine power, while on the sandy soil an increase in forward speed was responsible for an increase in output power and thus power delivery efficiency.

A simulation was conducted using MSc Easy 5 software to help develop a better understanding of the behaviour of the tractor. This work demonstrated that it was possible to use this software to generate qualitatively similar power and torque flow data to that gathered in the field.

Acknowledgements

Any project that lasts four years will inevitably build up a substantial supporting cast, without whom the main plot will make little or no sense, and this project is no exception. The author would like to acknowledge the assistance of a number of people who, not being afflicted by a PhD project of their own, could easily have found less demanding things to do with their time.

First of all Will Turner whose idea this whole thing was, and who provided tireless support when Easy 5 appeared to be anything but. Will's support has kept me going through a series of increasingly impossible projects, and on many occasions stopped me from running away to join the circus when all seemed futile.

Dick Godwin and David White who had to wade through reams of thesis drafts to pick out the good bits. Dave Crolla who kept us all on the 'straight-and-narrow' when we could so easily have diverted off into the wilderness.

This project was made possible by the generous support of ABB AB. Phil Burcham in particular is an exceptional human being and has been a paragon of calm and kindness throughout the project. The staff at ABB Vasteras have made tremendous efforts to support the project and shown great hospitality, in particular Par Gustafsson, Sergio Castagna, Roger Agren, Christer Wallin and Lars Gustavsson, who made the not un-substantial trek from Vasteras to Newport on many occasions to help integrate the Torductors into the tractor, and Jan Nilsson and Mikael

Karlsson who had the unenviable task of turning my ideas into actual components.

The staff and students of Harper Adams University College who have given me an academic home since 2001, and turned me into an Engineer, of sorts.

At Harper Adams the assembly and testing of the instrumented tractor would have been very much harder without the technical expertise of the '*Tractor Fairies'* (a title they chose for themselves!) Dave Coleman, Tim Dicker and Andrew Weaver, while the academic part of this work was greatly aided by Janet Parnaby and her team in the excellent Harper Adams Library and Leticia Chico-Santamarta who is far far more organised than me and saw to it that tasks like the printing of theses actually happened on time even when she was trying to write one of her own!

This project was made possible by the financial support of the Douglas Bomford Trust, and Ray Clay, who acted as my mentor on behalf of the Trust, and made sure I hadn't run away with their money, has been a tremendous ally and source of countless Vauxhall Viva based anecdotes throughout the project.

At Ravenhill Farm Services Alan Owen, and at Teme Valley Tractors Martyn Hall and Peter Williams offered advice, sage remarks and allowed me to paw through their service manuals.

And last, but certainly not least, my partner Liann who had the often thankless task of having to live with me while I wrestled with the vagaries of tractor transmission dynamics.

Thank you all so much

Ianto Guy

Contents

List of Figures

List of tables

1.0 Introduction

1.1 Background

Agricultural tractors commonly employ a four-wheel drive transmission. The use of a four-wheel drive system offers a number of advantages over two-wheel drive, foremost amongst them; it improves the vehicle's ability to cross soft, slippery and uneven terrain. However, as noted by Wong (1970 and 2001), Wong *et al* (1998, 1999 and 2000), and Besselink (2003), amongst others, there is a tendency, under certain circumstances, for four-wheel drive tractors to suffer a reduction in power delivery efficiency as a result of the interaction between front and rear axles being less than optimal. One such phenomenon is the so-called 'push-pull' effect, noted by Murillo-Soto and Smith (1978). While the purpose of a four-wheel drive system is to transmit drive through all four wheels, thus reducing the force transmitted by any single wheel, and maximizing the thrust-weight relationship, Musonda and Bigsby (1985) demonstrated that, under certain circumstances, a four wheel-drive tractor can exhibit a phenomenon in which one of the axles is effectively pushing the other i.e. rather than transmitting drive, one axle will generate a force that opposes the motion of the vehicle, which the dominant driving axle must overcome to move the vehicle. This phenomenon reduces the power delivery efficiency of the tractor, since the resistance to motion of the vehicle is higher than it would otherwise be.

Current four-wheel drive tractors often have a fixed ratio connection between the front and rear wheels. In a tractor with front wheels of a different size to the rear, the ratio of this connection is set to compensate for the specified

difference in size between the front and rear wheels, i.e. being of smaller diameter, the front wheels rotate at a greater angular velocity than the rear. In addition to compensating for the difference in size of the front and rear wheels, the current accepted practice amongst tractor designers is to gear the front wheels to run slightly faster than the rear. This over-speeding, or 'lead', is thought to improve the steering response of four-wheel drive tractors, and eliminate the phenomenon colloquially referred to as scrock, in which drive rapidly alternates between front and rear axles, causing a characteristic chatter in the drivetrain. Unlike their on-highway counterparts, the design of agricultural tractor drivelines do not usually incorporate any mechanism to compensate for variations in effective wheel size, caused by changes in load state, tyre behaviour, tyre selection or wear.

Interaction between front and rear axles can generate considerable parasitic torque within the driveline (Brenninger 1999). As there is no mechanism for equalising torque in the driveline between the front and rear axles, they tend to act as a rigid, closed system. Thus when one axle over-speeds the other, torque builds up within the driveline. This phenomenon is closely analogous to the 'four-square rig', an apparatus used to test driveline components under high torque, which consists of a pair of axles whose wheelstations are linked via drive chains. The purpose of a four-square rig is to generate very high levels of component wear while requiring only enough input power to overcome losses. For the case of a tractor, the ground takes the place of the drive chains, but the behaviour of the two systems is the same. Torque and therefore power is trapped within the driveline, and circulates through the components of the system causing wear, and absorbing power, thus

reducing the efficiency of the machine. Tractor manufacturers have observed the results of this phenomenon in the form of prematurely worn driveline components. However, few attempts have been made to quantify the magnitude of the power losses associated with this effect.

Torque measurement in tractors has previously been principally undertaken using strain gauge based apparatus; Snyder and Buck (1990), McLaughlin *et al* (1993) and Jenane and Bashford (1992). ABB Automation Technologies AB have developed a torque sensor based on the magnetostrictive principle (Wallin and Gustavsson 2002), that has proved to be extremely durable in a wide range of applications, including maritime engineering, motorsport and steel processing. This new type of sensor, which is insensitive to the effects of temperature and vibration, offers the possibility of conducting in-field research under real operating conditions, over an extended experimental programme.

1.2 Aim

The aim of this research was to assess the effect of the speed ratio between the front and rear axles of a four-wheel-drive agricultural tractor on the power delivery efficiency of the machine.

1.3 Experimental Question

Does the speed ratio between the front and rear axles of a tractor affect power delivery efficiency?

1.4 Objectives

- To design, construct and evaluate an instrumentation system, based around Torductor-S magnetostrictive torque sensors, manufactured by ABB, for a four-wheel-drive tractor, to isolate engine, and front and rear axle power flows, and drawbar power.
- To evaluate the tractive performance and power flows through the front and rear axles of a four-wheel-drive tractor at a series of lead ratios, on soil and hard surfaces.
- To evaluate the potential of using computer software to model the tractive performance and power flows between front and rear axles of a four-wheel-drive tractor.

1.5 Outline Methodology

This project sought to develop an improved understanding of the effects of axle interaction in a four-wheel-drive agricultural tractor, through a series of experiments conducted using a tractor instrumented to measure power-flow, and a computer model of the same tractor built using MSc Easy5 software.

The project's main activity streams were to:

- Conduct a review of published literature in this field to determine the current level of knowledge and potential areas for experimentation
- Build and evaluate an instrumentation system, based around magnetostrictive torque sensors, capable of measuring the power flow through the transmission of a four-wheel-drive tractor
- Conduct a programme of experiments to determine the effect of inter-axle speed ratio and soil properties on the power delivery efficiency of the instrumented tractor when running at a range of drawbar pulls
- Build and correlate a computer simulation of the same tractor using an industrially recognised software package

2.0 Review of Literature

2.1 Introduction

The four-wheel drive tractor has become almost ubiquitous in European agriculture. In a review of the development of tractor driveline technology, Renius (1999) noted that at the time of writing, four-wheel drive tractors accounted for approximately 90% of sales in the European market. Sohne (1968) noted that the four-wheel drive tractor has a considerable advantage over its two-wheel drive equivalent in terms of drawbar pull and work rate. He commented that even in comparatively favourable traction conditions, at 20% wheel slip a four-wheel drive machine exhibits a tractive effort 27% greater than a comparable two-wheel drive machine. In more arduous conditions, running on wet clay loam soil, at 30% wheel slip the four-wheel drive machine produces 57% more drawbar pull than the two-wheel-drive equivalent.

Despite the benefits of the four-wheel drive system, both Renius (1999) and Brenninger (1999) noted that one of the remaining problems of the four-wheel drive tractor is the fixed ratio coupling between front and rear wheels, which leads to the creation of parasitic power-flows within the transmission. Wong (1970) suggested that the important factors affecting the efficiency of a four wheel drive tractor are the relative speeds of the front and rear wheels, weight distribution and the method used to transmit power from engine to drive wheels.

2.2 Experimental Determination of Tractive Efficiency and Power Delivery Efficiency

The efficiency with which a tractor converts input power into output power may be measured in a number of different ways. Zoz *et al* (2002) explain that tractive efficiency is generally used as a measure of the efficiency with which a traction device, i.e. a tyre or track, convert input power into output power. They suggest an alternative measure, which they refer to as power delivery efficiency, which includes the cumulative efficiencies of all of the driveline components between the engine and the ground. Wong (2001) incorrectly referred to this measure as *tractive efficiency* (η_d), but noted that the measure more correctly called power delivery efficiency is a composite of three distinct efficiencies (Figure 2.1):

1. efficiency of motion (η_m), an indication of the losses due to resistance to the vehicles forward progress, this includes rolling resistance, obstacle resistance, gradient and aerodynamic resistance, Wong regards these factors as constant, and thus efficiency of motion relative to drawbar pull increases linearly with pull
2. efficiency of slip (η_s), a measure of the power consumed by slip between the vehicle and the ground. Slip reduces the forward speed of the tractor and also, on unprepared surfaces, consumes power by remoulding the running surface, or, on prepared surfaces, by warming the tyres. Slip efficiency has a negative relationship with drawbar pull, since wheel slip increases with drawbar pull, slip efficiency must reduce as drawbar pull increases, reaching 0% at maximum drawbar pull.

3. transmission efficiency (η_t), a measure of the losses within the driveline as a result of friction or churning of the lubricating oil.

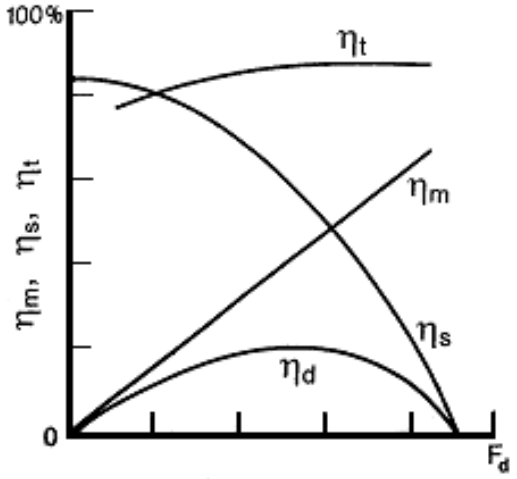

Figure 2.1: The relationship between power delivery efficiency (η_d), transmission efficiency (η_t), efficiency of motion (η_m), slip efficiency (η_s) and drawbar pull (F_d). (Wong, 2001)

A variety of approaches to measuring tractive efficiency and power delivery efficiency have been employed. Khalid and Smith (1981), Murillo-Soto and Smith (1978) and Wang *et al* (1989) used scale models of tractors running in indoor soil bins, while Erickson and Larsen (1983), Wong (2001), Jenane and Bashford (1992), Kim *et al* (2001), and others instrumented full size tractors to measure power both at some point within the driveline and at the drawbar when operating under field conditions.

Wang *et al* (1989) used a quarter scale model of a John Deere 8640, equal wheel, four-wheel drive tractor to assess the tractive performance of a tractor operating in front, rear and four-wheel drive modes. The use of a scale model rather than a full size tractor allowed them to use chains rather than shafts in the driveline. This substitution allowed them to easily measure axle

torque by measuring the tension in the drive chains. They found that the four-wheel drive mode produced approximately three times more drawbar pull than either of the two wheel drive modes, while rear wheel drive was somewhat superior to front wheel drive. Comparison with the work of Sohne (1968) suggests that this effect cannot be scaled accurately up to a full size machine. The dynamic load on the front wheels was 1.2 times that on the rear. Wang *et al* (1989) suggested that the superior performance of the rear wheel drive mode was due to the rear wheels running in the track created by the front wheels.

Wang *et al*'s (1989) conclusion that the tractive performance of the rear wheel of their model was being influenced by the passage of the front wheel substantiated the earlier work of Dwyer *et al* (1977), who conducted a series of experiments using a powered single wheel tester, in which the rig was run alternately on un-trodden soil and then the rut created by the first pass. They demonstrated that the tractive performance of the tyre was generally higher on the second pass, when compared to the first. They showed that on average the coefficient of traction increased by 7%, rolling resistance reduced by 11%, and maximum tractive efficiency increased by 5%. However, they concluded that the improvement in performance demonstrated, could not entirely account for the differences observed by previous workers when comparing two and four-wheel drive machines.

Komandi (2006) adopted a theoretical approach, and devised a general equation for a driving wheel, which allowed the peripheral force exerted by

that wheel to be calculated, which in turn allowed the pulling capacity of a tractor to be determined:

$$F_K^{h4k} = (Ac + \mu Q_{st}^h)[\frac{S_R}{S} - \mu m/(Z_h L]^{-1}$$

Where:

F_K^{h4k}=*peripheral force exerted by one wheel*
A = contact area of tyre
c = coefficient of stickiness
μ = coefficient of friction
Q_{st}^h*= static load on wheel*
S_R *= relative slip*
S = slip as defined by ISTVS
m = height of drawbar over soil surface
Z_h *= proportion of total peripheral force attributable to rear wheels*
L = wheel base of tractor

(Komandi, 2006)

While de Souza and Milanez (1991) proposed a method for predicting the theoretical tractive performance of a tractor based on its engine output, overall gear ratio, physical size and drawbar performance, when running on concrete. They concluded that it is possible to accurately predict the tractive performance of both two and four-wheel drive tractors running on concrete.

2.3 Experimental Determination of Torque and Power Flow

The experimental determination of wheel or axle torque in agricultural tractors has historically been focused on the use of strain gauge based instrumentation combined either with electrical slip rings or radio telemetry systems. Several different configurations of torque sensor position and number have been employed (Table 2.1); Erickson and Larsen (1983), Woerman and Bashford (1983), Bashford *et al* (1987), Musonda and Bigsby

(1985), Dudzinski (1986), Snyder and Buck (1990), Jenane and Bashford (1992), McLaughlin *et al* (1993), Kim *et al* (2001).

Erickson and Larsen (1983) investigated the field performance of an International Harvester Model 4386, pivot steer, equal wheel tractor. The machine had an operational weight of 11,300 kg, and a rated drawbar power of 126 kW. They fitted strain gauges to the front and rear driveshafts of the machine. Drawbar pull was recorded using a strain gauge pull-meter. Strain gauge readings were recorded on a strip chart, while forward speed and engine speed were taken from the gauges on the tractor's instrument panel. Shaft speeds were calculated from engine speed and previously measured gear ratios. No attempt was made to measure engine output. They conducted tests on 30 m strips of soil which had been prepared to represent Montana summer-fallow conditions. The average cone index of the soil was 1400 kPa, but ranged from 700 kPa in the dry, tilled upper layer to 2000 kPa in the more moist and cohesive lower layers. They found that summer-fallow tillage operations resulted in a nearly balanced front-rear power split. However, it should be borne in mind that they were using an equal wheel four-wheel drive tractor with a static front-rear weight distribution of 56:44, rather different to the front wheel assist machines commonly found on European farms. They also found that the front-rear weight transfer associated with drawbar pull only amounted to around 3% of the total.

Bashford *et al* (1987) used strain gauges to measure the front and rear axle torques in a front-wheel-assist Ford TW-15 tractor, and a Versatile 876 equal wheel four-wheel drive tractor on a sandy soil, a clay loam soil and concrete.

They altered the static weight distributions of their machines, and found that this had a significant impact on the magnitude of the torque transmitted by the front axle (Figure 2.2).

Most significantly perhaps, Bashford *et al* (1987) found that the torque response of the front axle of their front-wheel-assist tractor was almost constant, when ballasted to a 28:72 front-rear weight distribution.

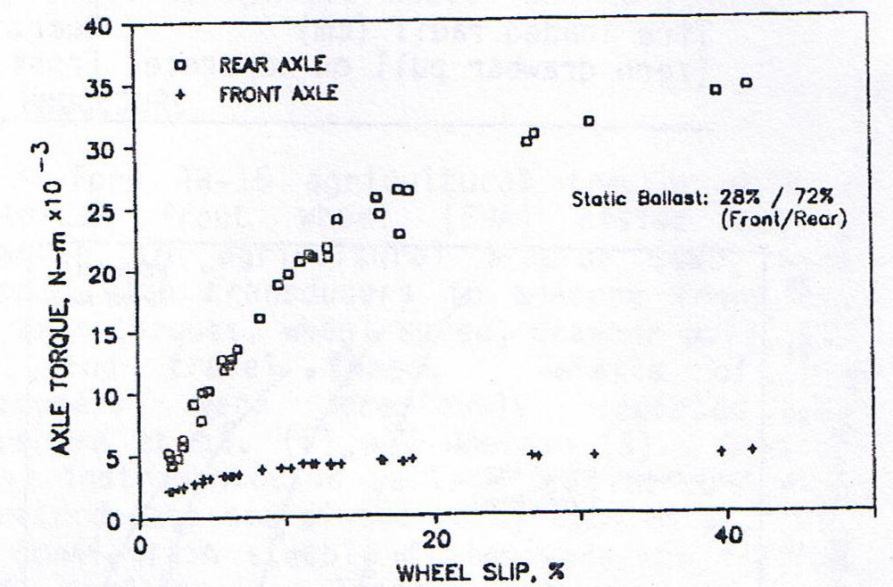

Figure 2.2: Axle torque versus wheel slip in a Ford TW-15 front-wheel-assist tractor operating on a sandy soil with a 28:72 front-rear weight distribution. (Bashford *et al,* 1987)

Jenane and Bashford (1992) used a single wireless torque sensor to measure the efficiency of power transmission between the gearbox and drawbar of a Massey Ferguson 3080 four-wheel drive agricultural tractor. They fitted an instrumented shaft in place of the drive shaft between the gearbox output and the rear differential. They did not attempt to measure engine output or front-rear power split. They operated their machine over a 100m course on a variety of surfaces, using a variable load unit to provide

steady retardation of the vehicle up to 60% slip. They performed duplicate runs with the machine operating in two and four-wheel drive modes. They demonstrated that applied drive torque and drawbar pull are directly related. They also showed that when operated in four-wheel drive mode, the efficiency of power delivery from the gearbox output to drawbar was between 56% and 78%, which represents an increase of between 17% and 28% respectively, when compared to the same vehicle operated in two wheel drive mode. Thus as well as attaining higher levels of drawbar pull for the same machine mass, the four-wheel drive machine was also more efficient.

Kim *et al* (2001) used strain gauges connected to a radio telemetry system, to measure the torque transmitted through the gearbox input shaft and the rear wheel hub of a 30.2 kW front wheel assist tractor. They investigated driving loads operating in Korean ploughing conditions, on soil with cone indices of between 46 kPa and 931 kPa; their main interest being the compilation of transmission torque spectra, rather than the characterisation of the relationship between drawbar pull and axle torque. They found that both the shape and magnitude of their load spectra varied with forward speed and soil conditions.

Snyder and Buck (1990) adopted a rather different approach to the problem of measuring traction in real time. They developed an axle shaft instrumented with strain gauges, but rather than attempt to directly measure torque, as other authors had previously, they instead measured the bending of the rotating shaft, and from this resolved the vertical and longitudinal forces acting on the axle, thus allowing them to measure both thrust and

normal load in real time. They combined this with a telemetry system based on the principle of capacitive transmission, (Snyder and Buck, 1991). However, their research was laboratory based and there is nothing in the literature to suggest that this system was ever tested on a tractor.

2.4 The Effect of Lead Ratio

In a four wheel drive tractor, the relative speeds of the front and rear axles may contribute to the overall efficiency with which the machine can transmit power to the ground. Subtle interactions may exist between the speed and torque transmitted by each wheel, and the soil conditions under that wheel. Indeed as indicated by Dwyer *et al* (1977) the soil conditions under the rear wheels may be modified by the passage of the front wheel. With this relationship in mind, Wong (1970), Besselink (2003) and Vantsevich (2007) conducted mathematical analyses of the behaviour of four-wheel and multi-wheel drive vehicles. Wong's (1970) theoretical analysis of the tractive efficiency of a four-wheel drive vehicle found that the optimum condition for tractive efficiency occurred when the rate of slip of the front wheels was the same as the rear, i.e. the ratio of the peripheral speeds of the front and rear wheels was equal to one. However, current design practice deliberately incorporates an element of 'lead', or front axle over-speeding, and thus, according to Wong's theory, sacrifices some proportion of tractive efficiency in exchange for improved vehicle control.

Vantsevich (2007) presents a mathematical analysis of the tractive performance and fuel efficiency of multi-wheel drive vehicles. His research,

in concurrence with Wong (1970), indicates that the optimum conditions for running gear efficiency occur when all the driving wheels have the same coefficients of slip.

Besselink (2003), however, disagrees with both Wong (1970) and Vantsevich's (2007) conclusions. Besselink conducted a mathematical analysis of the tractive efficiency of a four-wheel drive vehicle. Besselink suggested that Wong's (1970) conclusion is only applicable to situations in which the traction conditions for all wheels are the same, which, as Dwyer *et al* (1977) and others have demonstrated, is far from true. Besselink (2003) demonstrated mathematically that, since the shape of the slip pull curve changes with soil conditions, higher levels of tractive efficiency are attainable by altering the slip rate of each axle in response to its traction conditions. While Besselink offered a somewhat improbable scenario of a vehicle running with two wheels on soil and the other two on tarmac, his theory does have practical application to the situation seen in many off-highway vehicles in which the front wheels run on soft, un-trodden soil, while the rear wheels run in the compacted ruts created by the passage of the front axle. This dynamic difference in soil properties may have implications for the desirable magnitude of front axle lead ratio, and may also make Wong's (1970) hypothesis invalid.

In a paper on the determination of optimal torque distribution in multi-wheel drive electric vehicles, Yamakawa and Wanatabe (2006) noted that if all the driven wheels on a vehicle travelling on a straight path were rotated at the same rate, then the torque at each wheel would also be the same, assuming

that the sizes of the wheels were equal. They also noted that the optimum level of torque distribution is directly proportional to wheel loading, i.e. the most favourable condition occurs when the most heavily loaded wheel has the most torque. This offers a further dimension in the relationship between wheel speed, torque and soil conditions.

Woerman and Bashford (1983 and 1984) and Bashford *et al* (1985) sought to gather some experimental data to help understand these relationships. They conducted a series of experiments with the aim of measuring the performance of a Case 1490 front-wheel-assist agricultural tractor with a mass of 5172kg. The objectives of their research were to quantify the contribution to drawbar pull of the front and rear wheels, quantify the effect of front-rear speed ratio, establish optimal ballasting conditions, and measure the relative performance of the machine when operated in two and four-wheel drive modes. They measured the performance of their tractor at four different lead ratios; -3%, +1%, +7%, +13%, and three different ballast regimes; 28:72, 42:58 and 50:50 front-rear. Tests were undertaken on concrete and on clay-loam wheat stubble with a soil cone index of 427 kPa. Each run lasted 30seconds on concrete and 20seconds on soil.

Woerman and Bashford (1983) and Bashford *et al* (1985) found that the thrust contribution of the front axle increases with speed ratio, soil strength, and ballast, and decreases with slip. Contrary to Wong *et al's* (1998, 1999 and 2000) finding, they concluded that a speed ratio of between +1% and +5% provided the optimum tractive efficiency (Figure 2.3), front axle thrust and vehicle control characteristics. They demonstrated that the optimum

ballast conditions for two-wheel drive operation were different to that for four-wheel drive. They found that the tractive efficiency of their machine was between 3% and 5% higher when operated in four-wheel drive mode when optimally ballasted for that mode of operation, when compared to two-wheel drive mode, when optimally ballasted for that condition. They further discovered that the tractive efficiency of their machine was approximately 7% higher when operated in the four-wheel drive mode, compared to two-wheel drive, when the optimum ballast regime for four-wheel drive operation was used for both runs. It is intriguing that the performance difference demonstrated by these authors is somewhat less than that shown in Jenane and Bashford's (1992) paper.

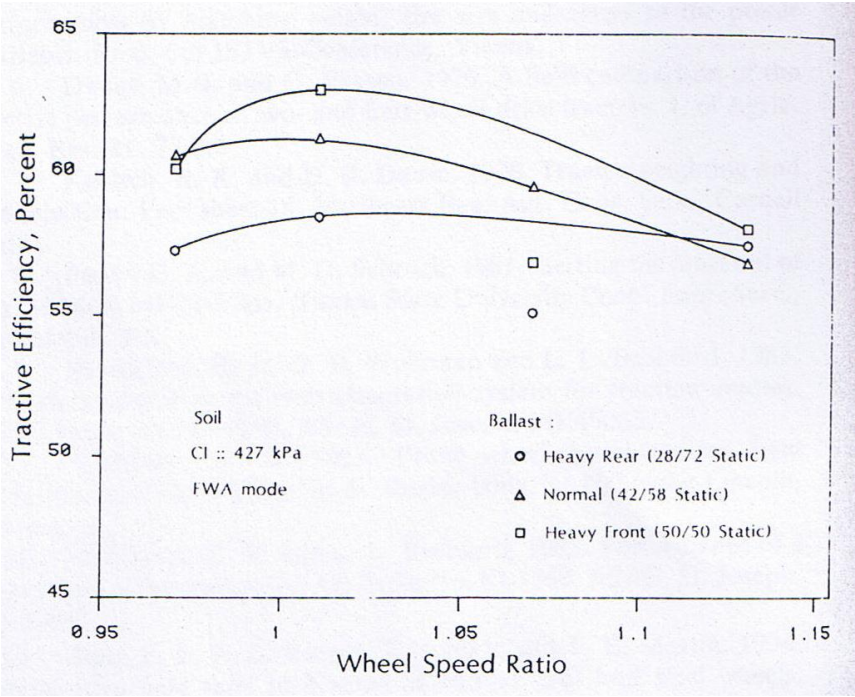

Figure 2.3: The effect of weight distribution on the relationship between front-rear wheel speed ratio and tractive efficiency of a Case 1490 tractor, operating on clay loam soil at 8 km/h. Note that a speed ratio of 1 is equal to 0% lead. (Bashford *et al,* 1985)

Musonda and Bigsby (1985) considered the influence of drawbar pull, tractor speed, axle load and relative tyre size on the ratio of torques transmitted by the front and rear axles of an equal wheel, articulated steer, four-wheel drive Steiger 220 Bearcat III tractor operating on tilled soil with an average cone index of 540 kPa. Their work indicated that at low draught levels, the rear wheels of the tractor did not contribute to overall thrust, as drawbar pull increased, then so too did the contribution of the rear axle. However, it must be remembered that this tractor had a static weight distribution of 62:38 front-rear. More significantly perhaps, Musonda and Bigsby demonstrated that the ratio of the torques transmitted by the front and rear axles is not fixed, but instead varies in a dynamic manner depending on instantaneous levels of axle load, soil cohesion, drawbar pull and vehicle speed. Their work also provided a practical demonstration of Besselink's (2003) theoretical conclusion that the optimum level of slip of the front and rear wheels may be different, and is influenced by the compaction of the soil by the passage of the front wheels, i.e. for the purposes of traction prediction, the soil properties under the front and rear wheels must be considered to be different to one another.

The phenomenon of dynamic torque variation was also observed by Murillo-Soto and Smith (1978) who conducted a series of experiments using a 1:10.94 scale model of a four-wheel drive tractor. In earlier work (Murillo-Soto and Smith 1977) they had noted that the forces and torques acting on the wheels of their machine varied instantaneously, causing noticeable longitudinal vibration, which they referred to as the 'push-pull' effect. Their model had equal size wheels fitted front and rear. They conducted tests on

clay-loam and sand using both smooth and lugged tyres. They varied the speed ratio and static weight distribution of the front and rear axles and drawbar height.

Murillo-Soto and Smith (1978) initially theorised that the push-pull effect was caused by both the lugs on the tyres and instantaneous relative slippage of the wheels. However, comparison of the behaviour of their vehicle when fitted with lugged and smooth tyres indicated that the push-pull effect was not related to tread pattern.

To their surprise they found that smooth tyres produced a higher maximum drawbar pull than their lugged equivalents, in both sand and clay-loam. They speculated that this result might have three possible causes. The passage of the smooth front tyres leaves a uniformly compacted running surface for the rear tyres, thus promoting adhesion. The presence of lugs might adversely affect the shape of the tyre-soil interface, causing localised changes in tyre contact pressure, leading to a variability of tyre thrust. Lugs might promote tyre sinkage, leading to an increase in rolling resistance. Like the findings of Wang *et al* (1989) it is questionable whether these results are scalable to full size machines.

In addition to their practical experimentation, Murillo-Soto and Smith (1977) also produced a computer simulation of their vehicle. Keen to simulate the irregular nature of unmade running surfaces, Murillo-Soto and Smith (1977) included a random number generator in the code for the soil properties under the wheels. This element enabled them to accurately reproduce the,

instantaneous wheel slip generated, push-pull effect witnessed in their model tractor. Their computer model produced data with an average error of 9% when compared to data gathered from the real vehicle. Both the simulation and experimental data show that tractive efficiency increases when the angular velocity of the more heavily loaded axle is increased.

Khalid and Smith (1981) also noted a dynamic torque variation in their scale model of a four-wheel drive tractor which they used to investigate the effects of front and rear axle speed differences. Khalid and Smith noted that the performance of a four-wheel drive tractor could be optimised by controlling the distribution of power between the front and rear axles. Axle power can be varied by changing either the speed of the wheels or the torque being transmitted through them, but they noted that introducing a difference between the speeds of the front and rear wheels caused longitudinal vibration or 'push-pull'. With this in view they postulated that a more effective means of optimising tractor performance might be to vary wheel torque, while maintaining a constant speed. They suggested that one method of doing this might be to produce an automated hitch position system, which would allow the vertical component of the hitch load on the wheels to be varied dynamically. This variation of force acted as a method of controlling wheel slip, and thus wheel torque; the more load the wheels saw, the more torque they were capable of transmitting. Their model allowed them to vary the torque and weight distributions between axles, and the vertical position of the hitch. This allowed them to demonstrate the effects of both static and dynamic weight transfer as well as the ratio of torques between the axles. Like Musonda and Bigsby (1985), they too agreed with Besselink's (2003)

theoretical assertion that the optimum levels of slip for the front and rear wheels may be different, and is influenced by the passage of the front wheels affecting the soil conditions under the rear wheels. Khalid and Smith (1981) also noted that the strength of the undisturbed soil had a minimal effect on torque ratio, with drawbar force and hitch position being the primary influences. Their model was not fitted with cleated agricultural tyres, but instead had block pattern tyres similar to those fitted to gravel rally cars. They assumed that the frictional component of soil strength, and thus vertical wheel load, was most important. This assumption was born out in their results.

Wong (2001), Wong *et al* (1998), Wong *et al* (1999) and Wong *et al* (2000) sought to substantiate experimentally his earlier conclusion that the optimum level of tractive efficiency is attained when the ratio of speeds of the front and rear wheels is equal to one. They conducted a series of experiments in which they altered the speed ratio between the front and rear wheels of a four-wheel drive Case IH Magnum tractor. They produced a range of seven lead ratios between -9.2% and +5.4%, by altering the relative sizes of the front and rear wheels through varying the sizes and pressures of the tyres. They operated the tractor at the Canadian Department of Agriculture and Agri-Food experimental farm, in a test field whose soil was classified as Dalhousie clay-loam, with a cohesion of c = 21.02 kPa and a shearing resistance of $\varphi = 29°$. This work confirmed Wong's (1970) theoretical assertion that the highest level of tractive efficiency is reached when the slip ratios of front and rear axles are matched, i.e. a lead ratio of 0% (Figure 2.4), but only considered the effect on a single soil type, and did not address the

phenomenon of a dynamically varying front to rear axle torque ratio demonstrated by Musonda and Bigsby (1985). In his experimental work, Wong considered the problem of axle interaction in a quasi-static manner, and ignored the possibility that dynamic phenomena within the tyres, driveline and running surface may have an effect on vehicle efficiency. Wong's work also overlooked the influence of dynamic weight transfer, which Musonda and Bigsby (1985) had noted as being significant. In particular, Wong considered front to rear axle speed ratio to be fixed, and thus ignored the possibility that the peripheral speeds of the tyres change dynamically with load and surface perturbations.

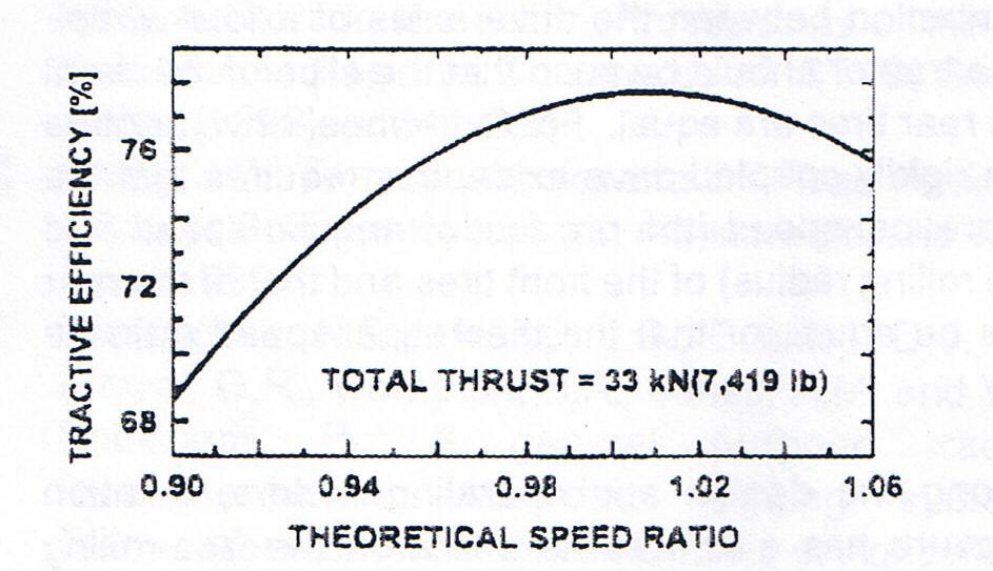

Figure 2.4: The effect of front-rear speed ratio on tractive efficiency, operating at 33 kN drawbar pull. (Wong, 2000)

Dudzinski (1986) sought to characterise the problems associated with the use of fixed ratio inter-axle couplings. Dudzinski's work focused on articulated frame steer, rather than Ackerman steered vehicles, but his data nevertheless has relevance to this project. Dudzinski noted that differences in the dynamic rolling radii of the tyres and differences in ground deformation under each wheel can lead to kinematic discrepancies between the front and

rear axles of a vehicle, which cause additional stress on the driveline, increased drive energy loss and tyre wear. Using a vehicle fitted with front and rear axle torque sensors, Dudzinski demonstrated that under certain circumstances one axle of a four-wheel drive vehicle would produce a negative wheel slip, while the other would produce a positive wheel slip, i.e. one axle was being pushed or pulled by the other. This phenomenon was particularly pronounced when running on concrete, where the higher levels of adhesion promote the development of transmission wind-up and thus make inter-axle interactions more evident.

Brenninger (1999) also observed the phenomenon of re-circulating power. He describes a situation in which a tractor, operating at a low slip level, exchanges power between the front and rear axles via the ground. The front axle, operating at a positive slip, pulls the rear axle, operating at a negative slip. He cites an experiment conducted on tarmac, in which a tractor was accelerated from rest, through a series of gears. This data shows that between 20 and 25km/h, the power circulating between the front and rear axles is equivalent to the vehicles 85kW rated engine power (Figure 2.5).

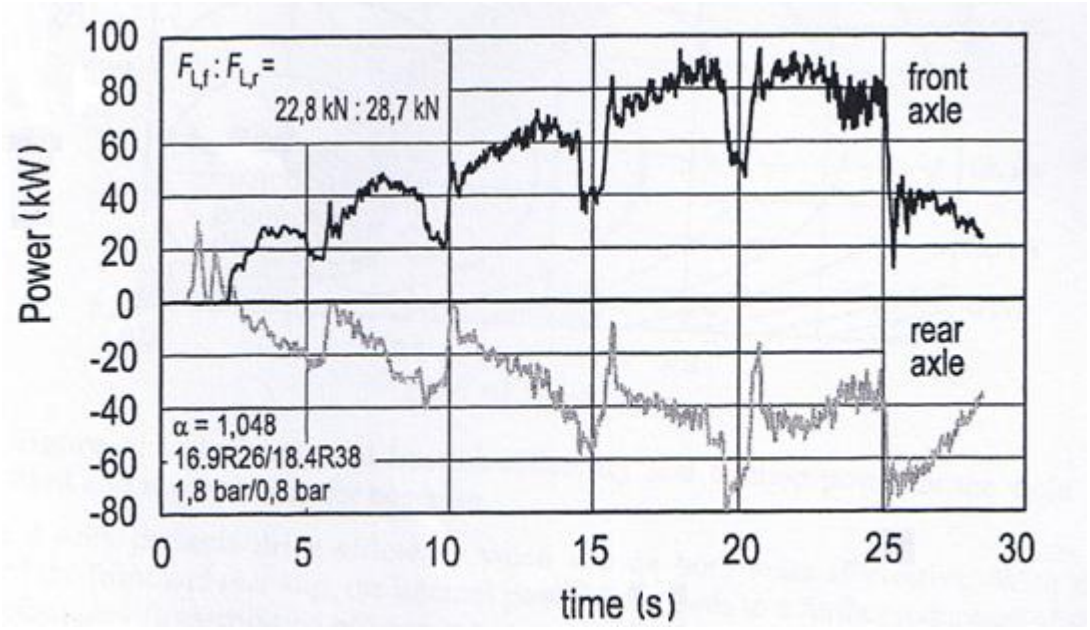

Figure 2.5: Power re-circulating through a tractor transmission as the machine accelerates. Note that a positive lead ratio is causing the rear axle to absorb power from the road, as indicated by the negative sign of the rear axle power. (Brenninger, 1999)

This circulating power causes additional wear on tyres and driveline components, but perhaps more significantly leads to a reduction in the overall efficiency of the vehicle. The power being exchanged between the axles is subject to a series of inefficiencies; between the front wheels and the ground, between the ground and rear wheels, and within the transmission between the rear and front axles. The power lost at each stage being replaced by the engine. Thus the power required to drive the tractor is rather more than if no power had been re-circulating.

Brenninger (1999) notes that the optimum speed ratio varies depending on whether the vehicle is travelling along a straight or curved path. Furthermore, he states, the optimum speed ratio alters depending on the radius of the path and the effective tyre radii. He also states that the effective radii of the tyres

can vary considerably as a result of variations in the production process, inflation pressure, tyre load and tyre wear. He suggests that variations in tyre properties can alter the ratio of peripheral speeds of the front and rear tyres by more than +/- 5%, while making a turn with a 50° steering angle at 15km/h can cause a variation of up to 30%. He concurs with Wong (1970) and others that the optimum condition for traction is to maintain equal levels of slip under all wheels, but he notes that a single fixed speed ratio can meet this condition in only one very specific set of circumstances. However, Brenninger (1999) cites data gathered by Steinkampf (1972), which shows that a 10% lead causes a reduction in tractive efficiency of only 2.5%, while a 20% lead reduces efficiency by 6%.

Rosa *et al* (2000) developed a system capable of automatically engaging and disengaging drive to the front wheels of an orchard tractor. They conducted both simulation studies and field trials to determine the effect of varying lead ratio on tractive efficiency and fuel consumption. They found no statistically significant differences between positive and negative lead modes.

2.5 Effects Associated with Steering

One of the reasons stated for the inclusion of a positive front axle lead in the design of a four-wheel drive tractor is a supposed improvement in the steering response of the machine. A fundamental dichotomy exists in the design of four-wheel drive systems for agricultural tractors. When operating on a straight and level path, the optimum speed ratio between front and rear wheels seems to be around one, as shown by Wong (2001), and others, but

when a tractor comes to make a sharp turn, such as at the headland, then, as demonstrated by Ikegami (1990), the optimum speed ratio is in the region of 1.7 – 1.9.

Ikegami *et al* (1990) documented the theoretical basis and experimental validation of the Kubota brand of tractor's *Bi-speed Turn* system, which allowed the lead ratio of a four-wheel drive tractor to be switched dynamically between two settings depending on the steering angle of the front wheels. Thus when the tractor was moving straight ahead, the speed ratio between front and rear wheels was one, but when the inner front wheel was turned to an angle greater than 25°, a clutch was engaged, which increased the speed of the front wheels to between 1.7 and 1.9 times the speed of the rear. Ikegami *et al* (1990) noted a reduction of between 18 and 20% in the turning radius of a tractor fitted with the Kubota system, when compared to an equivalent machine not using the system, although they did not actually document the nature of the experiments undertaken, or the running surface on which the vehicles were operated. It should be noted that the subject of this work was a small tractor with a mass of only 759kg and a wheelbase of 1470mm.

Ikegami *et al* agree with Sato *et al* (1999), who stated that one of the principle flaws of the four-wheel drive system most often found in agricultural tractors is its inability to deal with the difference between the distances travelled by the front and rear wheels when performing tight turns. The Kubota system clearly counters this shortcoming, by allowing the front wheels to rotate faster than the rear by a margin equivalent to the difference

in radii of the paths described by the front and rear wheels. However, Ikegami *et al* noted that the turn radius of a four-wheel drive tractor could be further improved by rotating the front wheels at a angular velocity greater than that required to simply overcome the difference in the length of front and rear paths. Figure 2.6 shows the change in turning radius as the ratio of front to rear speeds varies. Ikegami *et al* note that the speed ratio required to account for the difference in path lengths between front and rear wheels is 1.5. The area of the chart between a Bi-speed ratio of 1.0 – 1.5 shows a small progressive decrease in turning radius, associated with the steadily improving drive characteristics of the system as the braking effect of the front wheels lessens. Beyond a Bi-speed ratio of 1.5, there is a marked change in the gradient of the relationship between speed ratio and turning radius, indicating the existence of a further kinematic effect beyond that associated with the lengths of the front and rear paths.

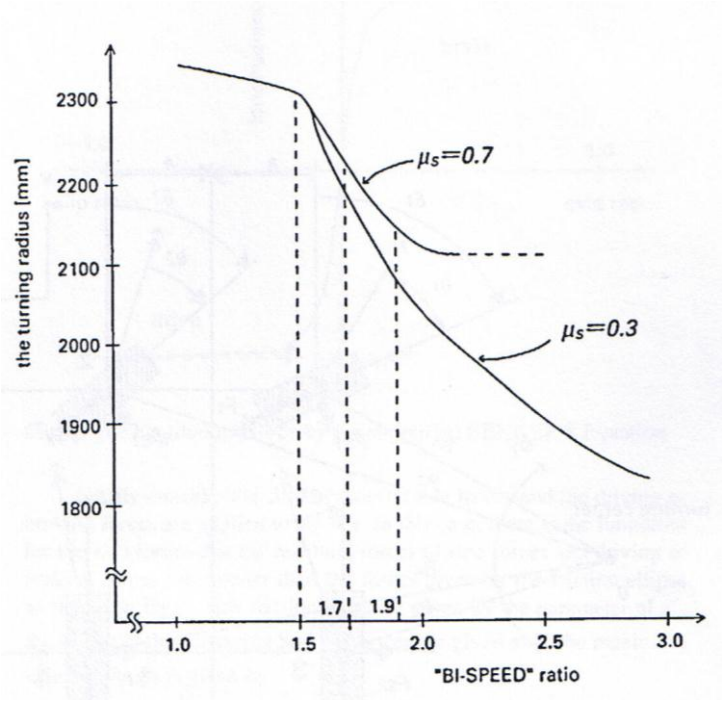

Figure 2.6: The relationship between “Bi-speed” ratio (speed ratio) and turning radius of the tractor. This chart was prepared using simulation data. (Ikegami *et al,* 1990)

Sato *et al* (1999) attempted to counter the steering problem associated with the rigid inter-axle coupling, typical of agricultural vehicles, by developing a torque proportioning centre differential. Their test vehicle was a 1720kg self-propelled orchard sprayer. They were able to demonstrate that the inclusion of a torque proportioning centre differential helped to improve the turning radius of the vehicle, from 7.70m to 7.55m, and reduce tyre wear due to excessive front wheel slip.

Crolla (1981) noted that the improvement in tractive performance of the rear wheels of a vehicle when running in the ruts created by the front, demonstrated by Dwyer *et al* (1977) and others, also applied when the vehicle was negotiating a turn. Thus a pivot steer vehicle, which produced only two ruts when turning, since the front and rear wheels follow the same path, had a superior tractive performance to that of an Ackerman steered vehicle, which produced separate ruts for all four wheels. Crolla (1981) also noted that the front and rear wheels of a pivot steer vehicle travel at the same speed as one another, thus eliminating the kinematic drag noted by Ikegami *et al* (1990).

Bottasso and Bandel (1988) conducted a mathematical study of road cars running on a circular path. They compared the behaviour of a four-wheel drive car with a centre-differential, a four-wheel drive car without a centre differential, and a rear-wheel drive car, with the intention of estimating the additional tyre wear caused to the four-wheel drive vehicle without centre differential, as a result of front and rear path length differences. They identified a critical speed, of *a few tens of kilometres per hour*, above which

the additional resistance caused by the difference in front and rear paths did not effect tyre wear. But they noted that below this speed, the kinematic differences between the front and rear axles did cause a significant longitudinal force, which would contribute to accelerated tyre wear. Bottasso and Bandel did not speculate on the influence of relative front and rear wheel speed on the straight-line performance of a vehicle.

2.6 Conclusions from the Review of Literature

Research into torque and power flow in agricultural tractors has in the past relied heavily on strain gauge based instrumentation. No previous attempts to measure axle and engine torque using magnetostrictive sensors are documented in the published literature. Also no previous attempt to measure power delivery efficiency, using Zoz *et al's* (2002) definition has been attempted in a four-wheel-drive or front-wheel-assist tractor.

Some disagreement exists between authors on the lead ratio that yields the highest tractive efficiency. Wong, Brenninger and Vantsevich maintain that the highest tractive efficiency is produced by running at zero lead, while Woerman and Bashford, Besselink and Musonda and Bigsby claim that the changing traction conditions between the front and rear axles mean that the optimum condition for tractive efficiency is different under each wheel.

Brenninger (1999) suggests that the concept of a fixed speed ratio is meaningless in any case, since changes in tyre load, pressure and wear can cause substantial changes in the effective rolling radii of the tyres.

Steinkampf (1972) showed that the magnitude of losses due to running with a sub-optimal lead ratio was perhaps only a few percent. However, Brenninger (1999) demonstrates that the magnitude of additional power being transmitted through driveline components and tyres might actually equal the power being delivered by the engine.

A limited amount of data exists on power flows within four-wheel drive tractors (Table 2.1). The vast majority of research has been carried out on North American soils. No power flow data exists in the literature for European soils.

Table 2.1: Summary of published research based on the use of torque sensors in off-highway vehicles

Authors	Tractor/Vehicle	Front Wheel Assist/4x4	Torque Sensors Front axle/Rear axle/Gearbox	Surfaces
Musonda and Bigsby 1978	Steiger 220 Bearcat III	4x4	F+R	CI 540 kPa
Erickson and Larsen 1983	126 kW International Harvester Model 4386	4x4	F+R	Clay Loam CI 1400 kPa
Woerman and Bashford 1983,1984, Bashford *et al* 1985	Case 1490	FWA	F+R	Clay/Concrete
Dudzinski 1986	Pivot Steer Dumper	4x4	F+R	Concrete
Bashford *et al* 1987	Ford TW-15	FWA	F+R	Sandy/Clay/Concrete
Bashford *et al* 1987	Versatile 876	4x4	F+R	Sandy/Clay/Concrete
Jenane and Bashford 1992	MF 3080	FWA	GB	Clay
Brenninger 1999	85 kW Tractor (Unknown)	FWA	F+R	Tarmac
Wong 1998, 1999, 2000, 2001, McLaughlin *et al* 1993	97kW Case IH Magnum	FWA	F+R	Clay Loam

3.0 Instrumentation and Methodology

3.1 Introduction

The experimental phase of this project had two main objectives:

- To evaluate an instrumentation system, based around magnetostrictive torque sensors manufactured by ABB, for a four-wheel-drive tractor, to isolate engine, and front and rear axle power flows, and drawbar power.
- To evaluate the power delivery efficiency and power flows through the front and rear axles of a four-wheel-drive tractor at a series of lead ratios, on soil and hard surfaces.

With these objectives in mind, a programme of field experiments was devised to gather data on the performance of a typical front-wheel-assist tractor operating under a range of field conditions. The programme was based around a model of tractor commonly found on European farms.

3.2 Tractor Specifications and Details

The tractor chosen for this study was a Case New Holland (CNH) TS90 (Figure 3.1). The tractor has a fixed ratio four wheel drive system, and is rated at 67 kW (90 hp). The particular vehicle used in this project was formerly a development prototype. The tractor has the model number APH90/01 and bears the serial number 153580B. It has four-speed, mechanical main gearbox, a three speed mechanical transfer box and an electro-hydraulically controlled splitter and forward and reverse shuttle, giving 24 forward and reverse gears (Figure 3.2).

The primary drivers for the selection of this tractor as the subject of this project were; the fact that it was a mid range, front wheel-assist tractor typical of those used on many northern European farms, and the gearbox architecture, which included sufficiently large spaces to accommodate the torque sensors (Appendix 3.1). Tractors from a number of alternative manufacturers were examined and then rejected on the grounds that the layout of their transmissions did not provide sufficient space to accommodate the torque sensors.

Figure 3.1: The Case New Holland TS90 tractor (Source, author)

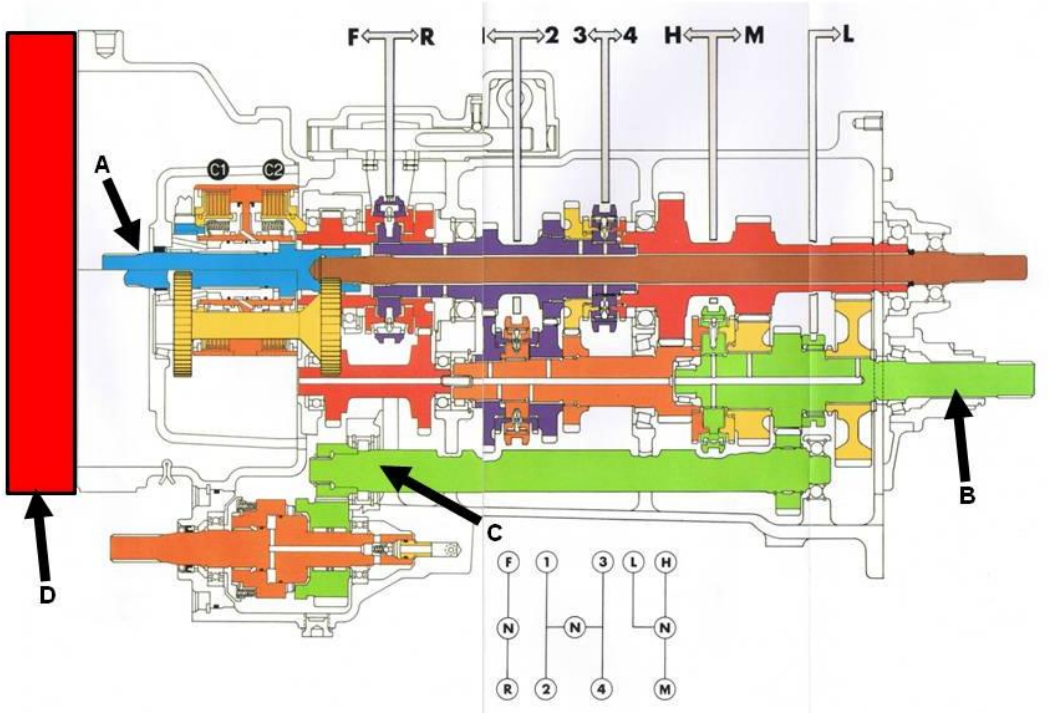

Figure 3.2: Schematic drawing of the main gearbox of the TS90. Torductor torque sensors were fitted at the input to the gearbox (A), output to the rear axle (B) and output to the front axle (C). Oxford TS180 shaft speed sensors were also fitted at locations B and C. The location of the extension plate (Figure 3.3) is shown at D. (Adapted from: CNH, 1998)

In the configuration used for this project, the tractor had a total mass of 4,600 kg (1,860 kg front, 2,740 kg rear) giving a 40/60 axle load split. The tractor was weighed with its fuel tank full, all instrumentation fitted, driver on board, and standard tyres fitted. The tractor was not fitted with any additional ballast.

In order to create sufficient space for a torque sensor at the gearbox input, the tractor was lengthened by 50mm by inserting a plate (Figure 3.3) between engine and bellhousing.

Figure 3.3: The 50mm steel plate used to extend the tractor (Source, author)

3.2.1 Tyres

In standard form the tractor was fitted with 420/24 Pirelli TM700 front tyres and 520/34 Pirelli TM700 rear tyres, giving a lead ratio of +2%. Following the method employed by Wong (1970 and 2001) and Wong *et al* (1998, 1999 and 2000) the lead ratio of the tractor was varied by changing either the front or rear wheels from the standard for ones of a different size. Three combinations were tested (Table 3.1) (See Appendix 3.11 for masses):

Table 3.1: Pirelli TM700 Tyre combinations used in the experimental programme

Lead Ratio	Front	Rear
-4%	420/70 R24	520/70 R38
+2% (As delivered)	420/70 R24	520/70 R34
+10%	420/70 R28	520/70 R34

The rolling circumference of each tyre was measured by making a reference mark on its sidewall, and a corresponding mark on the ground. The tractor was then driven forwards, on smooth, level tarmac, in two-wheel drive, until the tyre had completed five revolutions. A second mark was made on the ground adjacent to the mark on the tyre sidewall. The distance between the marks was measured using a tape measure. This process was repeated three times for each tyre. The average rolling circumference of each tyre was calculated by summing the three distances recorded, and dividing the result by 15. The results of this experiment are shown in Table 3.2.

Table 3.2: Rolling circumferences of the tyres used in the experimental programme

Replicate	420/70 R24	420/70 R28	520/70 R34	520/70 R38
1	18.54m	20.24m	24.28m	25.80m
2	18.54m	20.24m	24.26m	25.81m
3	18.54m	20.24m	24.26m	25.86m
Calculated rolling circumference	**3.708m**	**4.048m**	**4.853m**	**5.165m**

Tyre pressures were maintained at manufacturers recommended settings of 1.2bar front and 1.0bar rear.

3.2.2 Gear conditions

The TS90 was operated in gear 4LH, for all the field experiments, giving a reduction ratio between the gearbox input shaft and rear output shaft of 3.06:1, which, at maximum throttle setting, gave a forward speed, with no load, of 2.2m/s. The front wheel drive gears within the main gearbox gave a speed increase of 1:1.25. The reduction ratio between the front gearbox output shaft, where front axle torque was measured, and front hubs was 26.2:1 and between the rear output shaft, where rear axle torque was measured, and rear hubs 32.37:1.

3.3 Instrumentation

The TS90 was instrumented to measure a total of nineteen parameters (Appendix 3.1). Data from these sensors was recorded on a pair of Isaac Instruments BOX V8-STD solid-state data-loggers, mounted in the tractor cab. The approach taken to data collection was similar in principle to those employed by McLaughlin *et al* (1993) and Jenane and Bashford (1992), in that measurements of gearbox output shaft torque were combined with data from a drawbar loadcell and shaft and ground speed sensors to provide real-time indications of tractor input and output power, and thus the instantaneous tractive efficiency of the machine. However, this work differed from that of previous authors in that engine power was also measured in real time, allowing power delivery efficiency to be calculated.

3.3.1 Torque Sensors

Torductor-S torque sensors (Appendix 3.1), supplied by ABB AB of Sweden, were fitted in three locations. The Torductor-S is a non-contact, bi-directional torque sensor based on the magnetostrictive principle, described by Wallin and Gustavsson (2002). The sensor is in two distinct parts (Figure 3.4), the torque carrying shaft itself, and a sensor housing, which is concentric to, but separate from the shaft. The shafts used in this machine were manufactured by ABB from A354 stainless steel. The form of the shafts was modified (Appendix 3.7) from those originally fitted by the CNH in order to increase the stress within the shafts to a level compatible with the sensors.

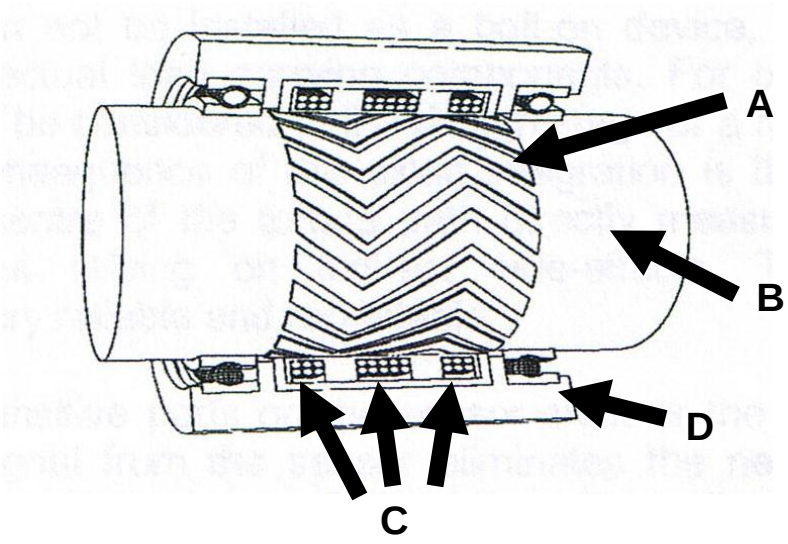

Figure 3.4: Cutaway drawing of a Torductor-S, showing the copper chevron pattern (A) on the shaft (B), and the three zone coil arrangement (C) in the sensor housing (D). (Adapted from Wallin and Gustavsson, 2002)

The sensor housing contains primary and secondary windings, which are separated into three areas. The shaft has a chevron pattern plated onto its surface in copper. Wallin and Gustavsson (2002) state that the shaft is excited with a rotationally symmetric magnetic field by the primary coil. The chevron pattern is aligned to the principle stresses in the torsionally loaded shaft. The induced magnetic field is aligned to the copper chevrons. When the shaft is loaded, the distribution of magnetic flux along the shaft is shifted due to the magnetoelastic effect. This change is detected by the secondary coils.

Wallin and Gustavsson (2002) note that the Torductor-S has a number of advantages over more conventional torques measuring methods; amongst these they list the Torductor-S' ability to operate reliably in hostile environments including gearboxes. They state that this ability is due to the lack of mechanical contact between the shaft in which the torque is being

measured and the sensor housing. They also note that the sensor does not generate a permanent magnetic field, and therefore is not susceptible to attracting metallic particles from the environment, which would damage the sensor. They also state that the sensor has a low electrical impedance and high signal to noise ratio (60dB), which gives it a high degree of immunity to external electrical interference. Finally they observe that the sensor components do not require any special handling during installation, which makes the Torductor-S easier to install than comparable torque sensing systems.

Calculations were carried out to estimate the torque levels likely to be encountered in the instrumented shafts while the tractor was being operated. These calculations (Appendix 3.6) were required to balance the requirements of adequate strength to ensure that the shafts would not fail under load, while also ensuring that they would be operating within the stress range specified by ABB for reliable operation of the Torductor (Appendix 3.1). The worst load case was assumed to be a situation in which the tractor was operating on a surface with a coefficient of friction of one and all the weight of the machine was being borne by one axle, a situation that might occur if the tractor had become unstable in pitch after hitting a bump at high speed on tarmac. These calculations suggested that the maximum torques likely to be encountered by the front and rear axles would be 923.94 Nm and 982.09 Nm respectively. The maximum torque likely to be encountered by the gearbox input shaft was assumed to be the maximum torque observed by Morgan *et al* (2000). The cross sectional areas and diameters of the instrumented shafts were then chosen based on these figures. This necessitated the

removal of a significant quantity of material compared to the original CNH design.

Each Torductor was calibrated by ABB before being shipped (Appendix 3.4). The sensors were then subjected to a further static calibration before final installation in the tractor (Appendix 3.4). The gearbox input and rear output Torductors were calibrated in position in the gearbox. The front output shaft Torductor was calibrated on the bench, as space constraints made it impossible to calibrate the sensor in position. Calibration involved fitting a splined fixture to one end of the shaft, which was then attached to the centre point of a steel bar which acted as a lever. Weights were then hung onto one end of the bar, producing a repeatable torque at the torque sensor. The distance between the centre of the shaft and axis of the weight carrier was set to 1019mm, so that a 10kg weight would produce 100Nm of torque at the torque sensor.

3.3.1.1 Rear Axle Torque Sensor

The torque transmitted to the rear axle was measured at the junction between the main gearbox and the rear axle housing (Figure 3.2). This location was chosen as it afforded the easiest access for fitting, and provided good protection for the sensor in service, being enclosed within an oil-filled casing. ABB were concerned that they would not be able to match the material properties of the working parts of this shaft using the A354 stainless steel required by the Torductor system. The decision was taken to manufacture a composite shaft using the front portion of the CNH made shaft, and a new rear section, manufactured by ABB, incorporating the

sensor zone. The original CNH manufactured part (Figure 3.5) was cut behind the low-ratio drive gear and a new section of shaft was machined from A354 stainless steel. Matching splines were machined onto the remaining part of the CNH shaft, and the new ABB manufactured part. The two parts finally being bonded together before fitting into the gearbox. The sensor housing was bolted to the rear output-shaft bearing carrier (Figure 3.6), which had been machined flat for that purpose. Radial location was provided by a locating ring on the sensor housing, which fitted into a corresponding machined hole in the bearing carrier. Opposing taper-roller bearings at either end of the shaft provided axial location. Shims either side of the rear bearing carrier were used to remove any float in the shaft, and position the sensor housing correctly.

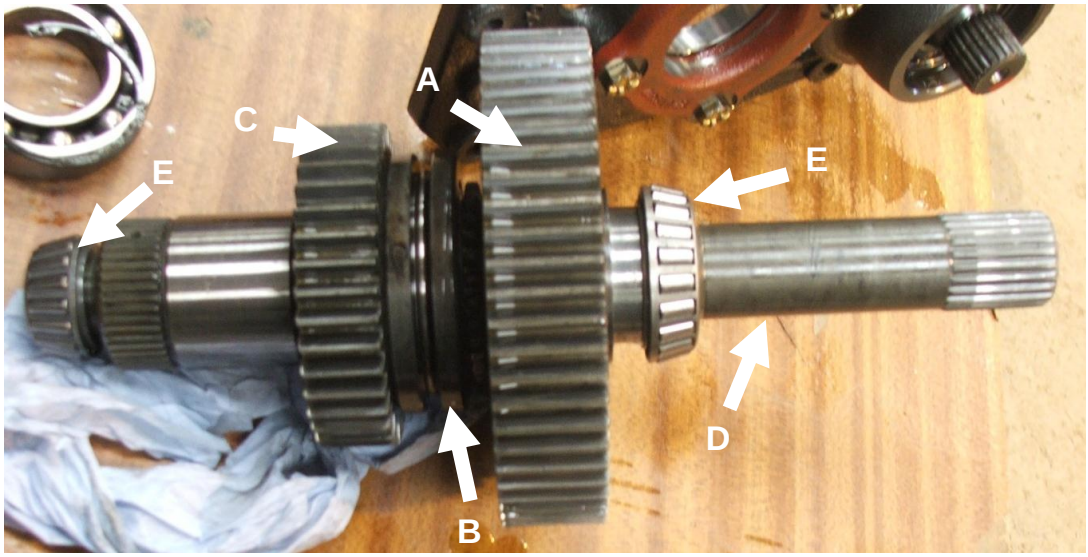

Figure 3.5: The rear output shaft, showing the low-ratio drive gear (A), and its dog clutch (B), the front wheel drive take-off gear (C), and the section of plain shaft used as the sensor zone for the rear Torductor (D). The axial location of the sensor zone is controlled by taper-roller bearings (E). (Source, author)

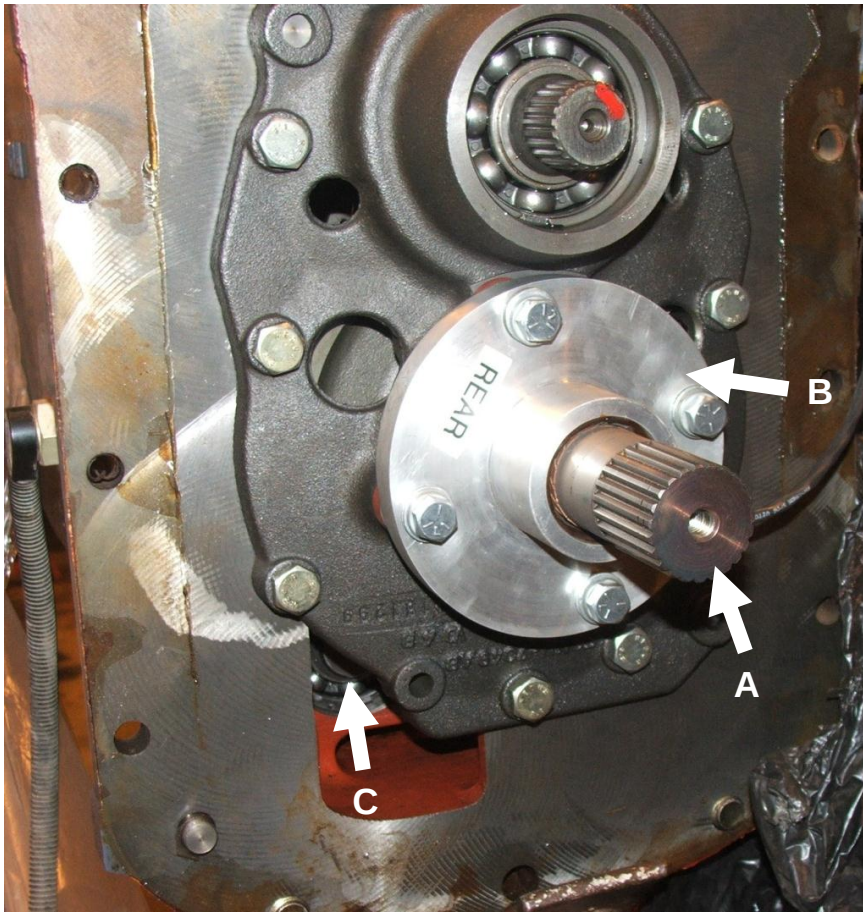

Figure 3.6: View of the rear of the main gearbox, showing the output shaft (A) and its associated Torductor housing (B). The front wheel driveshaft rear bearing (C) is also visible. (Source, author)

3.3.1.2 Front Axle Torque Sensor

The torque transmitted to the front axle was measured at the forward end of the internal front-wheel-drive shaft (Figure 3.2). This location (Figure 3.7) was chosen over the more easily accessible external shaft, as it afforded much better protection to the sensor. However, the close proximity of the front bearing carrier to the main gearbox casing necessitated some post-manufacture machining to the Torductor housing to create sufficient clearance for assembly to seat properly in the gearbox. Radial location was provided by an elevated lip on the sensor housing, which mated with the inner edge of the bearing carrier aperture. The internal front-wheel-drive

shaft was remanufactured in its entirety by ABB from A354 stainless steel. The external diameter of the shaft (Figure 3.8) was reduced from 45mm to 36.5mm in order to increase the stress level within the shaft to a range suitable for measurement by the Torductor. Axial location of the shaft was provided by a deep grove roller bearing at the rear end of the shaft. The Torductor was designed and calibrated with two torque ranges; +/- 1000Nm and +/- 2000Nm. The 1000Nm range was used throughout the experimental programme.

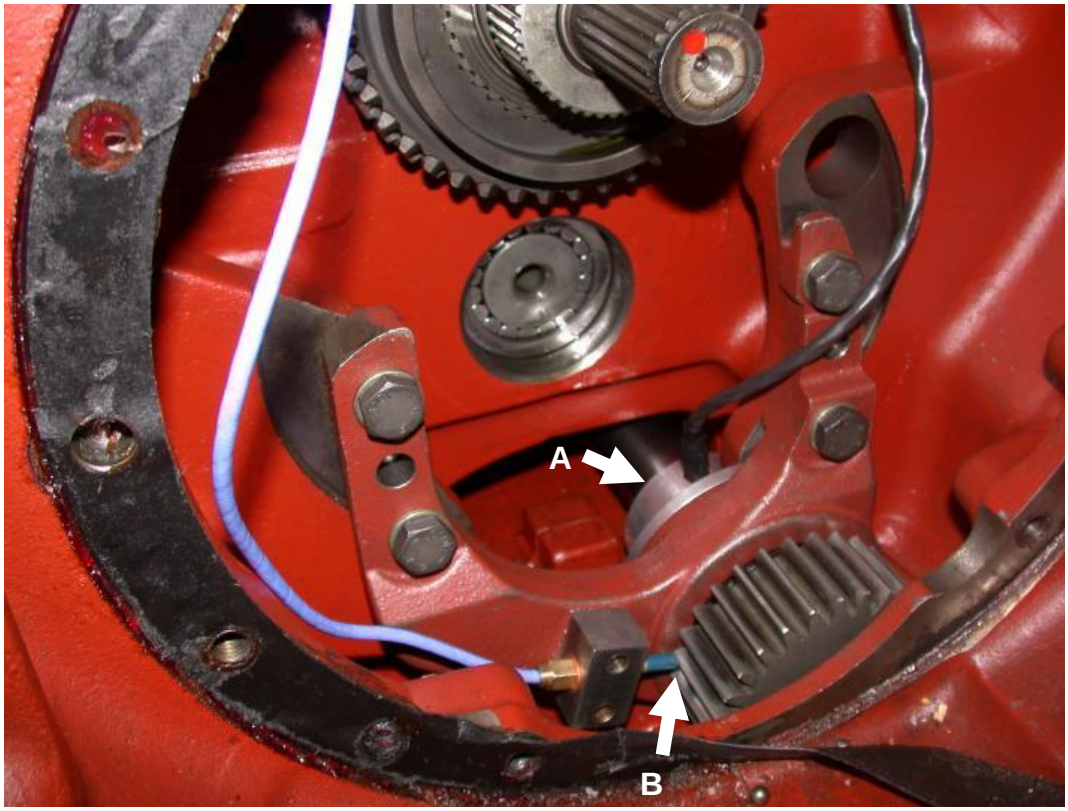

Figure 3.7: View from the front of the tractor, looking into the main gearbox, through the space normally occupied by the dual-power clutch assembly. The front-wheel-drive shaft torque sensor (A) and speed sensor (B) are visible. (Source, author)

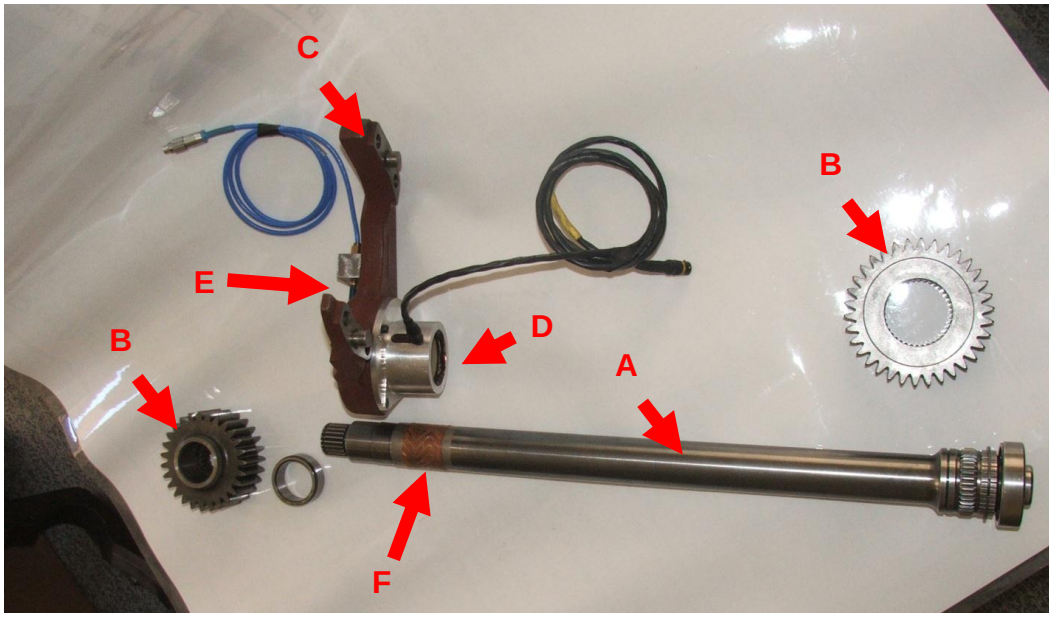

Figure 3.8: The internal front wheel driveshaft (A), drive gears (B), bearing carrier (C), Torductor housing (D) and speed sensor (E). The copper chevron of the Torductor sensing region (F) is visible on the left hand end of the shaft. (Source, author)

3.3.1.3 Gearbox Input Torque Sensor

The gearbox input Torductor (Figure 3.9) was fitted inside the bellhousing between the front of the dual power clutch housing and the engine flywheel (Figure 3.2). Since no suitable space existed at the input to the gearbox, the length of the gearbox input shaft was increased by 50mm to create a space suitable for the installation of the sensor housing. This necessitated the insertion of the spacer plate (Figure 3.3) between engine and bellhousing. In this location the Torductor was directly measuring the input torque to the gearbox. The gearbox input Torductor was designed to have a measuring range of -300Nm (i.e. against the normal direction of rotation) and +600Nm.

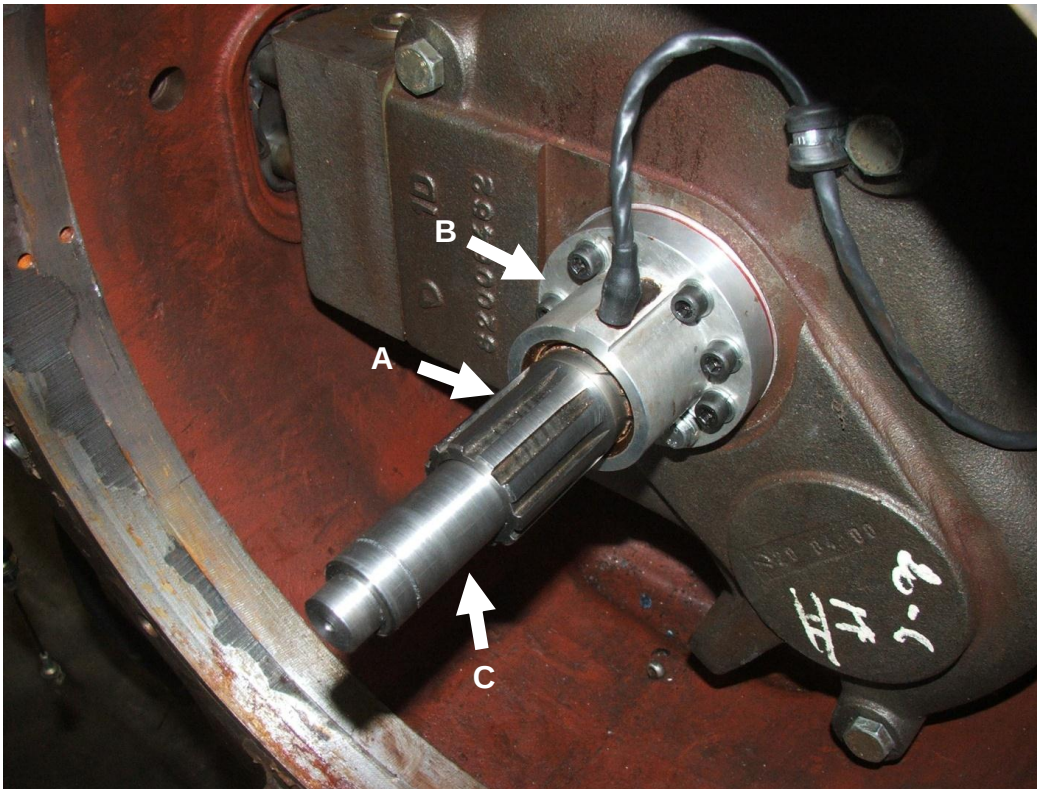

Figure 3.9: View from the front of the tractor looking into the bellhousing showing the gearbox input shaft (A) the Torductor housing (B) and the plunger mechanism used to maintain the axial position of the shaft (C). (Source, author)

3.3.2 Microwave Ground Speed Sensor

The absolute speed of the vehicle over the ground, as distinct from the wheel speed, was measured using a Pegasem GSS20 microwave speed sensor. The GSS 20 is a dual head microwave sensor. The heads are angled at 90° to one-another, and nominally 45° to the ground. This arrangement allows the sensor to derive its speed measurement from two independent sources, which are averaged together to reduce the effect of errors due to the vehicle pitching over uneven ground (Pegasem, 2009). The sensor was mounted on a bracket suspended below the left hand side of the engine, just behind the front axle. This position was chosen as it provided the best protection for the sensor, while still allowing an unobstructed view of the ground in an arc

below the sensor. The calibration of the sensor was checked by driving the tractor along a 100m tarmac test strip at a constant speed. The distance measured by the sensor was repeatable to within 0.4%. However, the absolute forward speed data recorded by the microwave speed sensor exhibited a perturbation with a frequency of around 0.2Hz and amplitude of around 0.2m/s. This perturbation was due to low frequency noise in the circuitry of the sensor itself (Mahr, 2010. Pers. Comm. Helmut Mahr is a representative of Pegassem GmbH). The effect of this noise was mitigated through filtering in the data processing stage of the experimental programme (Section 3.6.2) to the point where measured and calculated forward speed agreed to within 0.5%.

Figure 3.10: The Pegasem GSS20 dual head microwave speed sensor. (Source, Pegasem 2005)

3.3.3 Wheel Speed Sensors

The speed of each wheel was measured using a three wire Hall-effect sensor, which detects the passage of teeth on 60 tooth pole wheels fitted to each wheel hub (Figure 3.11). The pole wheels (Appendix 3.8) were laser-cut from 6mm steel plate, and sandwiched between the face of the wheel

drive flange and the wheel itself. The pulse streams from the Hall-effect sensors were converted into speed values by internal counters in the dataloggers. The sensors were calibrated by comparing the indicated speed to the average speed calculated by measuring the time taken to travel between two markers set 100m apart on a flat tarmac test track at a constant speed, in two-wheel-drive the maximum error of the sensors was found to be -0.85% of the timed speed (Appendix 3.12).

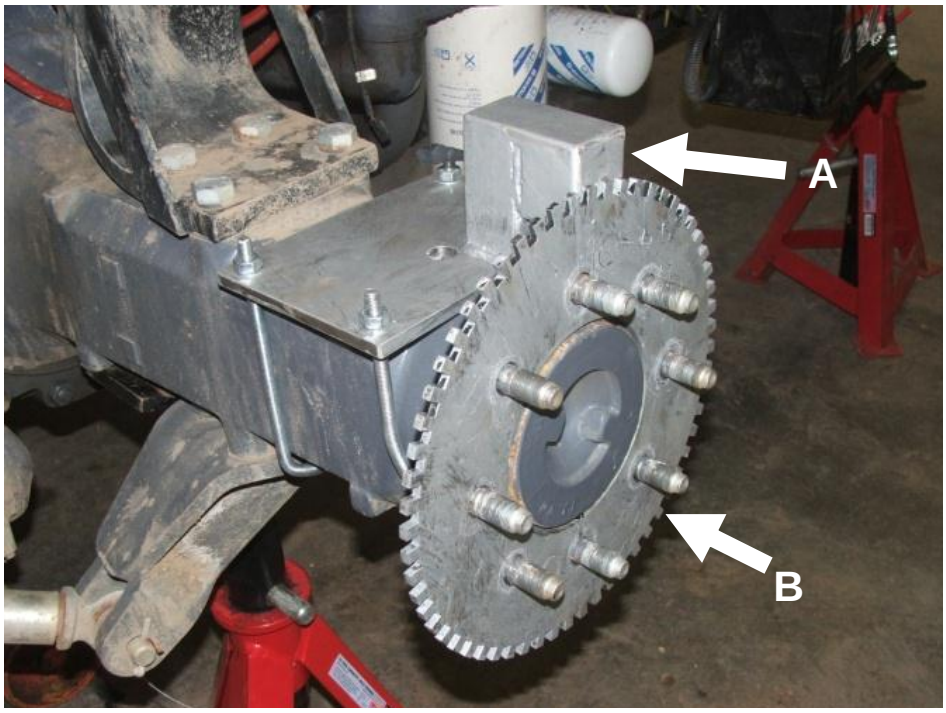

Figure 3.11: Rear wheel speed sensor (A) and its associated 60 tooth pole wheel (B). (Source, author)

3.3.4 Shaft Speed Sensors

Engine, front wheel driveshaft and rear wheel driveshaft speeds were measured using Oxford Instruments TS180 Hall effect probes. The speed of the front wheel driveshaft was picked up from the 27 tooth gear that drives the front wheel drive clutch, immediately adjacent to the Torductor position (Figure 3.6). The speed of the rear driveshaft is taken from the 31 toothed

wheel that forms the junction between the gearbox output shaft and axle input (Figure 3.12).

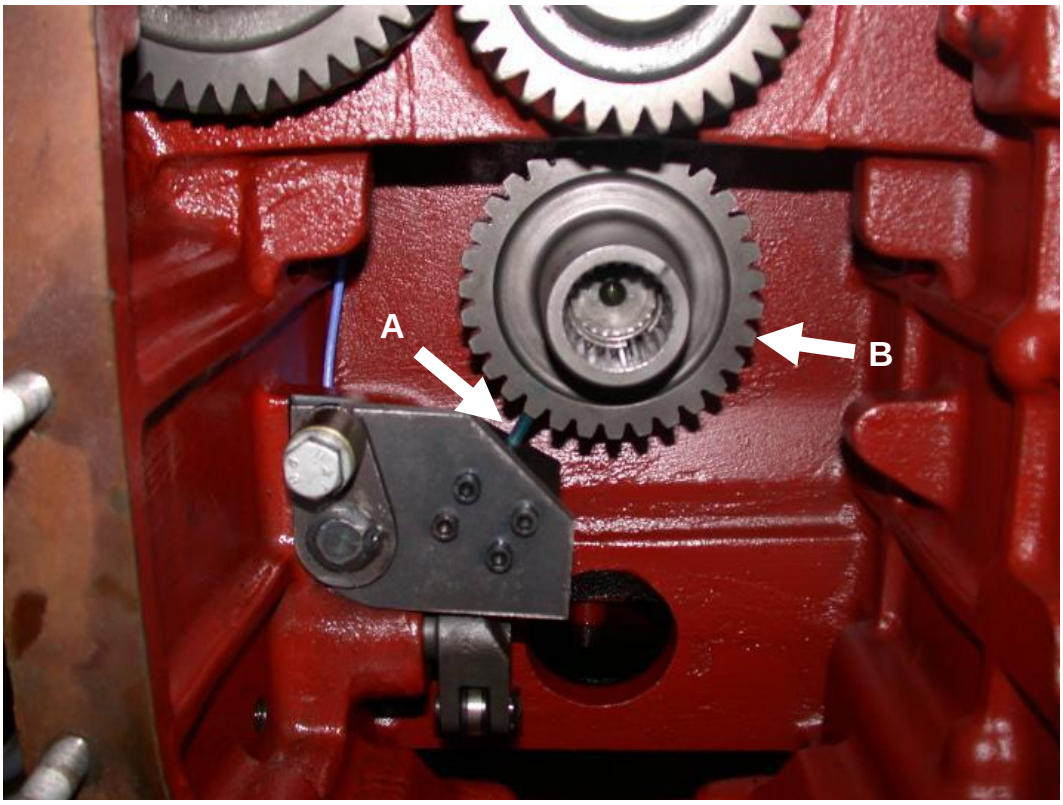

Figure 3.12: View from the front of the tractor showing the rear output shaft speed sensor (A) and its associated pole wheel (B). (Source, author)

The calibration of these sensors was verified prior to fitting into the tractor, by mounting each gear or toothed wheel into the chuck of a metalworking lathe, and rotating it adjacent to the Hall-effect probe at a range of different speeds. The speed of rotation was measured using an optical tachometer.

3.3.5 Data-loggers

The data-logging system consisted of a pair of Isaacs Instruments Box V8x/STD recorders, which were configured as a Master and Slave. The loggers communicated with one-another via a CANBUS link, with the Slave logger acting as a sensor interface for the Master. Data were collected at a rate of 100 samples per second, the highest rate at which the CANBUS

connection could operate. The loggers incorporated sensors to measure their own internal temperature and supply voltage, and a tri-axial accelerometer. Power for the data-loggers was supplied from the vehicle battery. The data-loggers supplied power to the shaft speed and wheel speed sensors.

3.3.6 Drawbar Loadcell

Drawbar pull was measured using a 10tonne Novatech loadcell coupled to a Vishay Measurements Group 2120B instrumentation amplifier. The 10tonne loadcell being selected over lower rated alternatives because of the danger of transient load spikes causing mechanical overload. The system was calibrated against a Denison hydraulic tensometer. The force on the loadcell being increased in 5kN steps over the range between 0 and 30kN, the maximum drawbar pull recorded during preliminary tests. This test was repeated three times. Over the range tested the loadcell exhibited a linear response (R^2=1), repeatability of +/- 0.04% and no hysteresis (Appendix 3.3). The sensitivity of the loadcell-amplifier combination was 0.1V/kN.

3.4 Experimental Procedure

Tests were conducted on two test sites at Harper Adams University College (Figs 3.13 and 3.14). The main body of data were collected in four days:

18th August 2009: testing on the sandy site at -4% lead

19th August 2009: testing on the sandy site at +10% lead

2nd September 2009: (AM) testing on the sandy site at +2% lead, (PM) testing on the clay site at +2% lead

3rd September 2009: (AM) testing on the clay site at +10% lead, (PM) testing on the clay site at -4% lead

The tractor was refuelled with 118litres of diesel between the morning and afternoon test sessions on the 2nd of September.

Within each lead condition tests were repeated three times. Tests were further replicated by conducting tests in opposite directions on the same test plot, giving two groups of three replicates in each lead on each surface. The two surfaces were treated as two separate experiments, with a common method but two sets of factors; lead ratio was a factor on both surfaces, but on clay direction of travel was treated as a factor, while on the sandy site, which had a slight slope, whether the tractor was travelling up or down hill was considered the second factor. Since one site sloped and the other did not, it was not possible or desirable to combine all the data from both sites into a common statistical analysis.

3.4.1 Sandy test site

The sandy test site (Figure 3.13) had a very light sandy soil. Immediately prior to testing a failed crop of beans, standing approximately 500mm tall, which had been sprayed with herbicide, was buried using a cultivator. The surface was then further treated with a power harrow to give a uniform running surface.

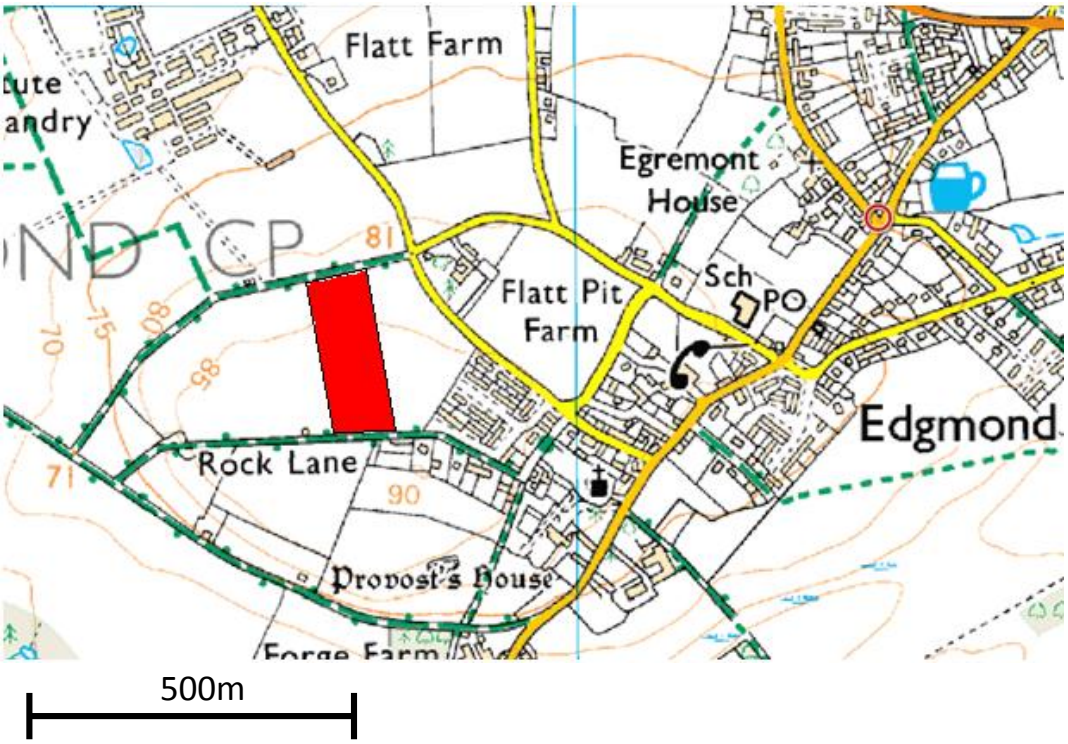

Figure 3.13: Location of the sandy test site (highlighted in red)

The test plot was divided into six test lanes, each approximately 250m in length. Each lane was used once in each set of trials. The surface was treated with the power harrow between sets to restore the uniform surface texture.

The sandy test site had a uniform gradient of approximately 1°. Tests were conducted both up and downhill.

3.4.2 Clay test site

The clay test site (Figure 3.14) had a heavy clay based soil. Immediately prior to testing a crop of wheat was harvested, leaving stubble approximately 75mm tall. The surface was not treated in any way prior to testing. Runs were conducted in between the windrows of cut straw. Each test lane was used only once. The field was divided into three strips. Each set of trials

included a run in each strip. Trials were conducted running towards both the north and south.

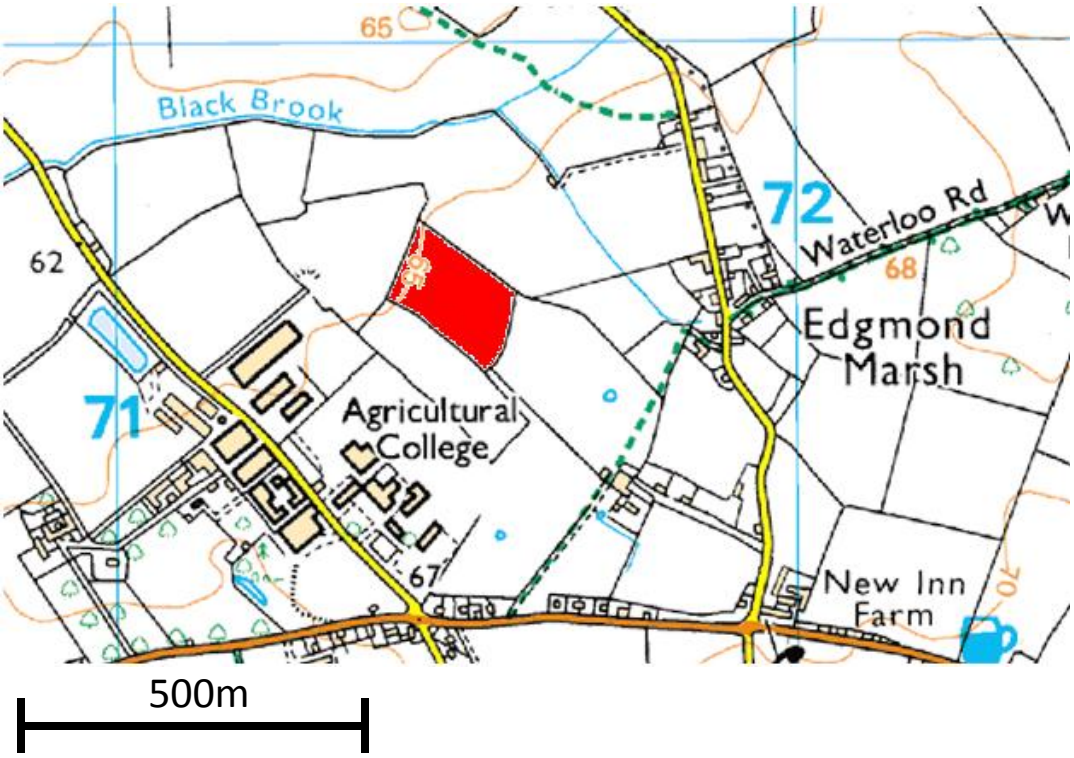

Figure 3.14: Location of the clay test site (highlighted in red)

3.4.3 Soil Conditions

A cone penetrometer with a 20mm cone was used to measure the properties of the soil on the two sites. Multiple measurements were taken at intervals across the test strips. The average soil cone index for the Sandy test site was 427 kN/m^2 while the Clay site had an average figure of 1,566 kN/m^2. Both sites exhibited considerable variability in their soil cone indices, as shown in Figure 3.15.

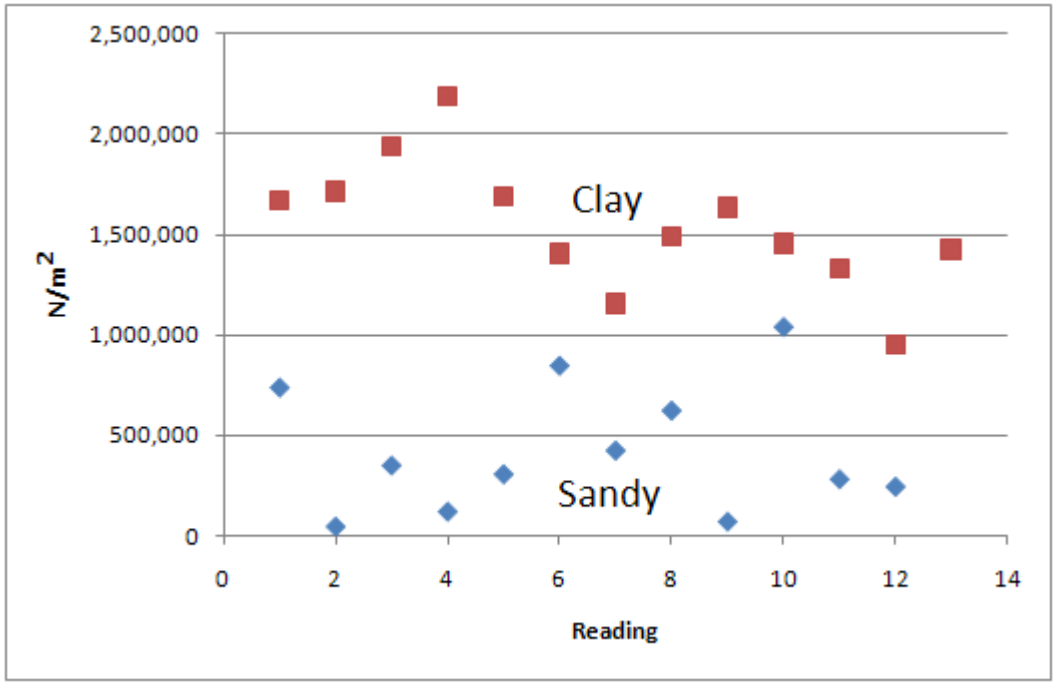

Figure 3.15: Average soil cone index at intervals along the test strips

3.4.4 Meteorological Conditions (Appendix 3.5)

18th August 2009, warm, dry, broken cloud

19th August 2009, warm, dry, clear sky

2nd September 2009, cool, occasional drops of rain, overcast, heavy rain the previous night

3rd September 2009, cool, occasional light showers, overcast

3.5 Test procedure

Following a technique used by Wong (2001 and 1970) and Wong *et al* (1998, 1999 and 2000) the TS90 subject tractor was coupled to a second tractor, whose purpose was to apply a retarding force to the drawbar of the subject tractor. The load tractor was a Case MXU135, which was carrying a Kverneland NGS301 power harrow. The total mass of the MXU135 and power harrow was around 10tonnes.

The TS90 ran in gear 4LH, at maximum throttle setting, which gave a forward speed, with no load, of 2.2m/s. The MXU 135 started in gear 10 at an engine speed of 2000rpm. As the test proceeded, the engine speed of the MXU135 was slowly reduced from 2000rpm to 1000rpm, thus reducing its forward speed from 2.2m/s to 1.1m/s. Since the mass of the MXU135 was much greater than that of the TS90, controlling the forward speed of the MXU135 effectively controlled the speed of the combination. Since the TS90 remained at a constant throttle and gear setting, slowing the MXU135 caused a steady increase in the TS90's wheel slip and drawbar pull.

Figure 3.16: Conducting a trial on the sandy test site.
(Source, Pickthall, 2009)

3.5.1 Rationale

The primary aim of the experimental programme was to gather data related to the effect of varying lead-ratio on the flow of power through the tractor's transmission. The effect of tractor-implement interaction was considered to

be beyond the scope of this project, and no attempt was made to address this phenomenon. Using a second tractor as a controlled rolling load allowed a retarding force to be applied at the drawbar, without the risk of inadvertently applying vertical forces, as might have been the case if a three-point linkage mounted implement had been used. The subject tractor was considered to be isolated from the load tractor, the sole connection between the two being the measured force applied to the drawbar via the chain. The choice of the MXU135 as the load tractor was purely expeditious.

The choices of speed and wheel slip ranges were selected to represent typical tillage operations in northern European agriculture. The subject tractor was not ballasted, as might be considered normal practice in farm operations, as the purpose of the study was to develop an understanding of the influence of lead, rather than optimise the performance of the tractor. A single gear ratio was employed to remove any variability associated with the main gearbox. The maximum throttle setting was employed as it provided an easily repeatable engine power reference point.

The test plots were chosen to provide contrasting field conditions representative of typical British arable farm land.

3.6 Data Processing

At the end of each run, the data collected was downloaded onto a laptop in Isaac's native ISA format. The data were then converted, using Isaac's software, into comma separated variable (CSV) format, and then imported into MathCAD 14.

3.6.1 Data Trimming

The raw data collected on each run included a quantity of extraneous measurements produced as the subject tractor took the strain on the drawbar, and transitioned into forward travel, and also as the tractor came to a halt at the end of each run. This spurious data were manually trimmed by setting individual range variables for each run (Figure 3.17). The trimmed data were then written out as a text file, which was used as the basis for all subsequent processing.

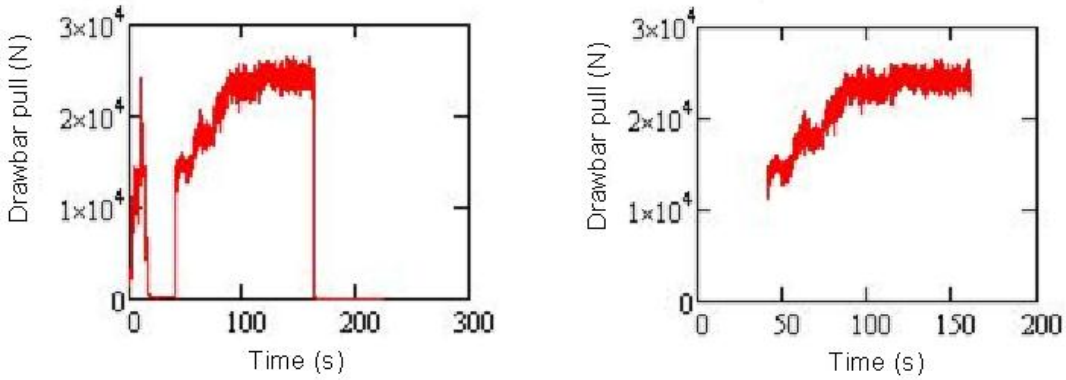

Figure 3.17: Drawbar pull data, untrimmed (left), and trimmed to remove extraneous data from the beginning and end of the test (right) Time (s)

3.6.2 Smoothing

This perturbation in the absolute forward speed data caused by low frequency electronic noise caused considerable variability in the secondary and tertiary parameters calculated using absolute forward speed as a factor. A moving average filter with a 1001 point sample frame was applied to the absolute forward speed data, to minimize the effect of this interference (Figure 3.18). The 1001 point sample frame was chosen to encompass ten seconds of data, or two complete cycles of the spurious signal.

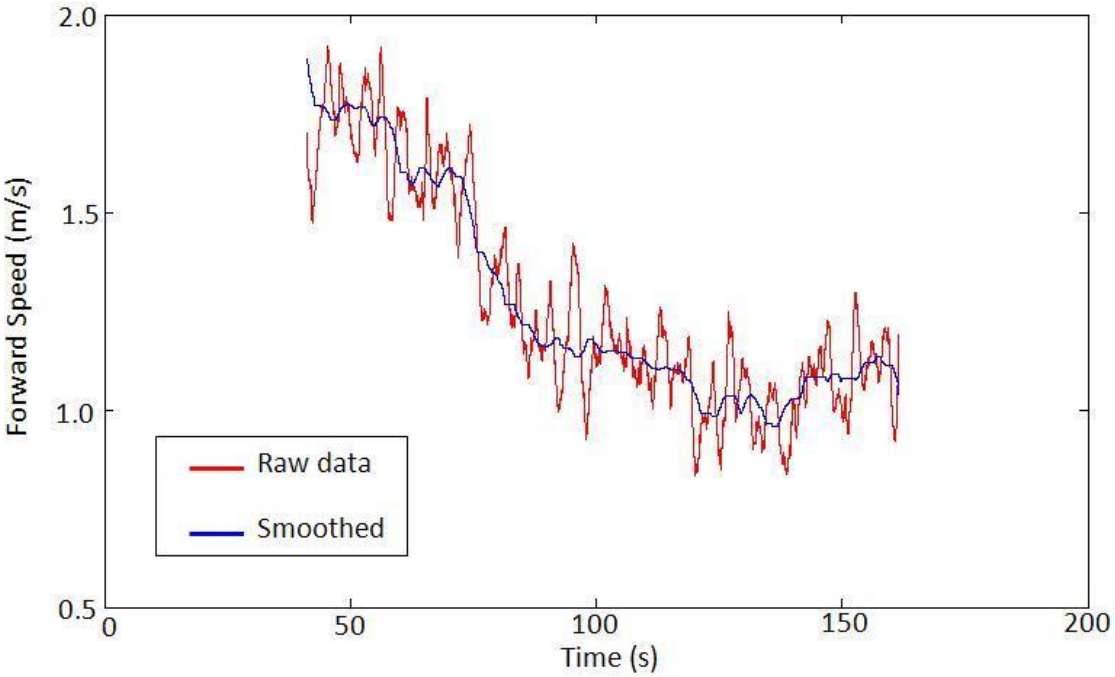

Figure 3.18: The effect of moving average smoothing on absolute forward speed data

3.6.3 Calculating secondary and tertiary parameters

The secondary parameters calculated from the raw data were:

- Engine power (calculated from engine speed and engine torque) (w)
- Front and rear shaft powers (calculated from the front or rear shaft speed and torque figures) (w)
- Drawbar power (calculated from drawbar pull and smoothed absolute forward speed) (w)
- Wheel slip at each wheel (calculated from wheel speed, wheel rolling circumference, and smoothed absolute forward speed. The ‘zero slip’ condition was specified as the ‘zero draught’ condition on tarmac) (%)

Power delivery efficiency was calculated as a tertiary parameter, by dividing drawbar power, by engine power, and multiplying the result by 100 to give the result as a percentage.

3.6.4 Statistical analysis of data

The experimental data was analysed using Genstat 13 software. All the data was analysed using a two factor analysis of variance, with lead ratio being one factor on both surfaces tested. On clay the second factor was direction of travel, while on the sandy site, which had a slight slope, the second factor was whether the tractor was travelling up or down hill. The data sets analysed were (Appendices 4.1 – 4.12):

- Power delivery efficiency
- Engine power
- Drawbar power
- Drawbar pull
- The slope of the front axle torque response to drawbar pull
- The slope of the rear axle torque response to drawbar pull

These data sets were chosen since they related most closely to the central aim of the research, which was to identify differences in power delivery efficiency and torque and power flow caused by changes in lead ratio.

4.0 Results and Analysis

4.1 Introduction to Data Analysis

This chapter presents the experimental data gathered while evaluating the field performance of the instrumented tractor. The chapter is divided into three sections; Section 4.2 examines the effect of lead ratio on drawbar performance and power delivery efficiency, Section 4.3 examines the effect of lead ratio on the way power and torque flows through the tractor's drivetrain, and Section 4.4 analyses the data gathered while operating on tarmac and gravel roads.

Among the key findings in this chapter; Section 4.2 illustrates the fact that the effect of lead ratio on power delivery efficiency and tractive performance changes with soil properties, Section 4.3 shows that power flow to the front axle remains constant as drawbar power increases, and Section 4.4 demonstrates the relationship between transmission wind-up and braking on hard surfaces.

4.2 Drawbar Performance and Power delivery Efficiency

4.2.1 Introduction

This section presents the results of experimental work conducted on the sandy and clay test sites at three lead ratios, and examines the effects of lead ratio and terrain on the performance of the TS90 tractor. Here performance is quantified in terms of the commonly applied criteria; wheel slip, drawbar pull, drawbar power and engine power. From these the power delivery efficiency of the machine is calculated, and related to drawbar pull and rear wheel slip.

Section 4.2.2 demonstrates the effects of the 1° gradient on the sandy test site and offers the distinct grouping of the up and downhill data as an indication of the reliability and repeatability of the data acquisition system, while section 4.2.3 demonstrates that on the flat clay test site, direction of travel does not influence the performance of the tractor.

Sections 4.2.4 to 4.2.7 illustrate the influence of lead ratio on the drawbar performance and power delivery efficiency of the tractor, and also demonstrate that the influence of lead ratio is not constant, but instead varies depending on the condition of the running surface.

4.2.2 The effect of gradient on the slip-pull curve

Figure 4.2.1 illustrates the effect of the 1° gradient of the sandy test site on the relationship between rear wheel slip and drawbar pull. This figure includes six plots of drawbar pull against rear wheel slip at the standard +2% lead. The distinct grouping of uphill and downhill data indicates that the modest gradient of the test site actually had a statistically significant

(p=<0.001, Appendix 4.4) and measurable effect on the draught performance of the tractor; operating downhill producing a higher maximum drawbar pull (average 25.2 kN), than operating uphill (average 24.4 kN). These results indicate that the data collection system is capable of gathering data in a repeatable fashion, and is also capable of detecting the effect of small changes in operating conditions.

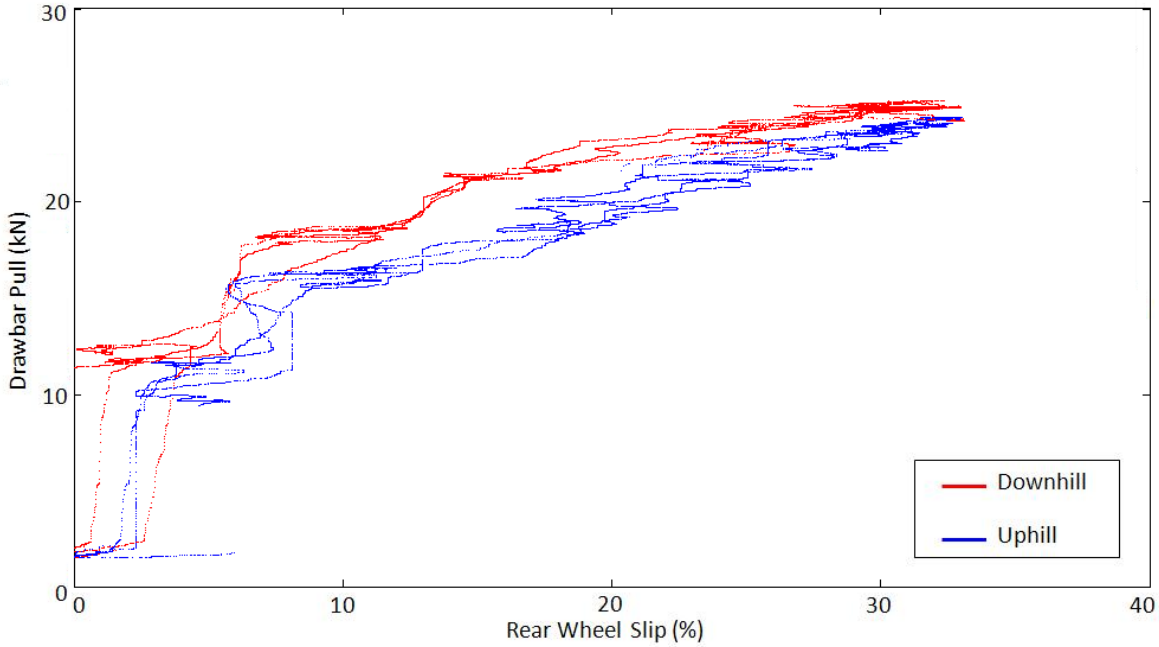

Figure 4.2.1: The effect of gradient on the slip-pull curve, operating at +2% lead on the sandy test site; three replicates in each direction

4.2.3 The effect of direction of travel on the slip-pull curve

The clay test site had no significant gradient, however, for the sake of consistency the data from the clay site was initially treated in the same way as that from the sandy site. Figure 4.2.2 shows the slip-pull curves for six runs on the clay site.

It is apparent from Figure 4.2.2 that the distinct grouping of runs seen on the sandy site was absent on the clay site. However, statistical analysis (Appendix 4.8) indicates that there is a small (204 N) but statistically

significant (p=<0.001) difference between the average maximum drawbar pulls recorded running in both directions. The average maximum drawbar pull running at +2% lead to the South was 27.56 kN, and to the North 27.50 kN. Given that there is no direction effect in the clay data, the North and South runs will be treated as a single data set from here on.

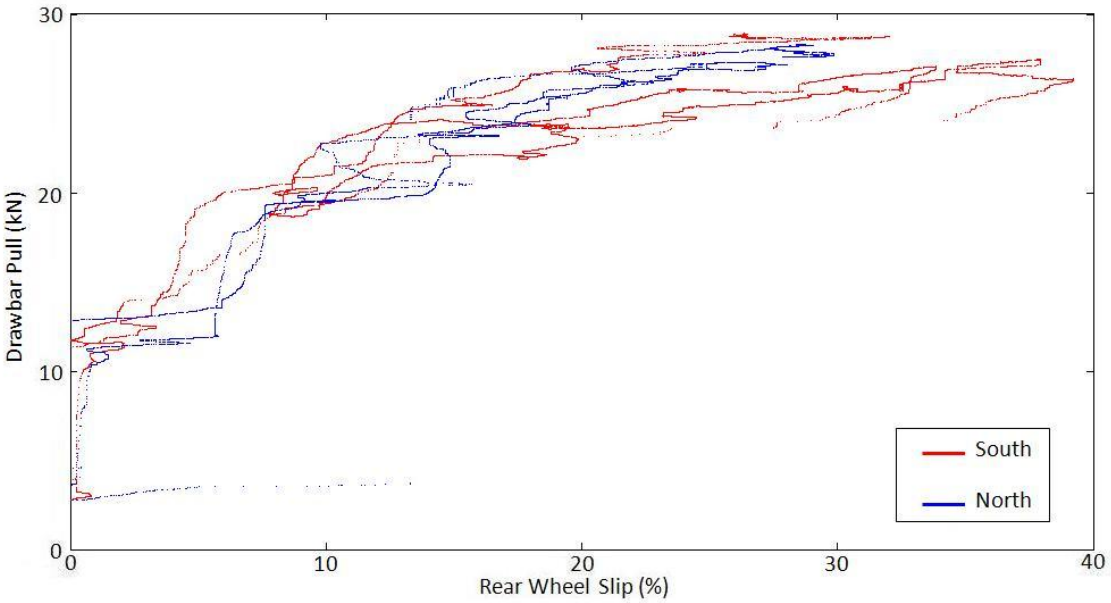

Figure 4.2.2: The effect of direction of travel on the slip-pull curve, operating at +2% lead on clay; three replicates in each direction

4.2.4 The effect of lead ratio on the slip-pull curve

Figures 4.2.3 and 4.2.4 illustrate the effect of lead ratio on the relationship between rear wheel slip and drawbar pull when operating downhill and uphill respectively on the sandy test site. To aid clarity curves with the form:

$$Y = A(1 - e^{-\frac{1}{b}X})$$

were manually fitted to the slip-pull data using the method outlined by Van De Vegte (1994) in which an initial approximation of the peak of the raw data is found and used as *'A'*. *'b'* is then made equal to the value of *'x'* that corresponds to 63% of *'A'*. *Values of 'A'* and *'b'* were then systematically

tested until a maximum R^2 value for each data set was found (Appendices 4.13.1 – 4.13.3). The purpose of this exercise was to find curves of a form that permitted the lead cases tested to be easily compared; the significance of the values of A, b and x found were not considered beyond the effect they had on values of R^2. The form and magnitudes of the relationships shown are in agreement with those quoted by Wismer (1982), citing Wismer and Luth (1972).

Table 4.2.1 shows the average maximum drawbar pull achieved by the TS90 on both the clay and sandy test sites at each of the three lead ratios tested. The figures quoted are an average of the one thousand highest data points in each of the replicates.

Table 4.2.1 indicates that the variation in drawbar pull caused by lead ratio is less on the sandy surface (1.1 kN) than on the clay surface (2.4 kN). On average operating on the clay surface produces 1.1 kN more drawbar pull than the sandy surface, although drawbar pull is not higher in every case on clay.

Table 4.2.1: Average maximum drawbar pull on the clay and sandy test sites

Lead ratio	**-4%**	**+2%**	**+10%**	**Average**
Av Max DBP Sand Uphill	24.8 kN	24.0 kN	24.5 kN	**24.4 kN**
Av Max DBP Sand Downhill	26.1 kN	24.6 kN	24.9 kN	**25.2 kN**
Av Max DBP Sand Total	**25.4 kN**	**24.3 kN**	**24.7 kN**	**24.8 kN**
Av Max DBP Clay Total	**25.1 kN**	**27.5 kN**	**25.1 kN**	**25.9 kN**

Operating on the sandy site -4% lead produced the highest drawbar pull (25.4 kN, p=<0.001), while on clay +2% lead produced the most (27.5 kN, p=<0.001).

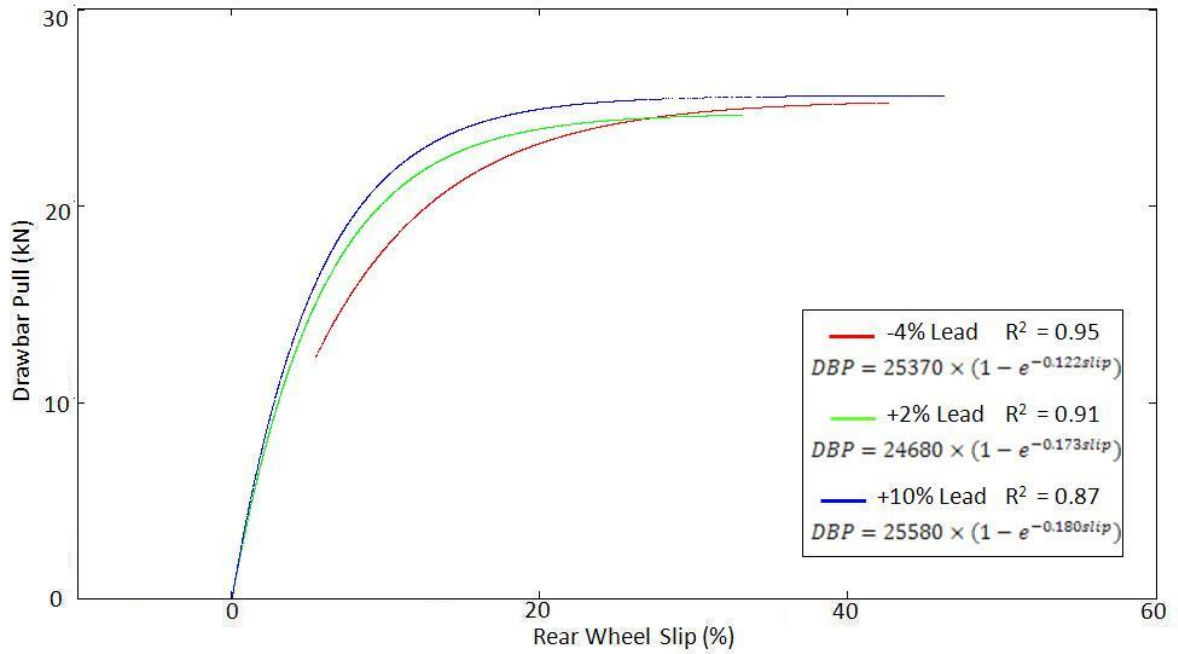

Figure 4.2.3: The effect of lead ratio on the slip-pull curve, operating downhill on the sandy test site (Appendix 4.13.2)

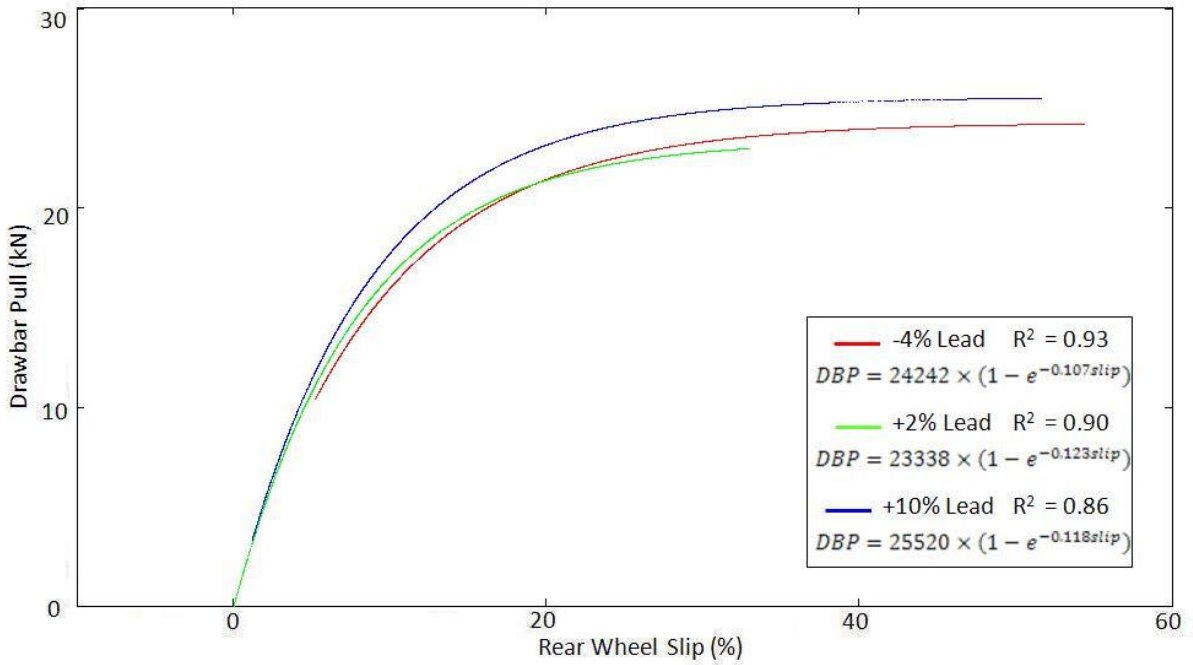

Figure 4.2.4: The effect of lead ratio on the slip-pull curve, operating uphill on the sandy test site (Appendix 4.13.1)

Figure 4.2.5 illustrates the relationship between rear wheel slip and drawbar pull when operating on the clay test site. At +2% lead, the relationship

between slip and the pull-weight ratio are in agreement with Wismer (1982), citing Zoz (1970). Unlike the results from the sandy test site, there is a clearer distinction between the three lead treatments. In the band between 0% and 30% rear wheel slip, the -4% lead case produces less drawbar pull, for a given slip, than either of the positive cases. This effect may be due to the retarding force of the slower moving front wheels. On the much less cohesive sandy surface the front wheels may be able to push forward through the soil, this force being balanced, as Dwyer *et al* (1977) observed, by the reduced rolling resistance and higher soil strength encountered by the rear wheels running in the ruts created by the front wheels. On clay the front wheels cause much less remoulding of the surface, producing no visible rut and thus negating Dwyer *et al*'*s* (1977) multi-pass effect, and also produce more mechanical interaction between tyre-cleat and soil, thus developing more negative thrust.

The +10% lead case initially produces more drawbar pull, replicating the effect of front wheel thrust seen in the sandy results. However, from 2% rear wheel slip onwards the +2% lead case produces more drawbar pull than either of the other two. This finding is in agreement with Wong (1970 and 2001) and Wong *et al* (1998, 1999 and 2000).

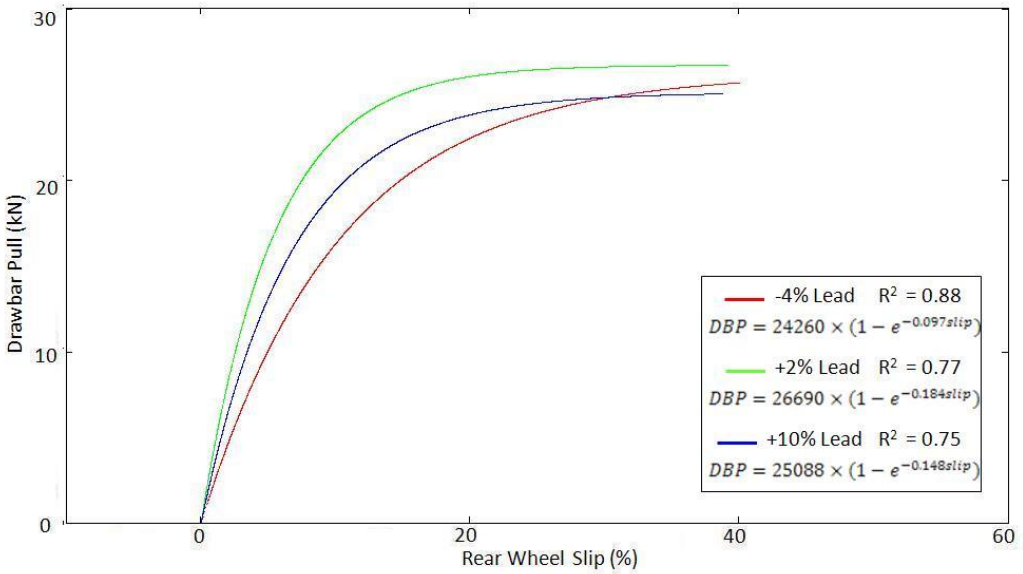

Figure 4.2.5: The effect of lead ratio on the slip-pull curve on clay (Appendix 4.13.3)

4.2.5 The effect of lead ratio on the relationship between power delivery efficiency and drawbar pull

Zoz *et al* (2002) described power delivery efficiency as the ratio of drawbar power to the corresponding power delivered by the engine. Power delivery efficiency was chosen here, in preference to the more commonly employed measure of tractive efficiency, the ratio of output power to the power delivered to a tractive device (Zoz *et al* 2002), since the phenomena under investigation involved the performance of the tractor as a whole rather than any single component. Table 4.2.2 shows the average maximum power delivery efficiency achieved by the TS90 on both the clay and sandy test sites at each of the three lead ratios tested. The figures quoted are an average of the one thousand highest data points in each of the replicates.

Table 4.2.2: Average maximum power delivery efficiencies

Lead ratio	**-4%**	**+2%**	**+10%**	**Average**
Av Max Power Delivery Efficiency Sand Uphill	51.1% @16.5 kN	47.4% @17.7 kN	48.2% @16.5 kN	48.9% @16.9 kN
Av Max Power Delivery Efficiency Sand Downhill	60.7% @18.6 kN	58.1% @17.1 kN	58.8% @17.3 kN	59.2% @17.7 kN
Av Max Power Delivery Efficiency Sand Total	55.9% @17.55 kN	52.7% @17.4 kN	53.5% @16.9 kN	54.1% @17.3 kN
Av Max Power Delivery Efficiency Clay Total	52.5% @20.3 kN	56.2% @19.5 kN	51.3% @19.6 kN	53.3% @19.8 kN

The results shown in Table 4.2.2 and Figures 4.2.6 and 4.2.7 mirror those for drawbar pull shown in Table 4.2.1, i.e. power delivery efficiency and drawbar pull are linked in these results. Second order polynomial curves were fitted to the data to ease interpretation; the raw data is shown in Appendices 4.13.4 and 4.13.5. The first point to note is that the lead ratio that achieved the highest power delivery efficiency was different on each surface; on the sandy site the -4% lead case achieved the highest power delivery efficiency (55.9%, p=<0.001), while on clay the +2% lead case was highest (56.2%, p=<0.001). It should also be noted that the average power delivery efficiency of the three lead ratios tested was lower on the clay than on the sand, even though the equivalent drawbar pull results were higher. This would seem to be related to the increased sensitivity of the tractor's power delivery efficiency to lead ratio when operating on clay, i.e. operating at a sub-optimal lead ratio was more damaging to efficiency on a strong clay soil than it was on a weaker sandy soil, perhaps as a result of power re-circulation, as noted by Brenninger (1999), i.e. on a stronger soil more torque wind-up can develop before being dissipated by wheel slip. A higher degree of torque wind-up will result in a higher degree of power re-circulation, a proportion of

which will be dissipated in the transmission in the form of heat. This finding would seem to be consistent with the power loss data shown in Section 4.3.6.

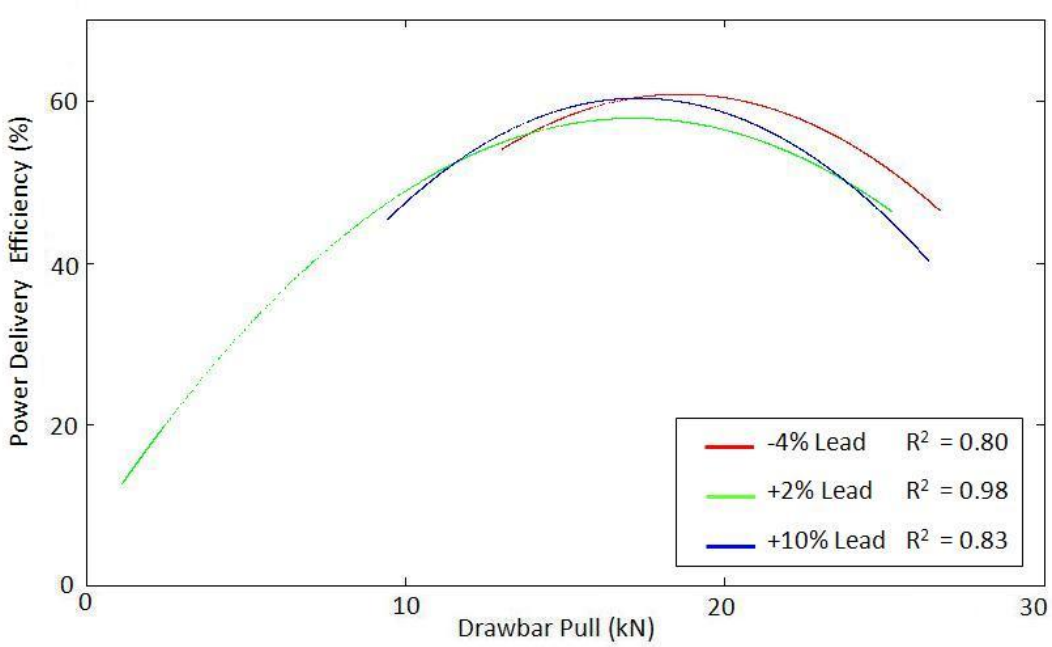

Figure 4.2.6: The effect of lead ratio on the relationship between power delivery efficiency and drawbar pull, operating downhill on the sandy test site (Appendix 4.13.5)

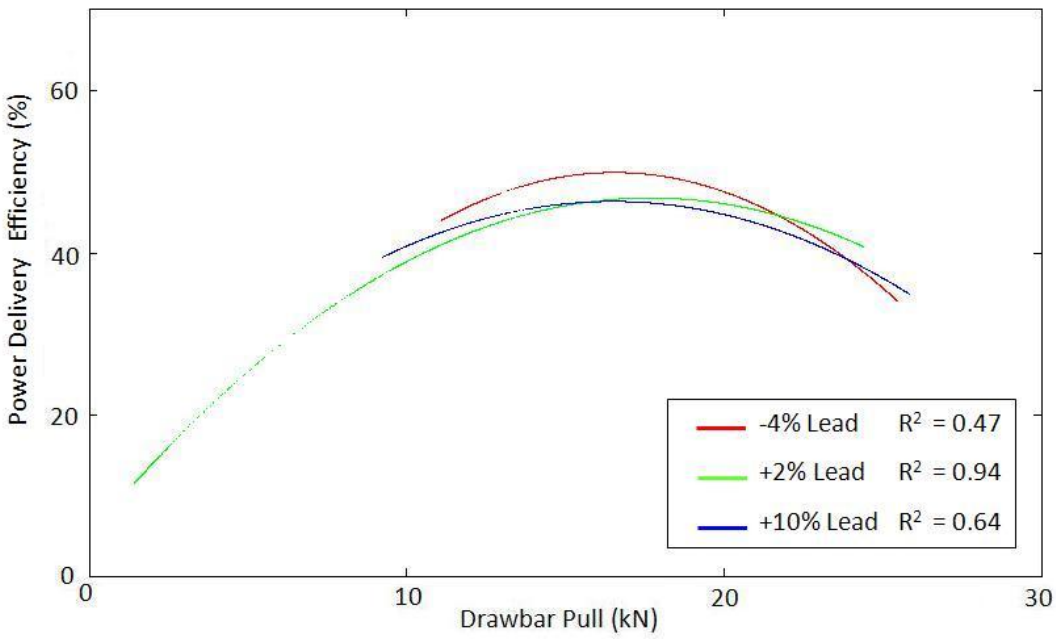

Figure 4.2.7: The effect of lead ratio on the relationship between power delivery efficiency and drawbar pull, operating uphill on the sandy test site (Appendix 4.13.4)

It is apparent from Table 4.2.2 that the 1° gradient of the sandy test site has a large and statistically significant (10.3%, p=<0.001) effect on the power delivery efficiency of the tractor. This effect is actually far more significant than the effect of varying the lead ratio (3.2%, p=<0.001). However, varying lead ratio does have an impact on the efficiency of the tractor. Paradoxically the effect of lead ratio on power delivery efficiency seems to be reversed on the sandy test site, with a deviation away from zero in either direction producing elevated power delivery efficiency. This finding directly contradicts those of Wong (1970 and 2001) and Wong *et al* (1998, 1999 and 2000), that a 0% lead ratio produces the highest efficiency.

Figure 4.2.8 illustrates the effect of lead ratio on the relationship between power delivery efficiency and drawbar pull when operating on the clay test site. Again, second order polynomial curves were fitted to the original data to aid clarity. The original data is shown in Appendix 4.13.6. The +2% lead case begins to demonstrate higher power delivery efficiency above 7 kN drawbar pull, and has a higher peak than either of the other two, reaching 56.2% (p=<0.001) at 19.5 kN drawbar pull.

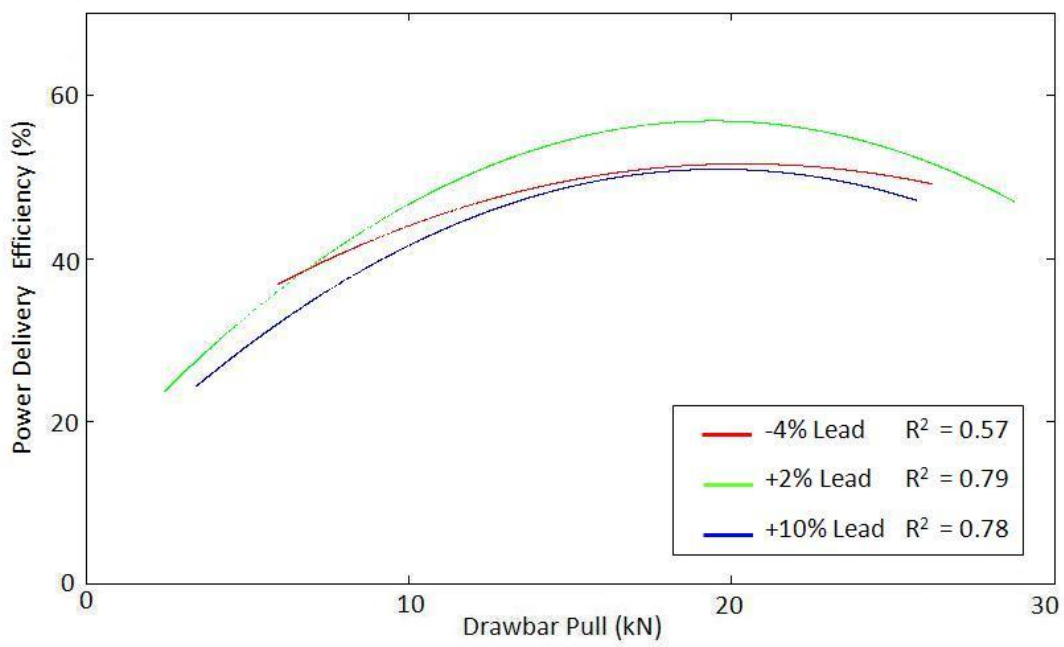

Figure 4.2.8: The effect of lead ratio on the relationship between power delivery efficiency and drawbar pull, operating to on the clay test site (Appendix 4.13.6)

4.2.6 The effect of lead ratio on the relationship between power delivery efficiency and rear wheel slip

Wheel slip has a negative impact on power delivery efficiency, since energy expended in generating slip cannot be used to produce drawbar pull or move the vehicle forward. The optimisation of power delivery efficiency must therefore be linked to the optimisation of slip performance. Table 4.2.3 shows the wheel slips associated with the maximum power delivery efficiencies under the range of conditions tested. The figures quoted are an average of the one thousand highest data points in each replicate.

Table 4.2.3: Wheel slip at average maximum power delivery efficiency

Lead ratio	**-4%**	**+2%**	**+10%**	**Average**
Av Max Power Delivery Efficiency Sand Uphill	51.1%	47.4%	48.2%	48.9%
Slip	@14.7%	@12.1%	@10.8%	@12.5%
Av Max Power Delivery Efficiency Sand Downhill	60.7%	58.1%	58.8%	59.2%
Slip	@12.2%	@8.7%	@9.2%	@10.0%
Av Max Power Delivery Efficiency Sand Total	55.9%	52.8%	53.5%	54.1%
Slip	@13.5%	@10.4%	@10.0%	@11.3%
Av Max Power Delivery Efficiency Clay Total	52.5%	56.2%	51.3%	53.3%
Slip	@21.4%	@12.4%	@15.7%	@16.5%

Consideration of Table 4.2.3 demonstrates that when operating on clay superior power delivery efficiency is associated with lower wheel slip. On the sandy test site, however, this effect is reversed, with higher power delivery efficiency being associated with elevated rear wheel slip. This is perhaps an indication that the energy expended in generating a given level of wheel slip is less on the weak sandy soil than it is on the stronger more cohesive clay.

To aid clarity curves with the form:

$$Y = A(1 - e^{-\frac{1}{b}X}) - dx$$

were manually fitted to the power delivery efficiency versus slip data using the method described in Section 4.2.4, with an additional variable *'d'* which was used to model the decay of power delivery efficiency with increasing wheel slip (Appendices 4.13.7 – 4.13.9). This approach did in some cases produce curves which had a low R^2 value; in the case of the +10% lead curve in Figure 4.2.9 (Appendix 4.13.8) this was the result of the fitted curve

reaching 0% power delivery efficiency at 0% wheel slip, as might be expected, while the raw data did not, since the zero slip condition, specified in Section 3.6.3 did not allow for the effective change in tyre rolling radius caused by wheel sinkage. In Figure 4.2.11 (Appendix 4.13.9) the R^2 values of all three lead cases were affected by the failure of the raw data to reach 0% power delivery efficiency and the greater variability of the power delivery efficiency data collected on clay.

Figures 4.2.9 and 4.2.10 illustrate the effect of lead ratio on the relationship between rear wheel slip and power delivery efficiency when operating on the sandy test site. The form and magnitudes of the curves shown in these figures are in agreement with Wulfsohn and Way (2009).

The curves shown in Figures 4.2.9 and 4.2.10 demonstrate that beyond the point of maximum power delivery efficiency there is a declining linear relationship between wheel slip and power delivery efficiency, indicating that there is a direct and negative relationship between slip and power delivery efficiency, i.e. increasing wheel slip absorbs increasing amounts of power which is lost in the form of surface remoulding and tyre carcass heating, but does not serve to increase drawbar power. This result conforms well to the models quoted by Inns and Kilgour (1978) and Wong (2001).

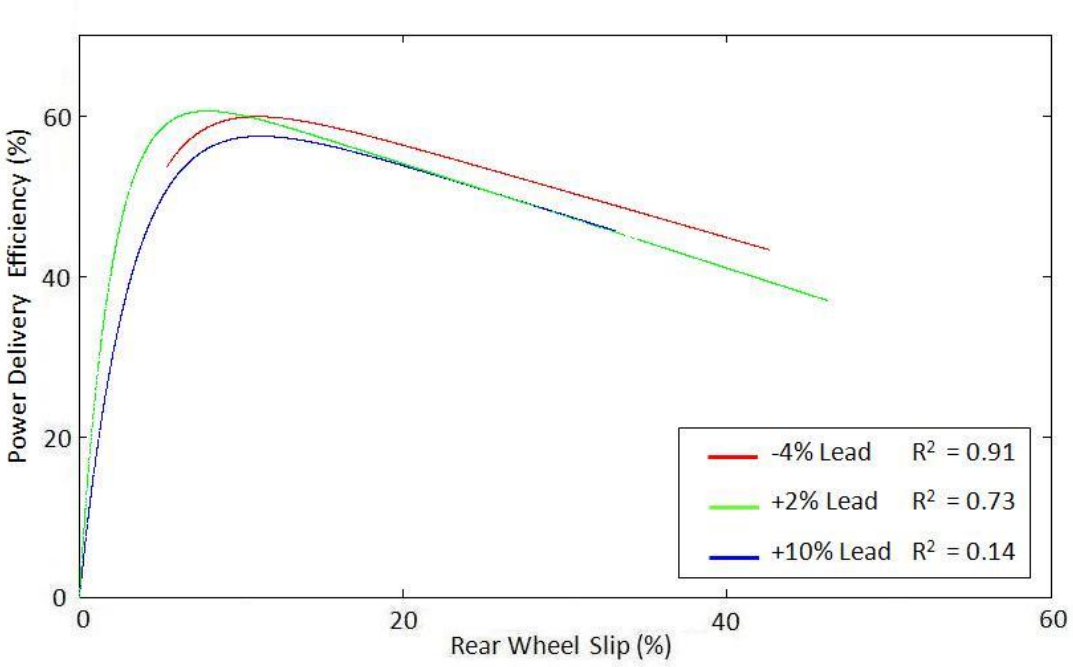

Figure 4.2.9: The effect of lead ratio on the relationship between power delivery efficiency and rear wheel slip, operating downhill on the sandy test site (Appendix 4.13.8)

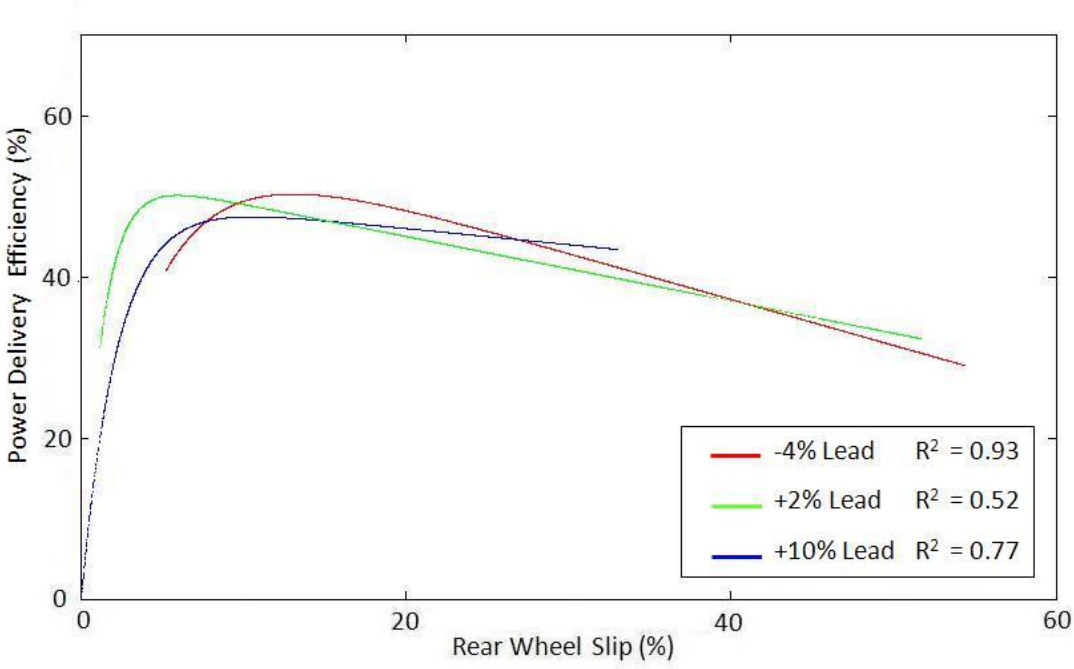

Figure 4.2.10: The effect of lead ratio on the relationship between power delivery efficiency and rear wheel slip, operating uphill on the sandy test site (Appendix 4.13.7)

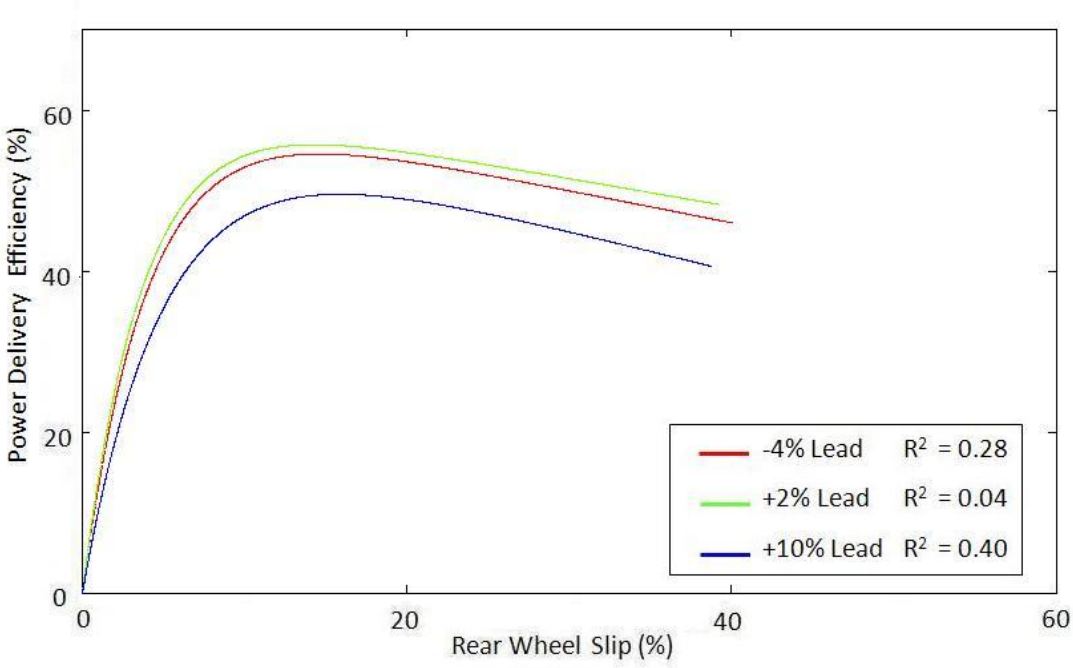

Figure 4.2.11: The effect of lead ratio on the relationship between power delivery efficiency and rear wheel slip, operating on clay (Appendix 4.13.9)

4.2.7 The effect of lead ratio on the relationship between engine power, drawbar power and forward speed

Table 4.2.4 shows the engine power, drawbar pull and forward speed at the maximum drawbar power produced. This table is intended to demonstrate how speed and drawbar pull combine to effect the tractive performance of the TS90.

The first interesting facet of Table 4.2.4 is the relationship between drawbar power and engine power. As noted in sections 4.2.5 and 4.2.6 the average power delivery efficiency of the TS90 was higher on the sandy test site than it was on the clay test site. This might be interpreted as an indication that the drawbar power produced on the sandy test site was higher than on the clay site. This was not actually the case, but while the tractor produced more drawbar power on clay (31.9 kW) than on sand (30.4 kW) it also expended more engine power in the process, 61.9 kW on clay compared to 59.3 kW on

the sandy site. Figures 4.2.12, 4.2.13 and 4.2.14 illustrate the effect of lead ratio on the relationships between drawbar power, engine power, forward speed and drawbar pull. Third order polynomial equations have been fitted to these data to improve their clarity. These graphs help to highlight the fact that power delivery efficiency is the product of the relationship between all these components. Figures 4.2.12, 4.2.13 and 4.2.14 all exhibit common trends, increasing drawbar pull is associated with increasing engine power and decreasing forward speed, as increasing levels of slip develop. Declining forward speed results in a reduction in drawbar power, as drawbar pull is maintained but forward speed is exchanged for increasing levels of wheel slip. Having reached a peak, engine power declines as the increasing torque demand associated with increasing slip pulls the engine speed down.

On the sandy test site the -4% case produced the both the highest power delivery efficiency (55.9%, compared to +2%=52.7% and +10%=53.5%, p=<0.001, Appendix 4.1) and drawbar power (31.2 kW, compared to +2%=30.0 kW and +10%=30.8 kW, p=0.001 Appendix 4.3). Examination of Figures 4.2.12 and 4.2.13 indicate that this elevation in performance was the result of a higher forward speed for a given drawbar pull, compared to the other two lead cases. At the point of maximum drawbar power, the -4% lead case also had the lowest engine power of the three cases tested (p=<0.001). It should be borne in mind that the power delivered by the engine is the result of both throttle setting and reacted load. Thus while the engine was given the same command for each run, the level of resistance to motion varied depending on rolling resistance and wind up. It is apparent from Figures 4.2.12 and 4.2.13 that the point of maximum drawbar power does not

coincide with either maximum forward speed or maximum drawbar pull, or indeed maximum engine power.

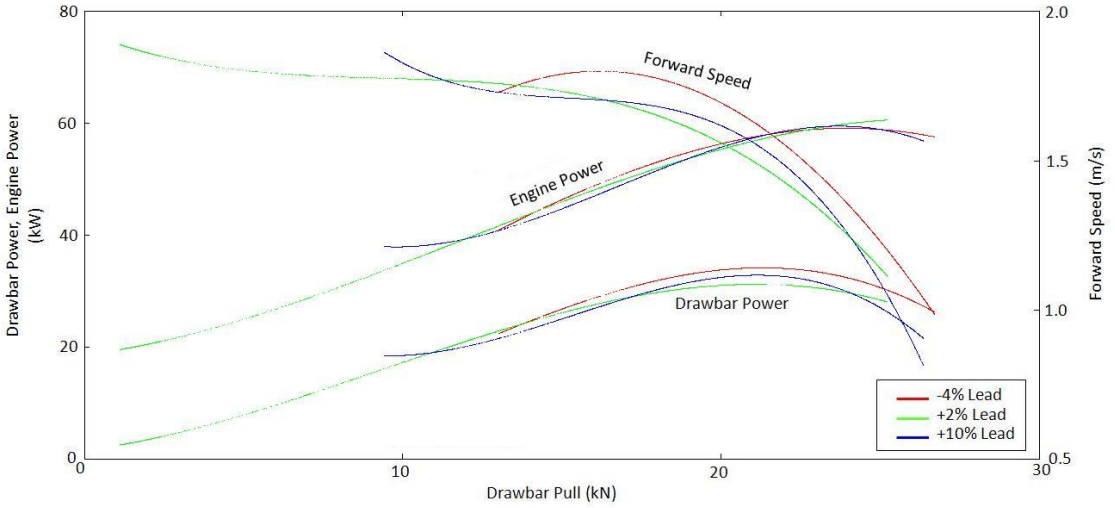

Figure 4.2.12: The effect of lead ratio on the relationship between drawbar power, engine power, forward speed and drawbar pull, operating downhill on the sandy test site (Appendix 4.13.14 and 4.13.17)

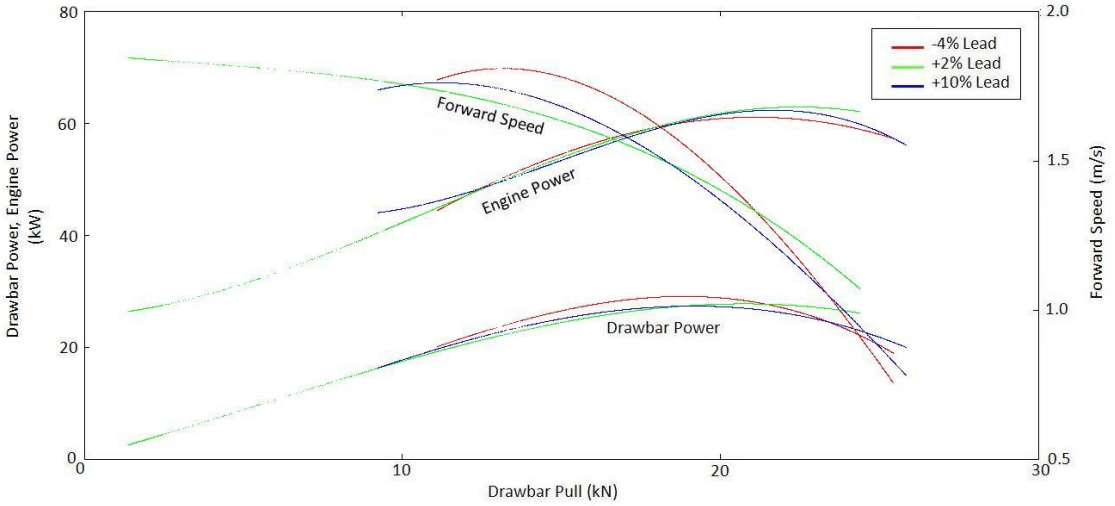

Figure 4.2.13: The effect of lead ratio on the relationship between drawbar power, engine power, forward speed and drawbar pull, operating uphill on the sandy test site (Appendix 4.13.13 and 4.13.16)

Table 4.2.4: Engine power, drawbar pull and forward speed at maximum drawbar power.

Lead ratio	**-4%**	**+2%**	**+10%**	**Average**
Uphill on sand				
Drawbar Power (kW)	29.1	27.8	27.4	**28.1**
Engine power (kW)	60.2	62.4	60.8	**61.1**
DBP (kN)	18.9	20.8	19.2	**19.6**
Speed (m/s)	1.66	1.17	1.02	**1.28**
Downhill on sand				
Drawbar Power (kW)	34.2	31.2	32.9	**32.8**
Engine power (kW)	57.8	56.9	57.6	**57.4**
DBP (kN)	21.3	21.1	21.2	**21.2**
Speed (m/s)	1.88	1.43	1.68	**1.66**
Average on sand				
Drawbar Power (kW)	**31.7**	**29.5**	**30.2**	**30.4**
Engine power (kW)	**59.0**	**59.7**	**59.2**	**59.3**
DBP (kN)	**20.1**	**21.0**	**20.2**	**20.4**
Speed (m/s)	**1.77**	**1.30**	**1.35**	**1.47**
Clay				
Drawbar Power (kW)	**31.5**	**32.8**	**31.3**	**31.9**
Engine power (kW)	**61.9**	**61.3**	**62.4**	**61.9**
DBP (kN)	**22.1**	**23.7**	**22.0**	**22.6**
Speed (m/s)	**1.72**	**1.87**	**1.70**	**1.76**

In Figure 4.2.14 it is apparent that the power-speed-pull relationship is rather different to that seen on the sandy test site. Here it is clear that maximum power delivery efficiency is achieved, not through elevating the drawbar power, but rather by reducing the engine power employed in producing a given level of output.

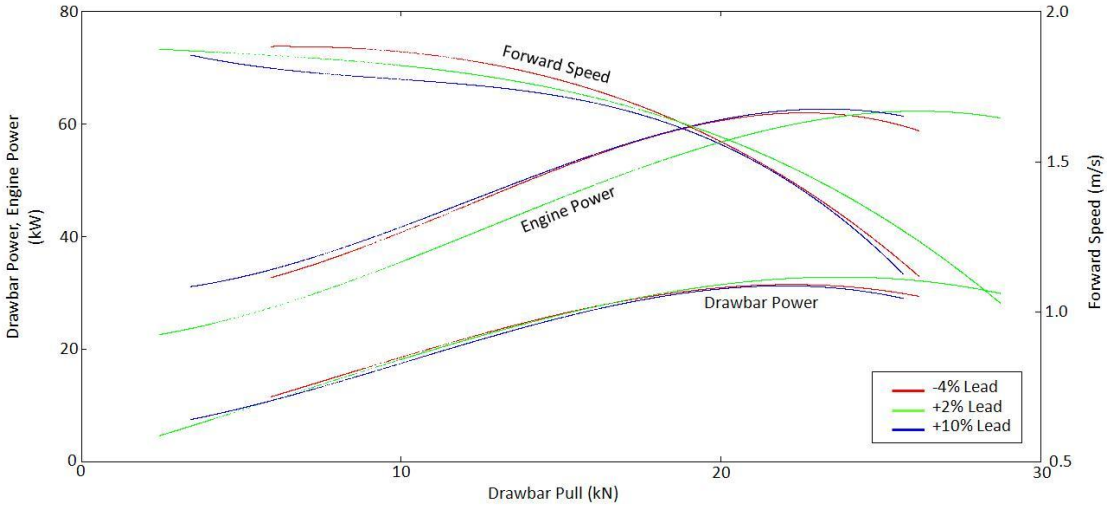

Figure 4.2.14: The effect of lead ratio on the relationship between drawbar power, engine power, forward speed and drawbar pull operating on clay (Appendix 4.13.15 and 4.13.18)

4.2.8 Conclusions

The results show that the data acquisition system is capable of distinguishing between relatively minor changes in operating conditions, and producing repeatable data (Figures 4.2.1 and 4.2.2 and Appendices 4.1 to 4.8).

Lead ratio was observed to have a stronger effect on power delivery efficiency when running on the clay soil (Figure 4.2.11) (max 56.2% @ +2% lead ratio, min 51.3% @ +10% lead ratio, p=<0.001, Appendix 4.5) than on

the sandy soil (Figures 4.2.9 and 4.2.10) (max 55.9% @ -4% lead ratio, min 52.7% @ +2% lead ratio, p=<0.001, Appendix 4.1). While perhaps not directly comparable, these results would seem to disagree with those of Rosa *et al* (2000) who noted a difference of less than 0.015% in the tractive efficiency of an orchard tractor operated in positive and negative lead modes.

The optimum lead ratio for both maximum drawbar pull (Table 4.2.1 and Figures 4.2.3 – 4.2.5) and power delivery efficiency (Table 4.2.2 and Figures 4.2.6 – 4.2.8) was a function of soil type, with -4% lead being highest on the sandy soil (Drawbar power = 31.2 kW, power delivery efficiency= 55.9%), but +2% lead ratio being highest on the clay test site (drawbar power = 34.3 kW, power delivery efficiency = 56.2%).

On the clay soil, divergence in either direction from a 0% lead ratio was observed to have a negative effect on drawbar pull. This result was reversed on the sandy test site.

On the clay soil a greater power delivery efficiency was associated with a reduction in wheel slip and a reduction in engine power for a given level of drawbar power, while on the sandy soil higher power delivery efficiency was associated with an increase in forward speed at a given drawbar pull and an increase in wheel slip (Figures 4.2.12 – 4.2.14).

4.3 Torque and Power Flow

4.3.1 Introduction

Section 4.2 concluded with an analysis of the relationships between engine power, drawbar power and forward speed. In this section that analysis is extended to include the relative contributions of the front and rear axles to the transmission of power from engine to drawbar.

This chapter examines the way in which lead ratio effects the flow of torque and power from the engine to the drawbar. Section 4.3.2 examines the effect of direction of travel on the relationship between drawbar pull and the torque transmitted by the front and rear axles. In Section 4.3.2 the behaviour of the front axle is shown to differ significantly from that of the rear, and from what might have been assumed. This phenomenon is examined in greater detail in the following sections.

The effect of lead on the torque response to drawbar pull of the front and rear axles is considered in Section 4.3.3. Section 4.3.4 examines the relative contributions of the front and rear axles to the overall power output of the tractor, and the relationship between axle powers and drawbar power. While Section 4.3.5 deals the overall cascade of power from engine to axles to drawbar, and offers some insight into the efficiencies of the tractor.

4.3.2 The effect of direction of travel on the relationship between axle torque and drawbar pull

For the purposes of this analysis, the torque measured at the gearbox output shafts was multiplied by the fixed speed ratios of the axles (front 26.2, rear 32.37) to give torque at the wheel hubs. This method is intended to normalise the data between the front and rear axles, thus allowing easier comparisons to be made between axles. This method does not, however, compensate for frictional losses within the axles and driveline downstream of the output shafts. Thus the figures quoted are idealised, and assume zero torque losses in the axles.

In Section 4.2 it was noted that the gradient of the sandy test site has a measurable influence on the drawbar performance of the tractor. Figure 4.3.1 shows a plot of axle torque against drawbar pull when travelling up and down the sandy test site, at +2% lead. The magnitude of the torque transmitted by the rear axle is influenced by the gradient of the site. This is reflected in the difference between the intercepts of the uphill (1.203 kNm) and downhill (-0.881 kNm) traces. This represents the difference in the static forces acting on the tractor, i.e. running downhill the machine will move forward due to gravity, hence the negative intercept, while running uphill the situation is reversed. Based on the static force due to gradient the torque at the rear axle due to gradient is +/-0.606 kNm.

The response of the rear axle torque to increasing drawbar pull is similar up (0.793Nm/N) and downhill (0.780Nm/N). This appears to be logical, since gradient applies a constant force, either positive or negative, to the tractor, and thus should have no effect on the response of the axle's torque to increasing drawbar pull. The torque required for a given drawbar pull will of

course vary by the magnitude of the intercept, which is the static torque due to gradient. The magnitude and response of the torque transmitted by the front axle, however, is unaffected by gradient.

Figure 4.3.2 illustrates the effect of direction of travel on the relationship between drawbar pull and axle torque when travelling to the North and South on the clay test site. It was noted in Section 4.2 that direction of travel does not affect drawbar performance on the clay test site, and that finding is repeated here.

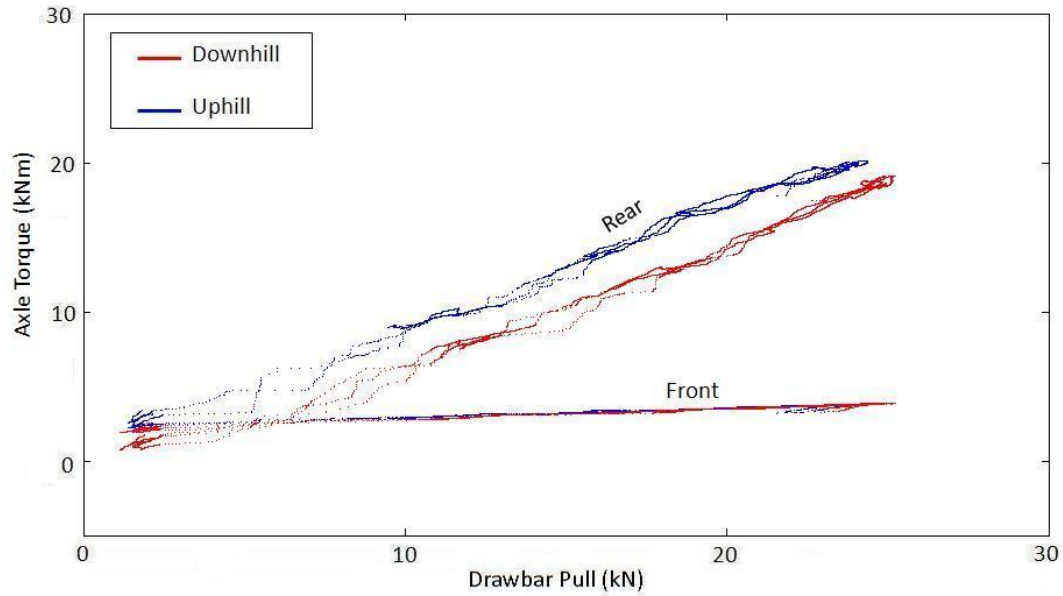

Figure 4.3.1: The effect of gradient on the relationship between front and rear axle torques and drawbar pull at +2% lead on the sandy test site; three replicates in each direction

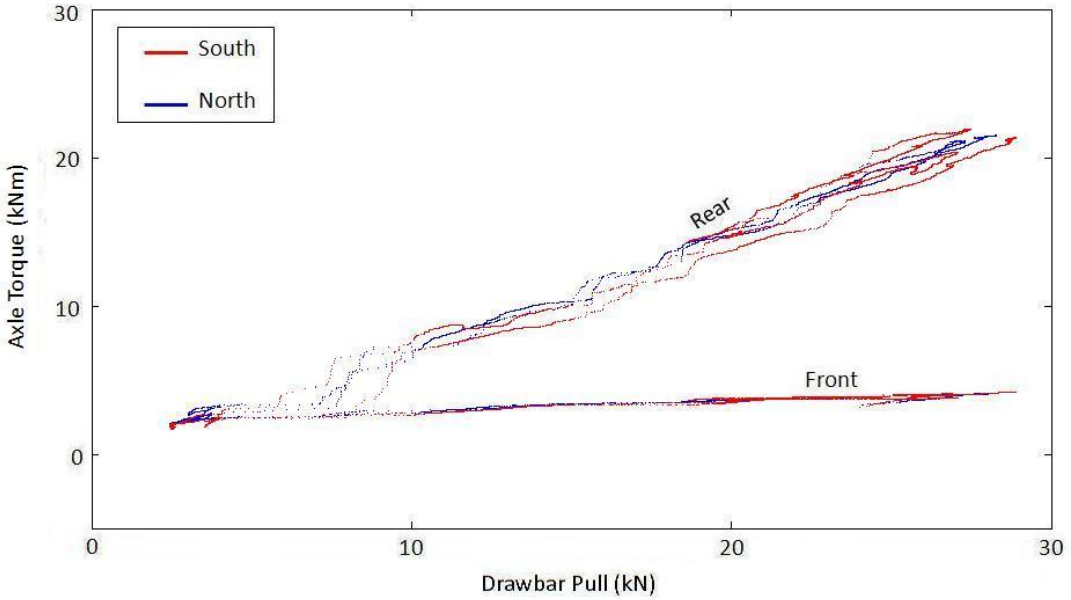

Figure 4.3.2: The effect of direction of travel on the relationship between front and rear axle torques and drawbar pull at +2% lead on the clay test site; three replicates in each direction

4.3.3 The effect of lead ratio on the relationship between drawbar pull and axle torque

The data collected exhibit a linear relationship between drawbar pull and front and rear axle torques, i.e. the combined torque transmitted by both wheels on the axle. Automated linear regression using the *least squares fit* method was carried out on this data using the *Linfit* function in *MathCAD* to fit equations with the form y = mx + c (Figure 4.3.3, 4.3.4, 4.3.5 and appendix 4.13.10, 4.13.11 and 4.13.12). The slopes and intercepts of the resulting lines are shown in Table 4.3.1. While increasing drawbar pull has a significant effect on the torque transmitted by the rear axle (slopes > 0.7 Nm/N), it has little effect on the front axle torque (slopes < 0.12 Nm/N). This result is counterintuitive, since it would seem reasonable to anticipate that the contribution of the front axle to overall thrust, and thus axle torque, would increase proportionally with increasing drawbar pull. This phenomenon may be the result of dynamic weight transfer between the axles as the drawbar pull increases. Since the drawbar is set 0.6m above the ground, the horizontal pull at the drawbar produces a significant moment about the rear contact patch, which causes the front of the tractor to unload progressively (0.25 kN for each 1 kN of drawbar pull). The weight lost from the front axle is transferred to the rear, thus magnifying the difference between the responses of the two axles.

Lead ratio has a statistically significant effect on the slope of response of both the front and rear axle torques on clay (p=<0.001, Appendix 4.11 and Appendix 4.12 respectively), and only the front axle torque on sand (p=<0.001, Appendix 4.9) (rear axle p=0.124, Appendix 4.10), although there is a difference in mean rear axle slope between the three lead ratios (-4% =

0.9530, +2% = 0.7853, +10% = 0.8967, LSD=0.1664). This result is repeated in the intercepts of the axle torque versus drawbar pull graphs (Table 4.3.1).

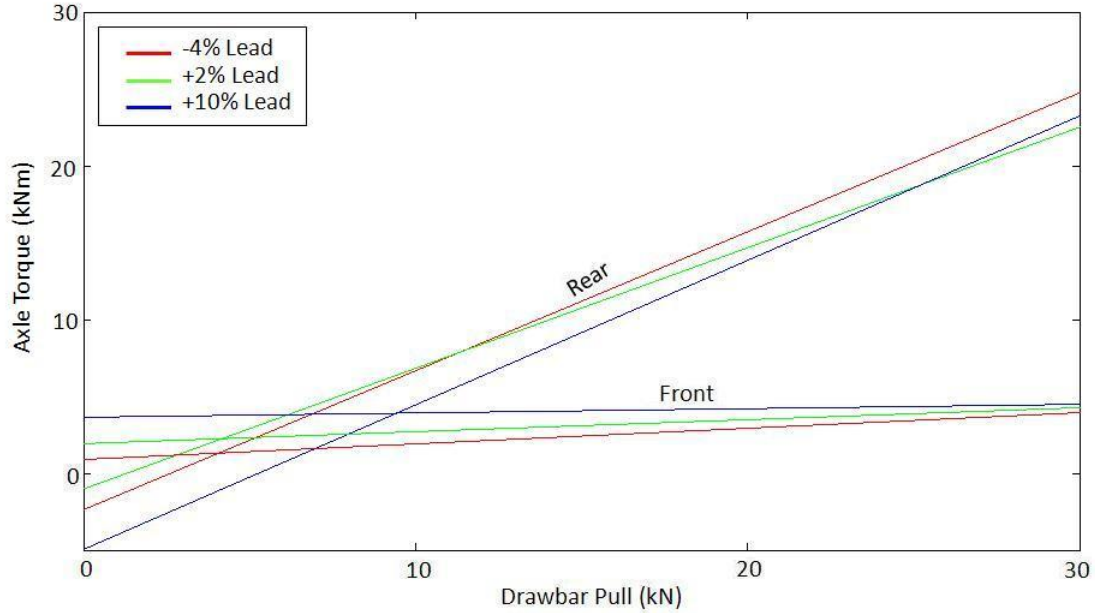

Figure 4.3.3: The effect of lead on the relationship between drawbar pull and front and rear axle torques, operating downhill on sand

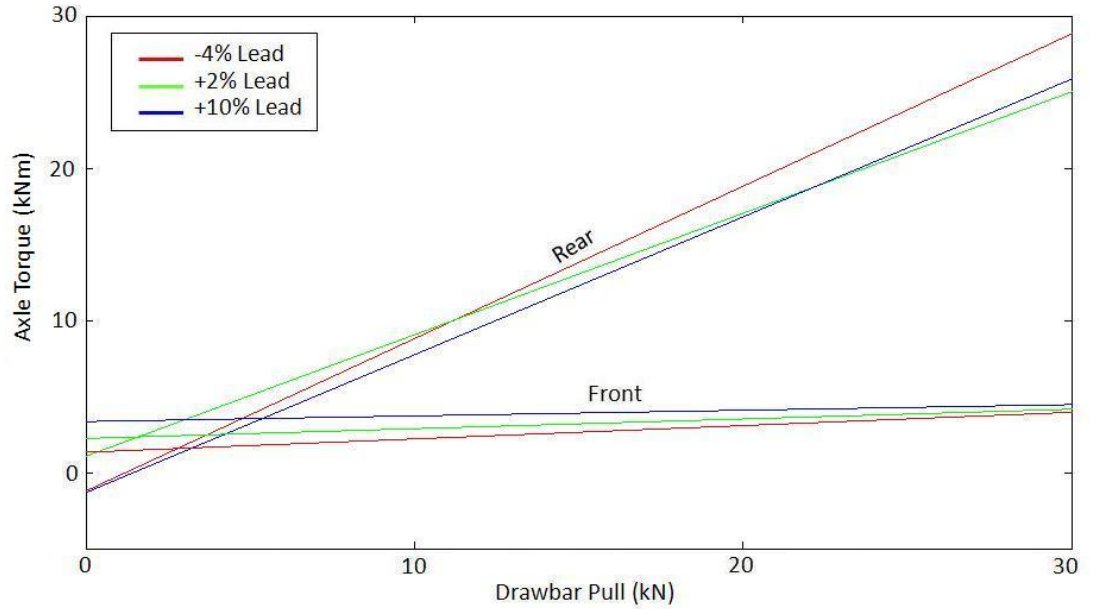

Figure 4.3.4: The effect of lead on the relationship between drawbar pull and front and rear axle torques, operating uphill on sand

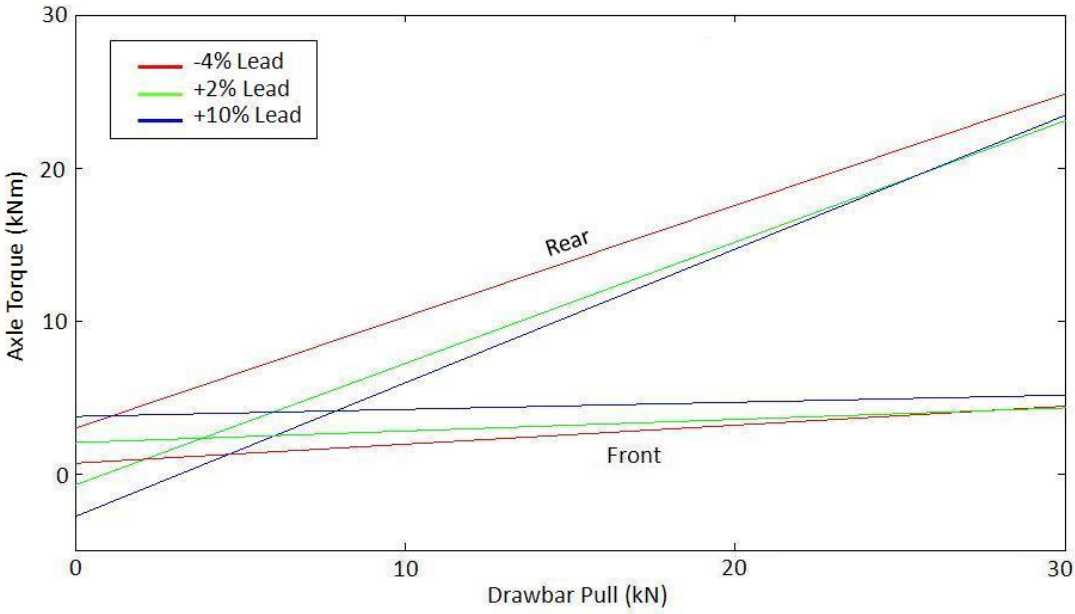

Figure 4.3.5: The effect of lead on the relationship between drawbar and pull front rear axle torques and operating on clay

Table 4.3.1: The slopes and intercepts of the Drawbar Pull v Axle Torque graphs shown in Figures 4.3.3, 4.3.4 and 4.3.5

Slope			Intercept		
	Sand Uphill			**Sand Uphill**	
Lead	**Front**	**Rear**	**Lead**	**Front**	**Rear**
-4%	0.084 Nm/N	0.933 Nm/N	**-4%**	1451 Nm	284 Nm
2%	0.063 Nm/N	0.793 Nm/N	**2%**	2292 Nm	1203 Nm
10%	0.031 Nm/N	0.89 Nm/N	**10%**	3508 Nm	959 Nm
	Sand Downhill			**Sand Downhill**	
Lead	**Front**	**Rear**	**Lead**	**Front**	**Rear**
-4%	0.093 Nm/N	0.874 Nm/N	**-4%**	1126 Nm	1621 Nm
2%	0.077 Nm/N	0.78 Nm/N	**2%**	1981 Nm	-881 Nm
10%	0.022 Nm/N	0.926 Nm/N	**10%**	3805 Nm	-4607 Nm
	Clay			**Clay**	
Lead	**Front**	**Rear**	**Lead**	**Front**	**Rear**
-4%	0.12 Nm/N	0.72 Nm/N	**-4%**	806 Nm	3206 Nm
2%	0.073 Nm/N	0.783 Nm/N	**2%**	2129 Nm	-462 Nm
10%	0.025 Nm/N	0.868 Nm/N	**10%**	4190 Nm	-2633 Nm

4.3.3.1 On Sand

On sand, the behaviour of the axles is less clearly related to lead. There is still a characteristic difference in the response of the front and rear axles, the slope of the front axle traces being much shallower than the rear in all cases (Table 4.3.1). At zero drawbar pull, the front axle produces positive torque in all three lead cases, and in both directions of travel. The front axle traces are ordered in line with lead, the -4% lead case exhibiting both the steepest slope (average 0.089 Nm/N) and smallest intercept (average -1289 Nm), and the +10% lead case the shallowest slope (average 0.027 Nm/N) and biggest intercept (average 3657 Nm). These results reflect the relative contribution of the front axle, which increases with increasing lead.

The results for rear axle torque are rather less clearly defined, and are not ordered in line with lead. In both the up and downhill cases, the +2% lead case has a shallower slope (average 0.787 Nm/N) than either of the other two cases. Visual analysis of the -4% and +10% rear axle torque traces in Figure 4.3.3 indicates that, running downhill on sand, lead has an effect on the intercepts of the rear axle torque/drawbar pull lines, but does not affect the slope of the lines. In Figure 4.3.4, running uphill, the situation is reversed, with intercept unaffected, but slope changed. Analysis of the -4% and +10% data indicates that the slope of the rear axle torque/drawbar pull line lies within 4% of the average value for both cases, both up and downhill.

4.3.3.2 On Clay

Varying lead alters the relative contribution of the front and rear axles, as indicated by the intercepts of the graphs (Table 4.3.1). On clay the -4% lead case is the only one that exhibits positive torques on both axles at zero

drawbar pull (Figure 4.3.5). This is paradoxical, as it might be expected that a negative lead case would exhibit negative front axle torque at close to zero drawbar pull. In the positive lead cases, some drawbar pull is developed even when the rear axle torque is zero. In these cases the front axle actually draws the tractor forward, with the rear axle making either no contribution (+2% lead), or a negative contribution (+10% lead), i.e. the rear axle actually develops negative torque, and thus retards the vehicle. The -4% case has the shallowest rear axle slope (average 0.719Nm/N) and steepest front axle slope (average 0.121 Nm/N) of the three cases, while in the +10% lead case, the situation is reversed (rear 0.876 Nm/N, front 0.025 Nm/N). The rear axle trace of the -4% case is visibly separated from, and higher than the other two, indicating that the -4% lead case produces less drawbar pull for a given rear axle torque than the other two cases. However, it should be borne in mind that the rolling radius of the rear wheels in the -4% case were 50 mm larger than in the other two cases, and thus the torque required to produce a given thrust was 6.5% greater.

4.3.4 The effect of lead on the relationship between drawbar power and front and rear driveshaft powers

Figures 4.3.6, 4.3.7 and 4.3.8 illustrate the relationship between drawbar power and front and rear shaft powers, i.e. the power measured at the gearbox output shafts. In all cases the increase in power transmitted by the front axle for a given increase in drawbar power was less than that for the rear axle, i.e. the slope of the front shaft traces was flatter than that of the rear. The front shaft power traces exhibited a linear response to increasing

drawbar power, reflecting the torque results seen in Figures 4.3.3 – 4.3.5. In all cases front shaft power is ordered in line with lead ratio; increasing lead ratio producing higher front shaft power. However, increasing lead ratio also produces a reduction in the increase of front shaft power for a given increase in drawbar power. Front shaft power is limited to below 15 kW in all cases. This limit may be the result of the relationship between traction, imposed load on the front tyres and drawbar pull.

4.3.4.1 On Sand

The rear shaft power traces in Figures 4.3.6 and 4.3.7 are more clearly defined than the equivalent traces recorded on clay. It was noted in section 4.2 that the homogenous nature of the sandy surface produced data with a narrower tolerance band than the clay. Though more clearly defined, the response of the rear axle power is not linear throughout the whole drawbar power range. The rear axle power traces of all runs exhibit a distinctly hooked profile. This result is consistent with the slip-pull data presented in Section 4.2. Drawbar power increases up to a maximum level of around 40 kW. At that point the tractor reaches its tractive limit. Beyond that point, increasing shaft speed is simply lost in the form of slip, thus rear axle power remains constant, while drawbar power falls.

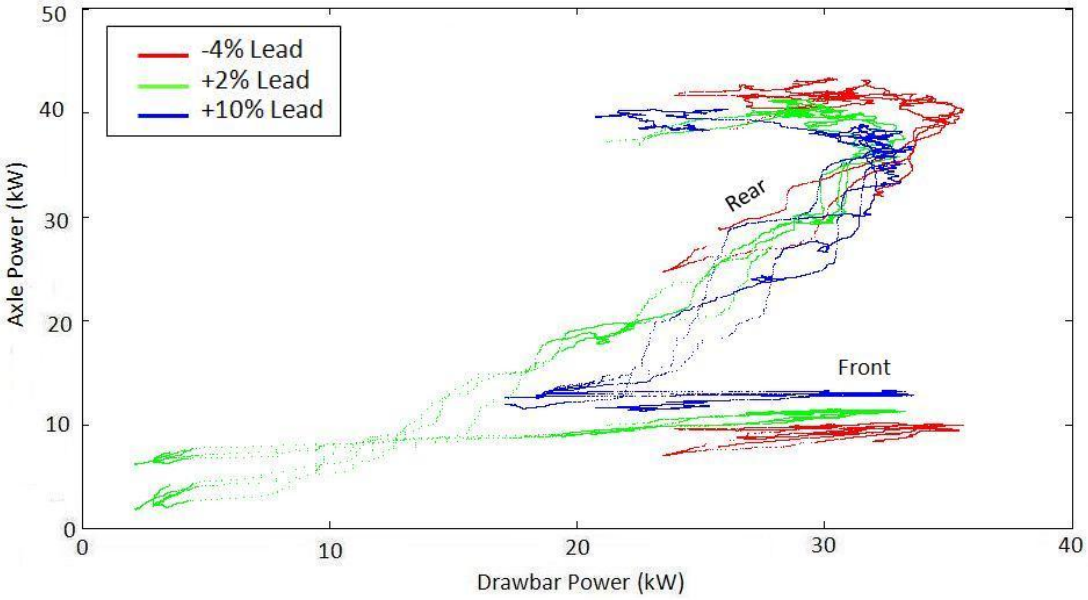

Figure 4.3.6: The effect of lead on the relationship between drawbar power and front and rear driveshaft powers operating downhill on sand; three replicates in each direction

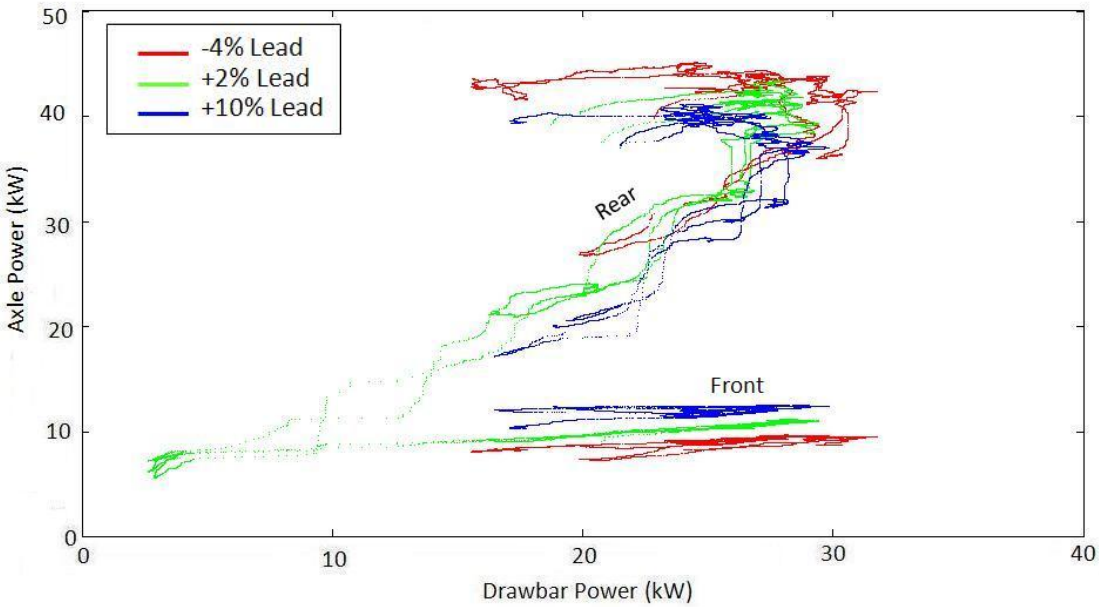

Figure 4.3.7: The effect of lead on the relationship between drawbar power and front and rear driveshaft powers operating uphill on sand; three replicates in each direction

4.3.4.2 On Clay

The rear shaft power data in Figure 4.3.8 is less clearly defined than the equivalent traces for the front. The general trend is that increasing drawbar power produces an equivalent increase in rear shaft power. However, some traces exhibit distinct flat spots, indicating that the relationship between rear axle power and drawbar power is not constant. Since the equivalent torque data does not exhibit this variability, the effect must be the result of the relationship between shaft speed and ground speed, i.e. the shape of these traces is affected by wheel slip.

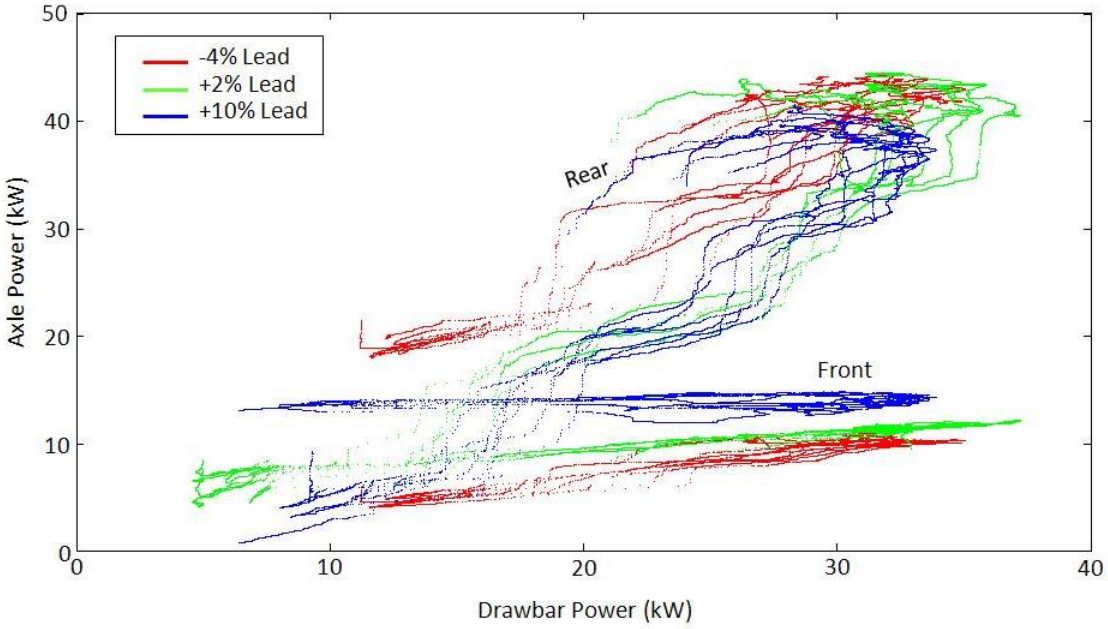

Figure 4.3.8: The effect of lead on the relationship between drawbar power and front and rear driveshaft powers operating to on clay; three replicates in each direction

4.3.5 The effect of lead ratio on the relationship between drawbar power, driveshaft power, engine power and drawbar pull

Figures 4.3.9, 4.3.10 and 4.3.11 provide an illustration of the power flowing within the tractor at the engine, gearbox output shafts and drawbar. The 'driveshaft power' traces represent the combined value of both front and rear shaft powers. For the sake of clarity, third order polynomial curves were fitted to the driveshaft, engine and drawbar power data (Appendices 4.13.13 – 4.13.15 and 4.13.19 – 4.13.21).

All the curves shown in Figures 4.3.9 – 4.3.11 exhibit a common form; initially increasing linearly with increasing drawbar pull, before reaching a maximum value beyond which they decline again. The primary influences on the form of these curves are the tractor's forward speed and engine speed; increasing drawbar pull giving rise to increasing slip and thus a reduction in drawbar power, while the increasing torque demand associated with increasing slip at a constant drawbar pull causes the engine speed to decrease, thus causing a reduction in engine power and an associated reduction in driveshaft power.

The peak in the drawbar power traces in all three figures indicates the point at which drawbar power becomes saturated; beyond the point at which maximum drawbar pull is reached, increasing engine and driveshaft power are lost as increasing slip. Comparison of the driveshaft power traces on clay and sand show that the peak is less pronounced, and at higher drawbar pull, on clay than on sand.

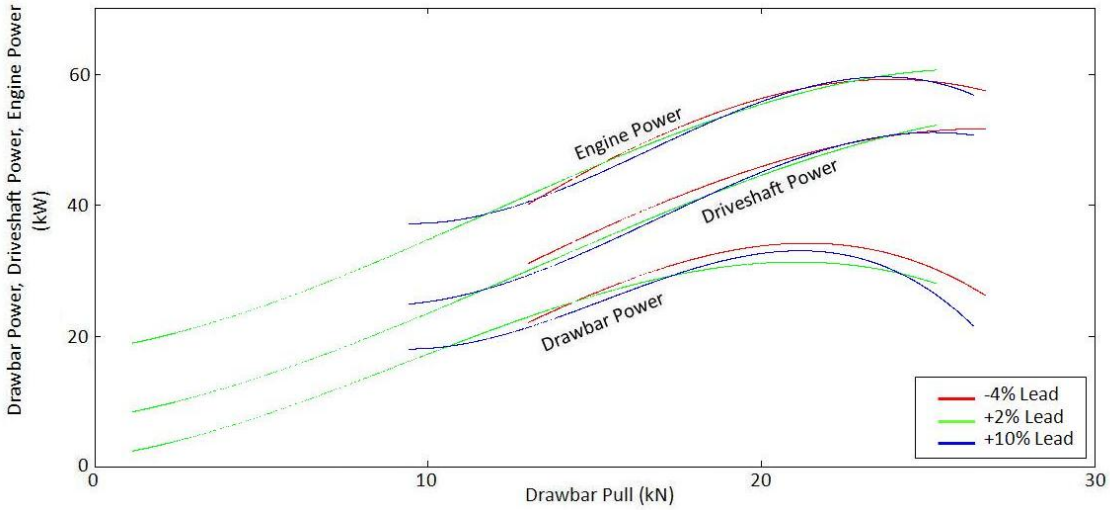

Figure 4.3.9: The effect of lead on the relationships between drawbar, driveshaft and engine powers, and drawbar pull, operating downhill on sand (Appendix 4.13.14 and 4.13.20)

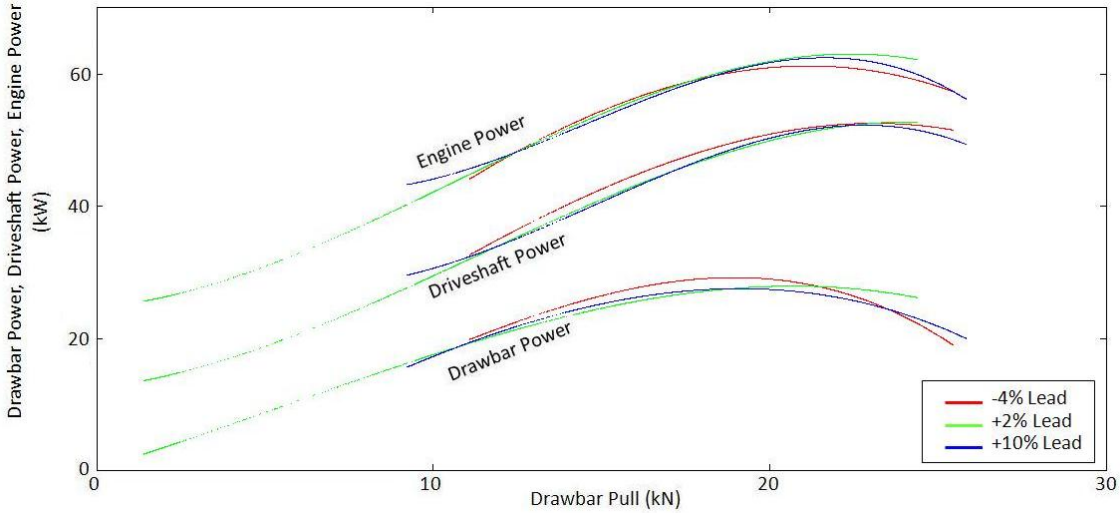

Figure 4.3.10: The effect of lead on the relationships between drawbar, driveshaft and engine powers, and drawbar pull, operating uphill on sand (Appendix 4.13.13 and 4.13.19)

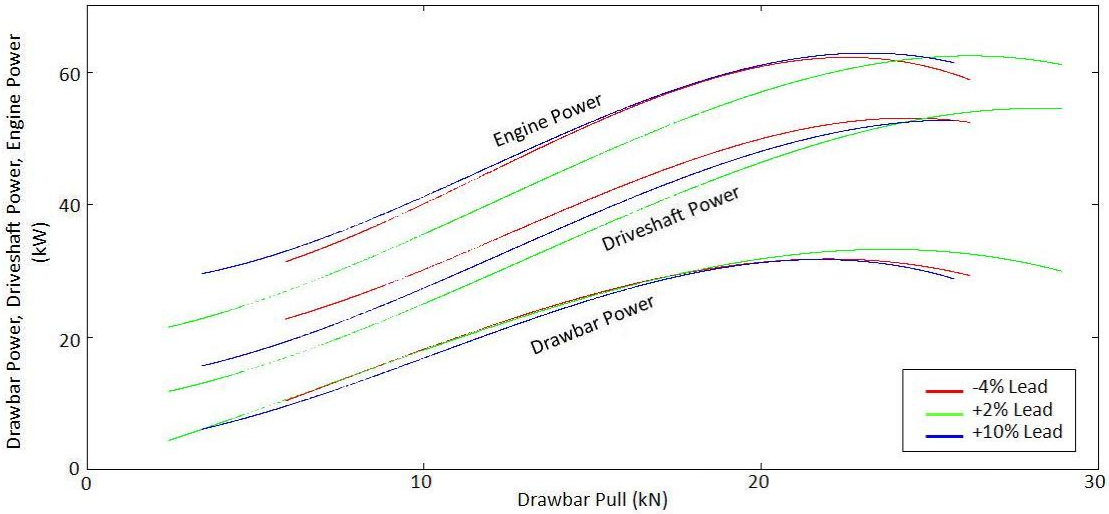

Figure 4.3.11: The effect of lead on the relationships between drawbar, driveshaft and engine powers, and drawbar pull, operating on clay (Appendix 4.13.15 and 4.13.21)

4.3.6 The effect of lead ratio on the magnitude of power consumed within the main gearbox

Figures 4.3.12, 4.3.13 and 4.3.14 were interpolated from the curves shown in Figures 4.3.9, 4.3.10 and 4.3.11, and show the magnitude of power consumed between the gearbox input and gearbox output shafts. These traces indicate that up to around 20 kN drawbar pull, the gearbox and its ancillaries consume between 8.5 and 14 kW. The majority of this power was consumed by the tractor's fixed displacement hydraulic pump, which is driven from the PTO, on the engine side of the PTO clutch. This pump has a maximum power requirement of 16.69 kW (Morgan *et al,* 2000). Beyond 20 kN drawbar pull the engine speed, and thus hydraulic pump speed reduced, thus reducing the power demand of the pump. This observation is consistent with that of Wong (2001), that transmission efficiency improves as drawbar pull increases, although Wong does not note that this effect is the result of the PTO driven, fixed displacement hydraulic pump slowing as the engine slows.

On sand lead ratio has less effect on the magnitude of power consumed in the transmission, with a difference of at most 2.6 kW on sand and 5 kW on clay. There is significant a separation between the traces for -4 % and +2%, and +10 % lead ratio cases on clay, which is not apparent on sand.

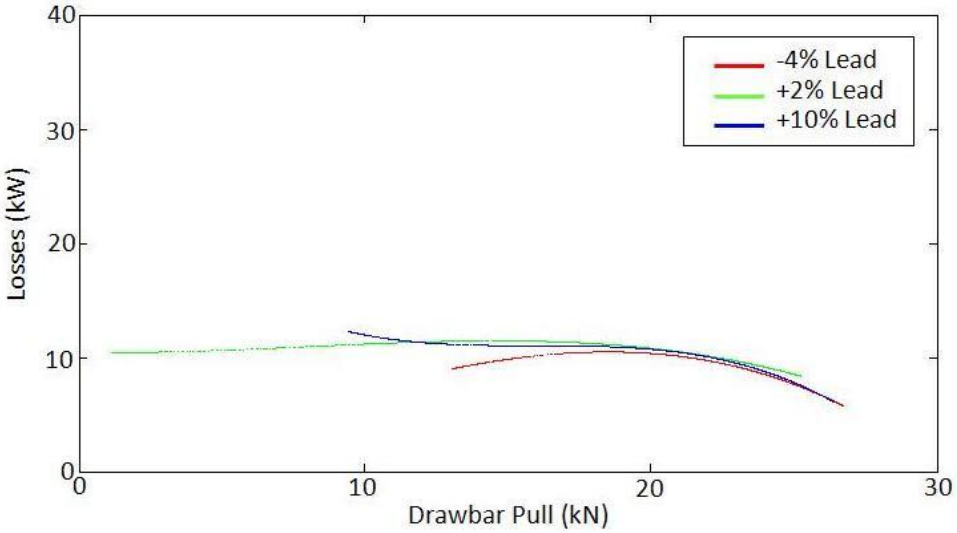

Figure 4.3.12: The effect of lead ratio on the relationship between power losses in the gearbox and drawbar pull, operating downhill on sand

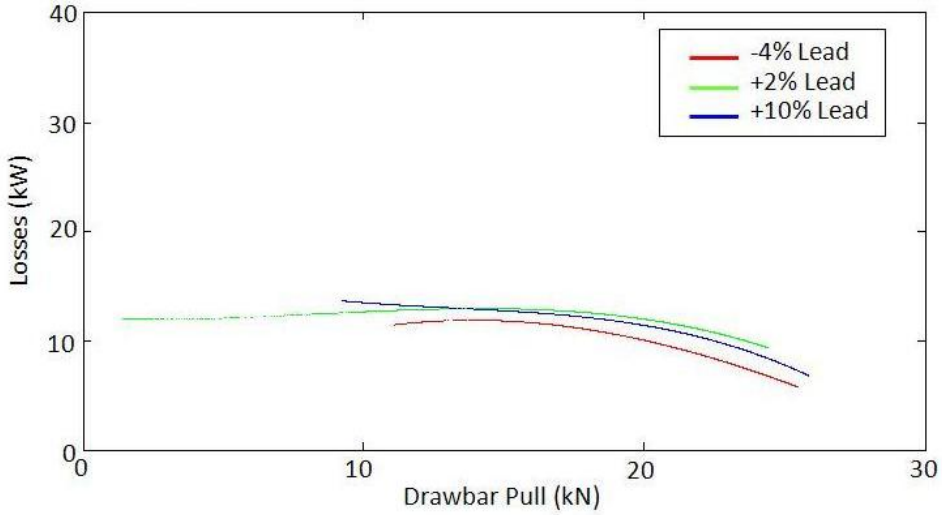

Figure 4.3.13: The effect of lead ratio on the relationship between power losses in the gearbox and drawbar pull, operating uphill on sand

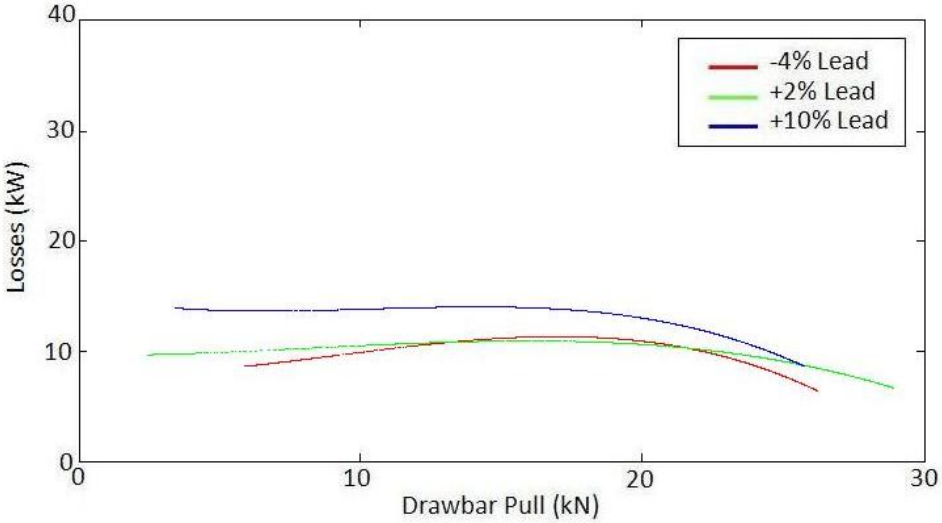

Figure 4.3.14: The effect of lead ratio on the relationship between power losses in the gearbox and drawbar pull, operating on clay

4.3.7 The effect of lead ratio on the magnitude of power consumed between the main gearbox output shafts and drawbar

Figures 4.3.15, 4.3.16 and 4.3.17 were interpolated from the curves shown in Figures 4.3.9, 4.3.10 and 4.3.11, and show the magnitude of power consumed between the gearbox output shafts and drawbar. On sand (Figures 4.3.15 and 4.3.16) there is little apparent difference between the traces for the three lead ratio treatments. However, on clay (Figure 4.3.17) it is apparent that lead ratio has a measurable effect on the magnitude of power lost downstream of the gearbox, with the +2% lead ratio case losing between 1.3 and 3.5 kW less power than either of the other two lead cases throughout the drawbar pull range tested. The differences between the power lost downstream of the gearbox on clay for the -4% case and +10% case are rather smaller (max 2.6 kW, min 0 kW) than the difference between both cases and the +2% case. This difference between the observations on sand and clay are consistent with the finding in Section 4.2 that power delivery efficiency was more strongly influenced by lead ratio on clay than on sand. Comparison of Figures 4.2.3, 4.2.4 and 4.2.5 showing the relationship between drawbar pull and wheel slip, and Figures 4.3.15, 4.3.16 and 4.3.17 indicate that the majority of the power lost between the gearbox output shafts and drawbar is lost as wheel slip. This observation is also consistent with that of Wong (2001). The +2 % lead ratio case exhibits the lowest power consumption between gearbox output and drawbar of the three treatments, which is consistent with the power delivery efficiency data presented in Figure 4.2.8.

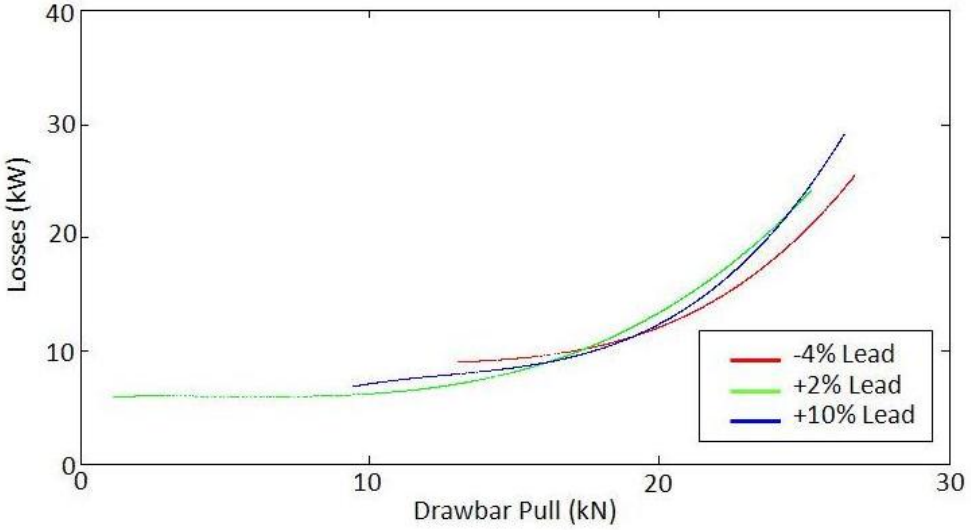

Figure 4.3.15: The effect of lead ratio on the relationship between power losses downstream of the gearbox, and drawbar pull, downhill on sand

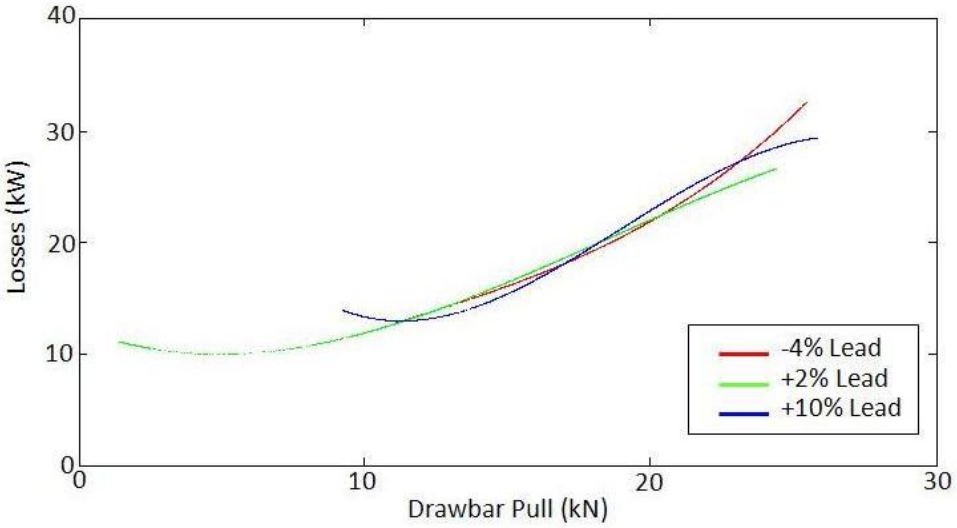

Figure 4.3.16: The effect of lead ratio on the relationship between power losses downstream of the gearbox, and drawbar pull, uphill on sand

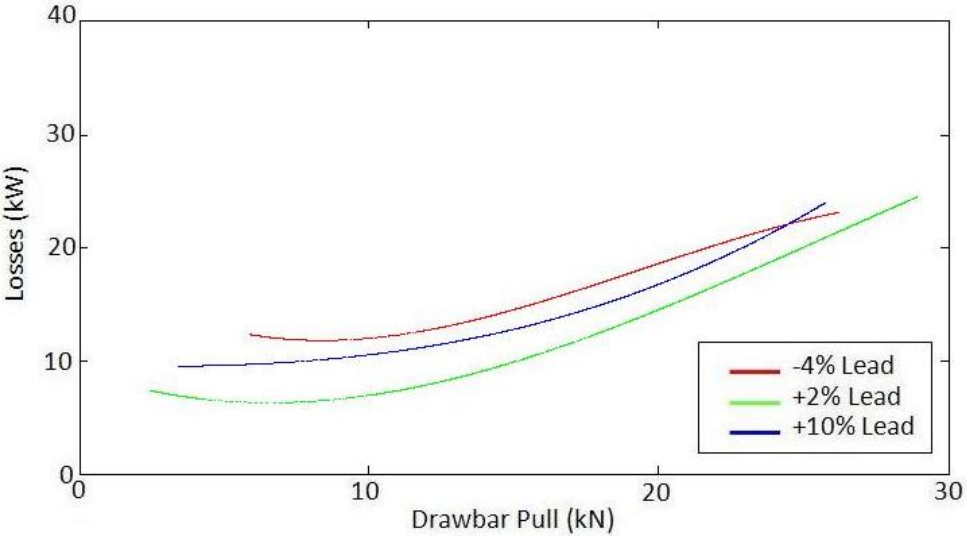

Figure 4.3.17: The effect of lead ratio on the relationship between power losses downstream of the gearbox, and drawbar pull, on clay

4.3.8 The effect of lead ratio on the overall magnitude of power consumed between the gearbox input and drawbar

Figures 4.3.18, 4.3.19 and 4.3.20 were interpolated from the curves shown in Figures 4.3.9, 4.3.10 and 4.3.11, and show the total magnitude of power consumed between the gearbox input shaft and drawbar. It is apparent from these Figures that the magnitude of power consumption is higher on sand (38 and 35 kW) than clay (32.5 kW), which is consistent with the analysis of power delivery efficiency in Section 4.2.5. It is also apparent that lead ratio has a larger effect on power consumption on clay than on sand, with the biggest difference in total power losses (7.3 kW) being between the +2% and +10% lead ratio cases on clay at 6.3 kN drawbar pull, while on sand the biggest difference was 4 kW, between the -4% and +10% lead ratio cases at 26.1 kN drawbar pull.

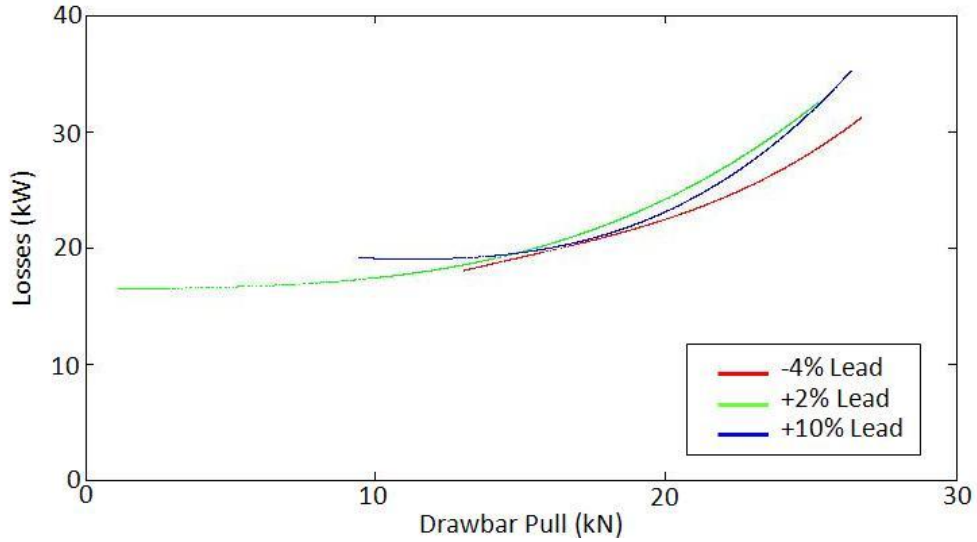

Figure 4.3.18: The effect of lead ratio on the relationship between total power losses and drawbar pull, operating downhill on sand

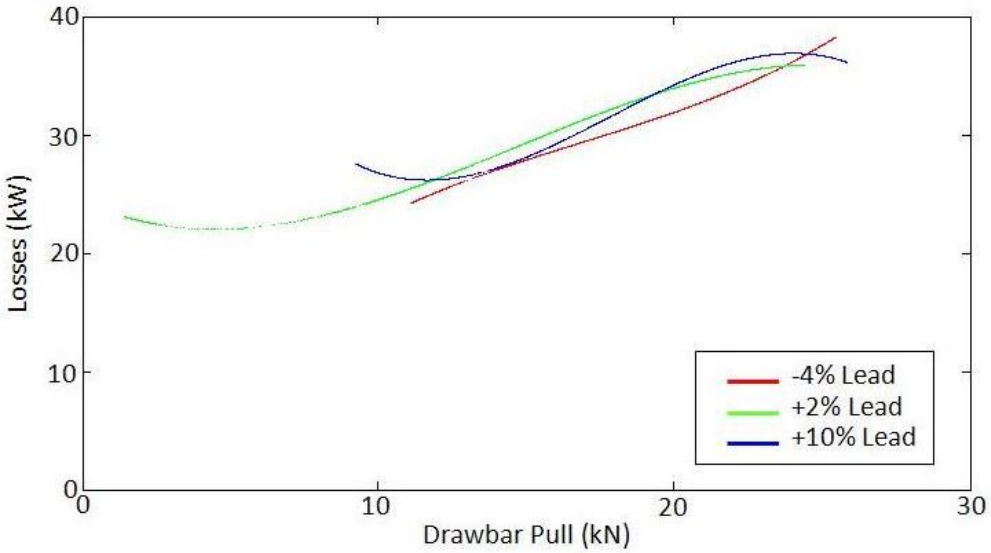

Figure 4.3.19: The effect of lead ratio on the relationship between total power losses and drawbar pull, operating uphill on sand

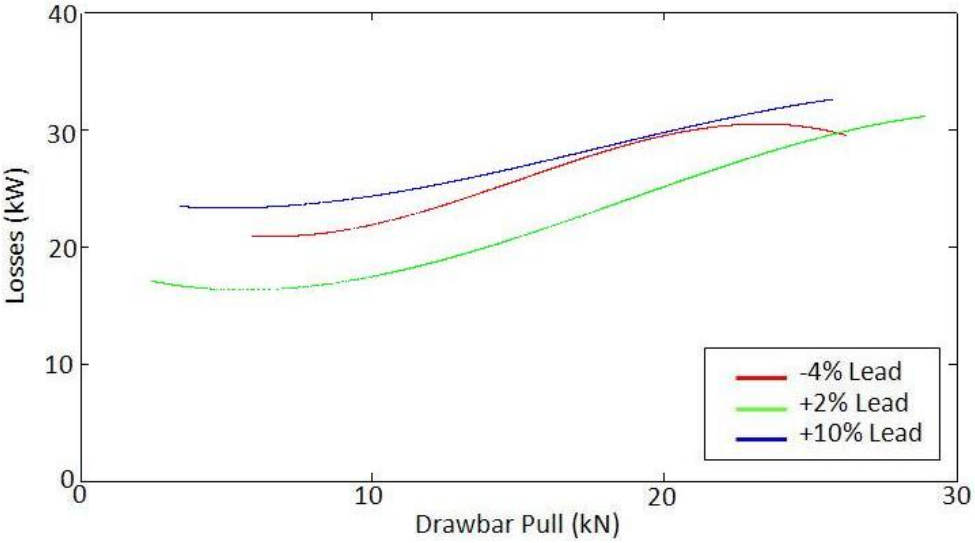

Figure 4.3.20: The effect of lead ratio on the relationship between total power losses and drawbar pull, operating on clay

4.3.9 Conclusions

The front axle of the tractor was found to transmit a near constant level of torque (max slope 0.12 Nm/N @ -4% lead ratio on clay) (Table 4.3.1and Figures 4.3.3 – 4.3.5) and power (Figures 4.3.6 – 4.3.8) throughout the drawbar pull and drawbar power ranges tested. These results concur with those of Bashford *et al* (1987). Additional thrust was produced almost exclusively via the rear axle (min slope 0.72 Nm/N @ -4% lead ratio on clay).

At drawbar pulls below 20 kN the fixed displacement hydraulic pump consumed a significant proportion of the TS90's engine power (Section 4.3.6). The magnitude of these losses (8.5 – 14 kW) was greater than the effect of varying lead ratio. Above 20 kN drawbar pull the slowing of the engine reduced the power demand of the pump, thus improving the overall efficiency of the transmission. These results concur with Wong (2001) who asserts that transmission efficiency increases with increasing drawbar pull.

Above 20 kN drawbar pull wheel slip accounted for the greatest power losses. At maximum drawbar pull (around 26 kN), the power lost between the gearbox output shafts and drawbar was up to 32 kW on sand and 24 kW on clay (Figures 4.3.15 – 4.3.17). These losses were primarily the result of wheel slip.

More power is consumed between the gearbox input and drawbar (Figures 4.3.18 – 4.3.20) when operating on sand than on clay, but lead ratio has a more pronounced effect on power consumption on clay than on sand.

The gradient of the sandy test site produced a statistically significant change in the slope of the front axle torque versus drawbar pull graphs (Figures 4.3.3 and 4.3.4), but not in the rear axle. However, the magnitude of the difference in front axle slope was only 0.004 Nm/N (Downhill=0.06444 Nm/N, uphill=0.06044 Nm/N, LSD=0.003372 Nm/N), compared to 0.044 Nm/N (Downhill=0.856 Nm/N, uphill=0.9 Nm/N, LSD=0.1359) (Appendices 4.9 and 4.10).

4.4 Measurements on Hard Surfaces

Through the course of the experimental programme a substantial quantity of data were gathered while operating on tarmac and compacted gravel roads. This data were not part of the formal experimental programme, and was not gathered using the same experimental procedure as the data presented in Sections 4.2 and 4.3, however, it does offer a useful insight into some aspects of the behaviour of the tractor's transmission.

4.4.1 Torque and power re-circulation

Brenninger (1999) reports observing a situation in which a four-wheel-drive tractor was able to transmit more power through one axle than was being delivered by the engine. This situation was caused by the phenomenon of power re-circulation, a condition in which power is delivered by one axle, but then absorbed the other. This phenomenon was reproduced during the experimental phase of this project.

Figure 4.4.1 shows a series of torque histories supplied by the engine, and transmitted by the front and rear axles, while travelling on a mixture of

compacted gravel and tarmac roads, in four-wheel-drive at -4% and +2% lead, and in four-wheel and two-wheel-drive at +10% lead. It proved very difficult to operate the tractor in four-wheel-drive on tarmac at +10% lead, since wind-up in the transmission caused significant vibration and longitudinal oscillation, thus at +10% lead the tractor was operated in four-wheel-drive for the first part of the journey on the compacted gravel road, but switched to two wheel drive for the section on tarmac. The tractor was not drawing a load while this data were being gathered.

Comparison of the three replicates shown in Figure 4.4.1 reveals a number of interesting facets to these data. In both of the positive lead cases, the rear axle exhibits negative drive torque, i.e. rather than the driveshaft turning the wheels forward, the wheels are actually absorbing thrust from the ground, and driving the driveshaft. In the +10% lead case this effect is more pronounced than in the +2% lead case. At -4% lead the effect is absent, and the rear axle exhibits positive driving torque. The front axle, however, does not transmit any torque and therefore does not contribute to driving the tractor forwards.

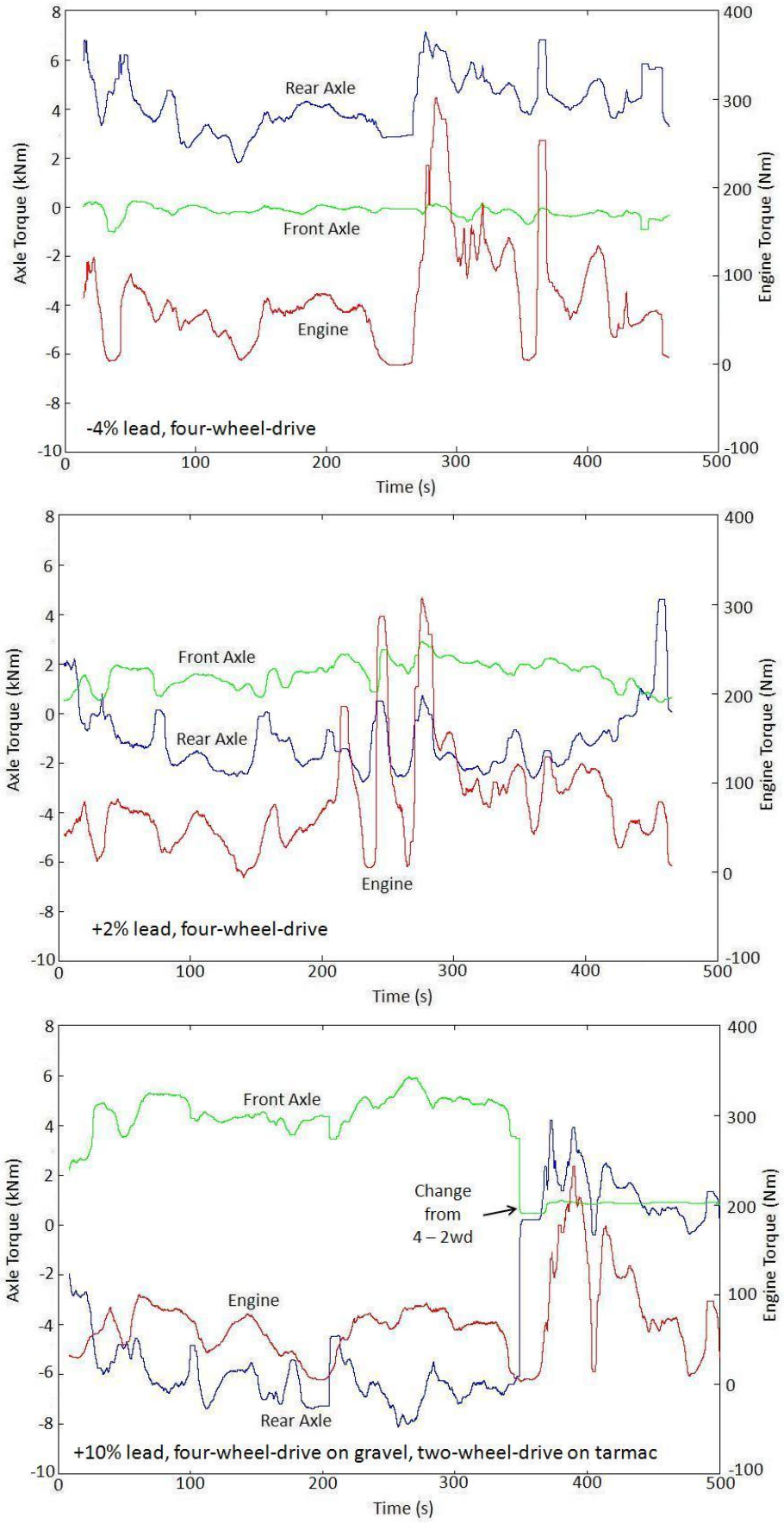

Figure 4.4.1: Front and rear axle and engine torque histories collected while travelling on compacted gravel and tarmac roads.

Figure 4.4.2 shows the equivalent power histories for the journeys shown in Figure 4.4.1. Comparison between the power histories shown in Figure 4.4.2 demonstrates the effect of varying lead on the magnitude of power transmitted by the front and rear axles. Increasing the percentage of front axle lead increases the amount of power transmitted by the front axle, and proportionately reduces the amount of power transmitted by the rear.

A notable feature of the power histories for the +2% and +10% lead cases is that the rear axle exhibits a negative power flow throughout much of the journey while operating in four-wheel-drive, i.e. the rear axle is being turned forward faster than the transmission is driving it, and actually absorbing power from the road. Secondly there are periods in the journey where the front axle is transmitting more power than is being delivered by the engine. This combination of behaviours is characteristic of power re-circulation.

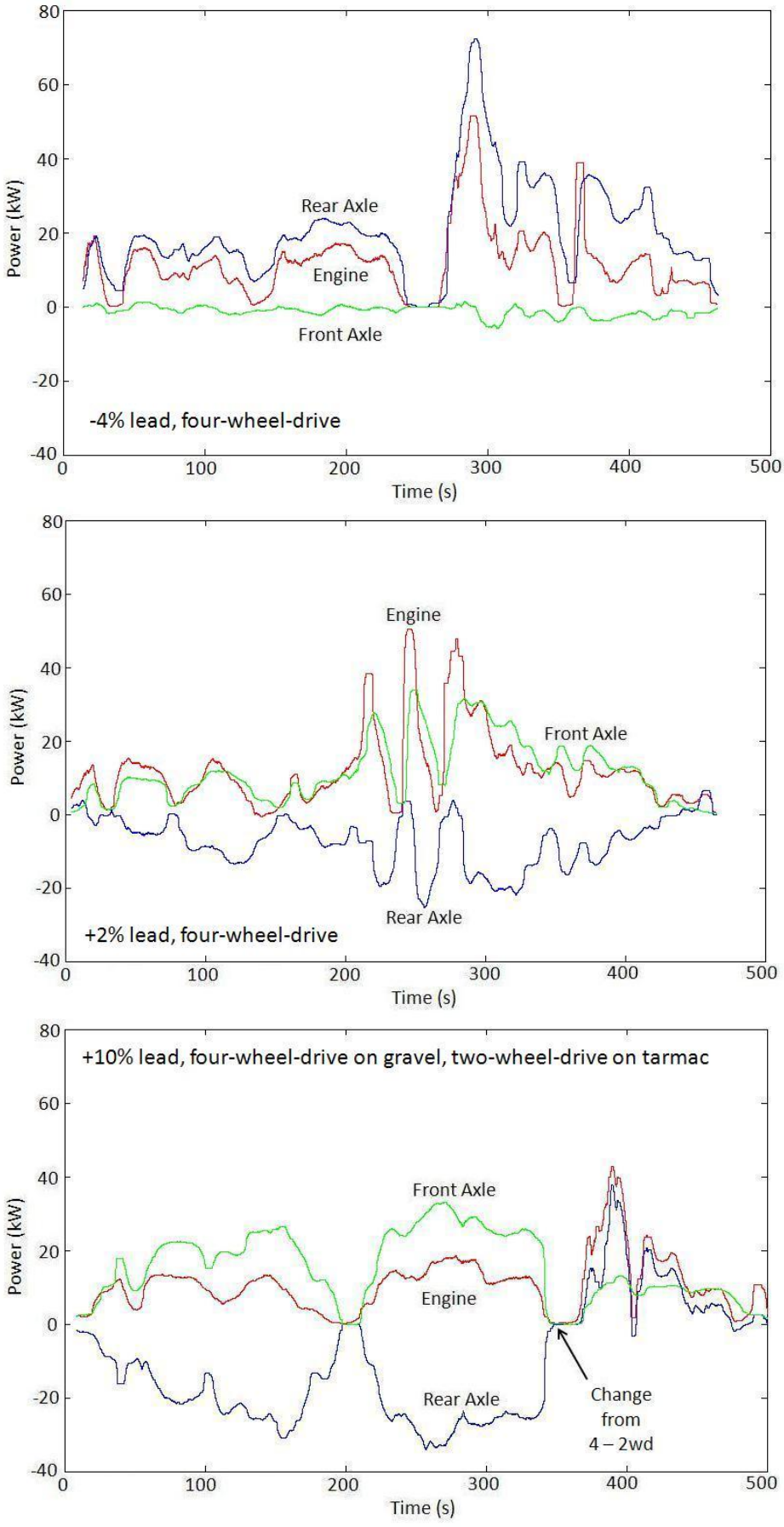

Figure 4.4.2: Front and rear axle and engine power histories collected while travelling on compacted gravel and tarmac roads.

4.4.2 Adverse effects under braking due to lead

It was noted in Section 4.4.1 that the TS90 exhibited some undesirable behaviour while operating in four-wheel-drive at +10% lead on tarmac, which necessitated using two-wheel-drive while travelling on the road. However, in common with many front-wheel-assist tractors, the TS90 only has wheel brakes on the rear axle, and engages drive to the front axle to brake the front wheels. This feature of the tractor's design created an unusual and undesirable phenomenon during one of the journeys on tarmac. Figure 4.4.3 is a section of time history for the journey in question, showing the tractor approaching and stopping at a road junction, waiting at the junction and then accelerating away. The footbrake was used to bring the tractor to a halt at the junction, engaging the front axle drive in the process. Initially the tractor is operating in two-wheel drive mode, driven only by the rear axle, which exhibits a gradually declining output torque as the tractor coasts to a halt. At the point where the footbrake is depressed the interaction between the front and rear axles causes an instantaneous wind-up condition within the transmission, with the torque being transmitted by the front axle becoming positive, and the rear axle becoming negative. It should be borne in mind that the rear axle torque sensor is between the rear axle brakes and the main gearbox, thus the retarding force from the brakes is transmitted through the sensor zone on the rear output shaft. The presence of positive torque in the front output shaft implies that depressing the footbrake actually has the effect of accelerating, rather than retarding, the front wheels.

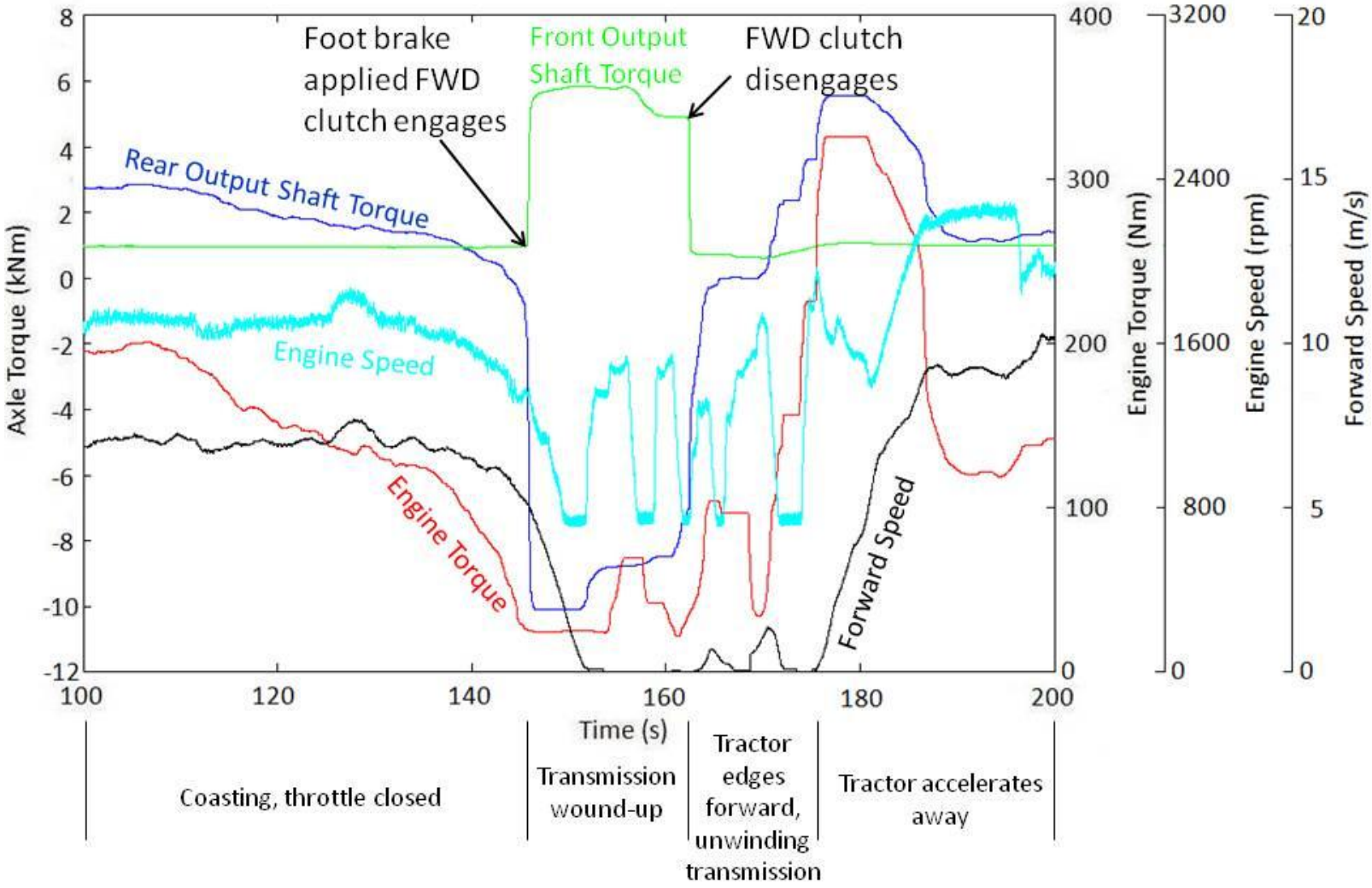

Figure 4.4.3: The effect of applying the footbrake when operating in two-wheel-drive at +10% lead on tarmac

Studying the relationship between front and rear axle torques and engine torque indicates that the torque flowing to the front axle comes from the rear axle, and not the engine, i.e. torque is being drawn from the rear axle and fed to the front. Considered in terms of wheel thrust rather than torque, the front wheels develop a peak thrust of 9.2 kN, while the rear wheels develop a retarding force of -13.2 kN. Thus the overall effect is still to decelerate the tractor with a force of 4 kN. However, it is not possible to reliably determine, with the data available, what effect the positive thrust developed by the front wheels has on braking efficiency.

When the tractor comes to move away, the negative torque wound into the rear axle as the tractor decelerated has to be overcome. In the case shown in Figure 4.4.3, the tractor was edged forward to allow the dog type front wheel drive clutch to disengage. As the clutch disengages, the torque wound into the system is released instantaneously.

A final observation from Figure 4.4.3 is that when the tractor is being operated in two-wheel-drive, the front axle transmits a constant torque of around 1000 Nm. This torque represents the drag of the front wheel drive clutch, which is only around 35 Nm at the clutch, but is multiplied by a factor of 26.2 by the front differential and reduction hubs. Thus in the case of this particular tractor, it can never be said to be truly operating in two-wheel-drive.

4.4.3 Conclusions

Torque and power is transmitted between the axles via the ground when the tractor operates at zero drawbar pull on compacted gravel and tarmac roads.

The rear axle was observed to generate up to 8 kNm of retarding torque and absorb 33 kW of power from the ground when the tractor was driven on gravel roads at +10% lead ratio.

When operating at +10% lead ratio it was observed that power re-circulation caused the front axle to transmit a higher magnitude of power (34.5 kW) than was being provided by the engine at the time (19 kW), the additional power being absorbed from the road surface by the rear axle (-33 kW).

The drag of the front-wheel-drive clutch meant that the front axle transmitted around 1000 Nm of torque to the front wheels, even when the tractor was operated in the two-wheel-drive mode.

Further research is required to determine the effect of inter-axle interaction on braking performance. It was noted that when operating with a positive lead ratio in two-wheel-drive mode, depressing the foot brake caused the front wheels to accelerate rather than decelerate, i.e. going from 0% slip to a positive slip equal to the lead ratio. No previous literature was found in this area.

5.0 Computer modelling

A computer model of the New Holland TS90 tractor was constructed, primarily as a diagnostic tool to investigate certain aspects of the behaviour of the tractor. In this investigative role, the absolute accuracy of the model was of secondary importance to its ability to replicate trends observed in the data collected in the field. This chapter describes the construction of the model and the modelling software employed.

5.1 Aim

To build a computer model of the TS90 test tractor, capable of predicting trends in drawbar pull, drawbar power, and driveshaft torque and driveshaft power on a range of surfaces, and at a range of leads.

5.2 Objectives

1. Assess the ability of a computer model to produce output data consistent with equivalent data gathered by experimental means.
2. Assess the ability of a computer model to predict the effects of soil strength and lead on powers and torques in the tractor.
3. Assess the relative accuracy of predictions generated using a simple friction coefficient based tyre model, and a more complex model based on Brixius (1987) using soil cone index and tyre stiffness as input parameters.
4. Assess the ability of a computer model to predict trends in the magnitude of re-circulating torque and power developed.

5. Utilise the model in a diagnostic role to explore aspects of the behaviour of the tractor.

5.3 Choice of modelling package

A number of modelling methods and packages were considered for this part of the project.

MSc Easy5 was selected for the construction of this model:

1. Easy5 is an integrated system that has previously been proven to be capable of combining the simulation of vehicle-terrain interaction and transmission behaviour in a single model
2. the package has previously been utilised for similar projects, most notably by Deere & Co who worked in association with Ricardo to develop the package of powertrain components utilised within the model
3. both the author and the broader Harper Adams community have some experience of developing models using the Easy5 platform
4. At the time the project began, Easy5 and the Ricardo Powertrain package of vehicle components was readily available at Harper Adams.

5.4 Easy5

MSc Easy5 is a graphical, schematic based, dynamic modelling system. Models are constructed in Easy5 from a library of generic components, which are represented by icons (Figure 5.1). Each of these components contains a mathematical sub-model representing the behaviour of the component. Components within the model are joined using visual lines, which represent numerical input and output paths between sub-models. The behaviour of

each individual component can be customised to match their real-world equivalents by changing relevant parameters within the component, and by connecting inputs from other components. So for example, the behaviour of a tyre component can be affected by a connected torque input from a shaft component, and by an internal parameter like rim diameter.

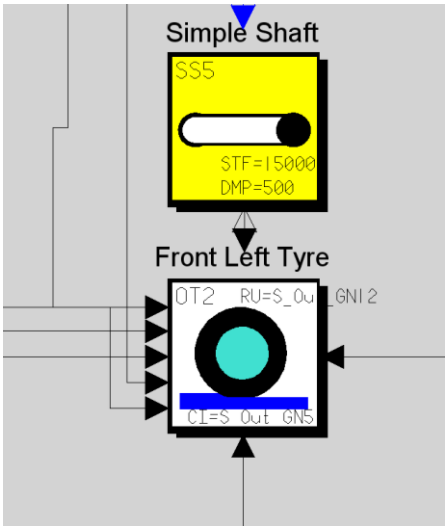

Figure 5.1: Easy5 icons representing an off-highway tyre and a simple shaft (Source, author)

Easy5 is a multipurpose modelling platform with a very wide range of applications. The powertrain components developed by Ricardo can be used to simulate, thermal performance, fuel consumption and even exhaust emissions. However, with this level of complexity available, care had to be taken to ensure that the model maintained an acceptable level of accuracy, while at the same time avoiding excessive complexity that would have both increased the simulation time for each run, and added many parameters not immediately relevant to this research.

5.5 Experimental method

A computer model of the powertrain of the TS90 test tractor was built using Easy5 and Ricardo Powertrain packages.

The model was populated with available data from the tractor and test sites.

The model was correlated with data gathered during field experiments on a single surface and at a single lead.

Predictive data were generated for the other leads and surfaces tested in the field experimental programme.

The accuracy of predictions was assessed and the model re-correlated where necessary.

A second model was constructed using an alternative tyre model and the process of correlation repeated.

Individual parameters were tested to assess their effect on power flow within the tractor.

5.6 The TS90 model

The model (Figure 5.2), follows a similar approach to that adopted by Summers *et al* (1986) and du Plessis and Marais (2003), and consists of generic engine and gearbox components which are connected via a shaft to a four-wheel drive system. This system replicates the numerical gear ratios between the main gearbox output and the wheels, and also the dimensions of the wheels and tyres, but does not seek to replicate the physical properties of the driveline components. The layout of the transmission is simplified in that the reduction hubs and the four wheel drive clutch are omitted; the main gearbox has only four speeds (Appendix 5.2); and there is no PTO or hydraulic system. While these omissions would prevent the model

from accurately predicting the behaviour of individual components, this macro-modelling approach allows the behaviour of the tractor as a whole to be simulated. Wherever possible, model parameters were taken from measurements of the TS90, or manufacturer's specifications. Where specific data for the TS90 was not available values were derived from published literature.

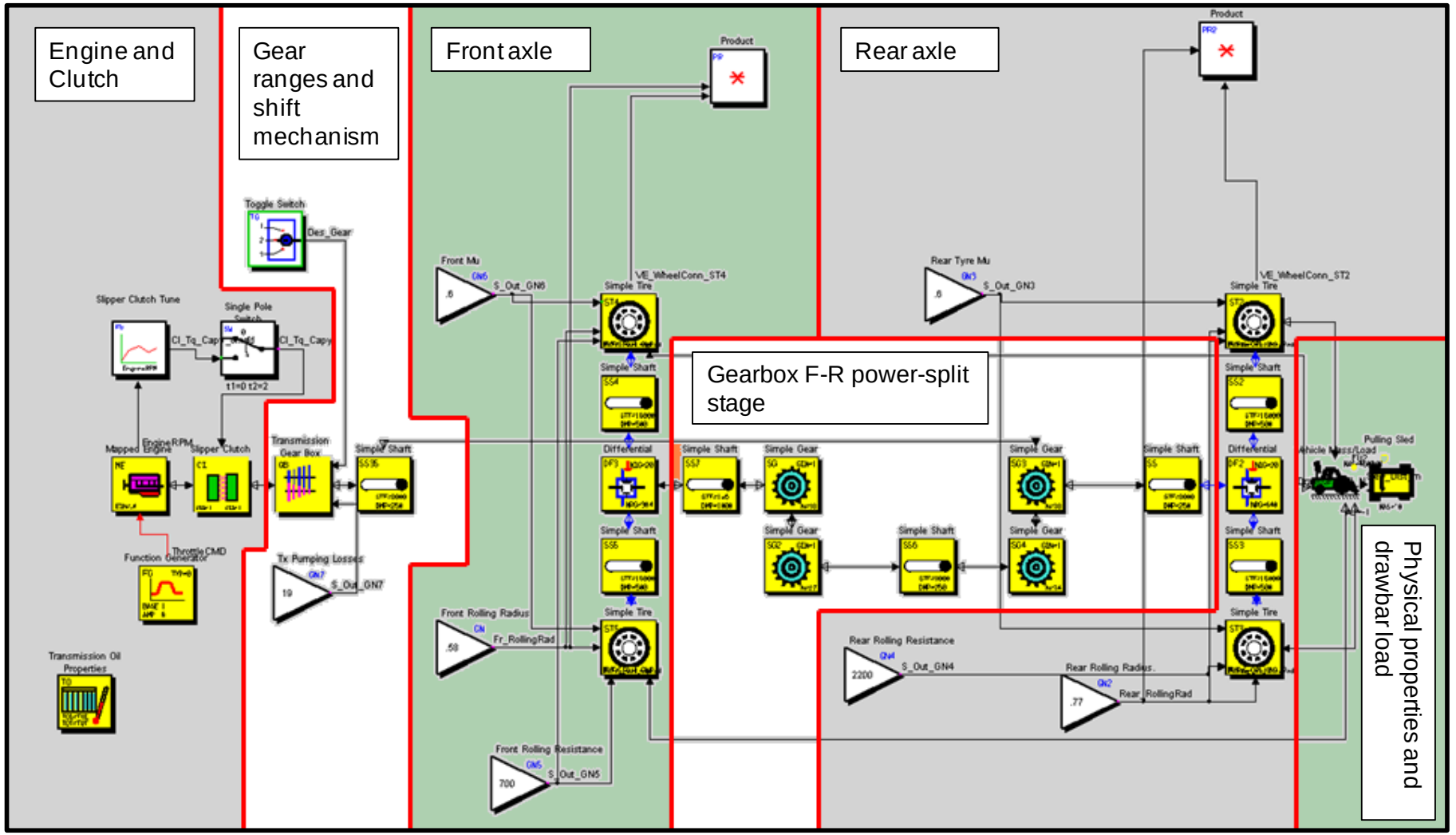

Figure 5.2: The Easy5 TS90 model built using the friction based Simple Tyre component (Source, author)

5.6.1 Physical properties of the tractor model

The physical dimensions of the tractor were represented by a *vehicle mass* component (Figure 5.3) which defined the relative positions of the four wheels and the position of the tow hitch relative to the back axle and ground (Appendix 5.3). The static mass and balance of the tractor was entered into the model (Appendix 5.3). Dynamic wheel loads were calculated by the model from the geometry of the axles and tow hitch, the gradient entered as a parameter in the model, and the drawbar pull calculated by the model. The load tractor was represented by a simple component that provided a load at the drawbar, which increased linearly with the distance travelled. No attempt was made to model the physical properties of the load tractor.

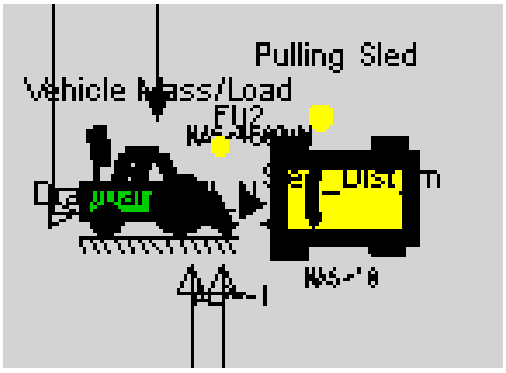

Figure 5.3: The *vehicle mass* component (left) that represented the physical dimensions and mass properties of the tractor and the *pulling sled* (right) which represented the rolling load imposed by the load tractor (Source, author)

5.6.2 Engine and transmission

The engine, clutch and gear ratio section of the gearbox were represented in the model by three discreet components (Figure 5.4). The behaviour of the engine component (Figure 5.4, second row from the bottom, far left) was derived from a simple look-up table of torque versus engine speed (Appendix 5.1) derived from CNH test data, and a reference value that represented

throttle position, fed into the engine component by a function generator component shown bottom left in Figure 5.4. For the purposes of this research the model was started with the throttle input set to maximum, where it remained throughout each simulation, this approach matched that employed in the field experiments.

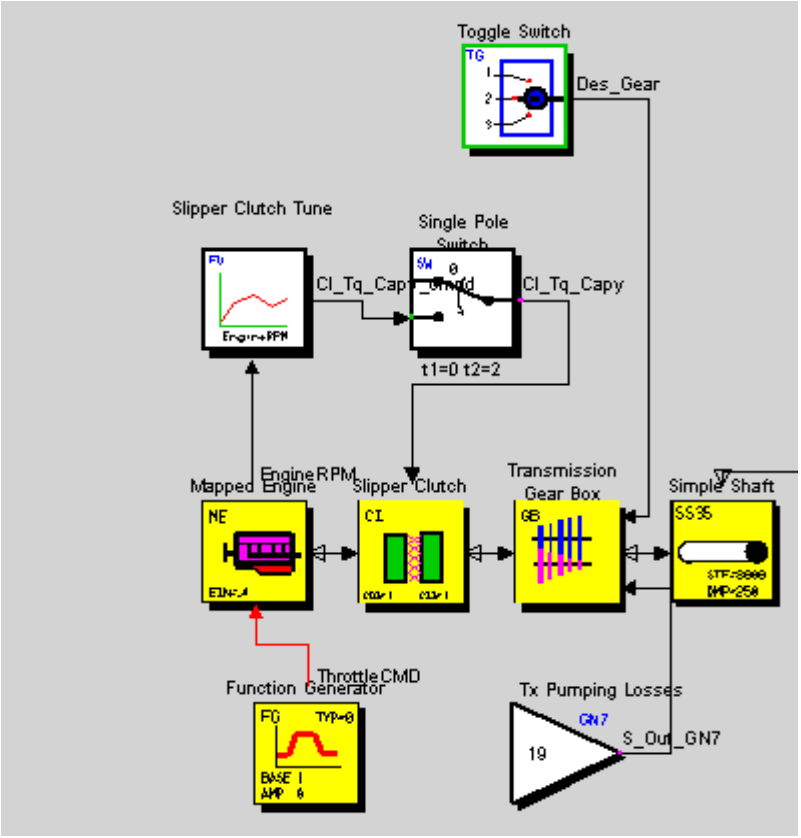

Figure 5.4: The engine, clutch and gear range section of the Easy5 TS90 model (Source, author)

The clutch (Figure 5.4, second row, second component from the left) was modelled as a simple dry-plate friction type clutch, rather than the multi-plate wet clutch employed in the instrumented tractor. The modelled clutch was controlled by a single pole switch (Figure 5.4, third row from the bottom, on the right) which initiated engagement of the clutch and a block that controlled the modulation of the clutch engagement in response to engine torque. In the model, as in the field experiments, the clutch was only used to control the

launch phase of the test. In the model the single pole switch was commanded to close at the start of each simulation. The modulation block controlled the torque capacity of the clutch up to the point where 100% of engine torque was being passed to the gear ratio section of the gearbox. This phase of the simulation was included as starting the simulation at maximum torque would have made the model unstable.

The tractor's gearbox (Figure 5.5) was modelled in two sections; a gear ratio selection component shown in Figure 5.4 and the power split section of the four-wheel-drive. The gear ratio selection component provided appropriate speed variation between the engine and four-wheel-drive system based on measured gear ratios. The model was only programmed with four ratios, as opposed to the twenty-four found in the instrumented tractor. Gear ratios were modelled as simple numeric relationships between input and output speed and did not attempt to represent the physical parameters of the instrumented tractor's gear clusters (Figure 5.5). Ratio selection was controlled by a four-position switch, shown at the top of Figure 5.4, which in turn was controlled by a subroutine in the simulation.

For the purposes of this research, the model was only operated in a single gear, whose ratio represented the 4LH gear used throughout the field trials. The gear ratio selection component also included a constant that deducted 14 kW of power to represent losses to the hydraulic system, consistent with data gathered during field experiments. In the model power was fed from the gear ratio component to the power split section of the gearbox via a simple shaft.

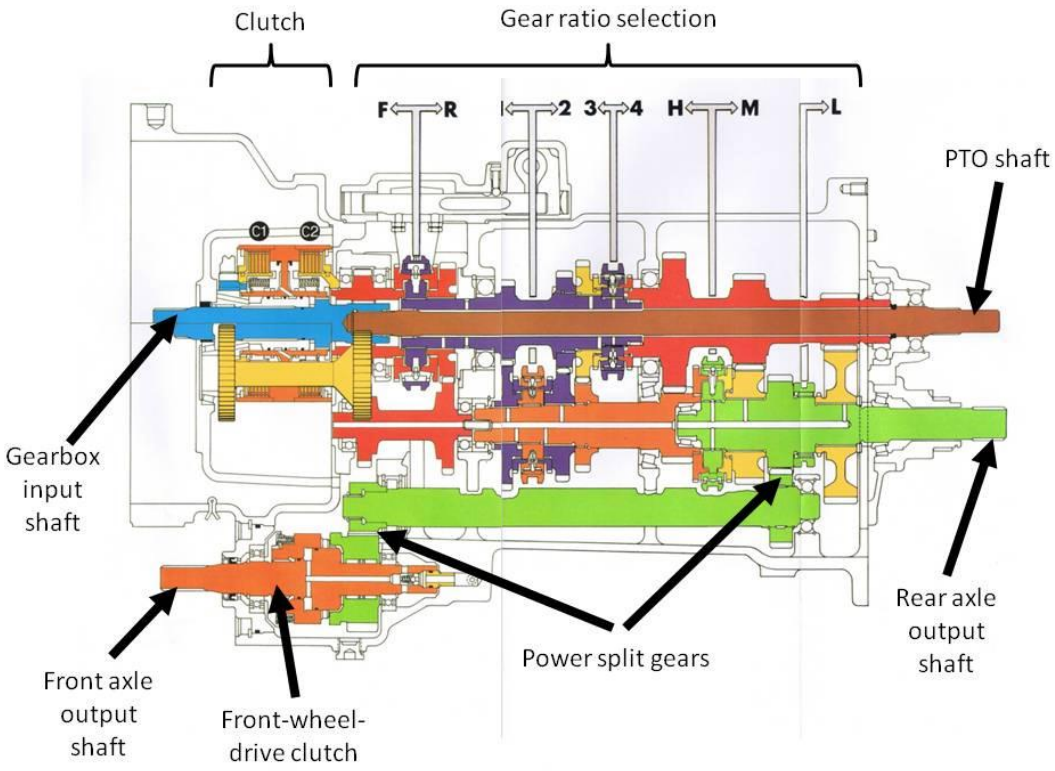

Figure 5.5: Schematic drawing of the main gearbox of the TS90. (Adapted from: CNH, 1998)

The four-wheel-drive power split section of the gearbox (Figure 5.6) was modelled as two pairs of intermeshing gears, which represented actual components in the instrumented tractor's transmission (Figure 5.5). The gear pairs in the model represent the tooth numbers, and thus the torque and speed ratios, of their equivalents in the instrumented tractor, but do not attempt to replicate their physical properties. The front-wheel-drive clutch (Figure 5.5) was omitted from the model, which was operated in four-wheel-drive throughout this research.

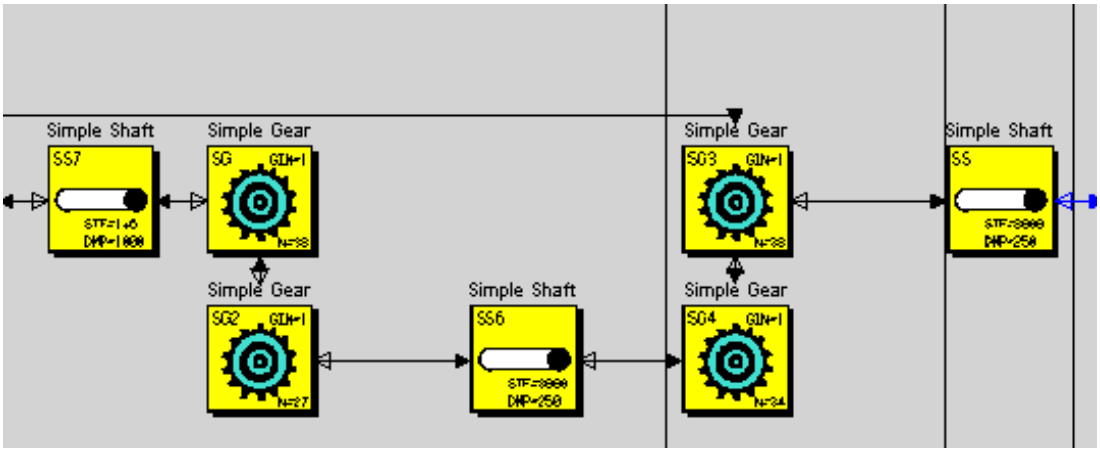

Figure 5.6: The power split section of the four-wheel-drive system modelled in Easy5 (Source, author)

The axles were modelled as crown-wheel and pinion type differential connected to the wheels by simple shafts (Figure 5.7). The ratios of the differentials were chosen to replicate the overall reduction ratio of the axles, including the reduction hubs, which were omitted from the model. The rear differential was locked in the model, as it was in the field trials. The front differential was open.

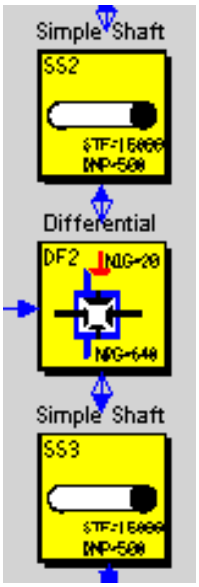

Figure 5.7: The rear axle modelled in Easy5 (Source, author)

5.6.3 Tyre models

The Ricardo library of powertrain components that works within the Easy 5 platform includes two alternative tyre models; a simple highway tyre model based on a look-up table of tractive force versus slip, and a more complex off-highway tyre model based on the traction equation developed by Brixius (1987), and described by Zoz and Grisso (2003) and Srivastava *et al* (2006). Both tyre models were tested and the accuracy of predictions produced were assessed.

5.6.3.1 Simple tyre model

The *Simple Tyre* model is a purely frictional model of tyre-terrain interaction. At the core of the model component is a predefined look-up table that defines tractive force values for a given wheel slip (Figure 5.8). The relationship between tractive force and wheel slip is scaleable by defining a variable that sets the maximum friction coefficient of each tyre (Appendix 5.4.1).

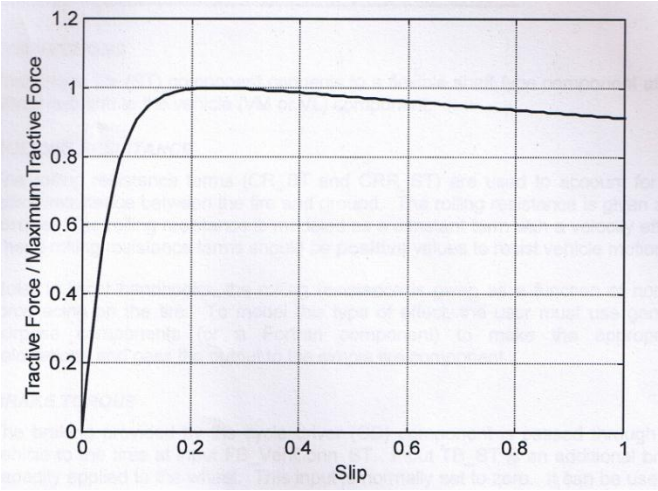

Figure 5.8: The relationship between wheel slip and tractive force used by the Easy 5 Ricardo simple tyre model (Ricardo, 2005a)

The *Simple Tyre* model also incorporates a term for rolling resistance (Appendix 5.4.2) of the tyre, which includes both a constant component and a velocity dependent component.

In operation, the primary means of manipulating the behaviour of the model was by adjusting the values of constant rolling resistance and maximum friction coefficient.

5.6.3.2 Off-highway tyre model

The *Off Highway Tire* used a set of equations (Appendices 5.4.3 – 5.4.15) to simulate the tractive behaviour of the tyre from the physical dimensions of the tyre (section width, rim diameter, rolling radius and unloaded radius), physical properties of the tyre (torsional stiffness and damping) and the soil cone index of the running surface. The physical dimensions of the tyres were all measured on the tractor. The model predicted the magnitude of torque transmitted from the wheel to the tyre tread by calculating the differences between wheel and tyre displacements, and wheel and tyre velocities (Appendix 5.4.15) using torsional stiffness and damping figures estimated from Pacey and Walker (1996) and Ramji *et al* (2002). The *Off Highway Tire* model used a formula to calculate a value for tyre rolling radius (Appendix 5.4.3) which was separate from its calculation of loaded tyre deflection (Appendix 5.4.4). The use of this formula produced a value for rolling radius equal to the static loaded wheel radius plus 38% of the difference between the loaded and unloaded wheel radii. In the case of this model, that equated to a difference of 19 mm for both the front and rear tyres. Since this value was not directly compared to any value measured in the field experiments it had no direct effect on the accuracy of the simulation data produced.

The model was found to be quite insensitive to the torsional stiffness of the tyres. The radial stiffness of the tyres, calculated from the difference between loaded and unloaded rolling radii was much more significant.

5.7 Model test procedure

As far as possible the test procedure in the model replicated that employed in the field experiments. Notable differences between the field and simulated testing were: the soil parameters used in the simulation were completely homogenous throughout each run; no attempt was made to simulate any transient effects created by the behaviour of the load tractor; and no attempt was made to simulate the two directions of travel tested on the clay site, although the gradient of the sandy site was replicated.

5.8 Model output

The output from the model took the form of a comma separated variable (CSV) file very similar in nature to the data files produced during the field testing of the tractor. These data files were imported into MathCAD, in the same way as the field data files. Comparison graphs were then created, which superimposed the simulated data onto the field test data. Working in the diagnostic mode, comparison graphs were also generated using multiple simulated data files, thus allowing the effect of model inputs to be assessed.

5.9 Initial proof of model validity

The model was run using the *Simple Tire* model and tested against data collected in the field experiments. The constant component of rolling resistance (Appendix 5.4.2) was optimised in the model to give the best fit between field and simulated data. It was not possible to experimentally measure these values, so they were extrapolated from values suggested by Wong (2001) and the normal force on each wheel. The front rolling resistance was set to 700 Nm per wheel, and the rear to 2200 Nm per wheel. The maximum friction coefficient for both axles was set to 0.6.

Figures 5.9 and 5.10 show comparison plots of field and simulation data, in these cases the tractor was being operated on the sandy test site, downhill at +2 % lead ratio. Both the forms and slopes of the responses show similarities between the simulation and field data. The simulation predicted the slopes of the front and rear axle torque responses to increasing drawbar pull (Figure 5.9) as -0.006 Nm/N for the front axle and +0.745 Nm/N for the rear, compared to the values observed in the field of +0.077 Nm/N (+0.083 Nm/N) for the front axle and +0.78 Nm/N (+0.035 Nm/N) for the rear.

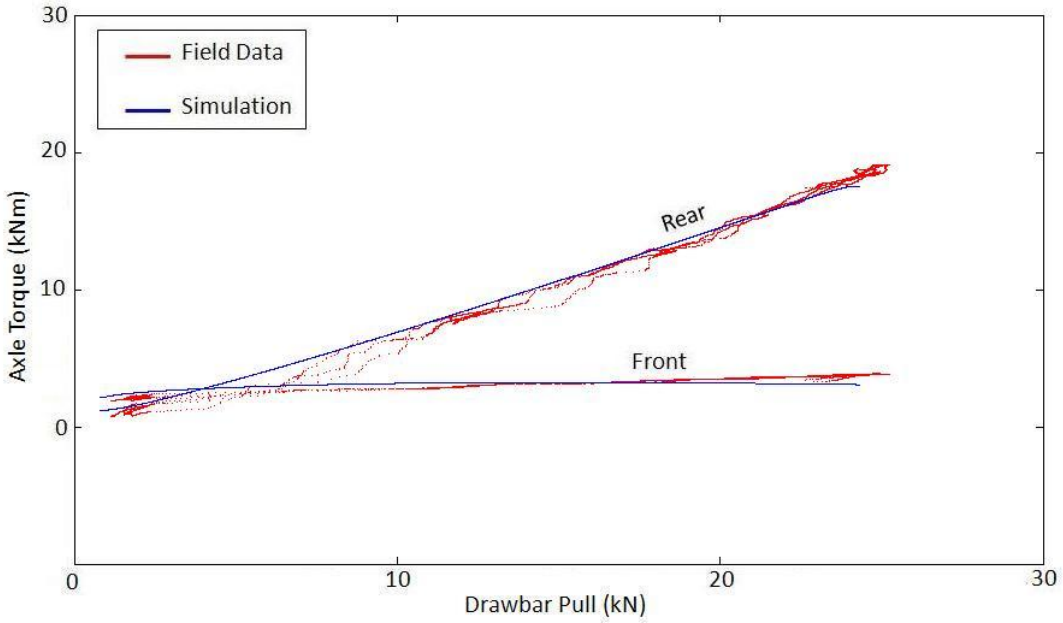

Figure 5.9: The relationship between the torques transmitted through the front and rear axles and drawbar pull; a comparison of field data, collected on the sandy test site at +2 % lead ratio operating downhill, and results from the Easy 5 simulation using the *Simple Tire* model.

The model predicted the maximum axle powers when operating downhill on sand (Figure 5.10) to be 11.7 kW for the front and 40.1 kW for the rear, compared to the values observed in the field of 11.5 kW (-0.2 kW) for the front and 41.2 kW (+1.1 kW) for the rear. The maximum drawbar power was predicted to be 36.2 kW, compared to the observed value of 33.3 kW (-2.9 kW)

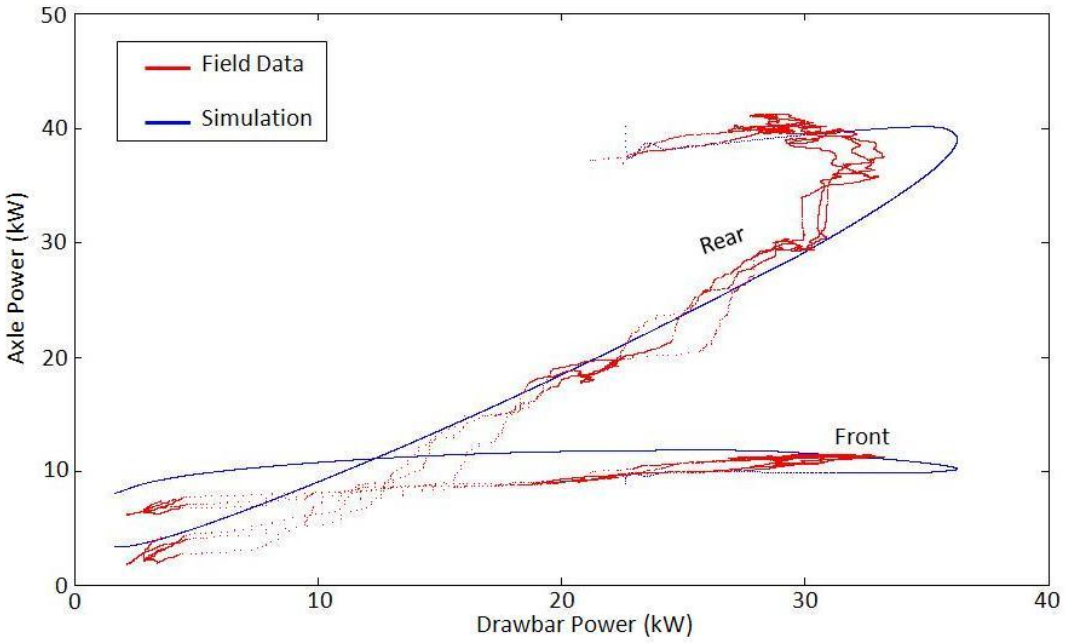

Figure 5.10: The relationship between the powers transmitted through the front and rear axles and drawbar power; a comparison of field data, collected on the sandy test site at +2 % lead ratio operating downhill, and results from the Easy 5 simulation using the *Simple Tire* model.

In order to test the validity of this model as a predictive tool, the lead ratio of the model was changed in the same way as it had been in the field experiments, i.e. by changing the diameter of the wheels and tyres fitted. Further comparative plots were prepared (Figures 5.11 – 5.14). These plots indicate that the simulation based around the *Simple Tire* model was capable of predicting the forms and magnitudes of responses of axle torque to drawbar pull, and axle power to drawbar power. However, the simulation consistently overestimated peak drawbar power by between 6.2 % and 8.7 %.

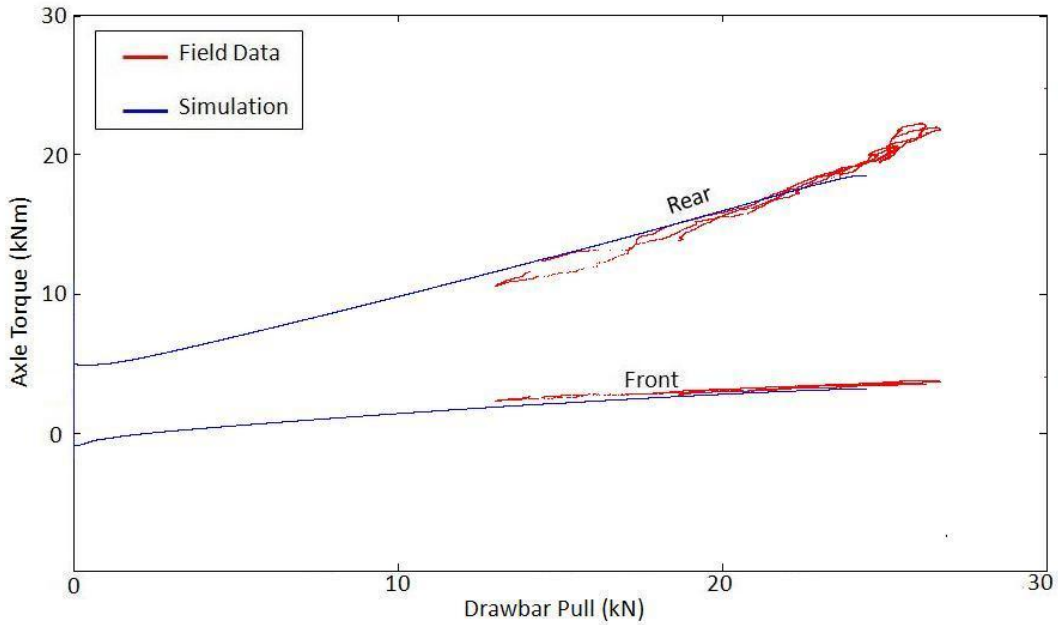

Figure 5.11: The relationship between the torques transmitted through the front and rear axles and drawbar pull; a comparison of field data, collected on the sandy test site at -4 % lead ratio operating downhill, and results from the Easy 5 simulation using the *Simple Tire* model.

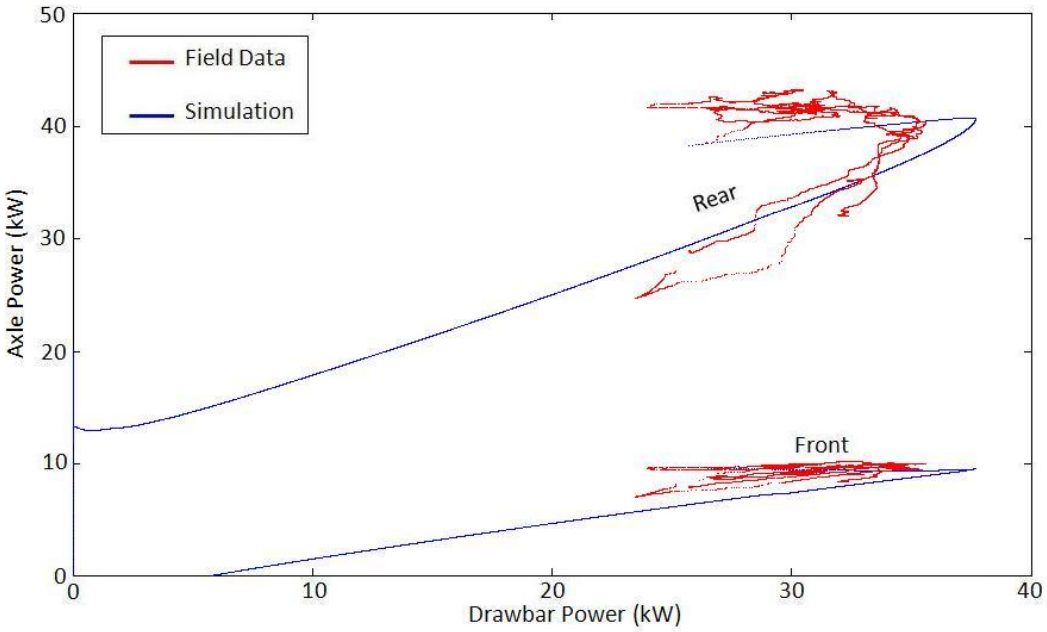

Figure 5.12: The relationship between the powers transmitted through the front and rear axles and drawbar power; a comparison of field data, collected on the sandy test site at -4 % lead ratio operating downhill, and results from the Easy 5 simulation using the *Simple Tire* model.

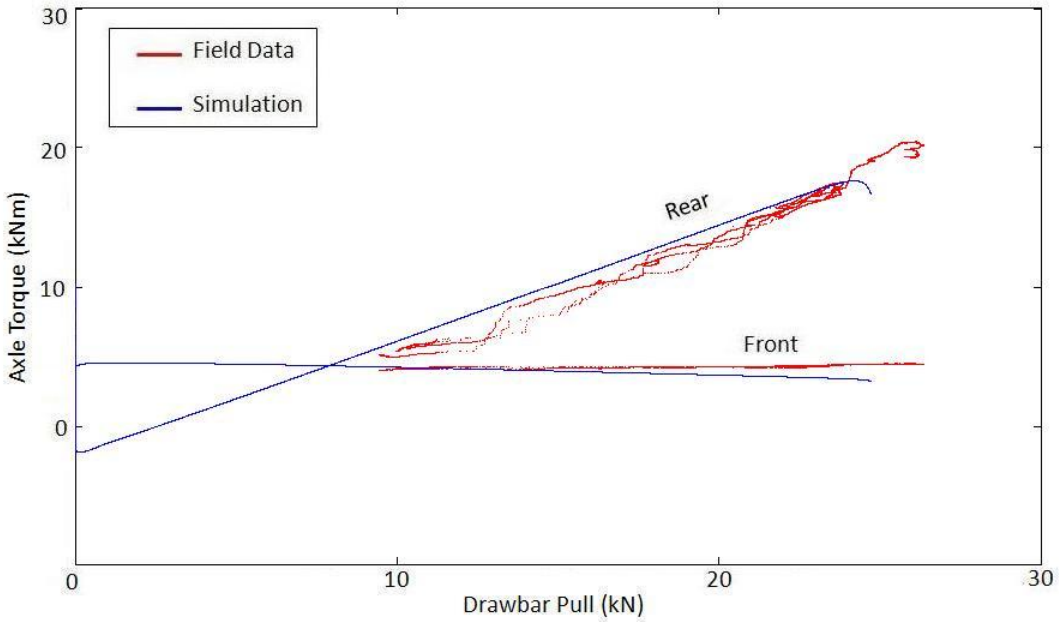

Figure 5.13: The relationship between the torques transmitted through the front and rear axles and drawbar pull; a comparison of field data, collected on the sandy test site at +10 % lead ratio operating downhill, and results from the Easy 5 simulation using the *Simple Tire* model.

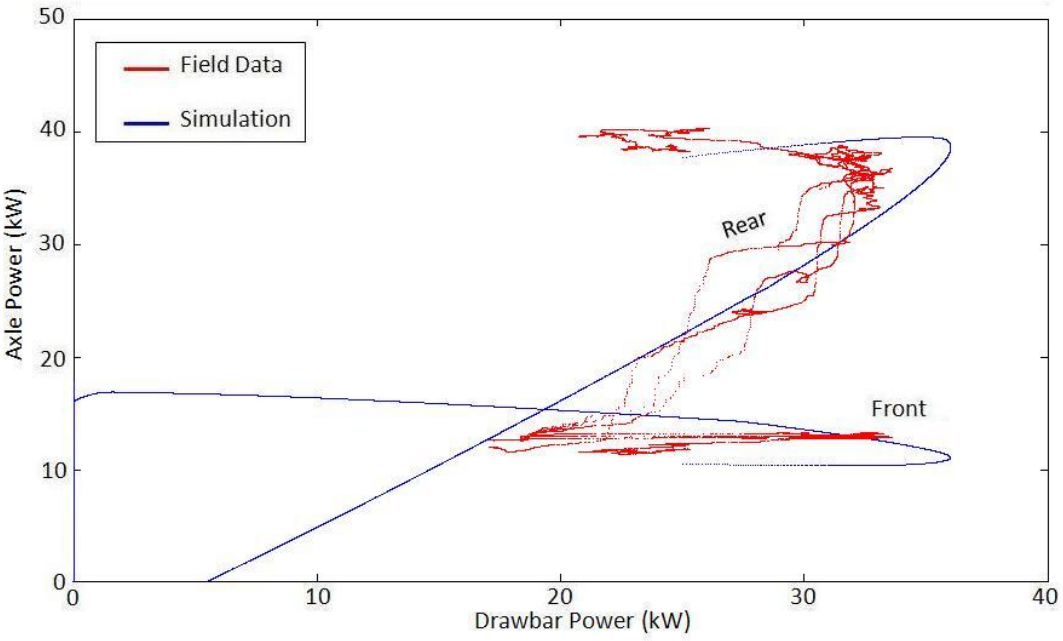

Figure 5.14: The relationship between the powers transmitted through the front and rear axles and drawbar power; a comparison of field data, collected on the sandy test site at -4 % lead ratio operating downhill, and results from the Easy 5 simulation using the *Simple Tire* model.

5.10 Testing of an alternative tyre model

In an effort to better relate the data generated by the Easy 5 simulation to measurable tractor and field properties, a second model was constructed using the *Off Highway Tyre* model. Figures 5.15 and 5.16 show data generated using both models and field data for comparison. These figures demonstrate that, like the *Simple Tire* model, the *Off Highway Tire* model is capable of predicting the forms and magnitudes of the relationships between axle torque and drawbar pull and axle power and drawbar power, but the fit of the data to the field data is no better and in many places worse than that generated by the *Simple Tire* model.

The Off Highway Tire model uses as one of its inputs the soil cone index under the wheels. As noted by Dwyer (1977) and Besselink (2003) the passage of the front wheels alters the properties of the soil and thus the soil conditions under the rear wheels are not the same as those under the front. Measurement in the field (Figure 3.15) showed that considerable variability existed in the cone indices of the soil on both test sites. Experimentation with different values of soil cone index in the model showed that this parameter had a significant effect on the data generated using the *Off Highway Tire* model. The data shown in Figures 5.15 and 5.16 was generated using a soil cone index of 160 kN/m^2 for the front axle and 350 kN/m^2 for the rear. However, the soil cone index value for the front wheels is in the lower range of those measured in the field (Figure 3.15), and no physical measurements were taken of the soil cone index of the soil between the front and rear wheels, thus the rear axle value is purely conjectural.

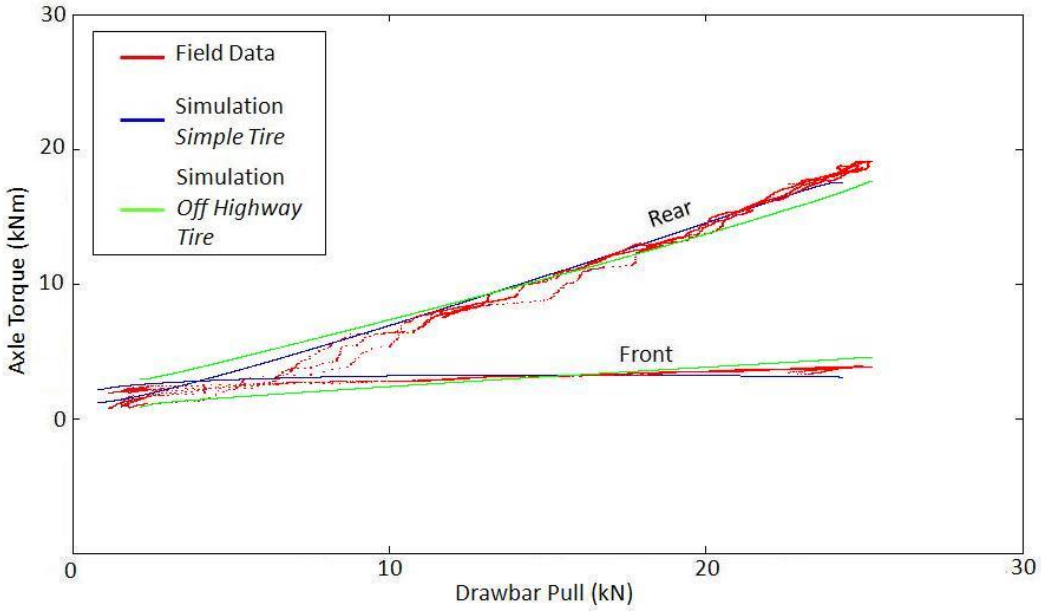

Figure 5.15: The relationship between the torques transmitted through the front and rear axles and drawbar pull; a comparison of field data, collected on the sandy test site at +10 % lead ratio operating downhill, and results from the Easy 5 simulation using the *Simple Tire* and *Off Highway Tire* models.

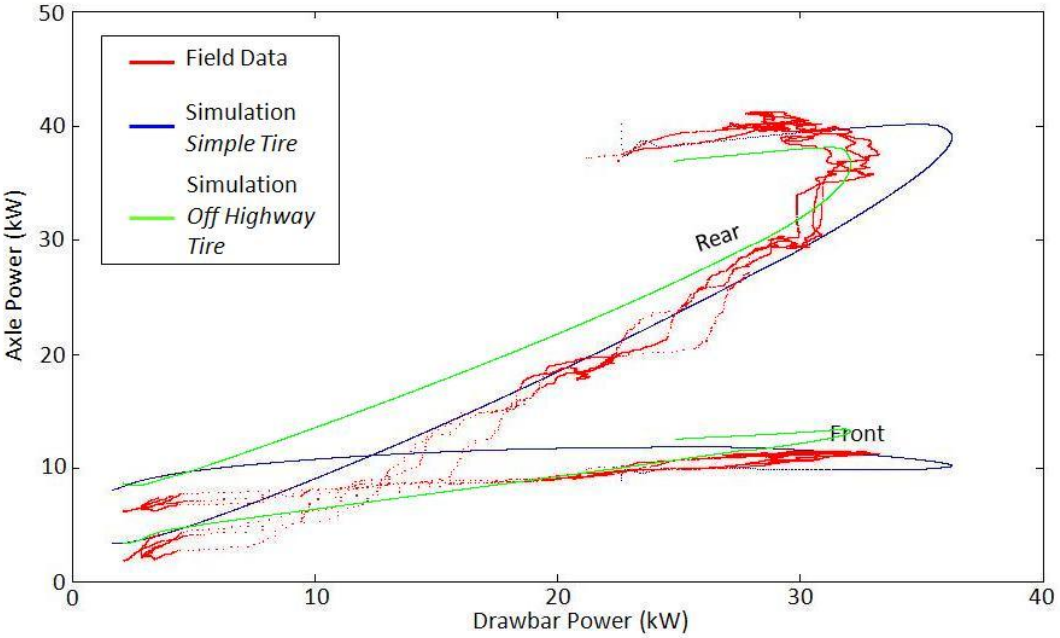

Figure 5.16: The relationship between the powers transmitted through the front and rear axles and drawbar power; a comparison of field data, collected on the sandy test site at +2 % lead ratio operating downhill, and results from the Easy 5 simulation using the *Simple Tire* and *Off Highway Tire* models.

5.11 Conclusions

It is possible using MSc Easy 5 and the Ricardo library of powertrain components to generate predictive axle torque and power data that is qualitatively and quantitively similar to data gathered through field experiments. The simulation was capable of predicting the response of the front axle torque to increasing drawbar pull to within 0.083 Nm/N and the rear axle to within 0.035 Nm/N. The simulation consistently overestimated drawbar power by between 6.2 % and 8.7 %. The simulation estimated front axle power to within 0.2 kW and rear axle power to within 1.1 kW.

Comparison of predictive data generated using the *Simple Tire* and *Off Highway Tire* showed that the latter offered no advantage over the former in terms of the accuracy of data generated, despite being a far more complex model.

When applied to the *Off Highway Tire* model, the variability of soil cone index data collected in the test fields used in this project made it an unreliable predictor of axle torques and powers.

6.0 Discussion

6.1 Instrumentation and field trials

The instrumentation system fitted to the TS90 was intended to be a permanent installation for teaching and research purposes. With that in mind the installation was undertaken in a more robust manner than might have been the case for a short programme of field trials. However, the installation of torque sensors in the transmission of an agricultural tractor does not lend itself to rapid implementation, requiring as it does the removal of the main gearbox from the centre of the tractor, an operation that necessitates splitting the machine into four major assemblies; engine and front axle, main gearbox, rear axle and cab. This level of mechanical intervention must form a considerable barrier to authors considering this type of research, and may go someway towards explaining the relative dearth of material in this field.

6.1.1 The use of ABB Torductors for torque flow research

In operation the Torductors proved to be extremely robust and reliable throughout the field trial programme and beyond. While the complexity of the design and installation process for the Torductors added considerably to the preparation time for the experimental phase of this research, in operation they proved to be entirely problem free, working affectively as soon as they were switched on.

One feature of the Torductor that made its application for this type of research more complicated was that it used the shaft through which the measured torque was passing as an integral part of the sensor. The

instrumented shafts therefore had to be precisely manufactured By ABB from their own specified material, a requirement that added considerably to the preparation time for the field trials. The instrumented shafts and sensor housings also had to be precisely located and restrained, particularly in the axial direction. One of the criteria that led to the selection of the TS90 for this research was the architecture of the transmission, which included front and rear output shafts restrained by deep-groove roller bearings, which therefore met the location tolerance requirements of the Torductor. This was found not to be the case in many of the other tractors considered for this project.

Authors who consider repeating or developing this research should give careful consideration to the locations they choose for their torque measurements. Future work could perhaps measure torque at the wheel hubs rather than within the transmission. This would allow a better understanding to be developed of the flow of power across the axles as well as between them. It might also make the task of instrumenting the vehicle slightly easier, although the additional space constraints associated with working within the hub would have to be considered carefully.

6.1.2 The use of the Pegasem GSS20 microwave speed sensor

The Pegasem GSS20 microwave speed sensor proved somewhat problematic in operation. The introduction by the sensor of low frequency interference into the forward speed data was mitigated through filtration in the post processing phase, but this requirement added an additional level of processing to the data analysis phase of the experimental programme. The sensor also proved to be incompatible with the Isaacs data loggers, which in

the field were unable to meet the sensor's power requirements, necessitating the construction of an additional wiring loom to power the sensor.

6.1.3 Measuring engine speed using Oxford TS180 speed sensors

The original instrumentation design utilised an Oxford TS180 hall-effect speed sensor which was inserted into a tapped and threaded hole in the bell-housing extension plate so as to detect the passage of the teeth of the starter ring on the engine flywheel. It was found that this approach would not work as the flywheel generated a considerable parasitic magnetic field, which interfered with the hall-effect probe. This problem was overcome by moving the speed sensor to the front of the engine where it measured the speed of the crankshaft.

6.1.4 Validity of data

Each of the sensors used to collect the experimental data presented here was calibrated before use (Appendices 3.3 and 3.4 and Section 3.3) against independently verifiable metrics. Data collected in repeated experiments exhibit a low level of variability, and low LSDs and SEDs, indicating that both the experimental method was repeatable, and the instrumentation system had a high degree of repeatability. The data from experiments with different treatments exhibit distinct separation of data, indicating that the instrumentation system was capable of distinguishing between the parameters tested.

One obvious concern with the experimental method employed in these field trials is the introduction of additional variables between treatments. The main

route for this un-intended variability is in the choice of tyres used to change the lead ratio between treatments. This effect was minimised by using tyres with the same tread pattern and section width, from the same manufacturer, of similar age and wear and inflated to the same pressure. Thus the only variables affected by changing the tyres was a slight variation in mass, which amounted to 89 kg (1.9% of the overall vehicle mass) difference between the lightest (+2% lead ratio = 702 kg) and heaviest (-4% lead ratio = 791 kg) combinations, and a change in the diameter and thus contact patch length of the tyres. An alternative approach, that would have negated this effect, would have been to use a single set of tyres and change the ratio of the front axle drive. However, in practice this method would not have been practical without making significant changes to the architecture of the tractor's transmission. While this method would have eliminated the possibility that the data could be influenced by changing the tyre contact patch length, in practice an operator would be more likely, either deliberately or accidentally, to change lead ratio by changing tyre sizes.

6.1.5 Choice of test site

With hindsight it would have been preferable to find a flat sandy test site on which to perform field trials. This would have eliminated the additional complexity introduced into the data analysis and processing phase of the experimental programme associated with the introduction of an additional and superfluous factor. However, at the time the field trials were conducted the sandy site used was the only one available on the Harper Adams estate.

6.1.6 Using a second tractor as a rolling load

Using a second tractor as a rolling load is a well proven method that has been used by many previous authors. The key advantages of this method are that it is straightforward to set up, does not require any bespoke experimental hardware, since the influence of the load tractor can be measured entirely via a drawbar loadcell and can simply be driven to the trial site. The disadvantages of this method are that it requires a second operator who must have a degree of skill in operating the machine and an understanding of the experimental programme, and it is susceptible to the introduction of random variation due to changes in operating method or physical parameters like fuel load or traction conditions. It would be beneficial for future field trials of this type to acquire or construct a system that could apply a constant drawbar load or maintain a set forward speed in a controlled and repeatable manner. Such a system would have to meet the requirements of portability and robustness that the current load tractor system provides.

6.2 Discussion of results

The features of the experimental data collected in this project were discussed in detail in Chapter 4. This section explores some possible theories to explain the more notable findings of the research.

6.2.1 Power delivery efficiency and transmission wind-up

Perhaps the most unusual aspect of this work, compared to other published literature in this field (Table 2.1), is that the experimental study was designed from the outset to study the power delivery efficiency of the subject tractor.

While a number of previous works have focused on understanding the tractive efficiency of four-wheel-drive systems, the effect of lead ratio on tractor performance is inherently related to the phenomena of transmission wind-up and re-circulating power, which by their very nature must affect the efficiency of the whole vehicle system, i.e. the power delivery efficiency of the vehicle rather than the tractive efficiency of the axles, which neglects the influence of transmission behaviour on the efficiency of the tractor. Simply put, if the transmission winds-up, as a result of a mismatch between front and rear wheel peripheral speeds, the forces between gear teeth within the transmission will be higher, which will create more friction and thus more heat, which will dissipate a greater proportion of the power flowing through the transmission.

Given the relative elasticity of components in the driveline, it seems likely that the major energy store in the wound-up tractor transmission is actually the tyres, which by stretching circumferentially can absorb a considerable quantity of torque. The magnitude of the energy that can be stored in this way is limited by the traction the tyres can develop; torque will build up in the tyre until the tractive limit is reached, at which point the tyre will slip. This would seem a logical explanation for the differences in power delivery efficiency noted between the sandy and clay test sites (Sections 4.2.5 and 4.2.6); since the limit of traction on the stronger clay soil is higher than on the sandy soil, the tyres can store more energy before slipping and thus generate a greater degree of wind-up.

6.2.2 Optimum lead ratio under different terrain conditions

A key finding of this work is that the optimum lead ratio changes depending on terrain conditions; in this case the -4% lead ratio producing the highest drawbar pull, drawbar power and power delivery efficiency on the sandy test site, and the +2% lead ratio producing the highest of each on clay. Rosa *et al* (2000) noted that the traction conditions for the front wheels of a tractor are different to those of the rear wheels. Dwyer *et al* (1977) partially characterised this phenomenon as the *multi-pass effect*, i.e. the change in the properties of the soil encountered by the rear wheels that is created by the passage of the front wheels, thus for any given field the front and rear wheels will be operating under a different set of conditions.

The two soil conditions tested in this study were very different from one another; the sandy test site had a soil with very little cohesion or structure, the organic matter in the soil was broken up first with a cultivator and then a power harrow thus minimising the structural effects of any buried root structure or plant stalks; the clay site by contrast had a much more cohesive soil, which was additionally bound together by a layer of stubble and the undisturbed root system of the recently harvested crop. These differences in surface condition had two important effects on the tractive behaviour of the tractor; firstly remoulding on the clay site was very limited; the passage of the tyres left cleat marks but no ruts, while the sandy site exhibited significant rut formation; secondly the soil at the clay site was much stronger and thus able to sustain higher levels of traction than the very weak soil at the sandy site. It would seem then that the clay soil, being stronger and better able to sustain higher levels of traction, favoured the +2% lead ratio because it was the

treatment that produced the most closely matched peripheral wheel speeds and thus the treatment that produced the lowest level of transmission wind-up. The soil at the sandy site, by contrast, being much weaker was less able to produce transmission wind-up and thus favoured the lead ratio treatment that produced the highest tractive efficiency for each axle.

6.2.1 The flow of power through the front axle

The data gathered in field experiments during this project showed that the front axle of the tractor transmitted no more than 15 kW under the conditions tested. Clearly the experimental programme of this project was confined to a limited range of surfaces and operations. The most compelling explanation for this phenomenon is that drawbar pull has a linear relationship with weight transfer; each additional Newton of drawbar pull transferring 0.25 N of normal load from the front axle to the rear. Thus as drawbar pull increases, the front axle's ability to generate traction and thus torque and power reduces, while the rear axle's ability to generate traction increases at the same rate.

This finding does suggest that scope might exist to optimise the design of the front axle drive on front-wheel-assist tractors. These modifications may simply take the form of a reduction in the quantity of material used in the construction of the front axle drive, but some benefit could be derived from replacing the mechanical drive with an electric motor and appropriate control system. Such a system would allow the lead ratio to be controlled and optimised in real time, eliminating the problems of power re-circulation and negative torque noted in Sections 4.3 and 4.4, while also allowing the

adoption of a system similar to the *Kubota Bi-speed Turn* system described by Ikegami *et al* (1990).

6.2.2 The effect of lead ratio on the proportion of power flowing to the front and rear axles

Lead ratio affects the balance of both the torque and power flowing through the front and rear axles; an increase in lead ratio being associated with an increase in both torque and power at the front axle. However, increasing the proportion of power transmitted by the front axle was not associated with any improvement in power delivery efficiency.

6.3 Relevance and applicability of this work

While this work was primarily focused on the performance of an agricultural tractor working in field conditions, it also has relevance to other types of vehicles that employ multi-axle drive with fixed speed ratio inter-axle couplings. Many such vehicles are employed in the off-highway setting, in particular by the construction and military sectors.

The changes in power delivery efficiency associated with changes in lead ratio found in this study are both statistically significant and economically and environmentally important. While changes in power delivery efficiency of a few percent might seem small, in economic terms where profit margins are small and fuel prices are increasing, they could have considerable importance to the agricultural vehicle industry. However, while this report has demonstrated the existence of these phenomena, considerable further work

is required before a definitive set of operational guidelines could be offered to tractor manufacturers or operators.

6.4 Reflections on the significance of this work in improving the efficiency of off-highway vehicles

The data presented in Sections 4.2 and 4.3 has demonstrated that a clear link exists between lead ratio and power delivery efficiency, a finding which is consistent with those of Wong (1970 and 2001) and Wong *et al* (1998, 1999 and 2000). Comparison of the power delivery efficiency data collected while operating on clay and sand indicate that the magnitude of the effect lead ratio has on power delivery efficiency is dependent on the running surface. On the sandy soil operating at -4% lead ratio increased power delivery efficiency by 3.1% compared with the +2% lead ratio case, which exhibited the lowest power delivery efficiency of the three lead ratios tested on that soil. However, on the clay soil the +2% lead ratio case had the highest power delivery efficiency of the three lead ratio cases tested at 4.9% higher than the +10% lead ratio case, which had the lowest power delivery efficiency on that soil. It is apparent therefore that the optimum lead ratio changes depended on the condition of the soil on which the machine was being operated.

Comparison of the power delivery efficiency data presented in Section 4.2, and the data on the power consumed within the main gearbox in Section 4.3.6, indicates that the optimisation of the operation of the constant displacement hydraulic pump has the potential to yield greater improvements in the efficiency of this particular tractor than does the optimisation of lead ratio. Field tests showed that changing lead ratio produced at most a 5 kW

difference in the magnitude of power lost in the transmission (Figure 4.3.14), while the hydraulic pump consumed between 8.5 and 14 kW (Section 5.3.6). Thus developing a control mechanism that allowed the hydraulic pump to be disengaged during phases of operation where it was not being used could potentially reduce transmission power losses to a greater degree than would optimising lead ratio. However, simply disengaging the hydraulic pump would only be possible under a limited range of conditions, i.e. where the hydraulic services were inoperative, for example driving straight ahead in a single gear and not using the three point linkage. Full optimisation of the use of hydraulic power on this tractor would require the installation of a variable displacement pump, whose output could be matched automatically to the instantaneous power requirements of each task.

6.5 Potential uses of the ABB Torductor in off-highway vehicles

Through the course of this project the ABB Torductor has demonstrated itself to be a robust and reliable sensor, capable of working effectively inside the transmission of an agricultural tractor. The ability of this sensor to work reliably on shafts whose positions were controlled by the production standard bearings suggests that the ABB Torductor could easily be incorporated into production vehicles, without the need for substantial modification to the other components in the transmission.

There are a number of areas in which the ability to measure torque in real time could be of benefit to the operation of off-highway machines.

- There is scope to optimise the relationship between axle and drawbar powers in real-time, as indicated by the data in Section 4.3.4.
- On harder surfaces four-wheel-drive systems are prone to developing negative power flow in one axle. This phenomenon is both inefficient, since it actually opposes the forward motion of the vehicle, and potentially damaging to the transmission since it causes rapid torque reversals. The ABB Torductor could be employed as part of a four-wheel-drive control system to sense when the torque in one axle was tending towards zero, and to disconnect power from it, thus improving the overall efficiency of the machine.

6.6 Using MSc Easy5 to model torque and power flow

The data presented in Chapter 5 demonstrates that it is possible to use MSc Easy5 to produce a simulation of a tractor operating in the field which is qualitatively similar to experimental measurement of the same tractor. Some work has already been conducted using the simulation described in this report to study experimental treatments that could not be produced in the field; these include running the tractor with a 50:50 weight distribution and running the tractor with the hitch set at ground level. These preliminary studies, which will be reported in greater depth in later papers, suggest that front axle power flow is indeed strongly influenced by static and dynamic weight distribution.

7.0 Conclusions and recommendations for further work

7.1 Conclusions

- This project demonstrated that the ABB Torductor-S torque sensors were a reliable instrument for measuring in real-time, the flow of torque between the engine and the front and rear axles of a four-wheel drive agricultural tractor. However, while the sensors themselves are extremely robust, accurate measurement relies on controlling the relative positions of the instrumented shafts and sensor housings, care must therefore be taken to ensure that the instrumented shafts are located with an axial float of less than +/- 0.5 mm and concentricity between shaft and sensor housing of less than +/- 0.2 mm.
- Power delivery efficiency was affected by lead ratio. The optimum lead ratio for both maximum power delivery efficiency (Section 4.2.5) and drawbar pull (Section 4.2.4) was a function of soil type. On the sandy soil the -4% lead ratio had the highest power delivery efficiency, which was 3.1% higher than the +2% lead ratio which was the lowest on that soil. On the clay soil the +2% lead ratio had the highest power delivery efficiency, which was 4.9% higher than the +10% lead ratio which was the lowest on that soil. Of the three lead ratios tested, none provided optimal power delivery efficiency on all surfaces. The 3.1 % increase in power delivery efficiency between the +2 % lead case and the -4 % lead case when operating on the sandy test site represents a saving that may be sufficiently large to warrant the cost of developing

and manufacturing a system to allow an operator to quickly adjust the lead ratio of tractors that operate on a range of different soils.

- The front axle of the tractor transmitted an almost constant amount of power and torque, regardless of the drawbar pull or power being generated. Any additional torque and power was transmitted via the rear axle alone. The maximum amount of powered transmitted by the front axle was observed to be 14.7 kW, when operating on clay, and 13.1 kW when operating on sand, both at +10% lead. The front axle transmitted a maximum of 5 kNm of torque, when operating on clay and 4.5 kNm, when operating on sand, again both at +10% lead. The maximum response of the front axle torque to increasing drawbar pull was 0.12 Nm/N, which occurred at -4% lead when operating on clay. The minimum response of the rear axle torque to increasing drawbar pull was 0.72 Nm/N, which also occurred at -4% lead when operating on clay.
- On hard surfaces it was observed that interaction between the front and rear axles could cause one axle to transmit more power than was actually being delivered by the engine at that point. This phenomenon was observed in both the front axle when operating at +2% and +10% lead and in the rear axle when operating at -4% lead. The highest magnitude of power re-circulation observed occurred at -4% lead, when the power being transmitted by the rear axle exceeded that being supplied by the engine at the time by 20 kW (Figure 4.4.2).
- The fixed displacement hydraulic pump fitted to this tractor absorbed up to 14 kW of power, representing 21% of the tractor's rated engine

power. These losses were observed under conditions where no demand for hydraulic power was being made. This magnitude of power loss was greater than the difference in power losses between the best and worst performing lead ratio cases**.**

- Computer modelling using MSc Easy 5 produced simulation data that was qualitatively consistent with experimental data on a limited range of surfaces (Section 5.9). Data produced using the friction based *Simple Tire* model was closer to measured values than that produced using the *Off Highway Tire* model (Section 5.10). Further experimentation is required to fully prove Easy5 as a tool for predicting the flow of torque and power in agricultural tractors.

7.2 Recommendations for Further work

As with almost scientific endeavour the completion of this work gives rise to a number of related questions.

7.2.1 Understanding what effect using a mounted, rather than trailed, implement has on the flow of torque and power

An important aspect of agricultural tractor performance that was not addressed by this work was the effect of using a mounted, rather than trailed, implement on the flow of torque and power in the transmission. The dynamics of a mounted implement are very different to those of a trailed load, and the ability of a mounted implement to transfer weight on to the front axle is likely to have a significant effect on the balance of power flowing through the front and rear axles. However, while measuring the behaviour of a mounted implement is a far more complex task than a trailed load, this aspect of tractor performance has significant implications for the efficiency of tillage operations.

7.2.2 Understanding the effect of changes in soil property, caused by the passage of the front wheels, on torque and power flow

Modelling using Easy 5 suggested that the change in soil conditions caused by the passage of the front wheels has a significant effect on the flow of power between the front and rear axles; a finding that supports the work of Dwyer *et al* (1977). However, the change in soil conditions following the passage of the front wheels was not quantified under field conditions. It would therefore be useful, in order to develop a better understanding of the influence of changing soil properties, to construct an experiment in which it

was possible to measure the soil properties between the front and rear axles, and correlate that data to axle torque and power data.

7.2.3 Investigating whether the findings of this work are scaleable

The experimental work in this paper was conducted on what might be considered a medium size European tractor. It is unclear both from experimental results and the published literature whether the behaviour of this tractor can be scaled to the larger machines now commonly employed for tillage operations on European farms. Further work is required to validate the findings of this project on other larger tractors.

7.2.4 Investigating how torque flow under braking effects the safety of front-wheel-assist tractors

The data collected while operating on the road indicated that the braking system of front-wheel-assist tractors, which retard the front wheels by engaging the front-wheel-drive clutch, might adversely affect brake performance. The data collected in this project was insufficient to provide definitive evidence, and further data should be collected to develop a better understanding how torque flow affects brake performance.

7.2.5 Investigating the effect of changing lead on transmission behaviour at component level

It is apparent from the data collected in this project that interaction between the front and rear axles affect the power delivery efficiency of the tractor. However, the design of the instrumentation system employed in this study did not allow the exact mechanism by which power delivery efficiency was affected to be studied in detail. This report presents a view of power delivery

efficiency at a macro-vehicle level, but it is felt that to develop a greater understanding of the underlying mechanisms that affect power delivery efficiency at the component level further studies are required. One potential avenue for investigation is to study the forces acting on gear teeth within the four-wheel-drive power split gears at a range of lead ratios. This would help to develop an improved understanding of how transmission wind-up actually affects the forces between gears and thus the parasitic power consumed by them.

In a similar vein, it would also be useful to study the stresses and strains acting on the tyres at a range of lead ratios. This would help to quantify the amount of energy that is stored in or dissipated by the tyres when wind-up occurs.

7.2.6 Further modelling using MSc Easy5

As was mentioned in Section 6.6, work is underway using MSc Easy5 to develop both a more refined model of the instrumented TS90 and to use that model to develop an improved understanding of the effect of lead ratio on tractor behaviour. At this stage that model is at the macro-vehicle level presented in this report, but the potential exists within the software to refine the simulation to the point where it can produce component level predictions for the behaviour of the transmission. That work would of course have to be validated by further field and laboratory trials.

8.0 References

ABB. 2008a. Ingaende Axel. [Drawing] Un-published: ABB AB.

ABB. 2008b. House for front wheel driveshaft. [Drawing] Un-published: ABB AB.

ABB. 2008c. House for input shaft. [Drawing] Un-published: ABB AB.

ABB. 2008d. House for output shaft. [Drawing] Un-published: ABB AB.

Anon. 2008. ABB Torductor-S Design Guidelines for Motorsport. Vasteras, Sweden: ABB AB

Bashford, L. L., Von Bargen, K. 1985. Front Wheel Assist: Does it Pay Off? *Agricultural Engineering*, v 66, n 5, May, 1985, p 7-9

Bashford, L. L., Woerman, G. R., Shropshire, G. J. 1985. Front Wheel Assist Tractor Perfomamce in Two and Four-Wheel Drive Modes. *Transactions of the ASAE*, v 28, n 1, Jan-Feb, 1985, pp 23-29

Bashford, L. L., Von Bargen, K, Esch, J. H. 1987. Torque in Agricultural Tractor Axles. *Transactions of the Society Automotive Engineers*, Paper Number 871607.

Besselink, B. C. 2003. Tractive efficiency of four-wheel-drive vehicles: an analysis for non-uniform traction conditions. *Journal of Automobile Engineering*, 217, 363-374.

Brenninger, M. 1999. Four-Wheel-Driven Tractors and the Effect of Circulating Power. *Proceedings of the 13th International Conference of the ISTVS.* 1999. Sept 14-17, Munich, Germany. pp613-620

Bottasso, F., Bandel, P. 1988. Four-wheel drive cars without intermediate differential gear: impact on tire tread wear. *Tire Science & Technology*, v 16, n 3, Jul-Sep, 1988, pp 187-197

Brixius, W. W. 1987. Traction Prediction Equations for Bias Play Tyres. Paper 87-1622 – American Society Agricultural Engineers.

CNH. 1998. TS Range Training: Service Training. [Drawing] Un-published: Case New Holland

Crolla, D. A. 1981. An Analysis of Off-Road Vehicle Steering Behaviour. *Proceedings of the 7th Annual ISTVS Conference.* 1981. Calgary, Canada. pp1265-1290

Derbyshire, H. 1993 Shaft – transmission input. Part number 82010653. [Drawing] Un-published: Case New Holland

de Souza, E.G., Milanez, L.F. 1991. Prediction of tractor performance on concrete. *Transactions of the ASAE*, v 34, n 4, Jul-Aug, 1991, pp 727-732

Dudzinski, P. A. 1986. The problems of multi-axle vehicle drives. *Journal or Terramechanics,* 23 (2), 85-93.

Du Plessis, H. L. M., Marais, C. L. 2003. Computer modelling for the traction performance of four wheel drive tractors. *Proceedings of the 9th European Conference of the ISTVS.* 2003. Sept 8-11, Harper Adams University College, UK. pp93-107

Dwyer, M. J., McAllister, M., Evernden, D. W. 1977. Comparison of the Tractive Performance of a Tractor Driving Wheel During Its First and Second Passes in the Same Track. *Journal of Terramechanics*, v 14, n 1, Mar, 1977, pp 1-10.

Erickson, L. R., Larsen, W. E. 1983. Four Wheel Drive Tractor Field Performance. Transactions of the American Society of Agricultural Engineers, v26, n5, Sep-Oct 1983, pp1346-1351.

Goering, C. E., Hansen, A. C. 2005. Engine and Tractor Power. 4th edition. St Joseph, Michigan: American Society of Agricultural Engineers.

Ikegami, S., Matsushita, Y., Osuga, M., 1990. Kubota's new 'BI-SPEED TURN' mechanism. *SAE (Society of Automotive Engineers) Transactions*, v 99, n Sect 2, 1990, pp 523-530

Jenane, C., Bashford, L.L., 1992. Field evaluation of tractive efficiency using a wireless torque meter. *Applied Engineering in Agriculture*, v 8, n 2, Mar, 1992, pp 141-145

Khalid, M., Smith, J. L. 1981. Axle torque distribution in 4wd tractors. *Journal of Terramechanics,* 18 (3), 157-167.

Kim, D. C., Ryu, I. H., Kim, K. U. 2001. Analysis of Tractor Transmission and Driving Axle Loads. *Transactions of the ASAE*, v 44, n 4, Jul-Aug, 2001, pp 751-757

Komandi, G. 2006. Soil vehicle relationship: The peripheral force. *Journal of Terramechanics,* v 43, n 2, April, 2006, pp 213-223

Lach, B. 1997. Tyre Inflation Pressure Control. In: *The proceedings of the 7th European Conference of the International Society for Terrain –Vehicle Systems Ferrara, Italy 8-10 October 1997.*

McLaughlin, N. B., Heslop, L. C., Buckley, D. J., St Amour, G. R., Compton, B. A., Jones, A. M., Van Bodegom, P. 1993. A General Purpose Tractor Instrumentation and Data Logging System. Transactions of the American Society of Agricultural Engineers, v36, n2, March-April 1993, pp 265 – 273.

Morgan, D. L., Bashford, L. L., Kocher, M. F., Grisso, R. D. 2000. Summary of OECD Test 1829 – Nebraska Summary 294 New Holland TS90 Diesel 24

Speed Diesel. Agricultural Research Division Institute of Agriculture and Natural Resources University of Nebraska–Lincoln.

Murillo-Soto, F., Smith, J. L. 1977. Traction Efficiency of 4wd Tractors: A Model Study. *Paper - American Society of Agricultural Engineers for Winter Meet*, Chicago, IL, USA, Dec 13-16 1977. Paper Number 77-1522

Murillo-Soto, F., Smith, J. L. 1978. Push-Pull Characteristics of the 4WD Tractor. Proceedings of the 1978 summer meeting of the American Society of Agricultural Engineers. Utah State University, Logan, Utah. June 27-30, 1978. Paper number 78-1041

Musonda, N. G., Bigsby, F. W. 1985. Traction characteristics of a four-wheel drive tractor. Proceedings of the 1985 Summer Meeting of the American Society of Agricultural Engineers, Michigan State University, East Lansing, June 23-26, 1985. Paper No. 85-1046.

Pacey, D. A., Walker, H. S. 1996. Modelling the dynamics of vehicles with differential speed steering. *Transactions of the ASAE*, v 39, n 2, 1996, pp 431-434

Pegasem. 2005. Pegasem GSS series ground speed sensors. Un-published: Pegasem Gmbh.

Pickthall, T. 2009. Photograph of the instrumented TS90 tractor and the Case load tractor operating on the sandy test site. [Photpgraph] Un-published.

Ricardo. 2005a. Simple Tire. Ricardo Powertrain Library – Version 5.1 User's Guide. Un-published: Ricardo

Ricardo. 2005b. Off Highway Tire. Ricardo Powertrain Library – Version 5.1 User's Guide. Un-published: Ricardo

Ramji, K., Goel, V. K., Saran, V. H. 2002. Stiffness properties of small sized pneumatic tyres. *Proceedings of the Institution of Mechanical Engineers, Part D: Journal of Automobile Engineering*, v 216, n 2, 2002, pp107-114

Renius, K. Th. 1999. Generation Change in Tractor Drivelines – A Review. *Proceedings of the 13th International Conference of the ISTVS.* 1999. Sept 14-17, Munich, Germany. pp 495 – 502

Rosa, U. A., Upadhyaya, S. K., Chen, P. 2000. Modelling and Verification of an Auto Front-Wheel-Drive System. *Transactions of the ASAE*, v 43, n 1, Jan-Feb 2000, pp 23-29.

Sato, K., Yamashita, J., Kanaya, T., Fukumoto, Y. 1999. Running Performance of Hillside Terrain Four-Wheel-Drive Farming Vehicles with Built-in Torque-Proportion-Type Centre Differential. *Proceedings of the 13th*

International Conference of the ISTVS. 1999. Sept 14-17, Munich, Germany. pp 629-636

Shropshire, G. J., G. R. Woerman and L. L. Bashford. 1983. A Microprocessor Based Instrumentation System for Traction Studies. ASAE Paper No. 83-1048. ASAE, St. Joseph, MI 49085.

Snyder, K. A., Buck, N. L. 1990. Axle Instrumentation for Tractive Performance Parameter Measurement. *Transactions of the ASAE*, v 33, n 1, Jan-Feb 1990, pp 290-297

Snyder, K. A., Buck, N. L. 1990. Capacitively Coupled Telemetry for Rotating Shafts. *Transactions of the ASAE*, v 34, n 1, Jan-Feb 1991, pp 296-300

Sohne, W. 1968. Four-Wheel Drive or Rear-Wheel Drive for High Power Farm Tractors. *Journal of Terramechanics.* v5, no3, pp 9-28.

de Souza, E.G., Milanez, L.F. 1991. Prediction of tractor performance on concrete. *Transactions of the ASAE*, v 34, n 4, Jul-Aug, 1991, pp 727-732

Srivastava, A. K., Goering, C. E., Rohrbach, R. P., Buckmaster, D. R. 2006. Engineering Principals of Agricultural Machines. 2nd edition. St Joseph, Michigan: American Society of Agricultural and Biological Engineers.

Steinkampf, H. 1972. Die Auswirkungen untershieldlicher Radumfangsgeschwindigkeiten der Rader eines Ackerschleppers auf seine

Zugfahigkeit. (The Effects of Different Peripheral Tyre Speeds of an agricultural tractor on its abilities to pull.) Grundlagen der Lantechnik 22 (1972) No.6 pp 166-170.

Summers, J. D., Ekstrom, R. E., Von Bargen, K. 1986. Development of a tractor performance simulation model. *Transactions of the ASAE*, v 29, n 3, May-June 1986, pp 661-666

Van De Vegte, J. 1994. Feedback Control Systems 3rd ed. New Jersey, USA: Prentice Hall.

Vantsevich, V. V. 2007. Multi-wheel drive vehicle energy/fuel efficiency and traction performance: Objective function analysis. *Journal of Terramechanics,* v 44, n 3, July, 2007, pp 239-253

Wallin, C., Gustavsson, L. 2002. Non-Contact Magnetostrictive Torque Sensor – Opportunities and Realisation. *Proceedings of the VDI/VDE-IT 6th International Conference – Advanced Microsystems for Automotive Applications.* 2002. March 21-22. Berlin, Germany. pp 184 - 195

Wang, G., Kushwaha, R.L., Zoerb, G.C., 1989. Traction performance of a model 4WD tractor. *Canadian Agricultural Engineering,* v 31, n 2, Jul, 1989, pp 125-129

Wendel, T. N. J. 1989a. Shaft – transmission output. Part number 81866598. [Drawing] Un-published: Case New Holland

Wendel, T. N. J. 1989b. Countershaft – transmission (F/W/D). Part number 81864852. [Drawing] Un-published: Case New Holland

Wismer, R. D. 1982. Soil dynamics a review of theory and application. Conference Paper - Society of Automotive Engineering Earthmoving Industry Conference, Peoria, Illinois. April 19-21, 1982. Paper number 820656.

Wismer, R. D., Luth, H. J. 1972. Off-road traction prediction for wheeled vehicles. Paper 72-619. American Society of Agricultural Engineers

Woerman, G. R., Bashford, L. L. 1983. Performance of a Front Wheel Assist Tractor. Conference Paper - American Society of Agricultural Engineers 1983 Winter Meeting, Chicago, IL, USA,

Woerman, G. R., Bashford, L. L. 1984. How Much Does Front Wheel Assist Really Help? *Agricultural Engineering*, v 65, n 4, Apr, 1984, pp 31-35

Wong, J. Y. 1970. Optimization of the tractive performance of four-wheel-drive off-road vehicles. *Transactions of the Society Automotive Engineers*, 79, 2238–2245.

Wong, J.Y., McLaughlin, N.B., Knezevic, Z., Burtt, S. 1998. Optimization of the tractive performance of four-wheel-drive tractors: Theoretical analysis and experimental substantiation*. Proceedings of the Institution of Mechanical*

Engineers, Part D: Journal of Automobile Engineering, v 212, n 4, 1998, pp 285-297

Wong, J. Y., Mc Laughlin, N. B., Zhinwen, Z., Jianqiao, L., Burtt, S. 1999. Optimizing Performance of Four-Wheel Drive Tractors – Theory and Practice. *Proceedings of the 13th International Conference of the ISTVS.* 1999. Sept 14-17, Munich, Germany. pp 621 – 628

Wong, J. Y., Mc Laughlin, N. B., Zhinwen, Z., Jianqiao, L., Burtt, S. 2000. Optimization of the Tractive Performance of Four-Wheel Drive Tractors – Correlation Between Analytical Predictions and Experimental Data. *Transactions of the Society of Automotive Engineers.* Paper number 2000-01-2596. p252-260

Wong, J. Y. 2001. Theory of Ground Vehicles. 3rd ed. Chichester: John Wiley and sons.

Yamakawa, J., Watanabe, K. 2006. A method of optimal wheel torque determination for independent wheel drive vehicles.
Journal of Terramechanics, v 43, n 3, July, 2006, pp 269-285.

Zoz, F. M., Grisso, R. D. 2003. Traction and Tractor Performance. *American Society of Agricultural Engineers Distinguished Lecture Series, Tractor Design no27.* St Joseph, Michigan: American Society of Agricultural Engineers.

Zoz, F. M., Turner, R. J., Shell, L. R. 2002. Power Delivery Efficiency: A Valid Measure of Belt and Tire Tractor Performance. *Transactions of the ASAE*, v 45, n 3, 2002, pp 509-518.

Appendix to chapter 3

3.1 ABB Torductor-S Design Guidelines for Motorsport (Anon, 2008)

Torque sensor information

Torque Sensor Principle

The ABB Torductor®-S non-contact torque sensor operates using the magnetoelastic principle where the change in the magnetic property of a ferromagnetic material is measured when subjected to torque. The sensor is suitable for use on shaft diameters ranging from 10 to 70 mm, and a torque range of 10 to 5000 Nm with a non-repeatability of ±0.2 % of the nominal torque. Rotational speed of the shaft is normally within the range of 0 to 20,000 rpm, the only limiting factor being any shaft bearings. A typical Torductor®-S is designed for temperatures ranging from –40°C to +150°C and +200°C for short periods of time. If required, even higher temperatures can be catered for.

Torque Sensor Parts

The torque sensor consists of a shaft surrounded by sensing coils wound on a bobbin in a stator part called the yoke. Excitation, demodulation and signal processing is carried out in the electronic unit.

Technical specifications

Stress level

It is important to achieve the correct stress level in the sensor zone for the quality of the torque signal and the sensitivity to be optimised. A stress level of 150 MPa for the nominal torque gives a good sensitivity and the operating span of the sensor could be between 80 MPa and 250 MPa with overloads up to 400 MPa. Designing for the nominal torque to give stresses in the upper range will give better signal quality but the **overload limit must not be exceeded**.

It is possible to reduce the material thickness along the sensor zone and also reduce the sensor zone diameter in order to achieve the preferred stress level in the shaft.
The formula to calculate the maximum torsion shear stress for a hollow shaft is:

$$\tau_{max}(MPa) = \frac{16 \cdot Mv \cdot D \cdot 10^3}{\Pi \cdot (D^4 - d^4)}$$

Where D and d is the outer respectively inner diameter of the shaft given in mm and the torque *Mv* in Nm.

Material

The sensor shaft should be machined from an ABB stainless steel material. The mechanical properties of some of the available materials

are presented below.

Case hardening of the sensor shaft should be avoided. If required, greater surface hardness can be achieved through surface treatment, e.g. coating, of the sensor shaft.
Grinding, shot peening or other treatments of the sensor zone must be avoided. The final cut in the zone should not exceed 0.15 mm depth.

Properties	ABB A354	S155 (comparison)
Tensile Strength (MPa)	2010	1900
0.2% Yield Strength (MPa)	1950	1550
Hardness (HRC)	53	54
Fatigue Strength (Rotating Beam Fatigue, 10^8 cycles, MPa)	860	
Charpy V-Notch Impact Strength (Joule)	25	

Dimensions

To achieve maximum reliability it is essential that the cable connection is taken into consideration in the design. One way to achieve this is to use a boot, similar to a Deutsch or FCI connector. See the attached drawings for reference.
Based on the outer diameter of the sensor zone of the shaft the dimensions of the sensor parts can be derived. The following dimensions do not take the cable connection into consideration.

	Diameter	Length
Sensor zone of the shaft	$I.D_{Shaft}$ chosen for optimal stress level	40 mm
	$O.D_{Shaft}$ chosen for optimal stress level	
Yoke	$I.D_{Yoke} = O.D_{Shaft} + 1.5$	30 mm
	$O.D_{Yoke} = I.D_{Yoke} + 5.4$	
Yoke housing	$I.D_{Housing} = O.D_{Yoke}$	32 mm
	$O.D_{Housing} = I.D_{Housing}$ + thickness	

Shaft:-

- The sensor length on the shaft should be 40 mm. Shorter lengths are possible, please contact ABB for information.
- The outer diameter of the shaft ($O.D_{Shaft}$) should be chosen to give a sufficient stress level and to suit design requirements. If a spline is used this imposes restrictions on the minimum diameter possible since the bobbin has to fit over the spline.
- The inner diameter of the shaft ($I.D_{Shaft}$) should be chosen with regards to the stress level and in agreement with requirements dictated by mechanical strength.

Yoke:-

- The yoke has an optimal length of 30 mm.
- The inner diameter ($I.D_{Yoke}$) is obtained from the outer diameter of the shaft ($O.D_{Shaft}$) and adding an air gap of 0.75 mm per radius. In some cases an air gap of 0.5 mm can be acceptable.
- The yoke thickness is 2.7 mm per radius.

Yoke Housing:-

- The yoke housing is designed to carry the yoke and to allow the cable lead out.
- In order to terminate the wires from the bobbin the yoke-housing diameter has to be increased in one direction along the circumference. See attached drawings for clarification.
- The material usually used is high strength aluminium, 4338 (Swedish standard) and HE 15 (British standard). Hard anodising is recommended. Other materials are also possible.
- A plastic circlip with a width of 1.2 mm is used to secure the yoke position in the housing.

Total:-

A housing thickness of 2 mm gives an outer diameter of the sensor that is 10.9 mm (absolute minimum is 10 mm) greater than the outer diameter of the shaft. This does not take into account the cable connection.

General design considerations

The following general specifications need to be fulfilled to obtain a proper functionality:-

- The axial float of the shaft / yoke should not be greater than ± 0.5 mm. Less end-float will improve the accuracy.
- Concentricity between shaft and yoke should be better than ± 0.2 mm.
- The yoke (30 mm) must be axially symmetric around the sensor zone (40 mm).

Mounting /dismantling

Mounting and dismantling of the sensor should be made as simple as possible and the procedure must be straightforward.
It is good to have a reference dimension that can be measured during installation and adjusted by shimming if necessary to achieve a positioning better than ± 0.5 mm including end-float.

Electronic unit

The specification for the electronic unit is presented in a data sheet attached.

- Note that the operating temperature should be maximum 65°C so a location in the cockpit is preferable.
- The dimensions of the electronic unit case are 81 x 56 x 31 mm.
- A cable with a diameter of approximately 4 mm (4 leads) is needed to connect the sensor to the electronic unit. The cable needs to be properly fixed with strain relief.
- A twisted pair cable can be used instead of a screened cable.
- Note also that the electronic unit is not CE-marked.

Torque measuring system

	Typical Data
Transducer Type	Torductor®-S
Output	0-5 V
Linearity Deviation Including Hysteresis (related to nominal sensitivity) **Signal Variation due to Rotation** (related to nominal sensitivity) **Repeatability Error** (related to nominal sensitivity)	< ±2% < ±0.4% ±0.2%
Temperature Drifts Zero-signal (related to nominal sensitivity) Gain (related to reading)	 < ±0.02 %/°C < ±0.04 %/°C
Operating Temperature Range **Storage Temperature Range**	- 40°C to + 150°C (200°C for short periods) - 40°C to + 70°C
Bending Limit Moment on the Shaft **Axial Limit Force on the Shaft** For Ø20 mm shaft For Ø40 mm shaft	< 10%, no influence on reading < 500 N, no influence on reading < 2 kN, no influence on reading
Chemical Environmental Tolerance	Normal oils and dissolvents. Use of brake cleaner should be avoided.

Control unit

	Typical Data
Mains Voltage **Power Consumption**	9-36 V DC ~15 W
Output Signal **SNR** **Step Response** (0 - 90 %) **Bandwidth** (- 3dB)	0 V to 5 V DC > 60dB 1 ms 1 kHz
Environmental Tolerance Ambient Operating Temperature Storage and Transport Material	 - 40°C to + 65°C - 40°C to + 70°C Magnesium
Dimensions (L x W x H)	81 x 56 x 31 mm
Supply Voltage Connector **Torque Signal Connector**	To be specified by customer To be specified by customer
Cable	To be specified by customer

3.2 Data channels recorded

	Name	Units	Analogue/ Digital	Sensitivity	Resolution	Range
1	Time	s	D	NA	0.01 s	
2	Front right had wheel speed	rpm	D	60 pulses/rev	0.001 rpm	0 – 3000 rpm
3	Rear right hand wheel speed	rpm	D	60 pulses/rev	0.001 rpm	0 – 3000 rpm
4	Rear output shaft speed	rpm	D	3 pulses/rev	0.015 rpm	0 - 84,000 rpm
5	Front output shaft speed	rpm	D	2.7 pulses/rev	0.05 rpm	0 - 93,333 rpm
6	Datalogger internal temperature	°C	A	NA	0.25 °C	-40 +85 °C
7	Datalogger input voltage	V	A	NA	0.05 V	0 - 55 V
8	Lateral acceleration	G	A	NA	0.004 G	+/- 2 G
9	Longitudinal acceleration	G	A	NA	0.004 G	+/- 2 G
10	Vertical acceleration	G	A	NA	0.004 G	+/- 2 G
11	Front output shaft torque	Nm	A	0.0025 V/Nm	1.96 Nm	+/- 1000 Nm
12	Rear output shaft torque	Nm	A	0.0025 V/Nm	1.96 Nm	+/- 1000 Nm
13	Engine torque	Nm	A	0.0056 V/Nm	0.87 Nm	-300 +600 Nm
14	Gear selection		D	NA	NA	NA
15	Front left hand wheel speed	rpm	A	60 pulses/rev	0.001 rpm	0 – 3000 rpm
16	Rear left hand wheel speed	rpm	A	60 pulses/rev	0.001 rpm	0 – 3000 rpm
17	Absolute forward speed	m/s	D	100 pulses/m	0.00005 m/s	0.03 - 83.33 m/s
18	Engine speed	rpm	D	6 pulses/rev	0.2 rpm	0 – 42000 rpm
19	Drawbar pull	kN	A	0.1 V/kN	0.75 N	0 - 50 kN

3.3 Calibration statistics for the Novatech 10tonne loadcell and Vishay Measurements Group 2120B amplifier

Load (kN)	Recorded Voltage #1	#2	#3	Mean (V)	Variance (% of mean) #1	#2	#3
0	0.0089	0.0093	0.0096	0.0093	0.039568	-0.0036	-0.03597
5	0.4940	0.4990	0.4970	0.4967	0.005369	-0.0047	-0.00067
10	1.0000	1.0000	1.0010	1.0003	0.000333	0.000333	-0.00067
15	1.4990	1.5050	1.5070	1.5037	0.003104	-0.00089	-0.00222
20	2.0010	2.0060	2.0110	2.0060	0.002493	0	-0.00249
25	2.5190	2.5140	2.5150	2.5160	-0.00119	0.000795	0.000397
30	3.0230	3.0290	3.0340	3.0287	0.001871	-0.00011	-0.00176
					Max %	0.04	
					Min %	-0.04	

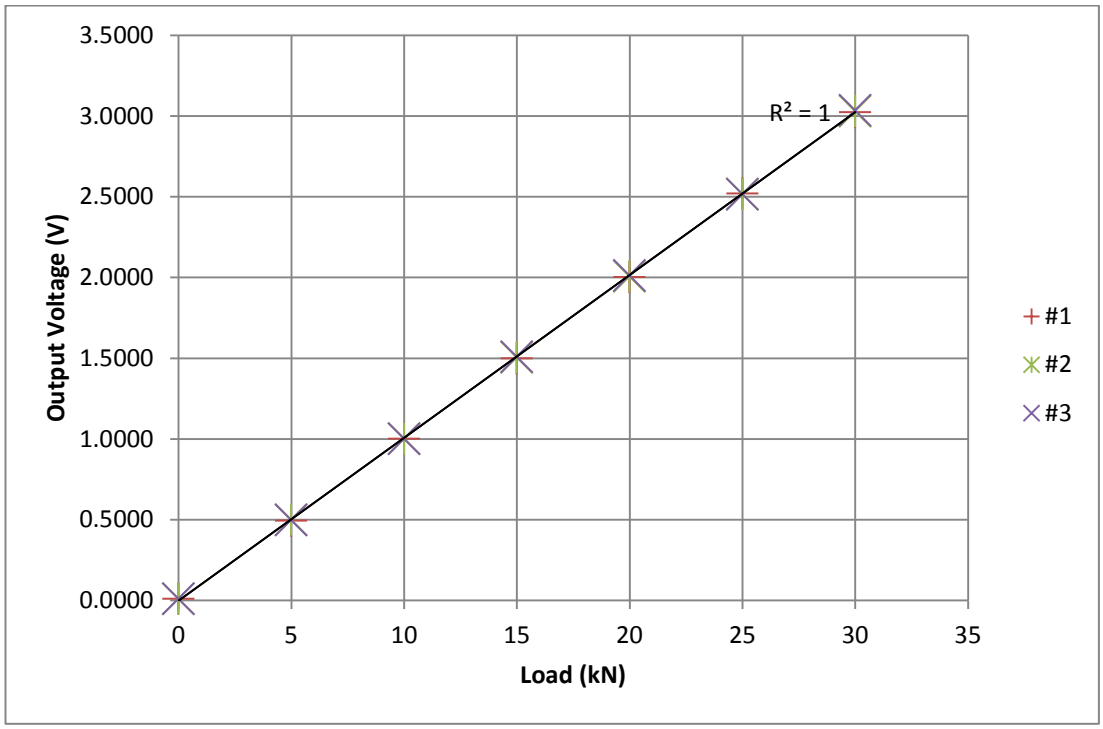

3.4 Calibration of the Torductor-S torque sensors

Calibration by ABB prior to shipment

Doc. no. FM-BM2008-000107 en
Rev. ind.
Date 2008-08-22

Calibration for torque output

Torque(Nm) = $\alpha(u-u_0)$

Where: α = calibration constant

u = Signal output in volts

u_0 = Signal output in volts at 0Nm

Shaft	Housing	u_0	α at 40°C	α at 100°C	Torque range
INPUT	INPUT	1.677	180	180	-300 to +600Nm
FRONT	FRONT	2.5	400	400	±1000Nm
FRONT	FRONT	2.5	800	800	±2000Nm
REAR	REAR	2.5	400	400	±1000Nm
REAR	REAR	2.5	800	800	±2000Nm

Verification of calibration at Harper Adams University College

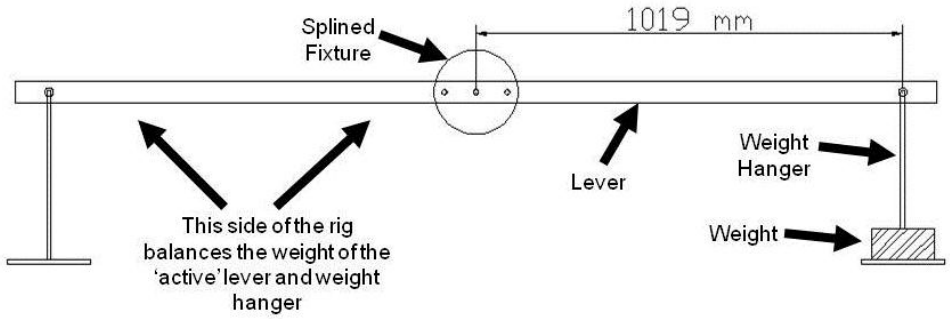

Harper Adams Torductor calibration rig

Gearbox Input

Applied Load (Nm)	Recorded Voltage (V) #1	#2	#3	Mean	Variance (%)		
600	4.9999	4.9957	4.9975	4.9977	-0.0004	0.0004	0.0000
500	4.4485	4.4445	4.4423	4.4451	-0.0008	0.0001	0.0006
400	3.8842	3.8890	3.8850	3.8861	0.0005	-0.0008	0.0003
300	3.3330	3.3321	3.3336	3.3329	0.0000	0.0002	-0.0002
200	2.7785	2.7770	2.7798	2.7784	0.0000	0.0005	-0.0005
100	2.2209	2.2215	2.2204	2.2209	0.0000	-0.0003	0.0002
0	1.6670	1.6660	1.6668	1.6666	-0.0003	0.0004	-0.0001
-100	1.1121	1.1113	1.1102	1.1112	-0.0008	-0.0001	0.0009
-200	0.5555	0.5570	0.5551	0.5559	0.0007	-0.0020	0.0014
-300	0.0031	0.0030	0.0031	0.0031	-0.0109	0.0217	-0.0109
					Max %	0.02	
					Min %	-0.01	

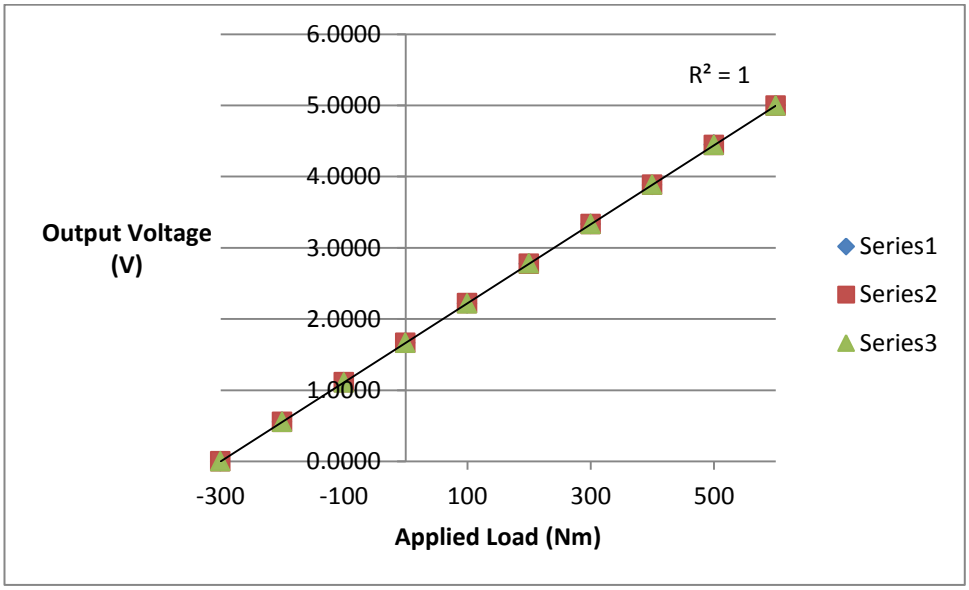

Rear Output Shaft

Applied Load (Nm)	Recorded Voltage (V) #1	#2	#3	Mean	Variance (%)		
1000	4.9998	5.0000	4.9975	4.9991	-0.0001	-0.0002	0.0003
750	4.3750	4.3737	4.3752	4.3746	-0.0001	0.0002	-0.0001
500	3.7500	3.7521	3.7502	3.7508	0.0002	-0.0004	0.0002
250	3.1252	3.1249	3.1244	3.1248	-0.0001	0.0000	0.0001
0	2.5001	2.5049	2.5001	2.5017	0.0006	-0.0013	0.0006
-250	1.8752	1.8751	1.8759	1.8754	0.0001	0.0002	-0.0003
-500	1.2526	1.2510	1.2501	1.2512	-0.0011	0.0002	0.0009
-750	0.6248	0.6249	0.6244	0.6247	-0.0002	-0.0003	0.0005
-1000	0.0040	0.0039	0.0037	0.0039	-0.0345	-0.0086	0.0431
					Max	0.0431	
					Min	-0.0345	

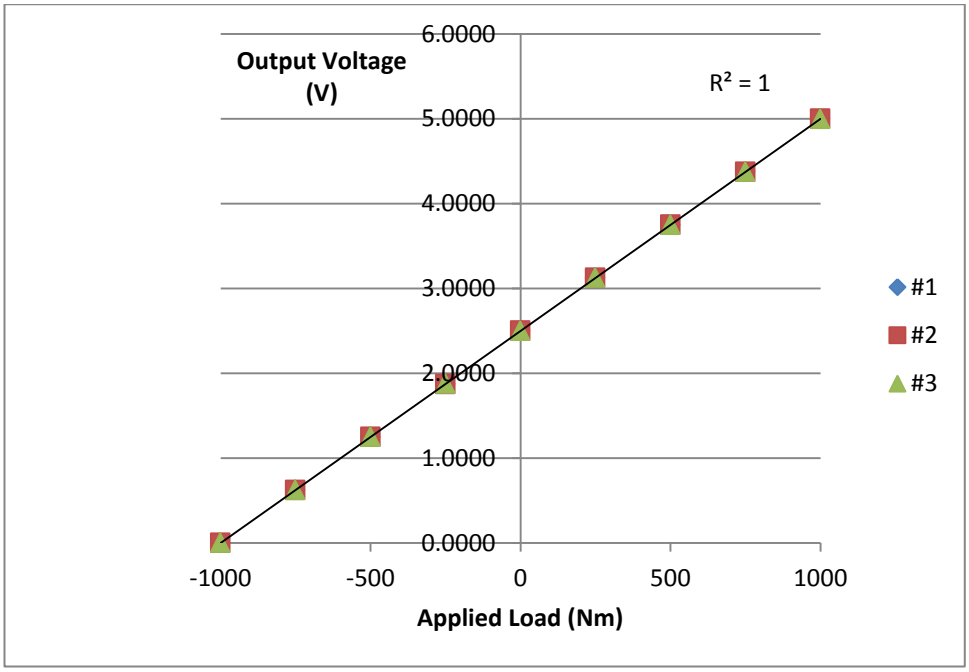

Front Output Shaft

Applied Load (Nm)	Recorded Voltage (V) #1	#2	#3	Mean	Variance (%)		
1000	4.9995	4.9987	4.9992	4.9991	-0.0001	0.0001	0.0000
750	4.3744	4.3770	4.3762	4.3759	0.0003	-0.0003	-0.0001
500	3.7516	3.7534	3.7522	3.7524	0.0002	-0.0003	0.0001
250	3.1255	3.1251	3.1249	3.1252	-0.0001	0.0000	0.0001
0	2.5010	2.5006	2.5023	2.5013	0.0001	0.0003	-0.0004
-250	1.8742	1.8748	1.8739	1.8743	0.0001	-0.0003	0.0002
-500	1.2524	1.2502	1.2485	1.2504	-0.0016	0.0001	0.0015
-750	0.6256	0.6255	0.6258	0.6256	0.0001	0.0002	-0.0003
-1000	0.0029	0.0030	0.0027	0.0029	-0.0116	-0.0465	0.0581
					Max %	0.06	
					Min %	-0.05	

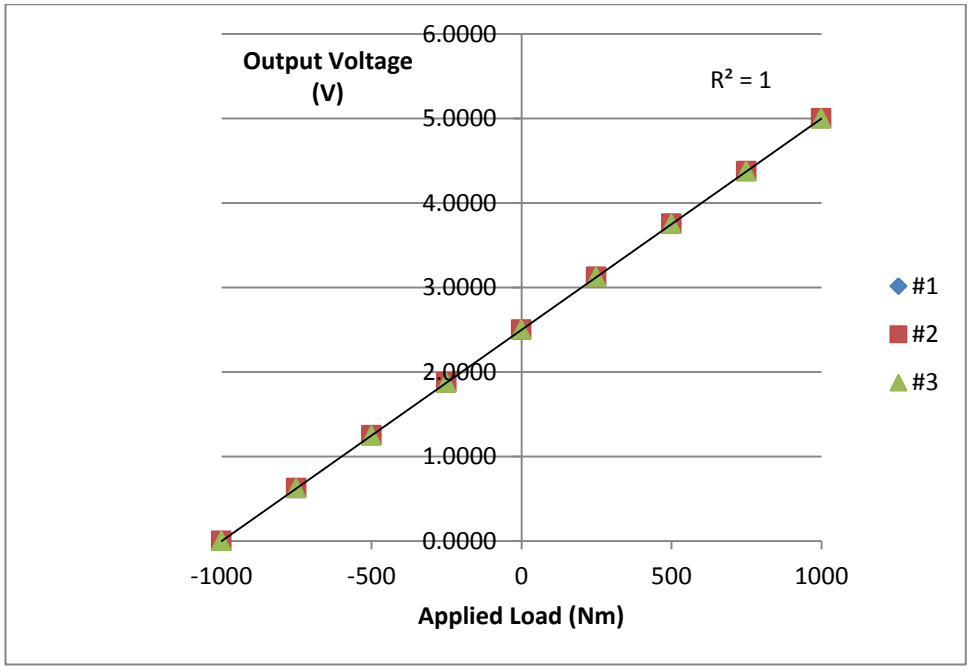

3.5 9:00am weather data collected by the Harper Adams Automatic Weather Station (no. 4787)

DATE August 2009	Wind dir	Wind sp	Dry bulb temp	Wet bulb temp	Max temp	Min temp 24 hrs	10cm soil temp	20cm soil temp	100cm soil temp	RH	Total rain 24 hrs
	°	m/s	°C	°C	°C	°C	°C	°C	°C	%	mm
1	196.1	0.8	15.2	15.0	17.9	12.5	14.9	15.6	16.3	98.0	1.8
2	297.8	0.8	16.8	13.4	20.8	8.4	13.6	14.7	16.2	66.1	0.0
3	176.5	3.1	16.9	15.2	21.3	11.3	15.4	15.8	16.2	83.2	1.2
4	186.2	2.7	18.3	18.2	22.0	15.9	16.8	16.8	16.2	98.6	2.8
5	210.3	0.5	18.7	17.2	23.8	14.7	17.2	17.1	16.1	85.7	0.2
6	287.2	0.7	18.1	15.4	21.8	10.4	16.1	16.9	16.2	74.0	0.0
7	324.4	1.7	18.8	16.2	23.5	10.7	16.0	16.8	16.3	75.1	0.0
8	248.7	0.8	17.6	15.0	22.5	7.9	15.0	16.3	16.4	74.3	0.0
9	no wind	0.0	19.8	16.8	24.4	8.0	15.2	16.4	16.5	72.5	1.0
10	221.6	1.5	17.5	16.5	21.6	13.5	17.1	17.6	16.7	89.5	0.0
11	313.7	1.0	19.3	16.9	25.3	12.9	17.1	17.4	16.7	77.2	9.2
12	8.1	0.8	16.2	15.5	21.8	15.7	18.1	18.6	16.8	93.0	2.0
13	337.7	2.4	16.2	14.6	20.6	11.3	16.7	17.6	16.9	83.5	0.0
14	no wind	0.0	18.3	15.6	21.8	9.9	16.4	17.3	17.0	74.1	0.0
15	228.8	1.9	20.4	18.4	24.1	16.7	17.8	17.9	17.0	81.6	0.0
16	261.0	2.0	18.3	15.5	20.6	10.8	16.7	17.6	17.0	72.8	0.6
17	262.5	2.0	17.9	15.6	22.0	12.6	16.9	17.3	17.0	77.4	0.0
18	189.8	2.0	17.5	16.0	22.2	10.7	16.6	17.2	17.0	84.9	0.0
19	199.9	2.3	19.9	18.0	25.8	14.7	17.3	17.6	17.0	81.6	0.0
20	219.8	1.9	18.1	16.2	21.8	17.3	18.0	18.2	17.0	81.2	0.2
21	226.4	0.9	15.0	12.9	19.0	10.4	16.0	17.0	17.0	77.5	2.8
22	no wind	0.0	17.9	15.3	23.4	7.8	14.8	16.1	17.0	73.9	0.0
23	184.3	3.0	18.3	16.3	21.9	14.0	16.8	17.4	17.0	80.6	0.6
24	no wind	0.0	14.9	14.6	18.9	13.8	17.0	17.5	17.0	97.3	3.0
25	213.7	1.3	17.5	14.9	21.5	9.4	15.6	16.6	17.0	74.4	5.6
26	181.4	4.5	15.9	15.7	19.4	10.5	15.8	16.7	17.0	97.4	3.4
27	176.5	0.8	18.6	16.3	22.4	12.6	16.5	17.0	17.0	78.2	0.6
28	238.6	1.7	12.8	12.6	16.9	8.8	15.3	16.6	17.0	98.3	1.6
29	268.5	2.2	16.0	13.1	19.3	7.3	14.0	15.6	17.0	70.0	0.0
30	no wind	0.0	15.1	13.9	21.0	9.7	14.9	15.9	17.0	87.6	0.6
31	209.3	2.5	20.5	19.9	21.9	15.1	16.7	16.6	17.0	94.7	0.6

DATE	Wind dir	Wind sp	Dry bulb	Wet bulb	Max temp	Min temp	10cm soil	20cm soil	100cm soil	RH	Total rain
September 2009	°	m/s	℃ temp	℃ temp	℃	℃ 24 hrs	℃ temp	℃ temp	℃ temp	%	mm 24 hrs
1	224.7	1.5	17.0	16.8	20.2	9.6	15.1	16.1	16.7	98.1	1.6
2	205.1	1.5	14.9	14.8	18.0	10.2	14.8	15.9	16.6	98.5	14.6
3	265.1	3.1	14.4	16.2	17.2	11.8	14.7	15.7	16.5	122.0	0.0
4	278.1	5.0	14.1	11.3	18.3	7.8	12.3	14.0	16.3	69.5	0.0

3.6 Instrumented shafts stress and torque calculations

Front Axle Ratios			**Notes**
Pinion/Crownwheel	3.2:1		CNH TS repair manual
Epicyclic	6:1		CNH TS repair manual
Overall	19.2:1		CNH TS repair manual

Rear Axle Ratios			
Pinion/Crownwheel	5.625:1		CNH TS repair manual
Epicyclic	6:1		CNH TS repair manual
Overall	33.75:1		CNH TS repair manual

Effective Wheel Sizes			
Rear Hub Height	0.77	**m**	Morgan *et al* 2000
Front Hub Height	0.58	**m**	Measured

Front wheel size (as delivered)	420/70 R24
Rear wheel size (as delivered)	520/70 R34

Instrumented Shafts Data			
FWD Shaft Diameter	0.045	**m**	
Rear Outputshaft Diameter	0.034	**m**	
GB Inputshaft Diameter	0.036	**m**	
FWD Shaft Ipolar	4.026×10^{-07}		(π x Shaft Diameter^4)/32
Rear Driveshaft Ipolar	1.312×10^{-07}		(π x Shaft Diameter^4)/32
GB input shaft Ipolar	1.649×10^{-07}		(π x Shaft Diameter^4)/32

Max Engine Torque	**324.70**	**Nm**	Morgan *et al* 2000

Assumed Load Case on Rear Axle			
Mu between tyre and running surface	1.00		Assumed on dry tarmac
Load on rear axle	43046.28	4388.00	**(N) (Kg)** Morgan *et al* 2000 (Unballasted) Assumes tractor with front wheels clear of the ground
Maximum rear wheel torque based on load and friction	33145.64	**Nm**	Rear axle load x Mu x Wheel radius
Rear Outputshaft torque	**982.09**	**Nm**	Rear wheel torque / overall axle ratio

Front Driveline Ratios

			Source
Gearbox output shaft FWD gear	38	**teeth**	
FWD shaft rear gear	34	**teeth**	
FWD shaft front gear	27	**teeth**	
FWD clutch drive gear	38	**teeth**	

Assumed Load Case on Front Axle

Mu between tyre and running surface	1.00		Assumed on dry tarmac
Load on front wheels	43046.28	4388.00	**(N) (Kg)** Morgan *et al* 2000 (Unballasted) Assumes tractor with rear wheels clear of the ground
Maximum front wheel torque based on load and friction	24966.84	**Nm**	Front axle load x Mu x Front wheel radius
Pinion shaft torque	1300.36	**Nm**	Front wheel torque/overall axle ratio
Internal FWD shaft torque	**923.94**	**Nm**	Pinion shaft torque / (FWD clutch drive gear teeth / FWD shaft front gear teeth)

Stresses in Instrumented Shafts Based on Assumed Load Cases

Internal FWD shaft stress	**51.64**	**MN/m^2**	FWD shaft diameter/2 x (internal FWD shaft torque/internal FWD shaft Ipolar)
Rear driveshaft stress	**127.26**	**MN/m^2**	Rear output shaft diameter/2 x (rear output shaft torque/rear output shaft Ipolar)
GB input shaft Stress	**35.44**	**MN/m^2**	Shaft diameter/2 x (Input shaft torque/Input shaft Ipolar)

3.7 Design of instrumented shafts

Author's design sketches for the instrumented front wheel drive shaft manufactured on his behalf by ABB

There is actually no need to change the front bearing. The shaft would be manufactured with a nominal 35mm bearing surface, which will be a press fit into the inner race from the existing roller bearing.

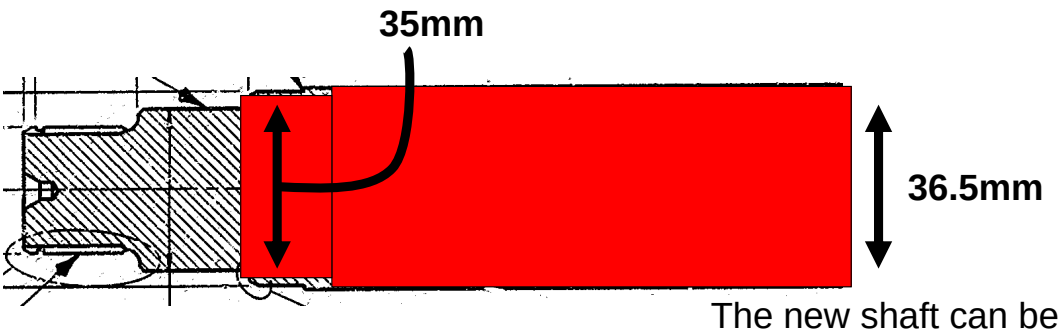

The new shaft can be made to a smaller diameter to suit ABB's needs

The shaft is located axially by an existing deep groove roller bearing at the rear end of the shaft

Cylindrical roller bearings, single row

Principal dimensions			Basic load ratings		Fatigue load limit	Speed ratings		Mass	Designation	Angle ring
			dynamic	static		Reference speed	Limiting speed			Designation
d	D	B	C	C_0	P_u				* - SKF Explorer bearing	
mm			kN		kN	r/min		kg	-	-
35	72	17	56	48	6,1	11000	12000	0,31	NU 207 ECJ *	HJ 207 EC

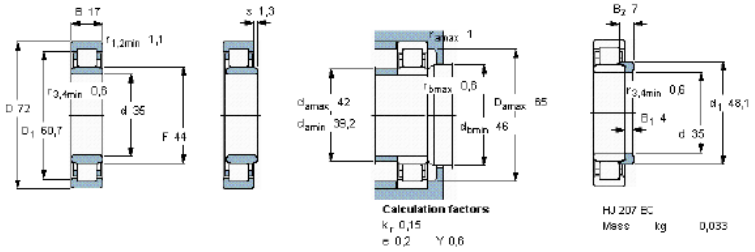

Data for the existing roller bearing:
SKF NU 207 ECJ

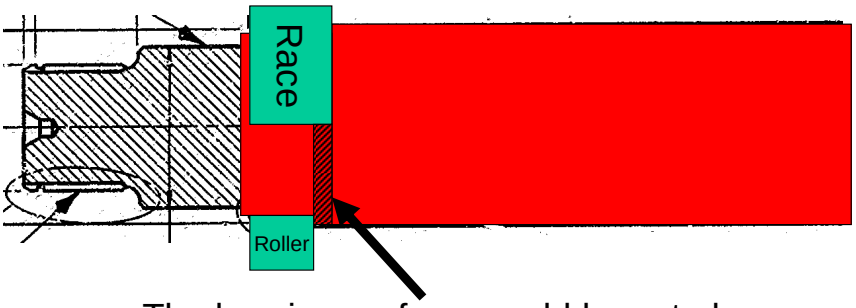

The bearing surface would have to be made slightly wider than it is currently, to accommodate the additional width of the race compared to the rollers

Inner race from the existing bearing, which is not currently fitted to the tractor

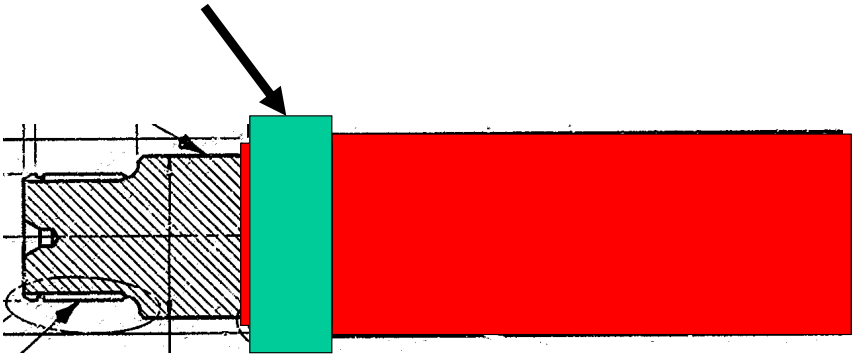

The new shaft can be made to a smaller diameter to suit ABB's needs

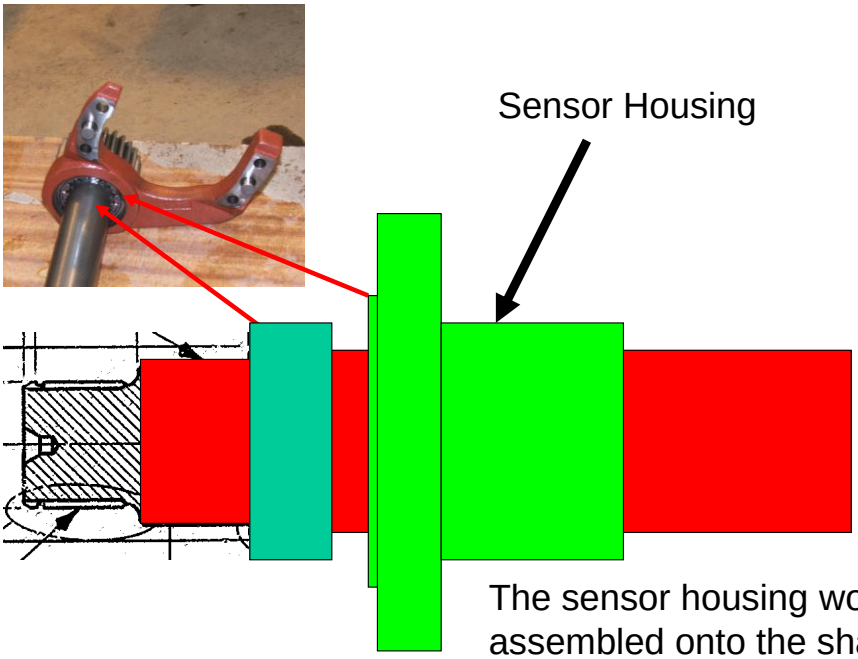

The sensor housing would be assembled onto the shaft before the race was fitted. The sensor housing would be bolted to the front bearing carrier.

Author's design sketches for the instrumented rear wheel drive shaft manufactured on his behalf by ABB

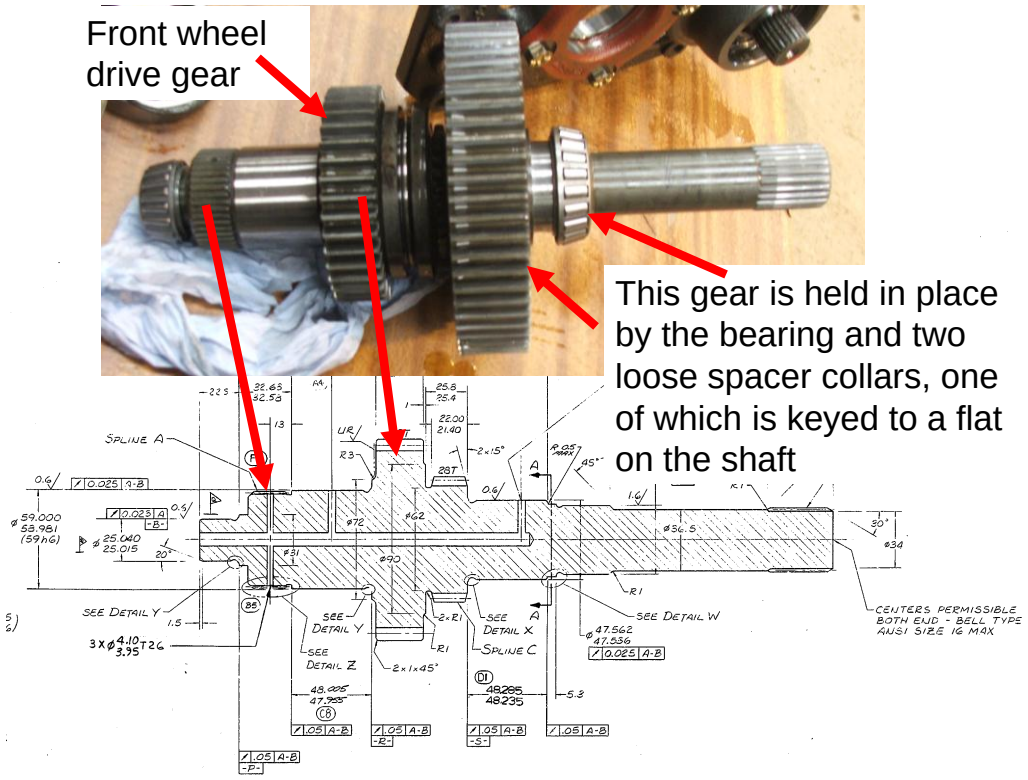

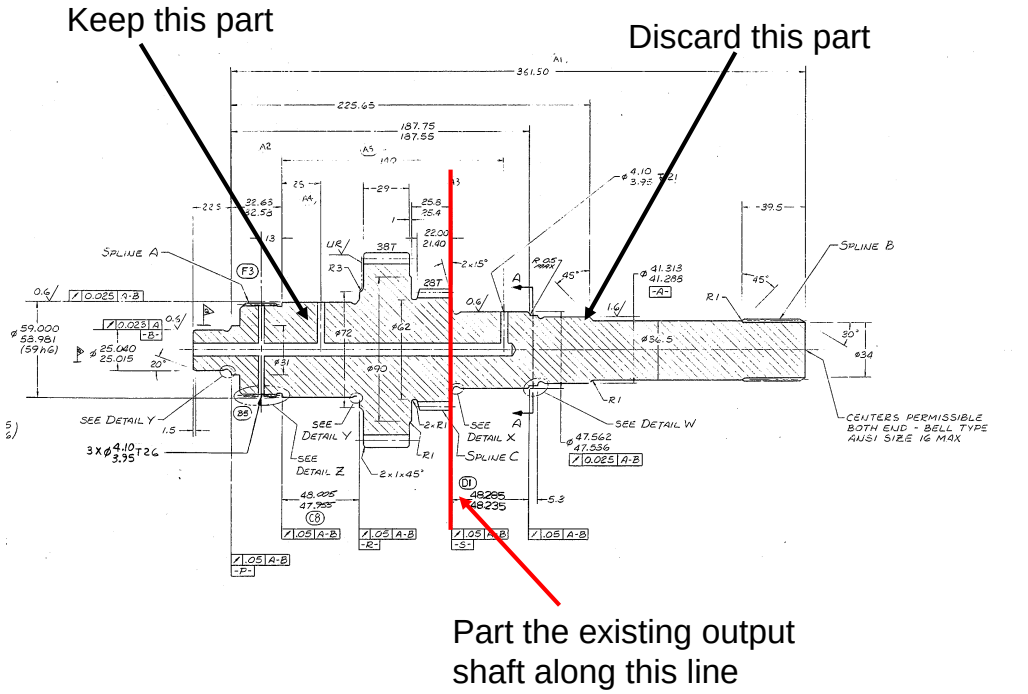

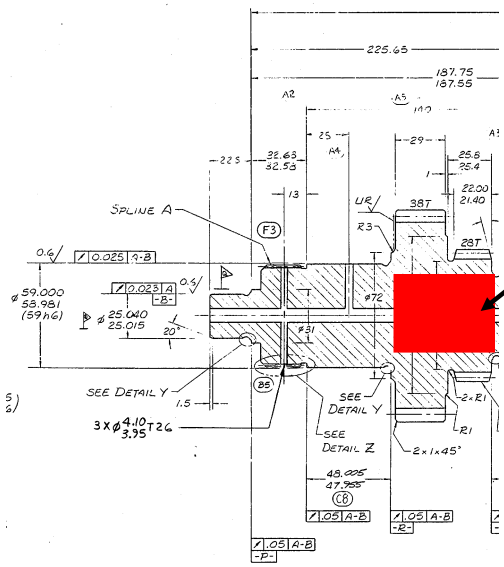

Machine a new internal spline into the shortened CNH shaft

Manufacture this section of the shaft from ABB's steel

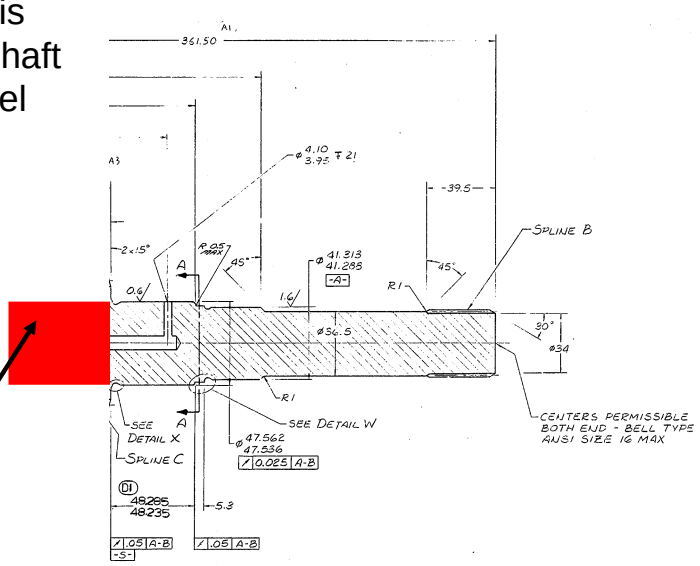

Add a new spline to mate the ABB part to the CNH part

Author's design sketches for the modified gearbox input shaft, manufactured on his behalf by ABB

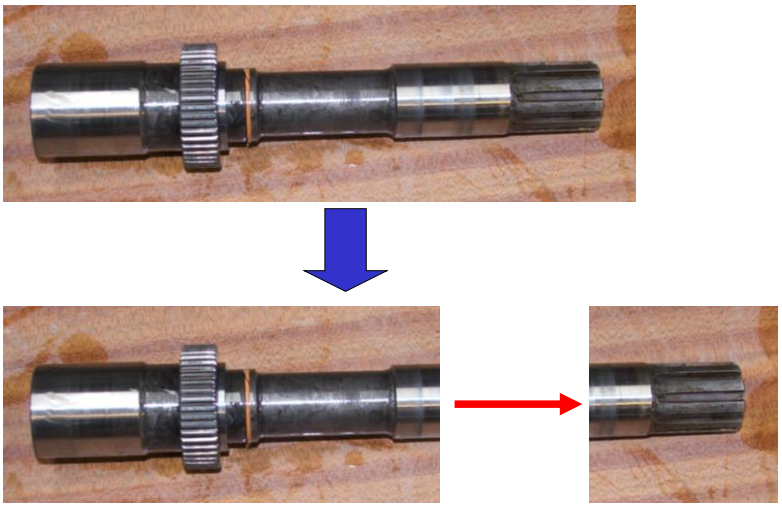

The ABB manufactured gearbox input shaft needs to be extended at the Dual Power clutch sealing surface, to accommodate the Torductor

Gearbox input Torductor

Engine flywheel. This tractor does not have a conventional friction clutch

A plate will be inserted between the engine and gearbox to extend the bellhousing by the same amount as the gearbox input shaft

Gearbox input shaft (removed from Dual Power clutch)

Gearbox input Torductor

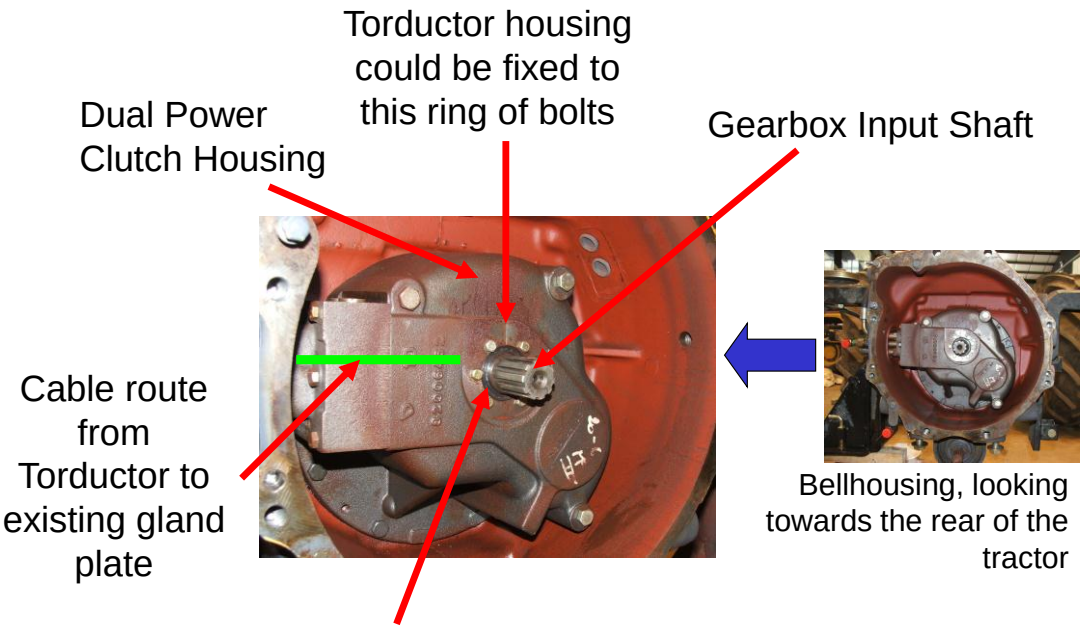

Gearbox input Torductor

3.8 CNH drawimgs of the shafts modified to accept the ABB Torductors

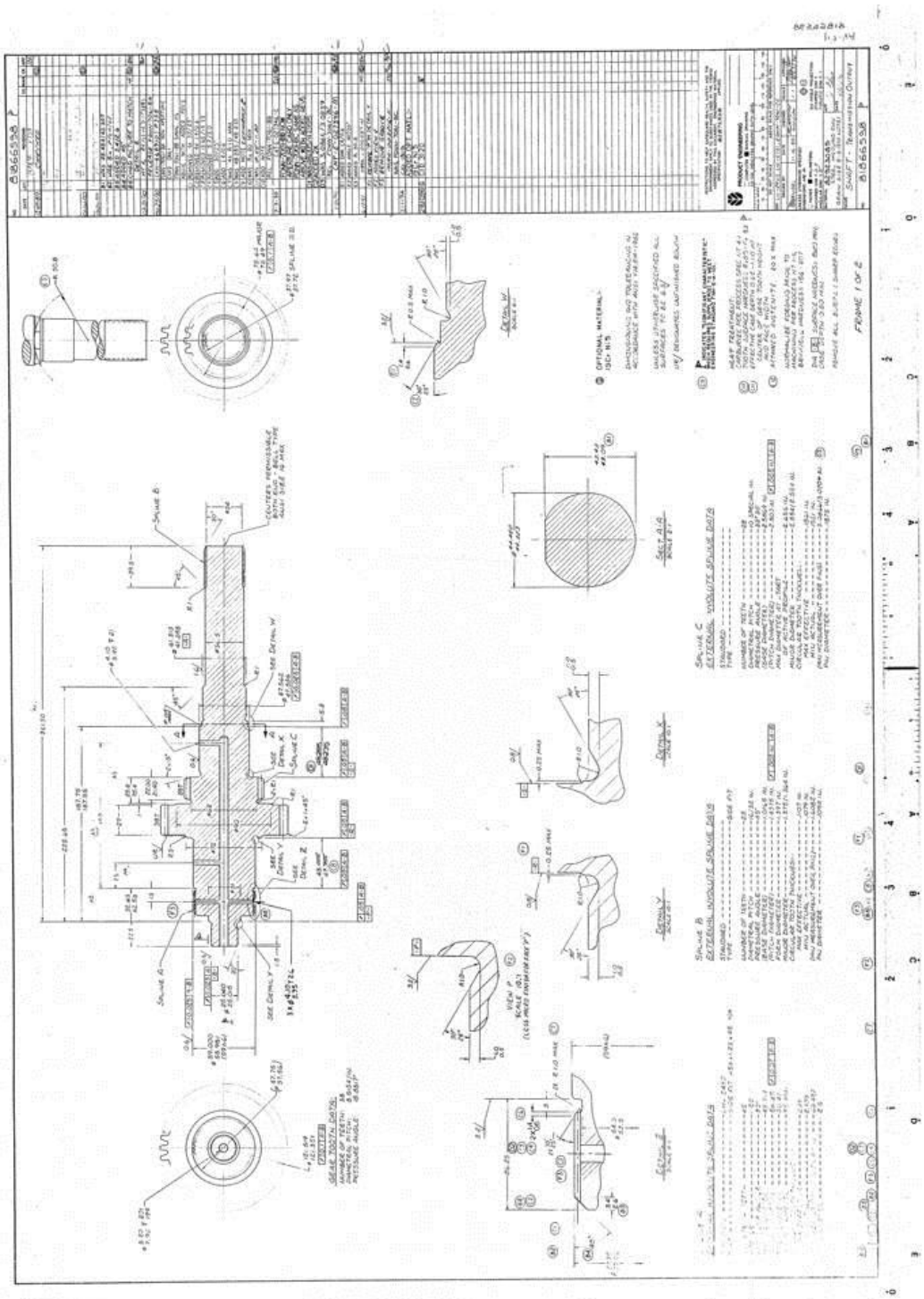

Un-modified TS90 rear output shaft (Wendel, 1989a)

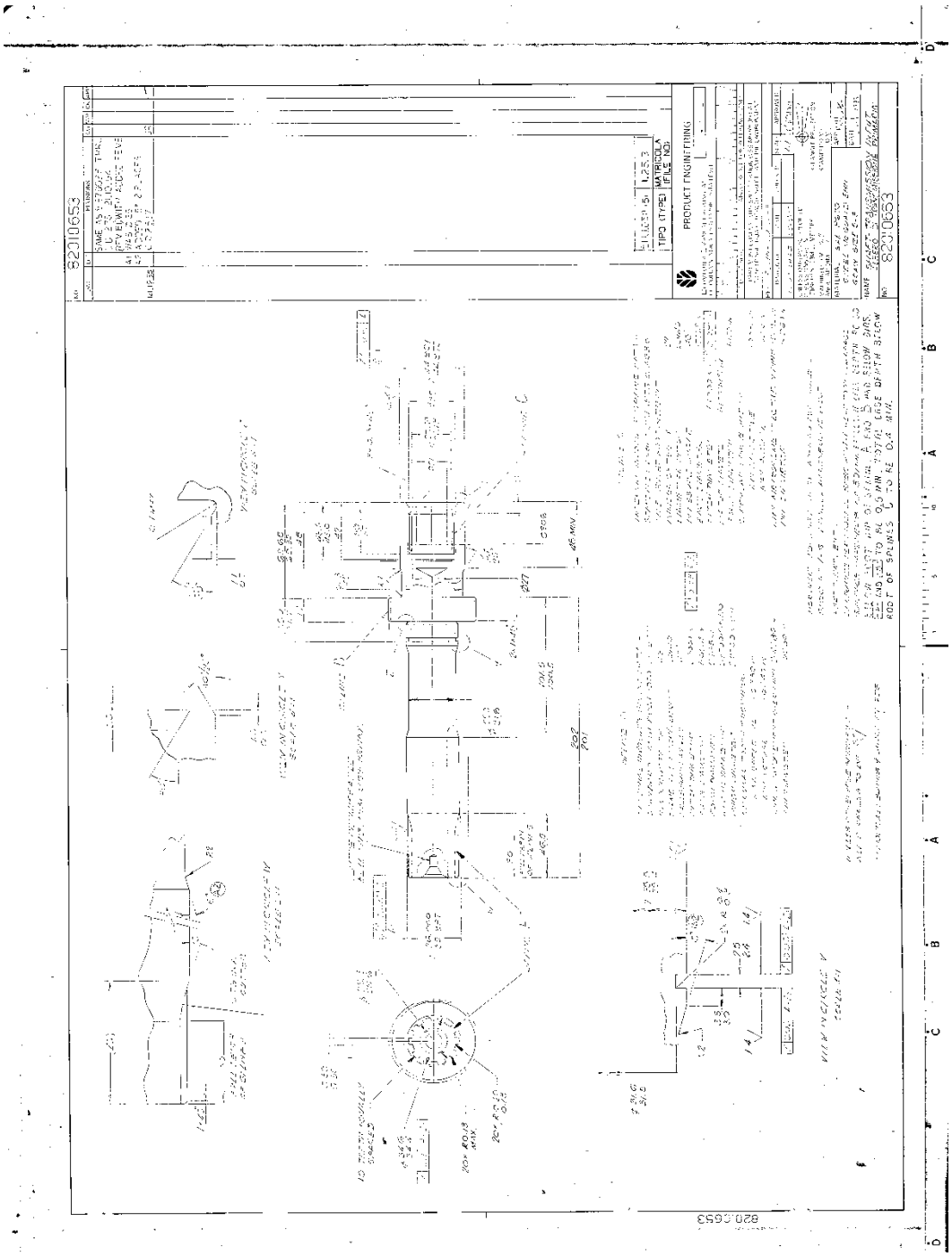

Un-modified TS90 gearbox input shaft (Derbyshire, 1993)

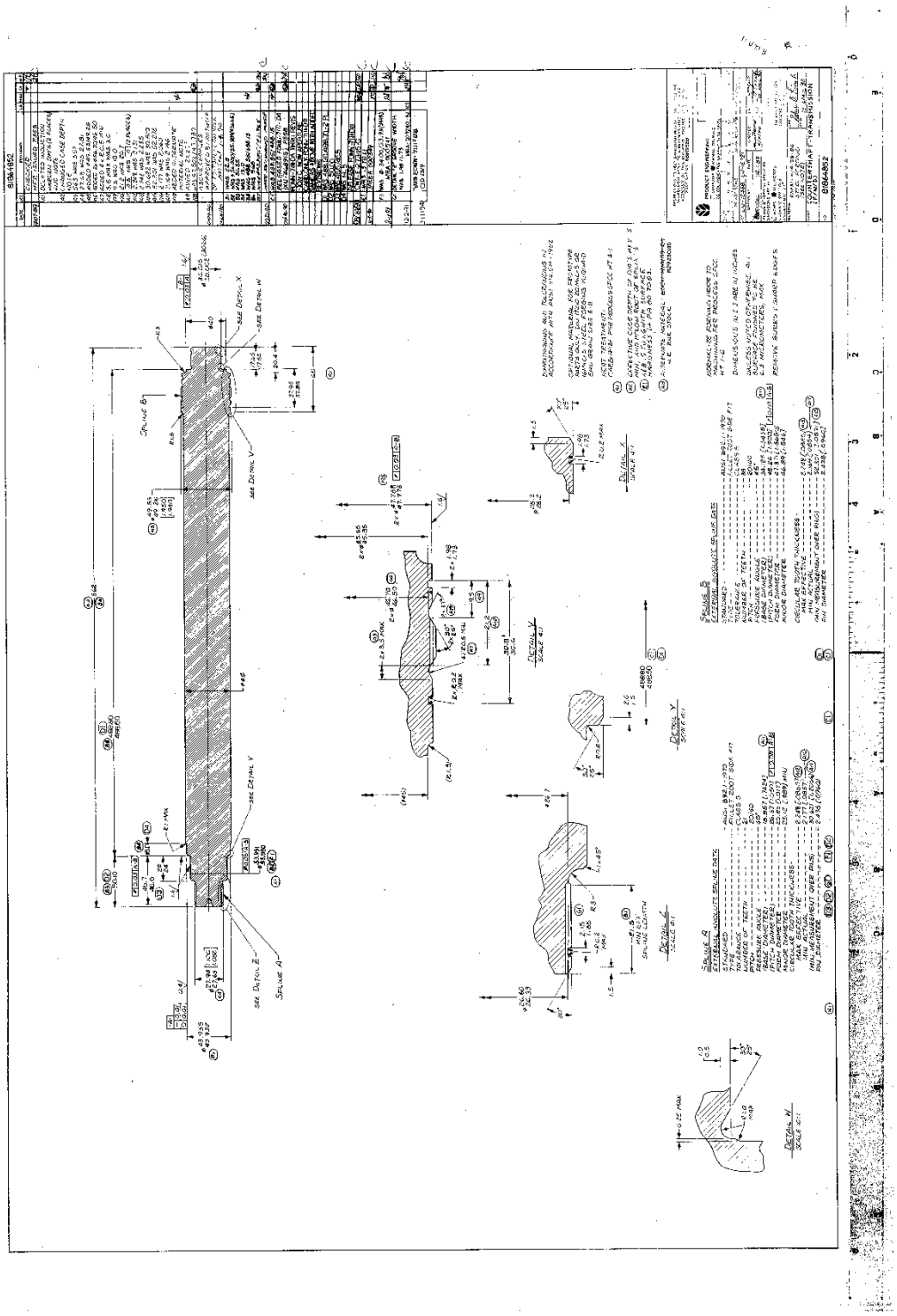

Unmodified TS90 front output shaft (Wendel, 1989b)

3.9 ABB drawings of the instrumented shafts

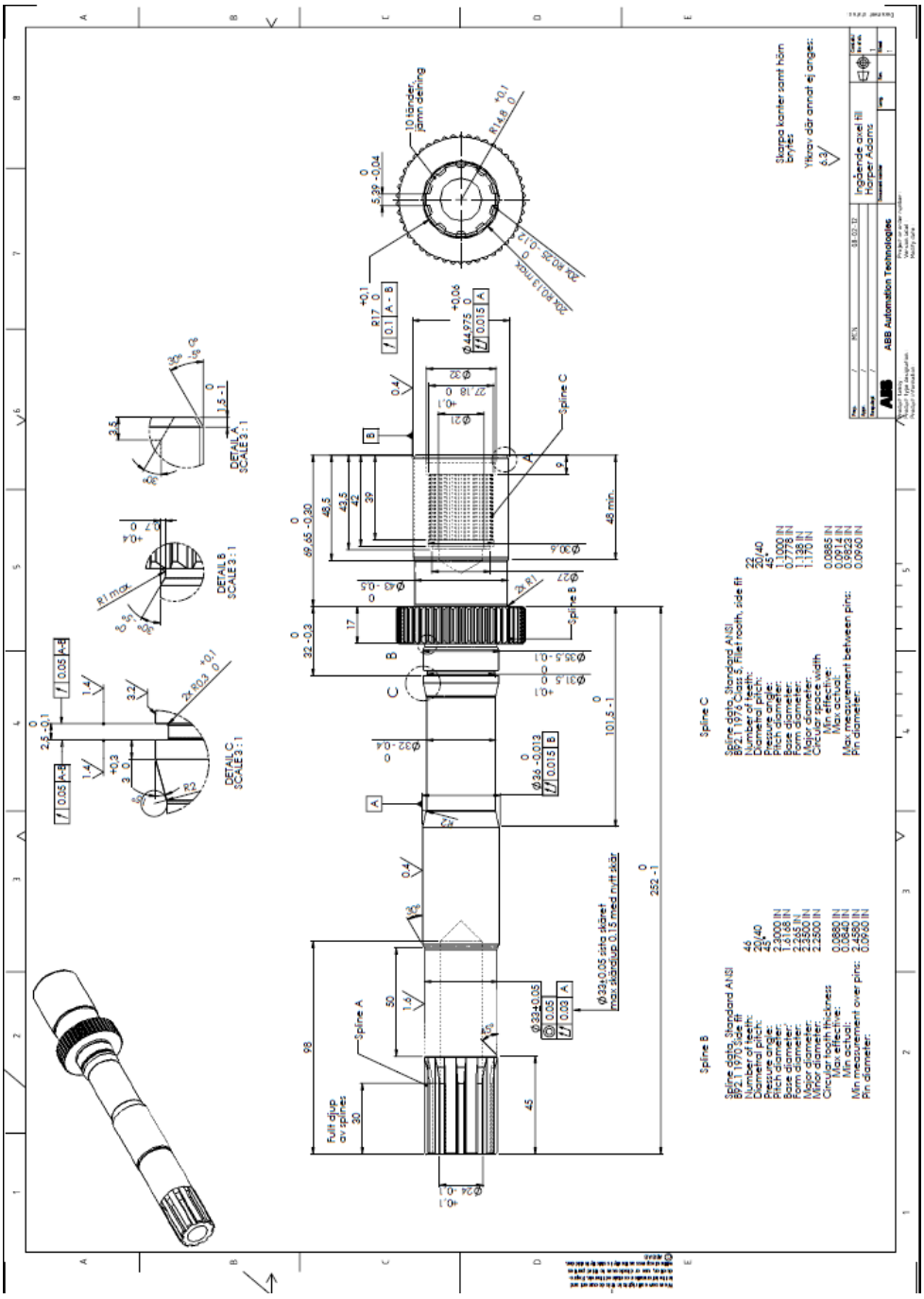

TS90 gearbox input shaft re-designed to accept the ABB Torductor (ABB,2008a)

3.10 Design of wheel speed pole wheels

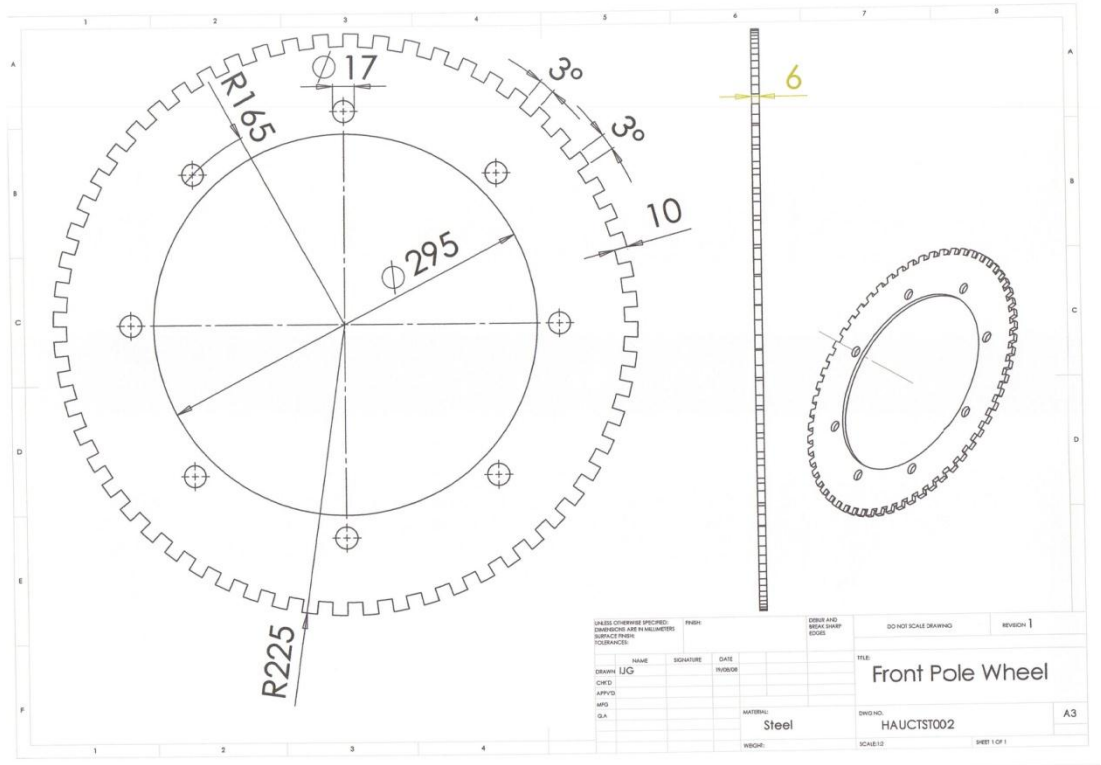

Drawing of front wheel speed pole wheel (Source, author)

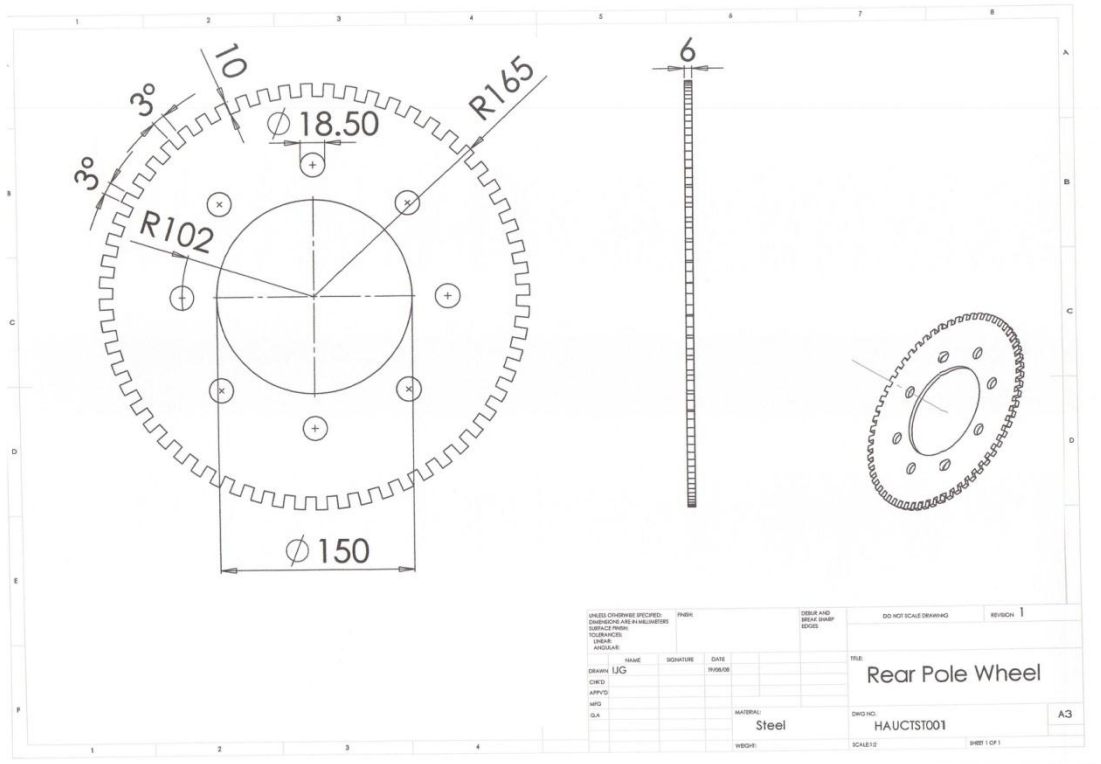

Drawing of rear wheel speed pole wheel (Source, author)

3.11 ABB drawings of the Torductor sensor housings

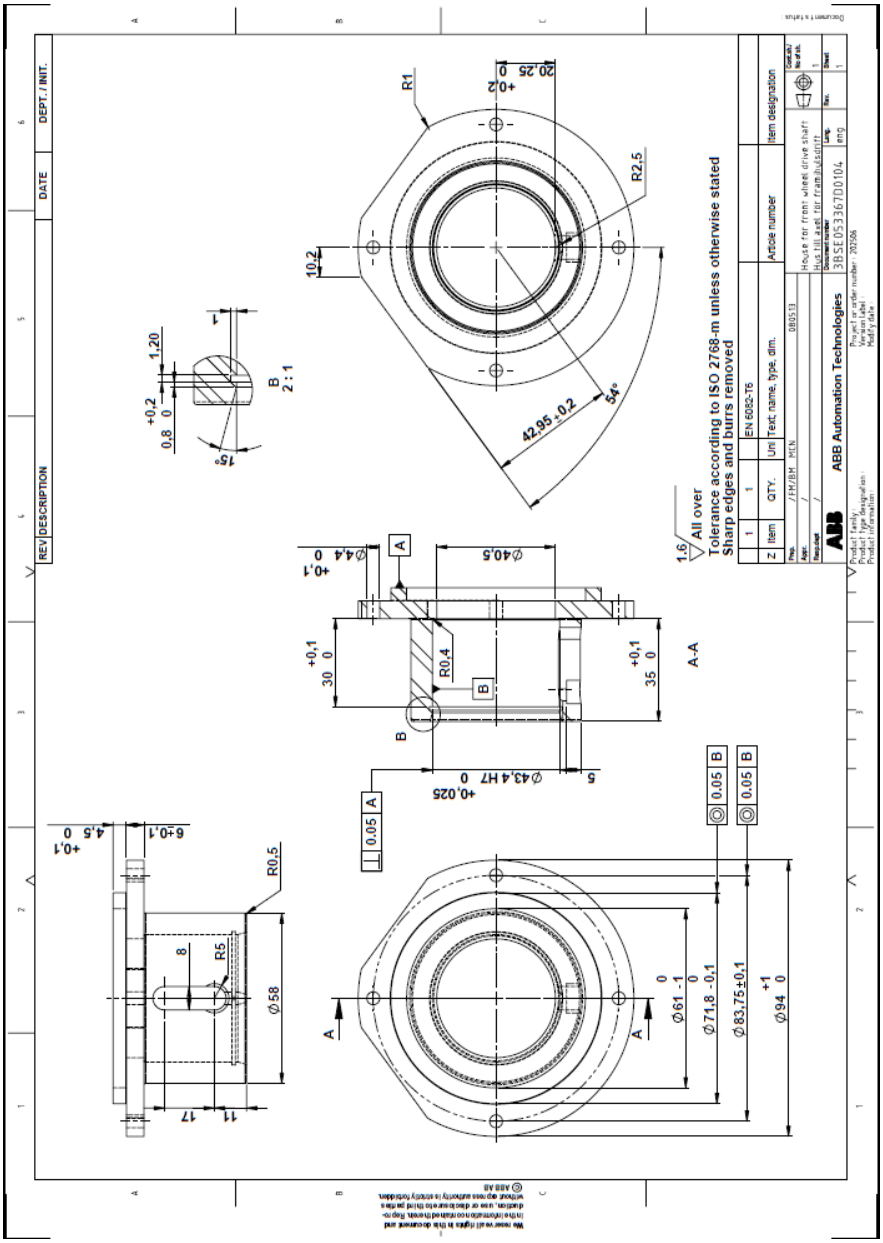

Drawing of the front-wheel-drive output shaft Torductor sensor housing (ABB, 2008b)

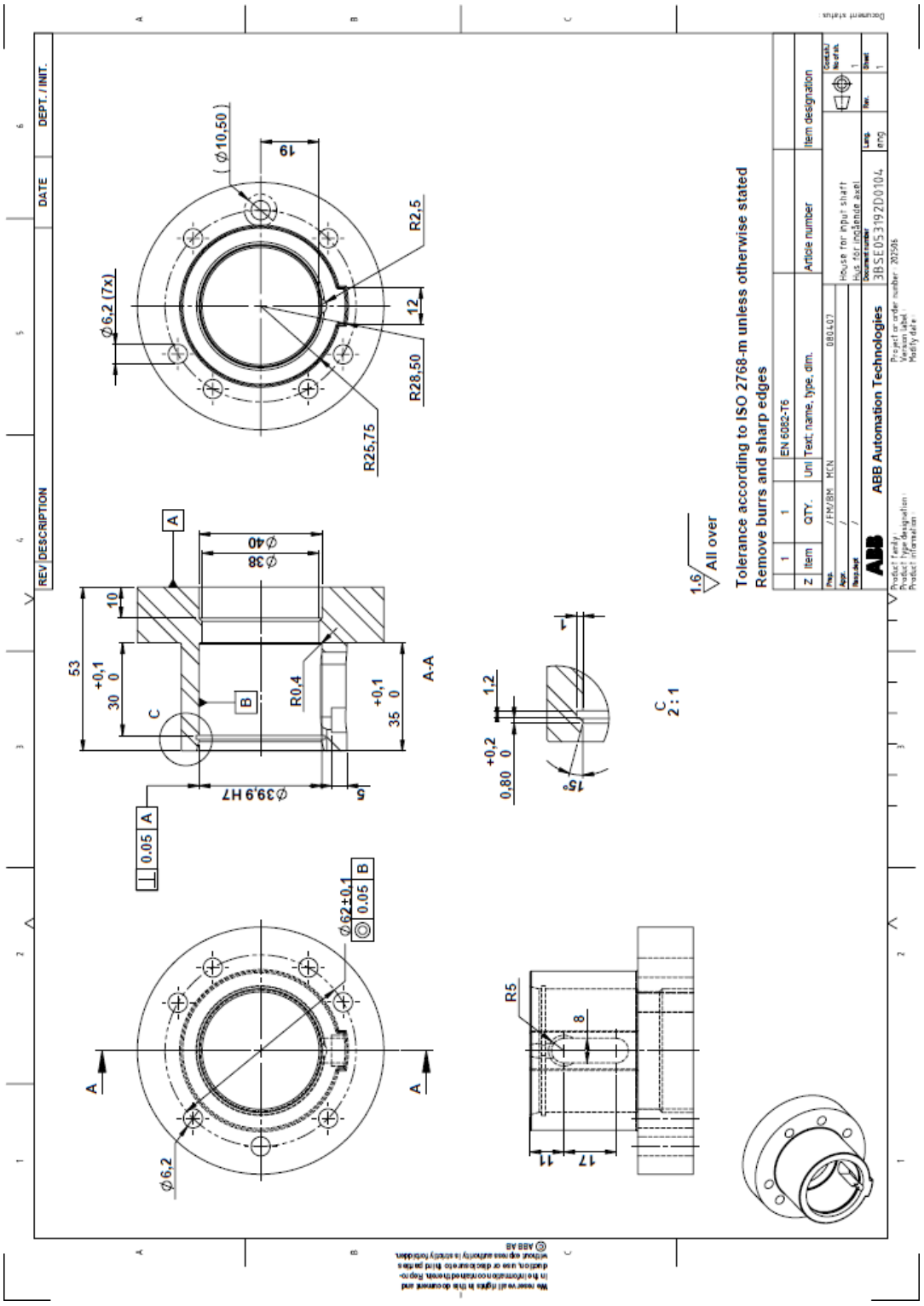

Drawing of the gearbox input Torductor sensor housing (ABB, 2008c)

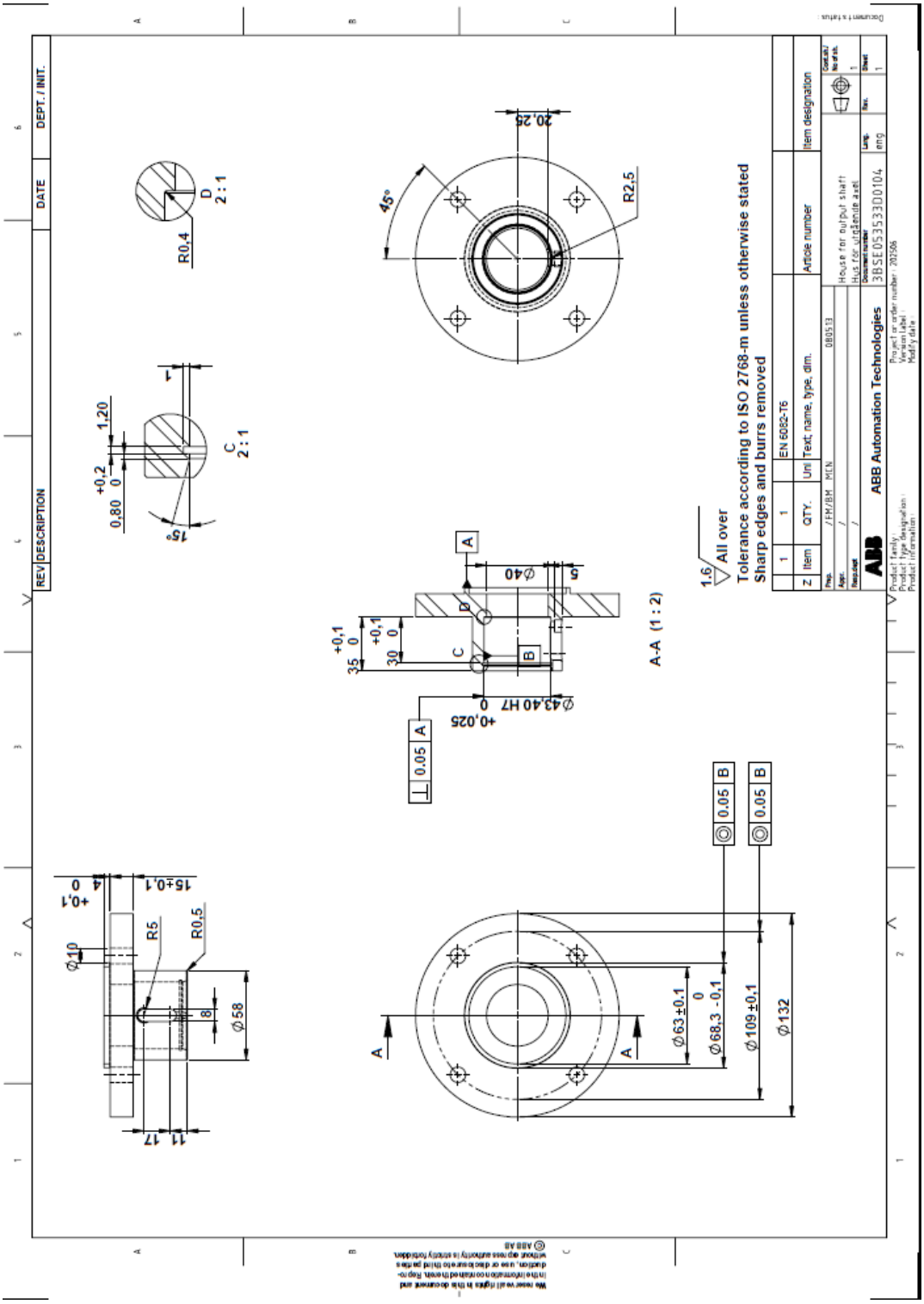

Drawing of the rear wheel drive output shaft Torductor sensor housing (ABB, 2008d)

3.11 Masses of wheel and tyre assemblies

Lead Ratio	Front Wheel and Tyre Masses	Rear Wheel and Tyre Masses	Total Wheel and Tyre Masses
-4%	111/113 kg	284/283 kg	791 kg
+2% (As delivered)	111/113 kg	239/239 kg	702 kg
+10%	154/157 kg	239/239 kg	789 kg

3.12 Calibration of wheel speed sensors

	#1	#2	#3	
Time for 100m (s)	45.3	45.1	45.9	
Measured average speed (m/s)	2.21	2.22	2.18	
Front right wheel average rpm	35.922	36.246	35.437	
Front left wheel average rpm	35.761	35.922	35.761	
Rear right wheel average rpm	27.694	27.818	26.829	
Rear left wheel average rpm	27.447	27.323	27.200	
Indicated average speed (front right) (m/s)	2.22	2.24	2.19	
Indicated average speed (front left) (m/s)	2.21	2.22	2.21	
Indicated average speed (rear right) (m/s)	2.24	2.25	2.17	
Indicated average speed (rear left) (m/s)	2.22	2.21	2.2	**Average**
Error (front right) %	-0.566	-1.024	-0.521	**-0.704**
Error (front left) %	-0.113	-0.122	-1.439	**-0.558**
Error (rear right) %	-1.472	-1.475	0.397	**-0.850**
Error (rear left) %	-0.566	0.329	-0.98	**-0.406**

Appendix to chapter 4

4.1 Analysis of variance: Power delivery efficiency on the sandy test site

Data imported from Excel file: G:\11188200 files\Thesis\Genstat\Peak Values Stats GENSTAT.xlsx
on: 22-Jun-2011 21:01:39
taken from sheet ""Genstat TE Sand"", cells A2:D18001

Identifier	Minimum	Mean	Maximum	Values	Missing
Site				18000	0

Identifier	Values	Missing	Levels
Direction	18000	0	2

Identifier	Values	Missing	Levels
Lead	18000	0	3

Identifier	Minimum	Mean	Maximum	Values	Missing
Power_Delivery_Efficiency	0.4577	0.5405	0.6360	18000	0

Analysis of variance

Variate: Power_Delivery_Efficiency

Source of variation	d.f.	s.s.	m.s.	v.r.	F pr.
Lead	2	3.2381245	1.6190622	6641.72	<.001
Direction	1	47.5979413	47.5979413	1.953E+05	<.001
Lead.Direction	2	0.0972031	0.0486016	199.37	<.001
Residual	17994	4.3864264	0.0002438		
Total	17999	55.3196953			

Information summary

All terms orthogonal, none aliased.

Tables of effects

Variate: Power_Delivery_Efficiency

Lead effects, e.s.e. 0.000202, rep. 6000

Lead	+10	+2	-4
	-0.00529	-0.01313	0.01842

Direction response -0.10285, s.e. 0.000233, rep. 9000

Lead.Direction effects, e.s.e. 0.000285, rep. 3000

Lead	Direction	downhill	uphill
+10		0.00146	-0.00146
+2		0.00182	-0.00182
-4		-0.00328	0.00328

Tables of means

Variate: Power_Delivery_Efficiency

Grand mean 0.54053

Lead	+10	+2	-4
	0.53524	0.52740	0.55895

Direction	downhill	uphill
	0.59195	0.48911

Lead	Direction	downhill	uphill
+10		0.58812	0.48236
+2		0.58065	0.47415
-4		0.60709	0.51081

Standard errors of means

Table	Lead	Direction	Lead Direction
rep.	6000	9000	3000
d.f.	17994	17994	17994
e.s.e.	0.000202	0.000165	0.000285

Standard errors of differences of means

Table	Lead	Direction	Lead Direction
rep.	6000	9000	3000
d.f.	17994	17994	17994
s.e.d.	0.000285	0.000233	0.000403

Least significant differences of means (5% level)

Table	Lead	Direction	Lead Direction
rep.	6000	9000	3000
d.f.	17994	17994	17994
l.s.d.	0.000559	0.000456	0.000790

Stratum standard errors and coefficients of variation

Variate: Power_Delivery_Efficiency

d.f.	s.e.	cv%
17994	0.015613	2.9

Tukey's 95% confidence intervals

Lead

	Mean	
+2	0.5274	a
+10	0.5352	b
-4	0.5589	c

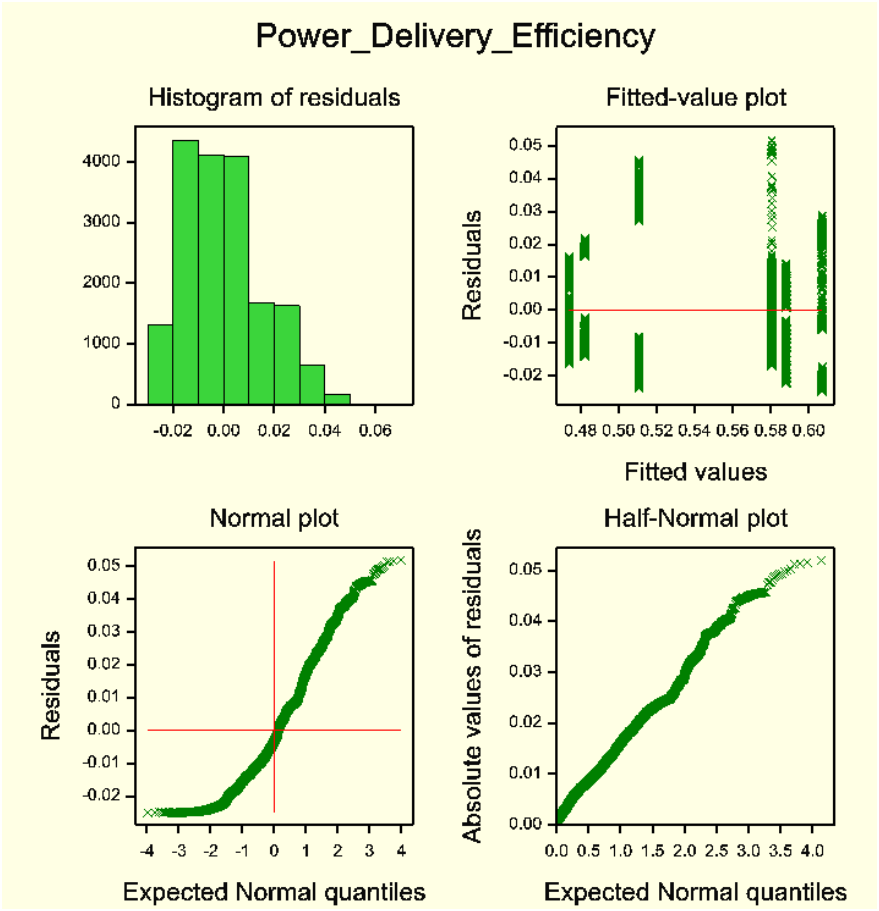
Power_Delivery_Efficiency
Histogram of residuals
Fitted-value plot
Residuals
Fitted values
Normal plot
Half-Normal plot
Absolute values of residuals
Expected Normal quantiles
Expected Normal quantiles

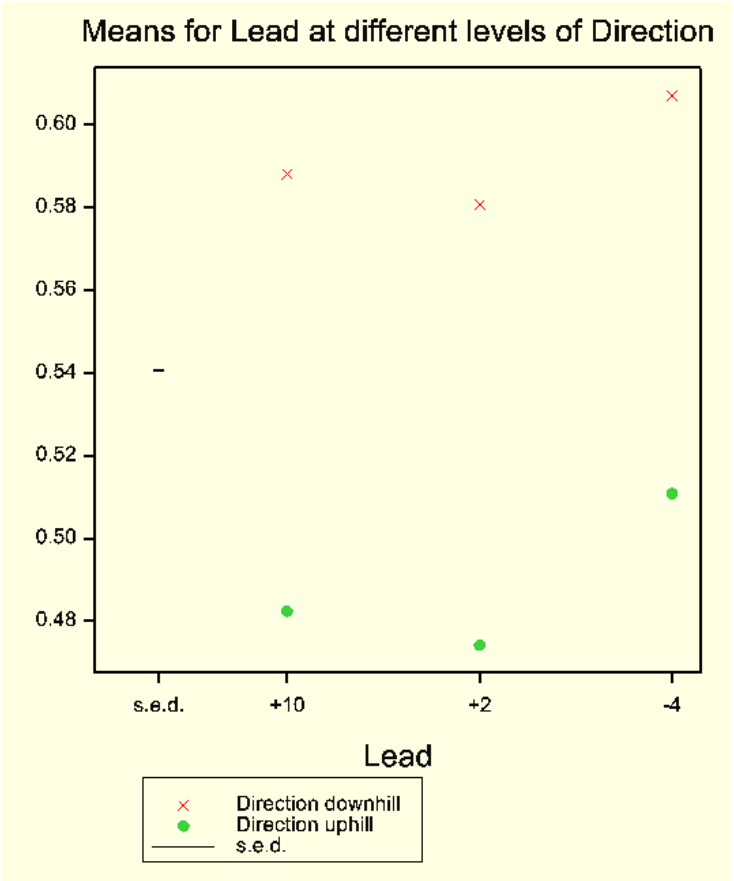
Means for Lead at different levels of Direction
s.e.d.
+10
+2
-4
Lead
Direction downhill
Direction uphill
s.e.d.

4.2 Analysis of variance: Engine power on the sandy test site

Data imported from Excel file: G:\11188200 files\Thesis\Genstat\Peak Values Stats GENSTAT.xlsx
on: 22-Jun-2011 23:30:59
taken from sheet ""Genstat Engine Power Sand "", cells A2:D18001

Identifier	Minimum	Mean	Maximum	Values	Missing
Site				18000	0

Identifier	Values	Missing	Levels
Direction	18000	0	2

Identifier	Values	Missing	Levels
Lead	18000	0	3

Identifier	Minimum	Mean	Maximum	Values	Missing
Engine_Power	59730	61315	63230	18000	0

Analysis of variance

Variate: Engine_Power

Source of variation	d.f.	s.s.	m.s.	v.r.	F pr.
Lead	2	1.602E+09	8.011E+08	10830.35	<.001
Direction	1	2.249E+10	2.249E+10	3.041E+05	<.001
Lead.Direction	2	4.614E+07	2.307E+07	311.92	<.001
Residual	17994	1.331E+09	7.397E+04		
Total	17999	2.547E+10			

Information summary

All terms orthogonal, none aliased.

Tables of effects

Variate: Engine_Power

Lead effects, e.s.e. 3.51, rep. 6000

Lead	+2%	-4%	10%
	418.6	-255.1	-163.5

Direction response 2235.6, s.e. 4.05, rep. 9000

Lead.Direction effects, e.s.e. 4.97, rep. 3000

Lead	Direction	Downhill	Uphill
+2%		-71.1	71.1
-4%		28.3	-28.3
10%		42.8	-42.8

Tables of means

Variate: Engine_Power

Grand mean 61314.9

Lead	+2%	-4%	10%
	61733.5	61059.9	61151.4

Direction	Downhill	Uphill
	60197.1	62432.7

Lead	Direction	Downhill	Uphill
+2%		60544.6	62922.4
-4%		59970.4	62149.3
10%		60076.4	62226.4

Standard errors of means

Table	Lead	Direction	Lead Direction
rep.	6000	9000	3000
d.f.	17994	17994	17994
e.s.e.	3.51	2.87	4.97

Standard errors of differences of means

Table	Lead	Direction	Lead Direction
rep.	6000	9000	3000
d.f.	17994	17994	17994
s.e.d.	4.97	4.05	7.02

Least significant differences of means (5% level)

Table	Lead	Direction	Lead Direction
rep.	6000	9000	3000
d.f.	17994	17994	17994
l.s.d.	9.73	7.95	13.76

Stratum standard errors and coefficients of variation

Variate: Engine_Power

d.f.	s.e.	cv%
17994	271.97	0.4

Tukey's 95% confidence intervals

Lead

	Mean	
-4%	61060	a
10%	61151	b
+2%	61734	c

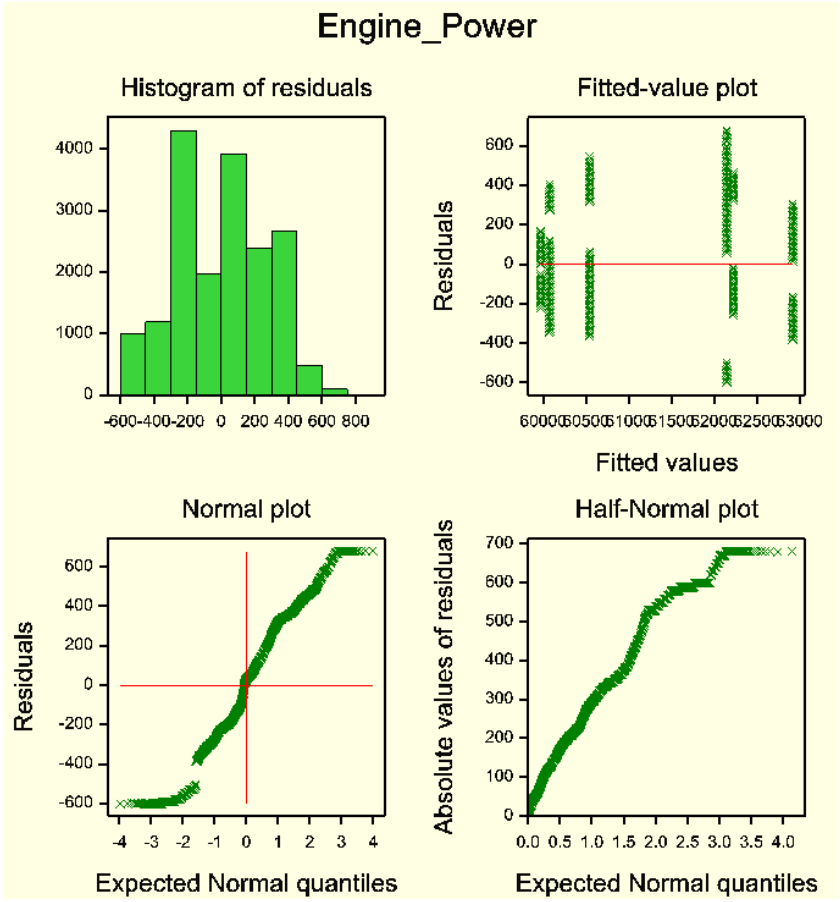
Engine_Power
Histogram of residuals
Fitted-value plot
Residuals
Fitted values
Normal plot
Half-Normal plot
Residuals
Absolute values of residuals
Expected Normal quantiles
Expected Normal quantiles

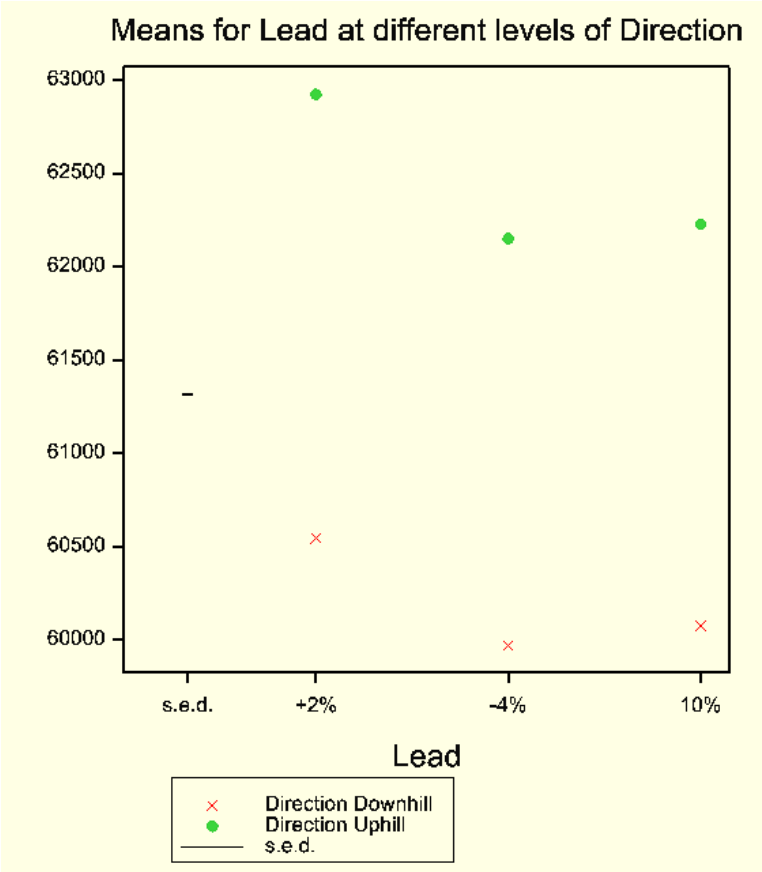
Means for Lead at different levels of Direction
s.e.d.
+2%
-4%
10%
Lead
Direction Downhill
Direction Uphill
s.e.d.

4.3 Analysis of variance: Drawbar power on the sandy test site

Data imported from Excel file: G:\11188200 files\Thesis\Genstat\Peak Values Stats GENSTAT.xlsx
on: 22-Jun-2011 21:49:17
taken from sheet ""Genstat Drawbar Power Sand"", cells A2:D18001

Identifier	Minimum	Mean	Maximum	Values	Missing
Site				18000	0

Identifier	Values	Missing	Levels
Direction	18000	0	2

Identifier	Values	Missing	Levels
Lead	18000	0	3

Identifier	Minimum	Mean	Maximum	Values	Missing
Drawbar_Power	26330	30658	35600	18000	0

Analysis of variance

Variate: Drawbar_Power

Source of variation	d.f.	s.s.	m.s.	v.r.	F pr.
Lead	2	4.382E+09	2.191E+09	619.16	<.001
Direction	1	4.179E+10	4.179E+10	11810.04	<.001
Lead.Direction	2	3.982E+09	1.991E+09	562.71	<.001
Residual	17994	6.367E+10	3.538E+06		
Total	17999	1.138E+11			

Information summary

All terms orthogonal, none aliased.

Tables of effects

Variate: Drawbar_Power

Lead effects, e.s.e. 24.3, rep. 6000

Lead	+10	+2	-4
	165.	-670.	505.

Direction response -3047., s.e. 28.0, rep. 9000

Lead.Direction effects, e.s.e. 34.3, rep. 3000

Lead	Direction	downhill	uphill
+10		655.	-655.
+2		-225.	225.
-4		-430.	430.

Tables of means

Variate: Drawbar_Power

Grand mean 30658.

Lead	+10	+2	-4
	30823.	29988.	31162.

Direction	downhill	uphill
	32181.	29134.

Lead	Direction	downhill	uphill
+10		33001.	28644.
+2		31287.	28689.
-4		32256.	30069.

Standard errors of means

Table	Lead	Direction	Lead Direction
rep.	6000	9000	3000
d.f.	17994	17994	17994
e.s.e.	24.3	19.8	34.3

Standard errors of differences of means

Table	Lead	Direction	Lead Direction
rep.	6000	9000	3000
d.f.	17994	17994	17994
s.e.d.	34.3	28.0	48.6

Least significant differences of means (5% level)

Table	Lead	Direction	Lead Direction
rep.	6000	9000	3000
d.f.	17994	17994	17994
l.s.d.	67.3	55.0	95.2

Stratum standard errors and coefficients of variation

Variate: Drawbar_Power

d.f.	s.e.	cv%
17994	1881.1	6.1

Tukey's 95% confidence intervals

Lead

	Mean	
+2	29988	a
+10	30823	b
-4	31162	c

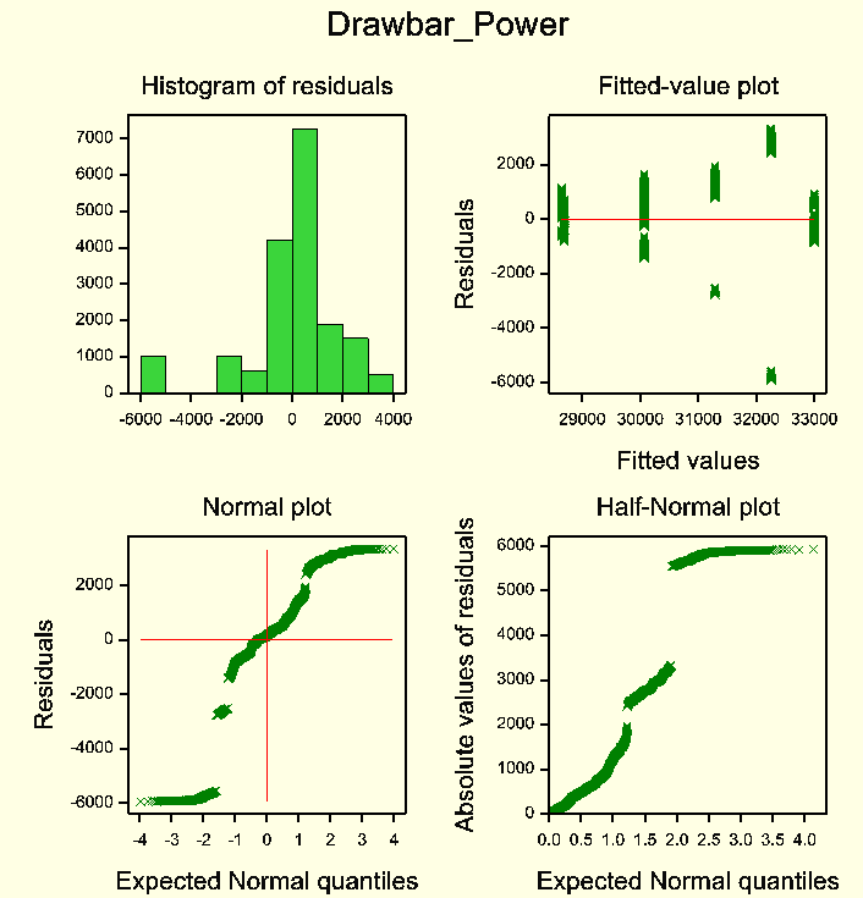
Drawbar_Power
Histogram of residuals
Fitted-value plot
Residuals
Fitted values
Normal plot
Half-Normal plot
Absolute values of residuals
Expected Normal quantiles
Expected Normal quantiles

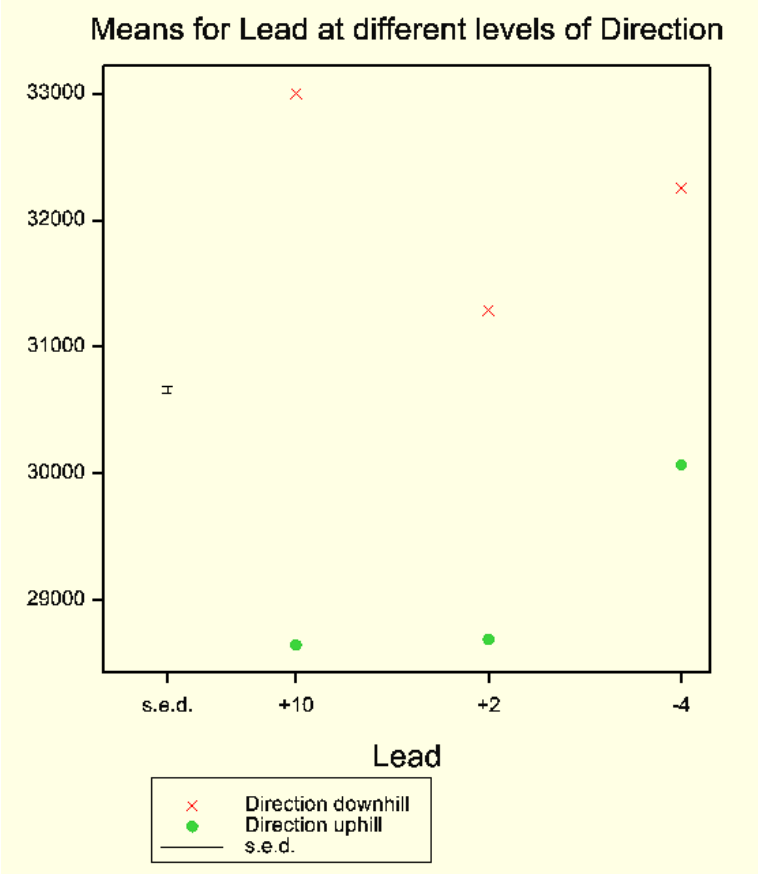
Means for Lead at different levels of Direction
s.e.d.
+10
+2
-4
Lead
Direction downhill
Direction uphill
s.e.d.

4.4 Analysis of variance: Drawbar pull on the sandy test site

Data imported from Excel file: G:\11188200 files\Thesis\Genstat\Peak Values Stats GENSTAT.xlsx
on: 22-Jun-2011 22:01:42
taken from sheet ""Genstat DBP Sand"", cells A2:D18001

Identifier	Minimum	Mean	Maximum	Values	Missing
Site				18000	0

Identifier	Values	Missing	Levels
Direction	18000	0	2

Identifier	Values	Missing	Levels
Lead	18000	0	3

Identifier	Minimum	Mean	Maximum	Values	Missing
Drawbar_Pull	23200	24820	26710	18000	0

Analysis of variance

Variate: Drawbar_Pull

Source of variation	d.f.	s.s.	m.s.	v.r.	F pr.
Lead	2	4.044E+09	2.022E+09	4116.81	<.001
Direction	1	2.542E+09	2.542E+09	5175.39	<.001
Lead.Direction	2	5.814E+08	2.907E+08	591.87	<.001
Residual	17994	8.837E+09	4.911E+05		
Total	17999	1.600E+10			

Information summary

All terms orthogonal, none aliased.

Tables of effects

Variate: Drawbar_Pull

Lead effects, e.s.e. 9.05, rep. 6000

Lead	+10	+2	-4
	-85.7	-532.9	618.6

Direction response -751.6, s.e. 10.45, rep. 9000

Lead.Direction effects, e.s.e. 12.79, rep. 3000

Lead	Direction	downhill	uphill
+10		-162.9	162.9
+2		-87.5	87.5
-4		250.4	-250.4

Tables of means

Variate: Drawbar_Pull

Grand mean 24820.4

Lead	+10	+2	-4
	24734.6	24287.5	25439.0

Direction	downhill	uphill
	25196.2	24444.6

Lead	Direction	downhill	uphill
+10		24947.5	24521.7
+2		24575.8	23999.3
-4		26065.2	24812.8

Standard errors of means

Table	Lead	Direction	Lead Direction
rep.	6000	9000	3000
d.f.	17994	17994	17994
e.s.e.	9.05	7.39	12.79

Standard errors of differences of means

Table	Lead	Direction	Lead Direction
rep.	6000	9000	3000
d.f.	17994	17994	17994
s.e.d.	12.79	10.45	18.09

Least significant differences of means (5% level)

Table	Lead	Direction	Lead Direction
rep.	6000	9000	3000
d.f.	17994	17994	17994
l.s.d.	25.08	20.48	35.47

Stratum standard errors and coefficients of variation

Variate: Drawbar_Pull

d.f.	s.e.	cv%
17994	700.81	2.8

Tukey's 95% confidence intervals

Lead

	Mean	
+2	24288	a
+10	24735	b
-4	25439	c

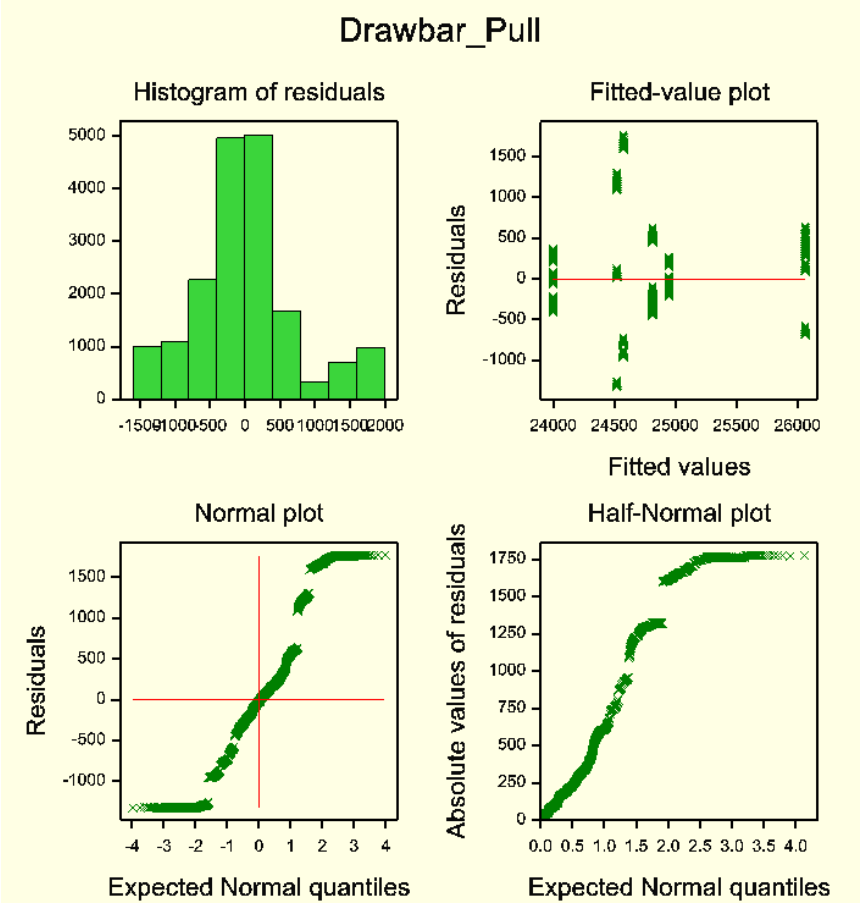
Drawbar_Pull
Histogram of residuals
Fitted-value plot
Residuals
Fitted values
Normal plot
Half-Normal plot
Absolute values of residuals
Expected Normal quantiles
Expected Normal quantiles

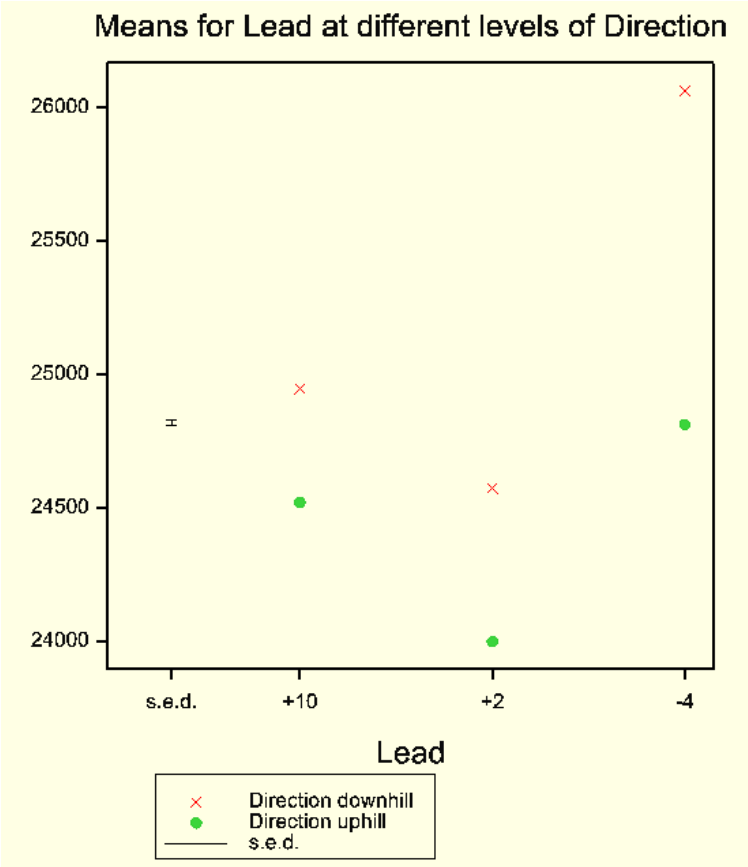
Means for Lead at different levels of Direction
s.e.d.
+10
+2
-4
Lead
Direction downhill
Direction uphill
s.e.d.

4.5 Analysis of variance: Power delivery efficiency on the clay test site

Data imported from Excel file: G:\11188200 files\Thesis\Genstat\Peak Values Stats GENSTAT.xlsx
on: 22-Jun-2011 21:12:59
taken from sheet ""Genstat TE Clay"", cells A2:D18001

Identifier	Minimum	Mean	Maximum	Values	Missing
Site				18000	0

Identifier	Values	Missing	Levels
Direction	18000	0	2

Identifier	Values	Missing	Levels
Lead	18000	0	3

Identifier	Minimum	Mean	Maximum	Values	Missing
Power_Delivery_Efficiency	0.4771	0.5334	0.6216	18000	0

Analysis of variance

Variate: Power_Delivery_Efficiency

Source of variation	d.f.	s.s.	m.s.	v.r.	F pr.
Lead	2	7.7144432	3.8572216	11444.69	<.001
Direction	1	0.0180498	0.0180498	53.56	<.001
Lead.Direction	2	4.3993061	2.1996531	6526.55	<.001
Residual	17994	6.0645459	0.0003370		
Total	17999	18.1963450			

Information summary

All terms orthogonal, none aliased.

Tables of effects

Variate: Power_Delivery_Efficiency

Lead effects, e.s.e. 0.000237, rep. 6000

Lead	+10	+2	-4
	-0.02042	0.02838	-0.00796

Direction response -0.00200, s.e. 0.000274, rep. 9000

Lead.Direction effects, e.s.e. 0.000335, rep. 3000

Lead	Direction	North	south
+10		-0.01517	0.01517
+2		-0.00634	0.00634
-4		0.02151	-0.02151

Tables of means

Variate: Power_Delivery_Efficiency

Grand mean 0.53343

Lead	+10	+2	-4
	0.51300	0.56180	0.52547

Direction	North	south
	0.53443	0.53242

Lead	Direction	North	south
+10		0.49883	0.52718
+2		0.55647	0.56714
-4		0.54798	0.50295

Standard errors of means

Table	Lead	Direction	Lead Direction
rep.	6000	9000	3000
d.f.	17994	17994	17994
e.s.e.	0.000237	0.000194	0.000335

Standard errors of differences of means

Table	Lead	Direction	Lead Direction
rep.	6000	9000	3000
d.f.	17994	17994	17994
s.e.d.	0.000335	0.000274	0.000474

Least significant differences of means (5% level)

Table	Lead	Direction	Lead Direction
rep.	6000	9000	3000
d.f.	17994	17994	17994
l.s.d.	0.000657	0.000536	0.000929

Stratum standard errors and coefficients of variation

Variate: Power_Delivery_Efficiency

d.f.	s.e.	cv%
17994	0.018358	3.4

Tukey's 95% confidence intervals

Lead

	Mean	
+10	0.5130	a
-4	0.5255	b
+2	0.5618	c


Power_Delivery_Efficiency
Histogram of residuals
Fitted-value plot
Residuals
Fitted values
Normal plot
Half-Normal plot
Residuals
Absolute values of residuals
Expected Normal quantiles
Expected Normal quantiles

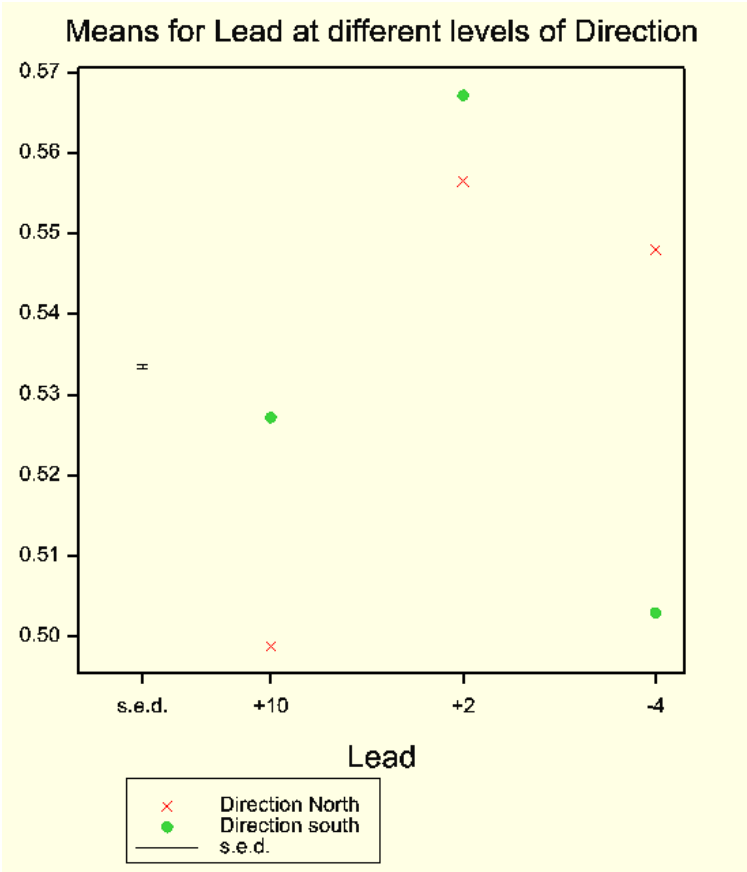
Means for Lead at different levels of Direction
s.e.d.
+10
+2
-4
Lead
Direction North
Direction south
s.e.d.

4.6 Analysis of variance: Engine power on the clay test site

Data imported from Excel file: G:\11188200 files\Thesis\Genstat\Peak Values Stats GENSTAT.xlsx
on: 22-Jun-2011 21:39:15
taken from sheet ""Genstat Engine Power Clay"", cells A2:D18001

Identifier	Minimum	Mean	Maximum	Values	Missing
Site				18000	0

Identifier	Values	Missing	Levels
Direction	18000	0	2

Identifier	Values	Missing	Levels
Lead	18000	0	3

Identifier	Minimum	Mean	Maximum	Values	Missing
Engine_Power	59890	62378	64220	18000	0

Analysis of variance

Variate: Engine_Power

Source of variation	d.f.	s.s.	m.s.	v.r.	F pr.
Lead	2	2.408E+09	1.204E+09	8559.23	<.001
Direction	1	1.074E+09	1.074E+09	7639.46	<.001
Lead.Direction	2	4.382E+09	2.191E+09	15579.85	<.001
Residual	17994	2.531E+09	1.406E+05		
Total	17999	1.040E+10			

Information summary

All terms orthogonal, none aliased.

Tables of effects

Variate: Engine_Power

Lead effects, e.s.e. 4.84, rep. 6000

Lead	+10	+2	-4
	371.8	125.4	-497.3

Direction response -488.6, s.e. 5.59, rep. 9000

Lead.Direction effects, e.s.e. 6.85, rep. 3000

Lead	Direction	North	south
+10		240.8	-240.8
+2		446.8	-446.8
-4		-687.6	687.6

Tables of means

Variate: Engine_Power

Grand mean 62378.0

Lead	+10	+2	-4
	62749.8	62503.4	61880.7

Direction	North	south
	62622.3	62133.7

Lead	Direction	North	south
+10		63234.9	62264.7
+2		63194.5	61812.3
-4		61437.4	62324.0

Standard errors of means

Table	Lead	Direction	Lead Direction
rep.	6000	9000	3000
d.f.	17994	17994	17994
e.s.e.	4.84	3.95	6.85

Standard errors of differences of means

Table	Lead	Direction	Lead Direction
rep.	6000	9000	3000
d.f.	17994	17994	17994
s.e.d.	6.85	5.59	9.68

Least significant differences of means (5% level)

Table	Lead	Direction	Lead Direction
rep.	6000	9000	3000
d.f.	17994	17994	17994
l.s.d.	13.42	10.96	18.98

Stratum standard errors and coefficients of variation

Variate: Engine_Power

d.f.	s.e.	cv%
17994	375.02	0.6

Tukey's 95% confidence intervals

Lead

	Mean	
-4	61881	a
+2	62503	b
+10	62750	c

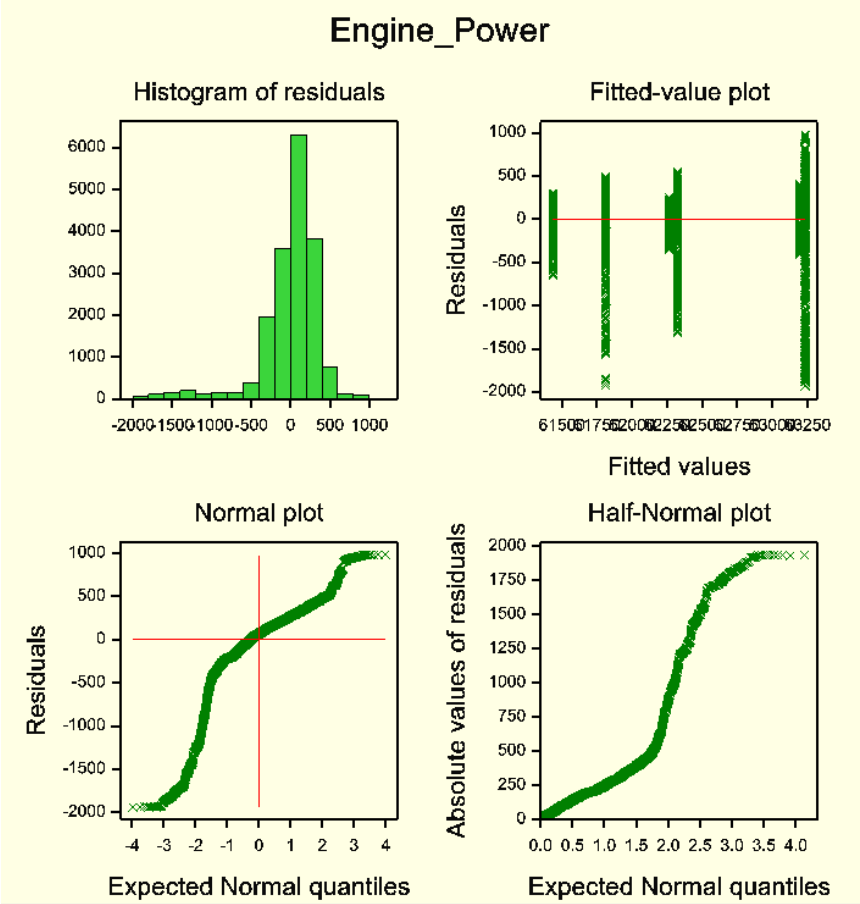
Engine_Power
Histogram of residuals
Fitted-value plot
Residuals
Fitted values
Normal plot
Half-Normal plot
Residuals
Absolute values of residuals
Expected Normal quantiles
Expected Normal quantiles

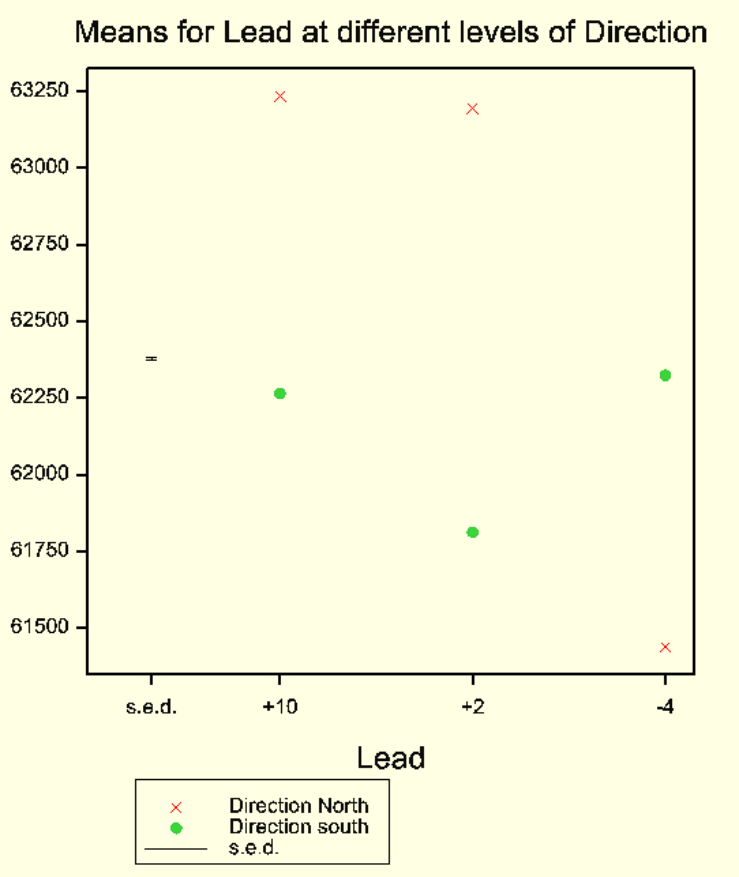
Means for Lead at different levels of Direction
s.e.d.
+10
+2
-4
Lead
Direction North
Direction south
s.e.d.

4.7 Analysis of variance: Drawbar power on the clay test site

Data imported from Excel file: G:\11188200 files\Thesis\Genstat\Peak Values Stats GENSTAT.xlsx
on: 22-Jun-2011 21:53:27
taken from sheet ""Genstat Drawbar Power Clay"", cells A2:D18001

Identifier	Minimum	Mean	Maximum	Values	Missing
Site				18000	0

Identifier	Values	Missing	Levels
Direction	18000	0	2

Identifier	Values	Missing	Levels
Lead	18000	0	3

Identifier	Minimum	Mean	Maximum	Values	Missing
Drawbar_Power	28640	32875	37230	18000	0

Analysis of variance

Variate: Drawbar_Power

Source of variation	d.f.	s.s.	m.s.	v.r.	F pr.
Lead	2	1.909E+10	9.543E+09	6088.14	<.001
Direction	1	8.342E+08	8.342E+08	532.20	<.001
Lead.Direction	2	1.081E+10	5.403E+09	3446.89	<.001
Residual	17994	2.820E+10	1.567E+06		
Total	17999	5.893E+10			

Information summary

All terms orthogonal, none aliased.

Tables of effects

Variate: Drawbar_Power

Lead effects, e.s.e. 16.16, rep. 6000

Lead	+10	+2	-4
	-845.5	1449.5	-604.1

Direction response -430.6, s.e. 18.66, rep. 9000

Lead.Direction effects, e.s.e. 22.86, rep. 3000

Lead	Direction	North	south
+10		-1025.0	1025.0
+2		177.1	-177.1
-4		847.9	-847.9

Tables of means

Variate: Drawbar_Power

Grand mean 32874.8

Lead	+10	+2	-4
	32029.4	34324.4	32270.8

Direction	North	south
	33090.1	32659.6

Lead	Direction	North	south
+10		31219.6	32839.1
+2		34716.8	33932.0
-4		33334.0	31207.6

Standard errors of means

Table	Lead	Direction	Lead Direction
rep.	6000	9000	3000
d.f.	17994	17994	17994
e.s.e.	16.16	13.20	22.86

Standard errors of differences of means

Table	Lead	Direction	Lead Direction
rep.	6000	9000	3000
d.f.	17994	17994	17994
s.e.d.	22.86	18.66	32.33

Least significant differences of means (5% level)

Table	Lead	Direction	Lead Direction
rep.	6000	9000	3000
d.f.	17994	17994	17994
l.s.d.	44.80	36.58	63.36

Stratum standard errors and coefficients of variation

Variate: Drawbar_Power

d.f.	s.e.	cv%
17994	1251.97	3.8

Tukey's 95% confidence intervals

Lead

	Mean	
+10	32029	a
-4	32271	b
+2	34324	c

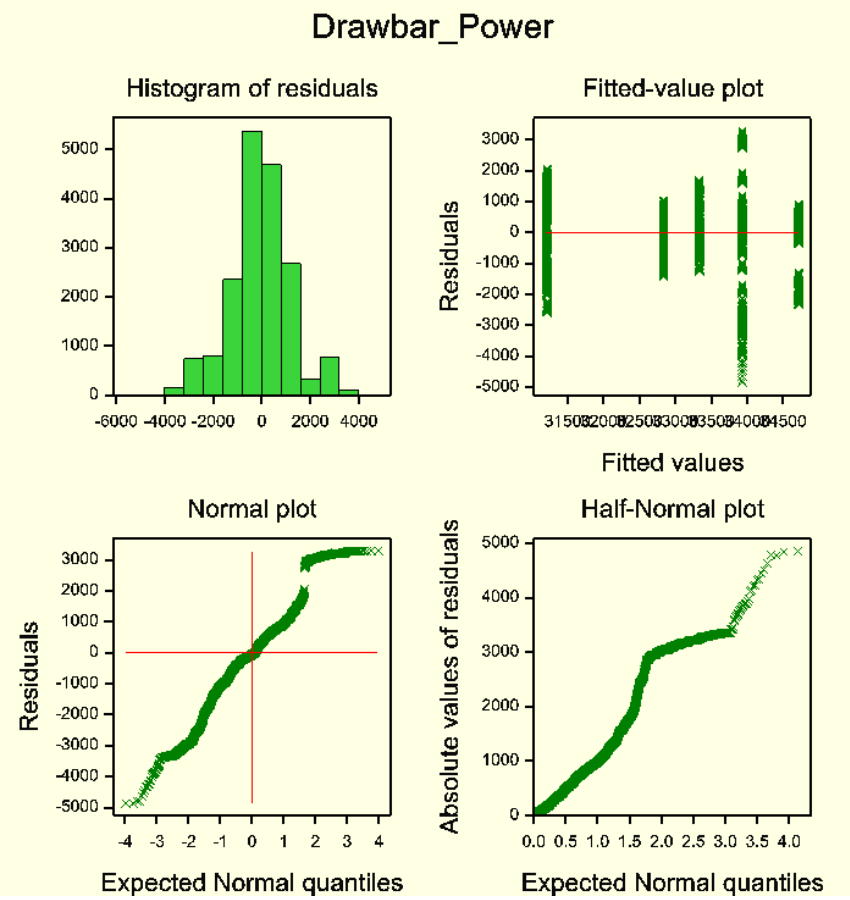
Drawbar_Power
Histogram of residuals
Fitted-value plot
Residuals
Fitted values
Normal plot
Half-Normal plot
Residuals
Absolute values of residuals
Expected Normal quantiles
Expected Normal quantiles

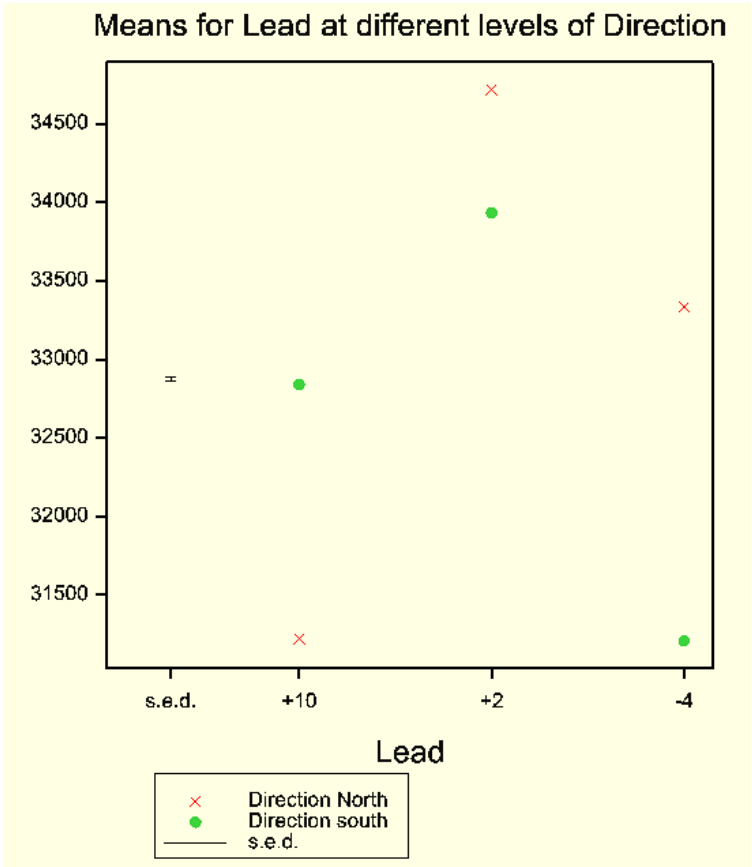
Means for Lead at different levels of Direction
s.e.d.
+10
+2
-4
Lead
Direction North
Direction south
s.e.d.

4.8 Analysis of variance: Drawbar pull on the clay test site

Data imported from Excel file: G:\11188200 files\Thesis\Genstat\Peak Values Stats GENSTAT.xlsx
on: 22-Jun-2011 22:05:33
taken from sheet ""Genstat DBP Clay"", cells A2:D18001

Identifier	Minimum	Mean	Maximum	Values	Missing
Site				18000	0

Identifier	Values	Missing	Levels
Direction	18000	0	2

Identifier	Values	Missing	Levels
Lead	18000	0	3

Identifier	Minimum	Mean	Maximum	Values	Missing
Drawbar_Pull	23110	25894	28890	18000	0

Analysis of variance

Variate: Drawbar_Pull

Source of variation	d.f.	s.s.	m.s.	v.r.	F pr.
Lead	2	2.399E+10	1.199E+10	30180.95	<.001
Direction	1	1.860E+08	1.860E+08	468.01	<.001
Lead.Direction	2	3.313E+09	1.657E+09	4168.25	<.001
Residual	17994	7.151E+09	3.974E+05		
Total	17999	3.464E+10			

Information summary

All terms orthogonal, none aliased.

Tables of effects

Variate: Drawbar_Pull

Lead effects, e.s.e. 8.14, rep. 6000

Lead	+10	+2	-4
	-797.4	1632.5	-835.1

Direction response -203.3, s.e. 9.40, rep. 9000

Lead.Direction effects, e.s.e. 11.51, rep. 3000

Lead	Direction	North	south
+10		-447.8	447.8
+2		-130.7	130.7
-4		578.4	-578.4

Tables of means

Variate: Drawbar_Pull

Grand mean 25894.3

Lead	+10	+2	-4
	25096.9	27526.8	25059.2

Direction	North	south
	25996.0	25792.7

Lead	Direction	North	south
+10		24750.8	25443.1
+2		27497.8	27555.8
-4		25739.3	24379.1

Standard errors of means

Table	Lead	Direction	Lead Direction
rep.	6000	9000	3000
d.f.	17994	17994	17994
e.s.e.	8.14	6.65	11.51

Standard errors of differences of means

Table	Lead	Direction	Lead Direction
rep.	6000	9000	3000
d.f.	17994	17994	17994
s.e.d.	11.51	9.40	16.28

Least significant differences of means (5% level)

Table	Lead	Direction	Lead Direction
rep.	6000	9000	3000
d.f.	17994	17994	17994
l.s.d.	22.56	18.42	31.90

Stratum standard errors and coefficients of variation

Variate: Drawbar_Pull

d.f.	s.e.	cv%
17994	630.41	2.4

Tukey's 95% confidence intervals

Lead

	Mean	
-4	25059	a
+10	25097	b
+2	27527	c

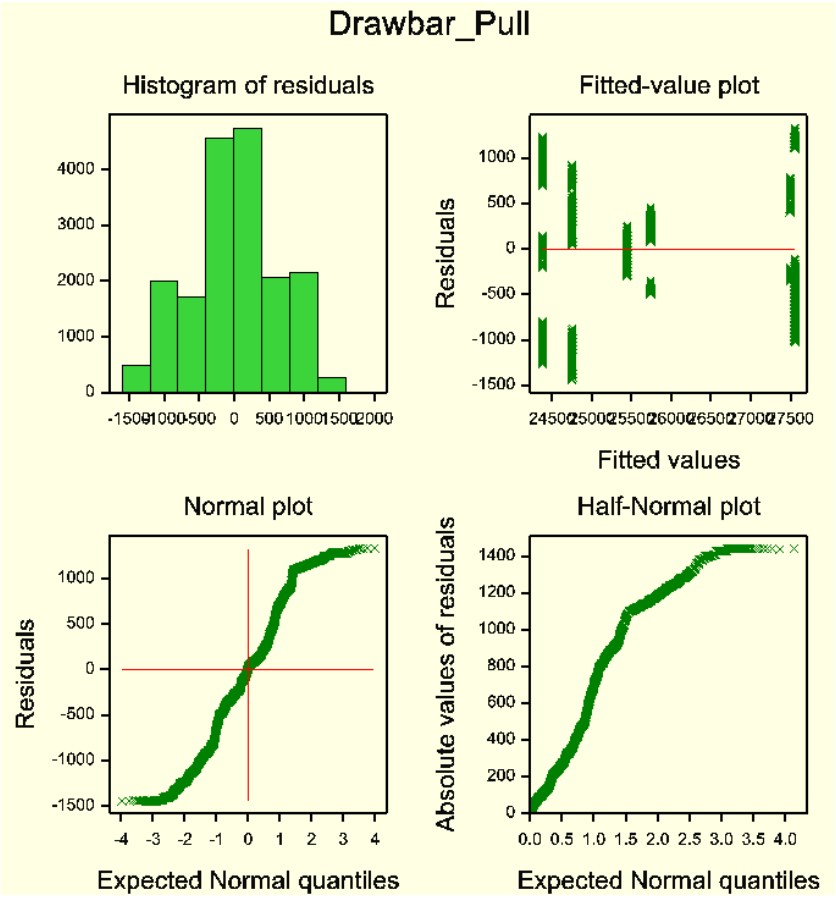
Drawbar_Pull
Histogram of residuals
Fitted-value plot
Residuals
Fitted values
Normal plot
Half-Normal plot
Absolute values of residuals
Expected Normal quantiles
Expected Normal quantiles

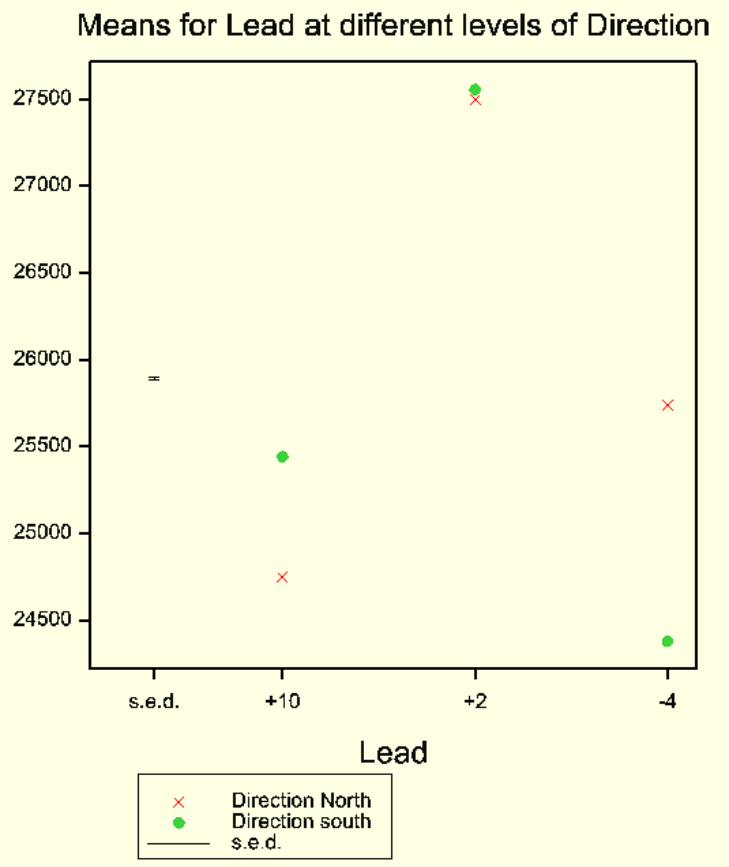
Means for Lead at different levels of Direction
s.e.d.
+10
+2
-4
Lead
Direction North
Direction south
s.e.d.

4.9 Analysis of variance: Slope of front axle torque v drawbar pull on sand

Data imported from Excel file: G:\11188200 files\Thesis\Genstat\Torque v DBP stats GENSTAT.xlsx
on: 22-Jun-2011 23:09:36
taken from sheet ""GENSTAT Sand Torque DBP F Slope"", cells A2:D19

Identifier	Values	Missing	Levels
Direction	18	0	2

Identifier	Minimum	Mean	Maximum	Values	Missing
Axle				18	0

Identifier	Values	Missing	Levels
Lead	18	0	3

Identifier	Minimum	Mean	Maximum	Values	Missing
Slope	0.01600	0.06244	0.09700	18	0

Analysis of variance

Variate: Slope

Source of variation	d.f.	s.s.	m.s.	v.r.	F pr.
Lead	2	0.01290878	0.00645439	598.86	<.001
Direction	1	0.00007200	0.00007200	6.68	0.024
Lead.Direction	2	0.00047233	0.00023617	21.91	<.001
Residual	12	0.00012933	0.00001078		
Total	17	0.01358244			

Information summary

All terms orthogonal, none aliased.

Tables of effects

Variate: Slope

Lead effects, e.s.e. 0.001340, rep. 6

Lead	+10%	+2%	-4%
	-0.03628	0.00872	0.02756

Direction response -0.00400, s.e. 0.001548, rep. 9

Lead.Direction effects, e.s.e. 0.001895, rep. 3

Lead	Direction	Downhill	Uphill
+10%		-0.00717	0.00717
+2%		0.00450	-0.00450
-4%		0.00267	-0.00267

Tables of means

Variate: Slope

Grand mean 0.06244

Lead	+10%	+2%	-4%
	0.02617	0.07117	0.09000

Direction	Downhill	Uphill
	0.06444	0.06044

Lead	Direction	Downhill	Uphill
+10%		0.02100	0.03133
+2%		0.07767	0.06467
-4%		0.09467	0.08533

Standard errors of means

Table	Lead	Direction	Lead Direction
rep.	6	9	3
d.f.	12	12	12
e.s.e.	0.001340	0.001094	0.001895

Standard errors of differences of means

Table	Lead	Direction	Lead Direction
rep.	6	9	3
d.f.	12	12	12
s.e.d.	0.001895	0.001548	0.002681

Least significant differences of means (5% level)

Table	Lead	Direction	Lead Direction
rep.	6	9	3
d.f.	12	12	12
l.s.d.	0.004130	0.003372	0.005840

Stratum standard errors and coefficients of variation

Variate: Slope

d.f.	s.e.	cv%
12	0.003283	5.3

Tukey's 95% confidence intervals

Lead

	Mean	
+10%	0.02617	a
+2%	0.07117	b
-4%	0.09000	c

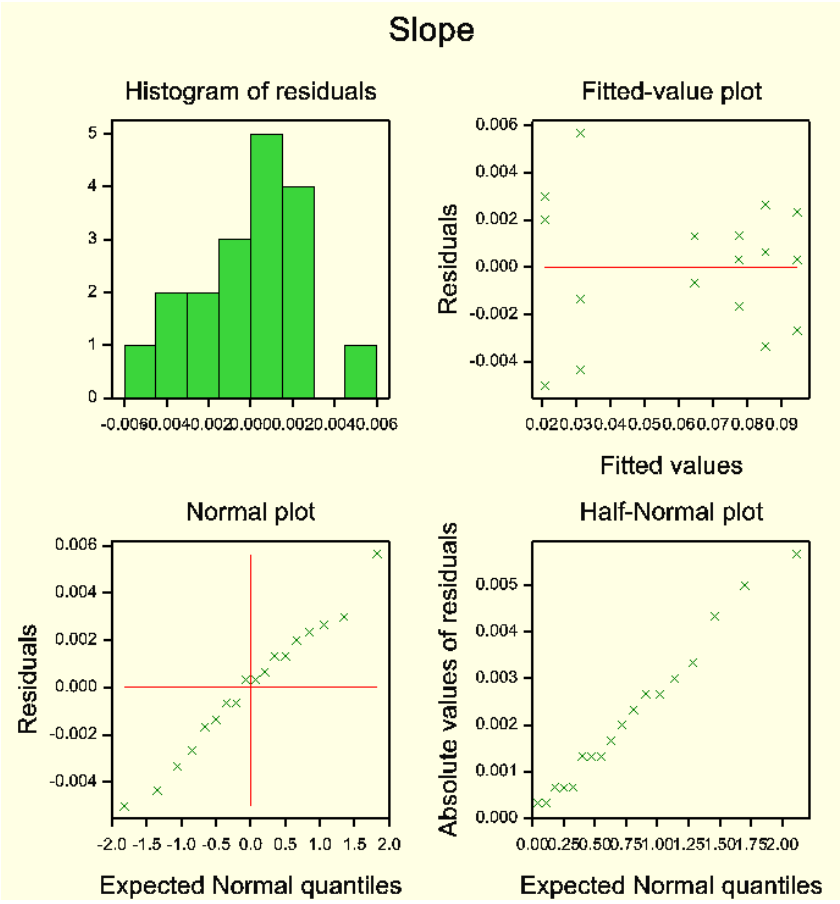
Slope
Histogram of residuals
Fitted-value plot
Residuals
Fitted values
Normal plot
Half-Normal plot
Absolute values of residuals
Expected Normal quantiles
Expected Normal quantiles

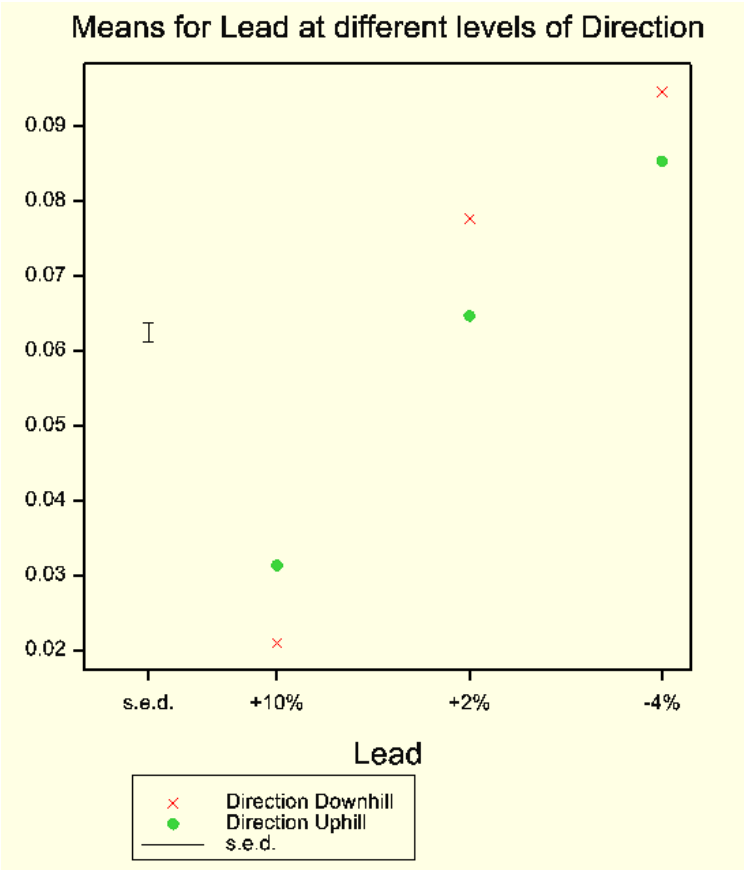
Means for Lead at different levels of Direction
s.e.d.
+10%
+2%
-4%
Lead
Direction Downhill
Direction Uphill
s.e.d.

4.10 Analysis of variance: Slope of rear axle torque v drawbar pull on sand

Data imported from Excel file: G:\11188200 files\Thesis\Genstat\Torque v DBP stats GENSTAT.xlsx
on: 22-Jun-2011 23:08:22
taken from sheet ""GENSTAT Sand Torque DBP R Slope"", cells A2:S19

Identifier	Values	Missing	Levels
Direction	18	0	2

Identifier	Minimum	Mean	Maximum	Values	Missing
Axle				18	0

Identifier	Values	Missing	Levels
Lead	18	0	3

Identifier	Minimum	Mean	Maximum	Values	Missing
Slope	0.7730	0.8783	1.340	18	0

Skew

Analysis of variance

Variate: Slope

Source of variation	d.f.	s.s.	m.s.	v.r.	F pr.
Lead	2	0.08736	0.04368	2.50	0.124
Direction	1	0.00871	0.00871	0.50	0.494
Lead.Direction	2	0.01440	0.00720	0.41	0.672
Residual	12	0.21002	0.01750		
Total	17	0.32049			

Information summary

All terms orthogonal, none aliased.

Tables of effects

Variate: Slope

Lead effects, e.s.e. 0.0540, rep. 6

Lead	+10%	+2%	-4%
	0.018	-0.093	0.075

Direction response 0.044, s.e. 0.0624, rep. 9

Lead.Direction effects, e.s.e. 0.0764, rep. 3

Lead	Direction	Downhill	Uphill
+10%		0.024	-0.024
+2%		0.015	-0.015
-4%		-0.040	0.040

Tables of means

Variate: Slope

Grand mean 0.878

Lead	+10%	+2%	-4%
	0.897	0.785	0.953

Direction	Downhill	Uphill
	0.856	0.900

Lead	Direction	Downhill	Uphill
+10%		0.899	0.894
+2%		0.779	0.792
-4%		0.891	1.015

Standard errors of means

Table	Lead	Direction	Lead Direction
rep.	6	9	3
d.f.	12	12	12
e.s.e.	0.0540	0.0441	0.0764

Standard errors of differences of means

Table	Lead	Direction	Lead Direction
rep.	6	9	3
d.f.	12	12	12
s.e.d.	0.0764	0.0624	0.1080

Least significant differences of means (5% level)

Table	Lead	Direction	Lead Direction
rep.	6	9	3
d.f.	12	12	12
l.s.d.	0.1664	0.1359	0.2353

Stratum standard errors and coefficients of variation

Variate: Slope

d.f.	s.e.	cv%
12	0.1323	15.1

Tukey's 95% confidence intervals

Lead

	Mean	
+2%	0.7853	a
+10%	0.8967	a
-4%	0.9530	a

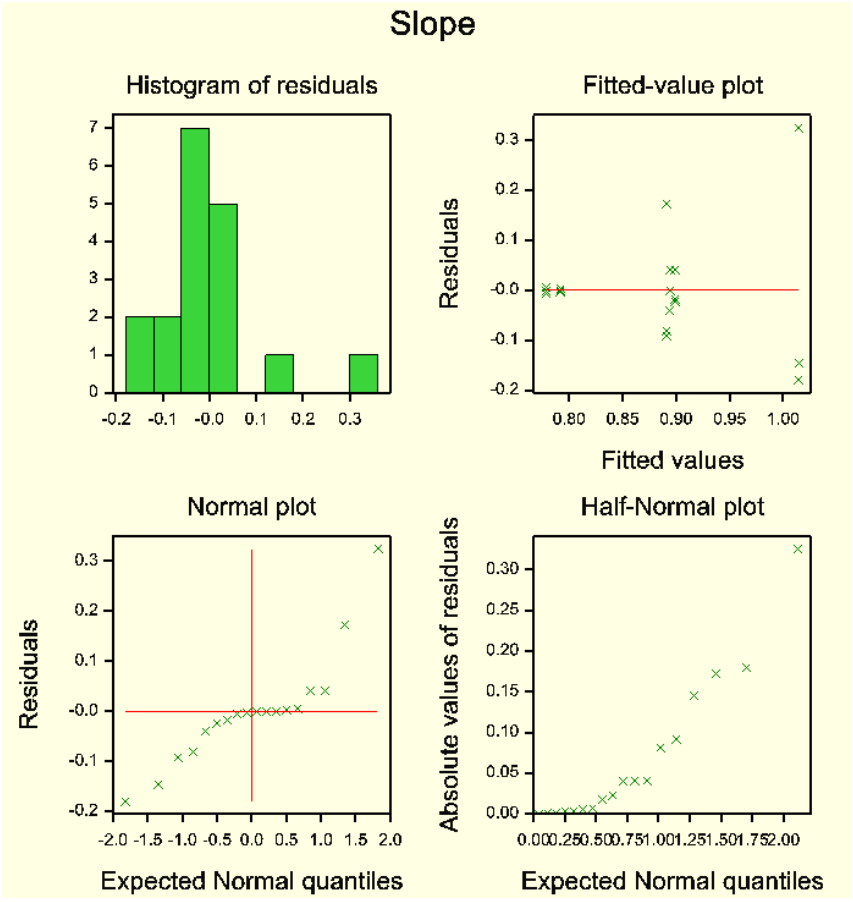
Slope
Histogram of residuals
Fitted-value plot
Residuals
Fitted values
Normal plot
Half-Normal plot
Residuals
Absolute values of residuals
Expected Normal quantiles
Expected Normal quantiles

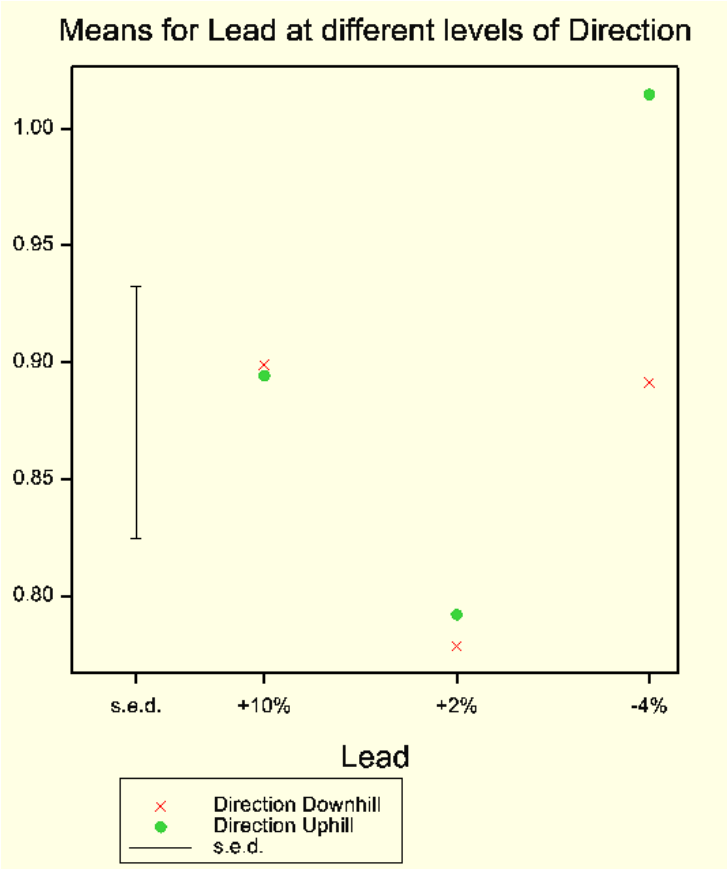
Means for Lead at different levels of Direction
s.e.d.
+10%
+2%
-4%
Lead
Direction Downhill
Direction Uphill
s.e.d.

4.11 Analysis of variance: Slope of front axle torque v drawbar pull on clay

Data imported from Excel file: G:\11188200 files\Thesis\Genstat\Torque v DBP stats GENSTAT.xlsx
on: 22-Jun-2011 23:16:27
taken from sheet ""GENSTAT Clay Torque DBP F Slope"", cells A2:D19

Identifier	Values	Missing	Levels
Direction	18	0	2

Identifier	Minimum	Mean	Maximum	Values	Missing
Axle				18	0

Identifier	Values	Missing	Levels
Lead	18	0	3

Identifier	Minimum	Mean	Maximum	Values	Missing
Slope	0.009492	0.07164	0.1260	18	0

Analysis of variance

Variate: Slope

Source of variation	d.f.	s.s.	m.s.	v.r.	F pr.
Lead	2	0.0287643	0.0143821	124.88	<.001
Direction	1	0.0000257	0.0000257	0.22	0.645
Lead.Direction	2	0.0001209	0.0000605	0.52	0.605
Residual	12	0.0013820	0.0001152		
Total	17	0.0302929			

Information summary

All terms orthogonal, none aliased.

Tables of effects

Variate: Slope

Lead effects, e.s.e. 0.00438, rep. 6

Lead	+10%	+2%	-4%
	-0.0472	-0.0033	0.0505

Direction response -0.0024, s.e. 0.00506, rep. 9

Lead.Direction effects, e.s.e. 0.00620, rep. 3

Lead	Direction	North	South
+10%		-0.0034	0.0034
+2%		0.0028	-0.0028
-4%		0.0006	-0.0006

Tables of means

Variate: Slope

Grand mean 0.0716

Lead	+10%	+2%	-4%
	0.0244	0.0683	0.1222

Direction	North	South
	0.0728	0.0704

Lead	Direction	North	South
+10%		0.0222	0.0267
+2%		0.0723	0.0643
-4%		0.1240	0.1203

Standard errors of means

Table	Lead	Direction	Lead Direction
rep.	6	9	3
d.f.	12	12	12
e.s.e.	0.00438	0.00358	0.00620

Standard errors of differences of means

Table	Lead	Direction	Lead Direction
rep.	6	9	3
d.f.	12	12	12
s.e.d.	0.00620	0.00506	0.00876

Least significant differences of means (5% level)

Table	Lead	Direction	Lead Direction
rep.	6	9	3
d.f.	12	12	12
l.s.d.	0.01350	0.01102	0.01909

Stratum standard errors and coefficients of variation

Variate: Slope

d.f.	s.e.	cv%
12	0.01073	15.0

Tukey's 95% confidence intervals

Lead

	Mean	
+10%	0.02442	a
+2%	0.06833	b
-4%	0.12217	c

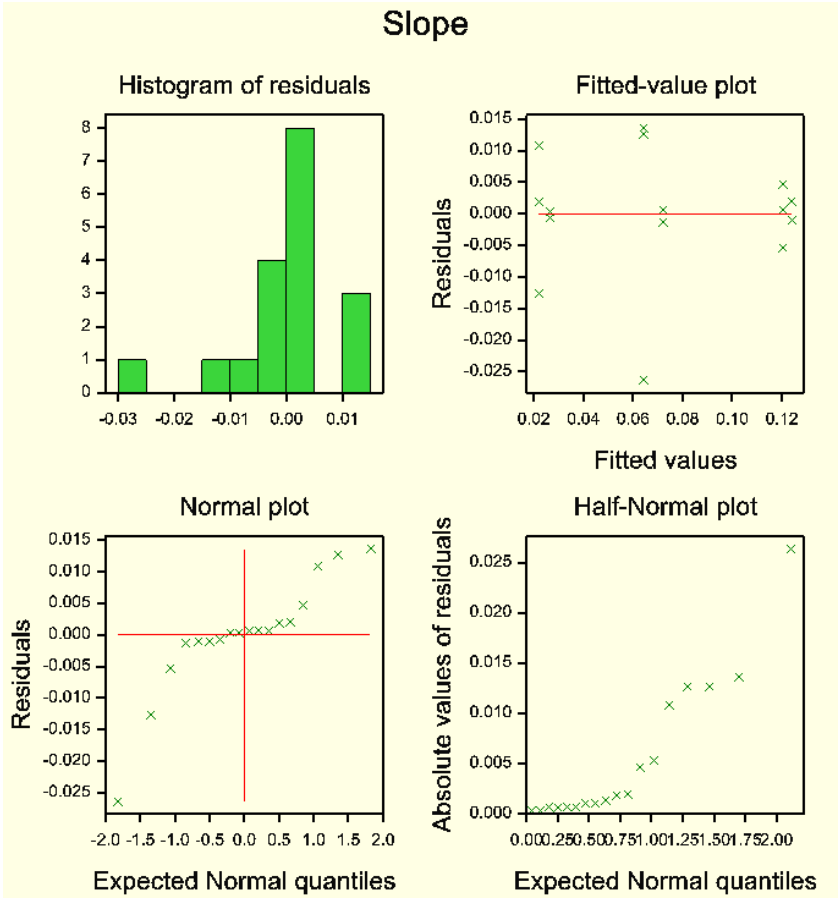
Slope
Histogram of residuals
Fitted-value plot
Residuals
Fitted values
Normal plot
Half-Normal plot
Residuals
Absolute values of residuals
Expected Normal quantiles
Expected Normal quantiles

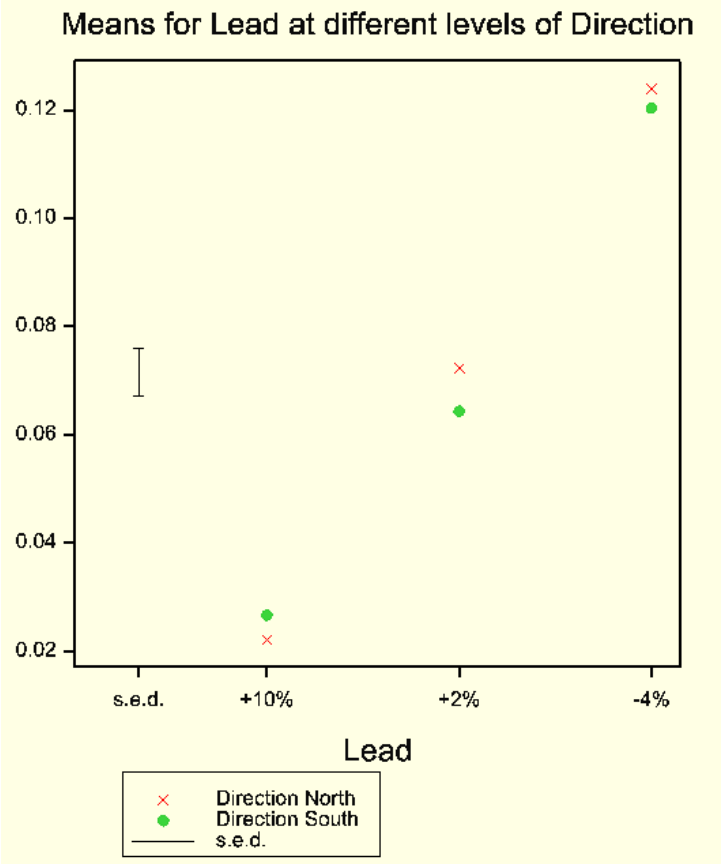
Means for Lead at different levels of Direction
0.12
0.10
0.08
0.06
0.04
0.02
s.e.d.
+10%
+2%
-4%
Lead
Direction North
Direction South
s.e.d.

4.12 Analysis of variance: Slope of rear axle torque v drawbar pull on clay

Data imported from Excel file: G:\11188200 files\Thesis\Genstat\Torque v DBP stats GENSTAT.xlsx
on: 22-Jun-2011 23:13:18
taken from sheet ""GENSTAT Clay Torque DBP R Slope"", cells A2:S19

Identifier	Values	Missing	Levels
Direction	18	0	2

Identifier	Minimum	Mean	Maximum	Values	Missing
Axle				18	0

Identifier	Values	Missing	Levels
Lead	18	0	3

Identifier	Minimum	Mean	Maximum	Values	Missing
Slope	0.6750	0.7939	0.9010	18	0

Analysis of variance

Variate: Slope

Source of variation	d.f.	s.s.	m.s.	v.r.	F pr.
Lead	2	0.075584	0.037792	30.96	<.001
Direction	1	0.000001	0.000001	0.00	0.974
Lead.Direction	2	0.004664	0.002332	1.91	0.190
Residual	12	0.014649	0.001221		
Total	17	0.094899			

Information summary

All terms orthogonal, none aliased.

Tables of effects

Variate: Slope

Lead effects, e.s.e. 0.01426, rep. 6

Lead	+10%	+2%	-4%
	0.0781	0.0026	-0.0806

Direction response -0.0006, s.e. 0.01647, rep. 9

Lead.Direction effects, e.s.e. 0.02017, rep. 3

Lead	Direction	North	South
+10%		-0.0039	0.0039
+2%		-0.0174	0.0174
-4%		0.0214	-0.0214

Tables of means

Variate: Slope

Grand mean 0.7939

Lead	+10%	+2%	-4%
	0.8720	0.7965	0.7133

Direction	North	South
	0.7942	0.7937

Lead	Direction	North	South
+10%		0.8683	0.8757
+2%		0.7793	0.8137
-4%		0.7350	0.6917

Standard errors of means

Table	Lead	Direction	Lead Direction
rep.	6	9	3
d.f.	12	12	12
e.s.e.	0.01426	0.01165	0.02017

Standard errors of differences of means

Table	Lead	Direction	Lead Direction
rep.	6	9	3
d.f.	12	12	12
s.e.d.	0.02017	0.01647	0.02853

Least significant differences of means (5% level)

Table	Lead	Direction	Lead Direction
rep.	6	9	3
d.f.	12	12	12
l.s.d.	0.04395	0.03589	0.06216

Stratum standard errors and coefficients of variation

Variate: Slope

d.f.	s.e.	cv%
12	0.03494	4.4

Tukey's 95% confidence intervals

Lead

	Mean	
-4%	0.7133	a
+2%	0.7965	b
+10%	0.8720	c

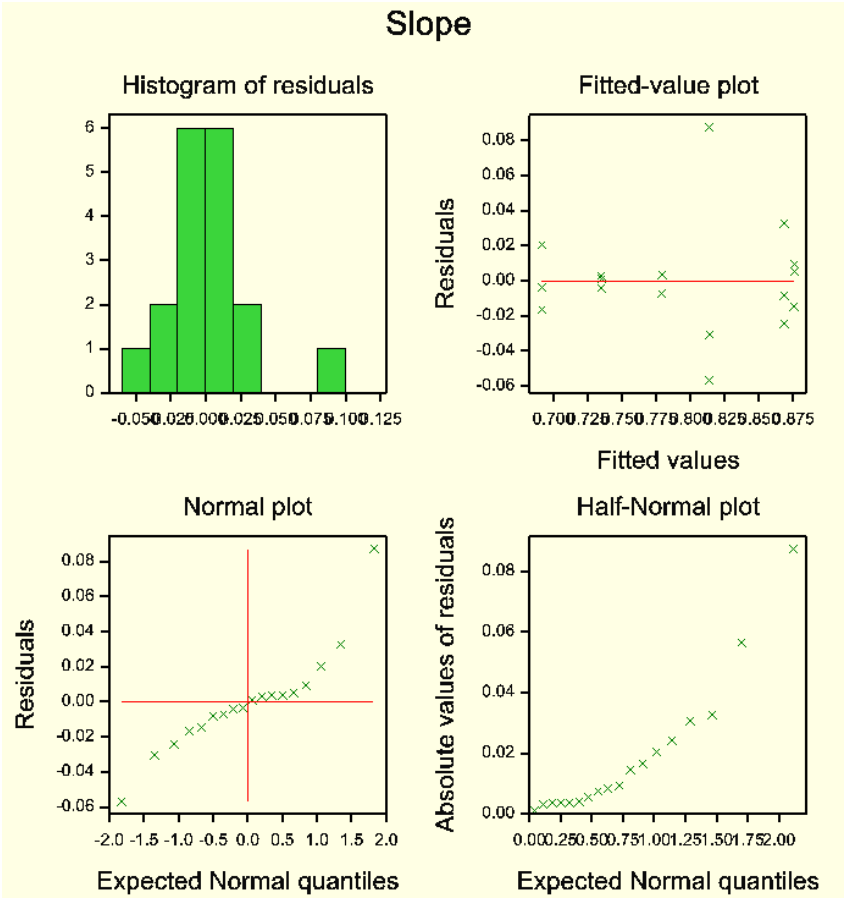
Slope
Histogram of residuals
Fitted-value plot
Residuals
Fitted values
Normal plot
Half-Normal plot
Residuals
Absolute values of residuals
Expected Normal quantiles
Expected Normal quantiles

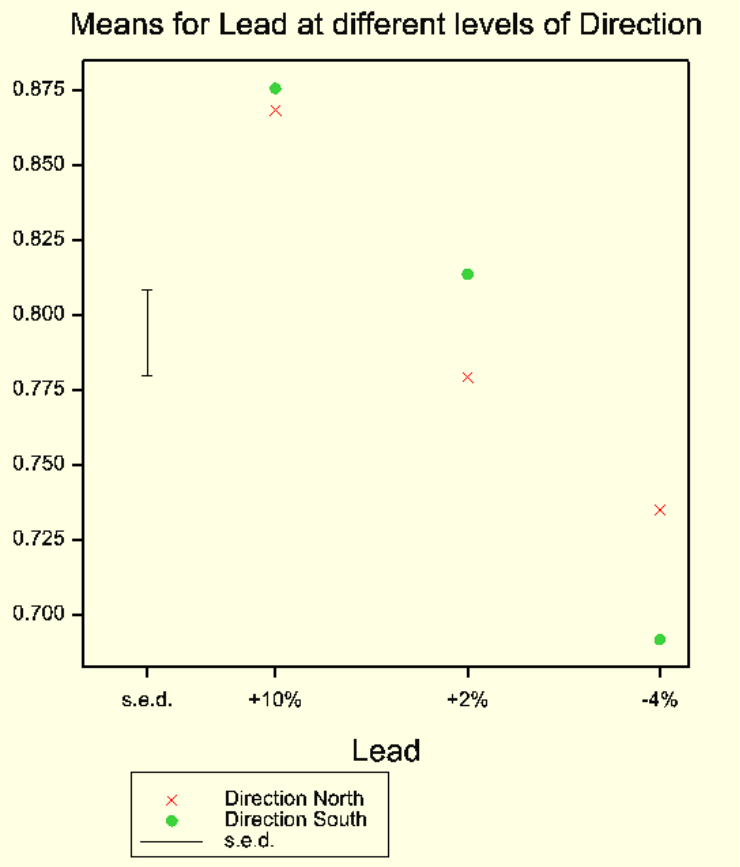
Means for Lead at different levels of Direction
0.875
0.850
0.825
0.800
0.775
0.750
0.725
0.700
s.e.d.
+10%
+2%
-4%
Lead
Direction North
Direction South
s.e.d.

4.13 Experimental data with fitted curves

4.13.1 Slip-pull uphill on sand

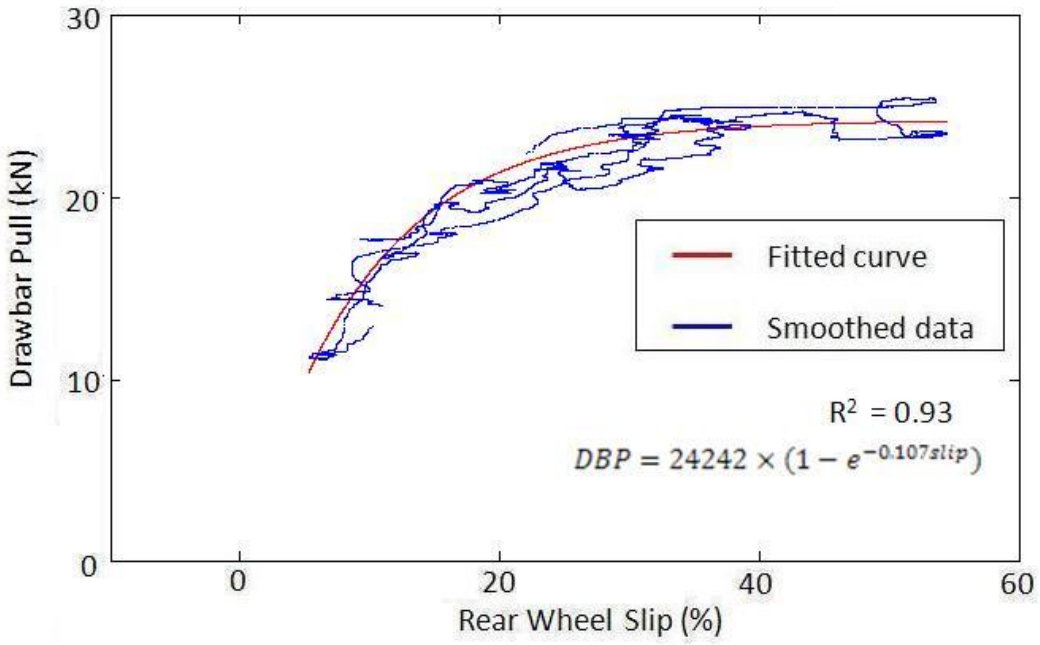

Slip-pull relationship at -4% lead uphill on sand; experimental data smoothed using a 1001 point moving average filter and a fitted curve

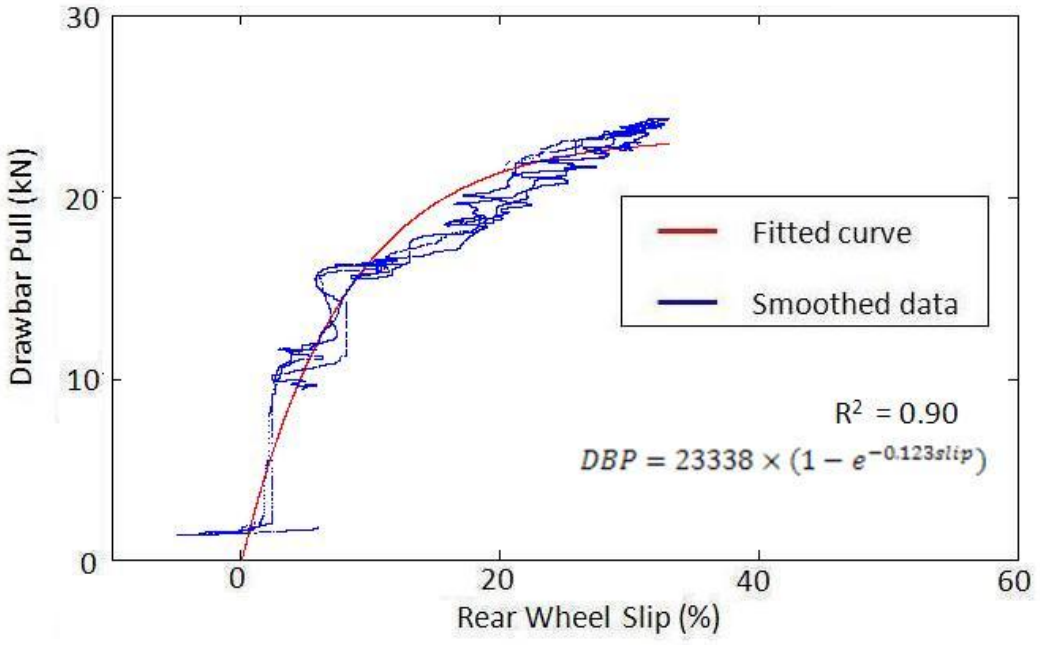

Slip-pull relationship at +2% lead uphill on sand; experimental data smoothed using a 1001 point moving average filter and a fitted curve

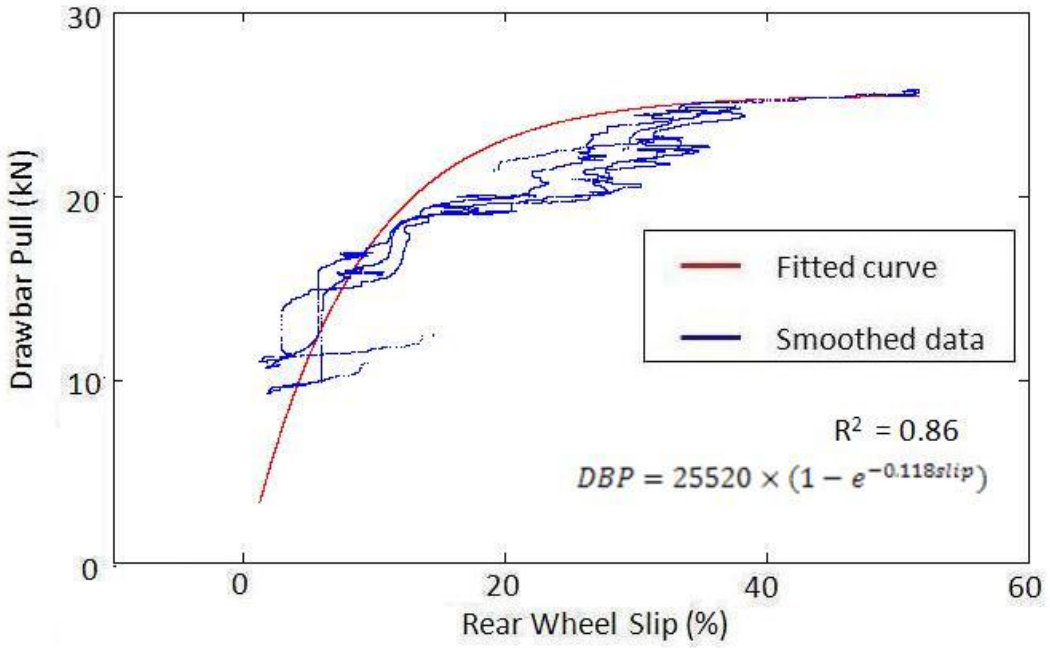

Slip-pull relationship at +10% lead uphill on sand; experimental data smoothed using a 1001 point moving average filter and a fitted curve

4.13.2 Slip-pull downhill on sand

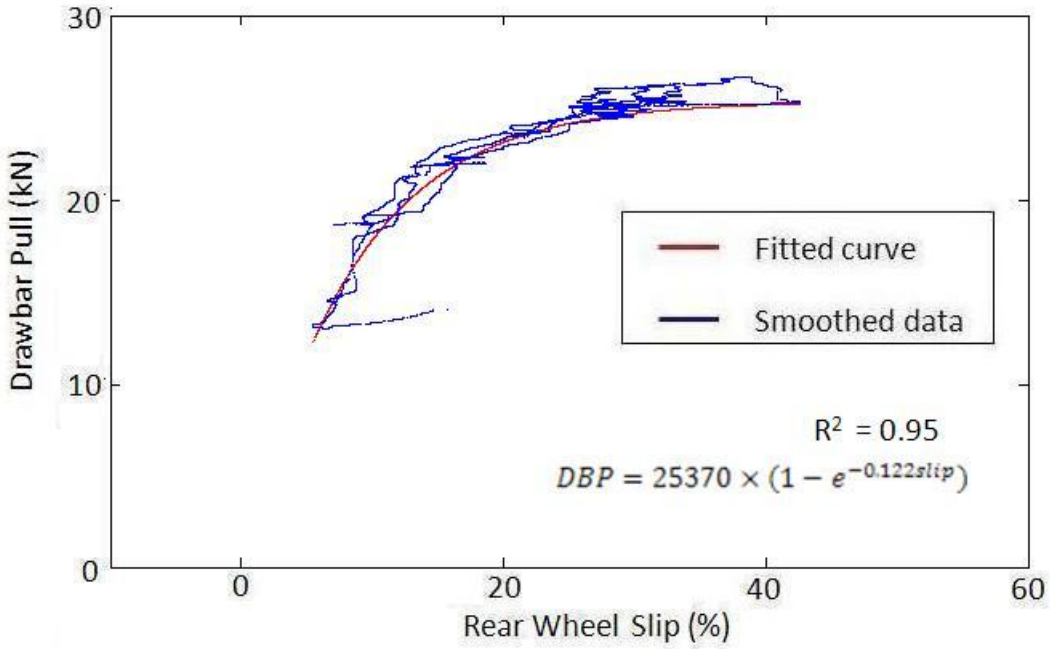

Slip-pull relationship at -4% lead downhill on sand; experimental data smoothed using a 1001 point moving average filter and a fitted curve

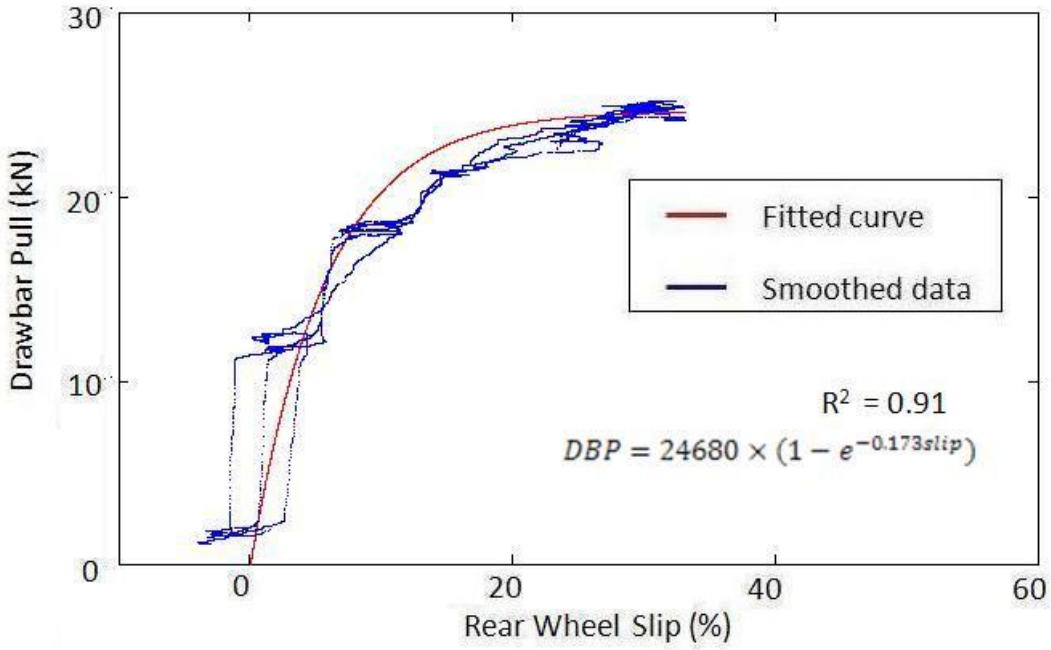

Slip-pull relationship at +2% lead downhill on sand; experimental data smoothed using a 1001 point moving average filter and a fitted curve

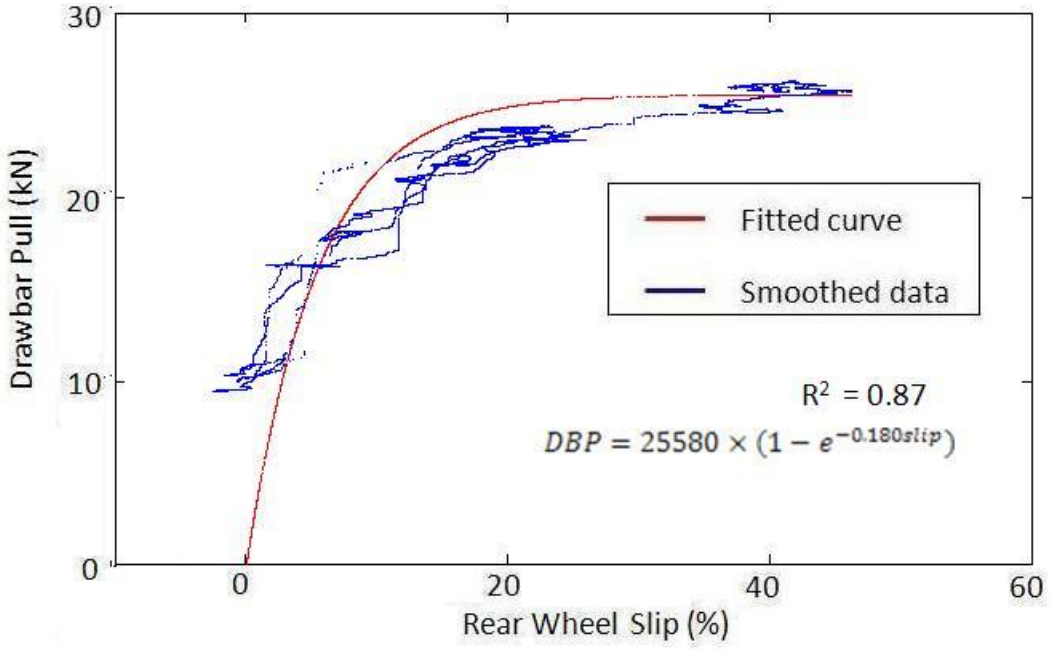

Slip-pull relationship at +10% lead downhill on sand; experimental data smoothed using a 1001 point moving average filter and a fitted curve

4.13.3 Slip-pull on clay

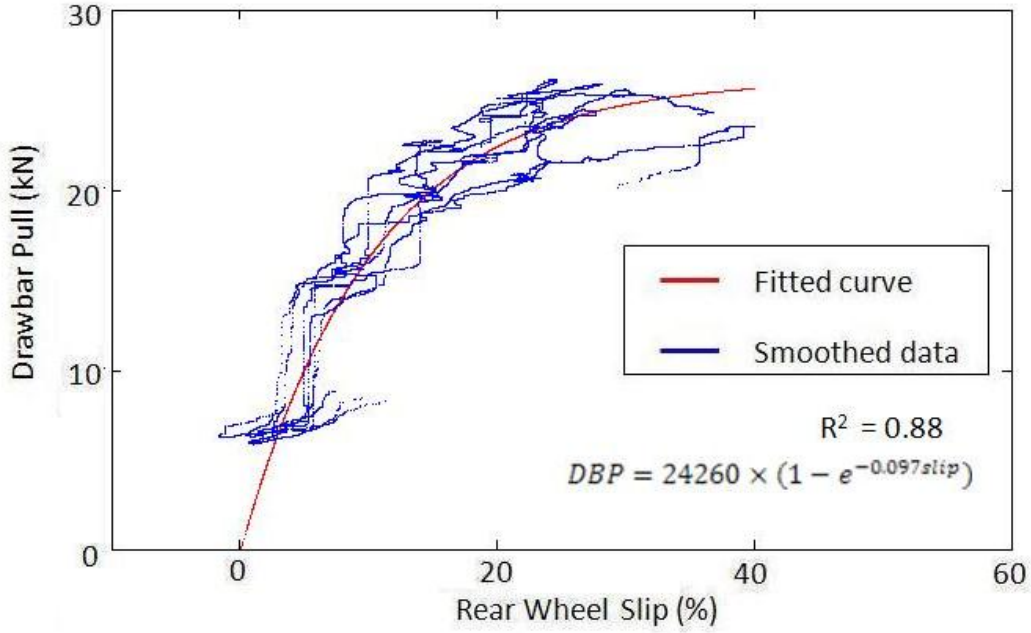

Slip-pull relationship at -4% lead on clay; experimental data smoothed using a 1001 point moving average filter and a fitted curve

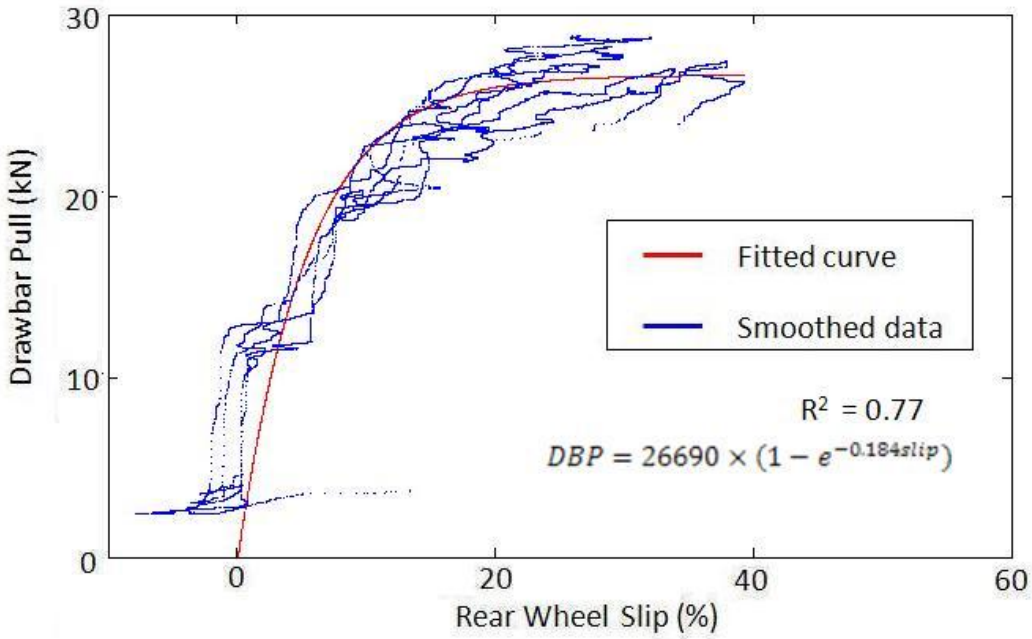

Slip-pull relationship at +2% lead on clay; experimental data smoothed using a 1001 point moving average filter and a fitted curve

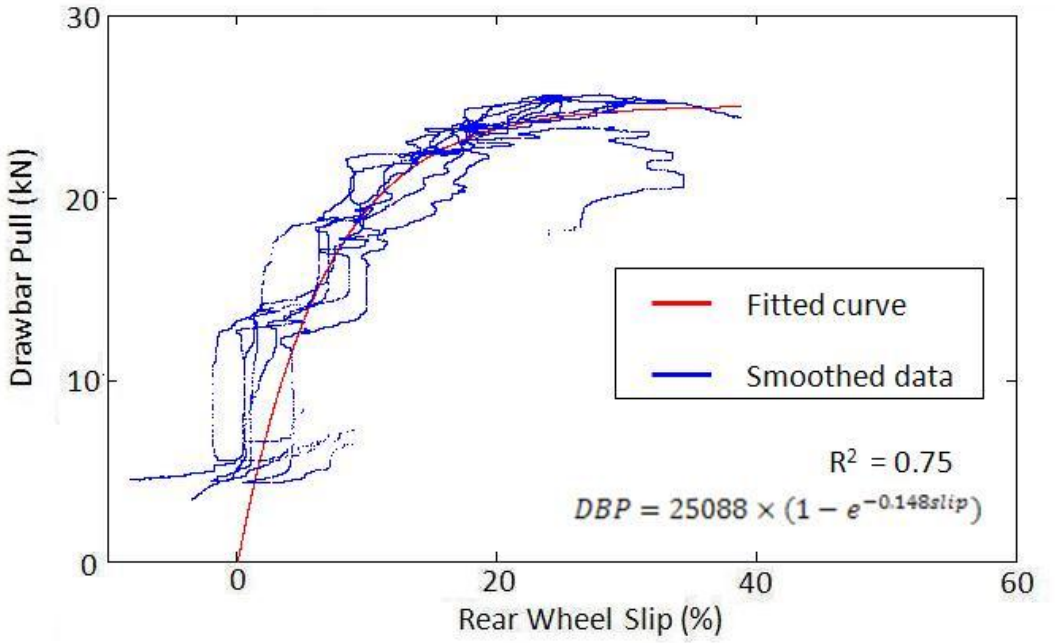

Slip-pull relationship at +10% lead on clay; experimental data smoothed using a 1001 point moving average filter and a fitted curve

4.13.4 Power delivery efficiency versus drawbar pull uphill on sand

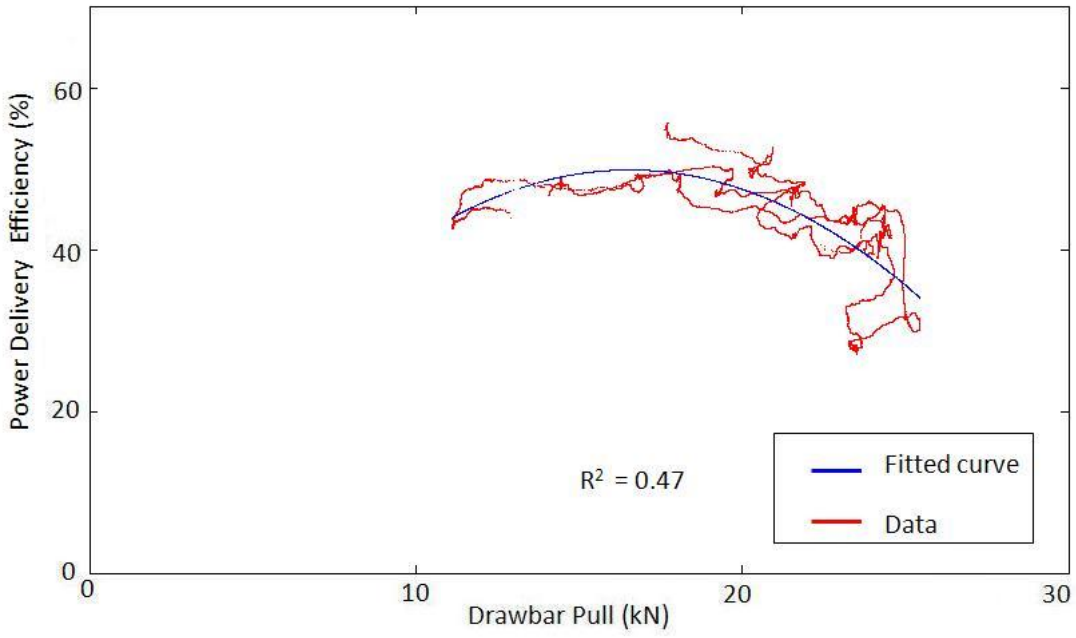

The relationship between power delivery efficiency and drawbar pull, operating uphill on sand at -4% lead

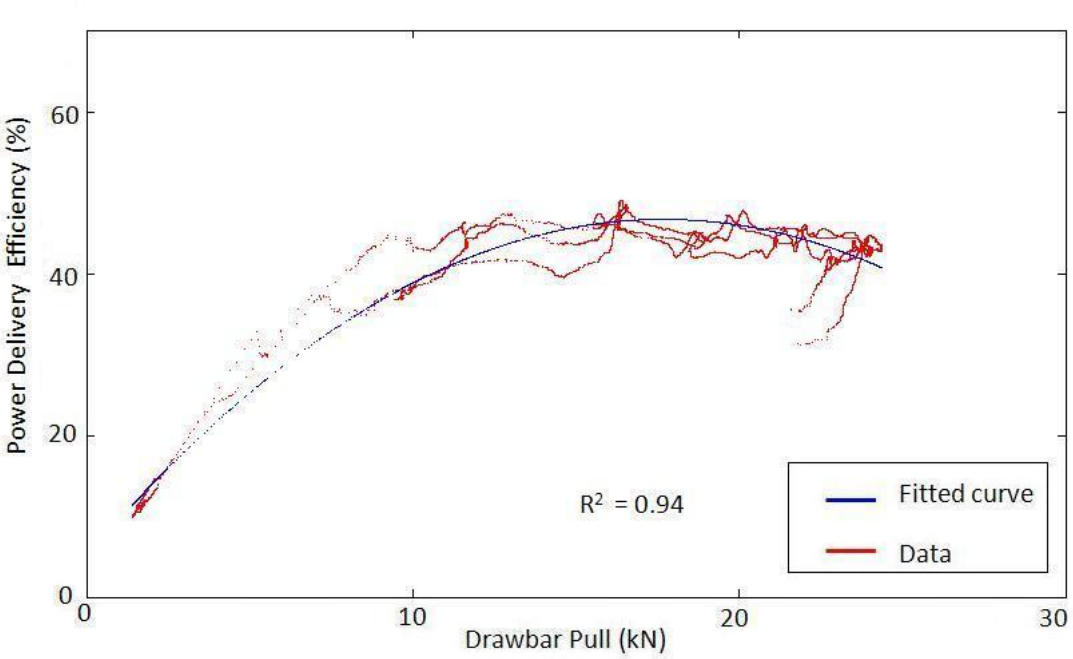

The relationship between power delivery efficiency and drawbar pull,

operating uphill on sand at +2% lead

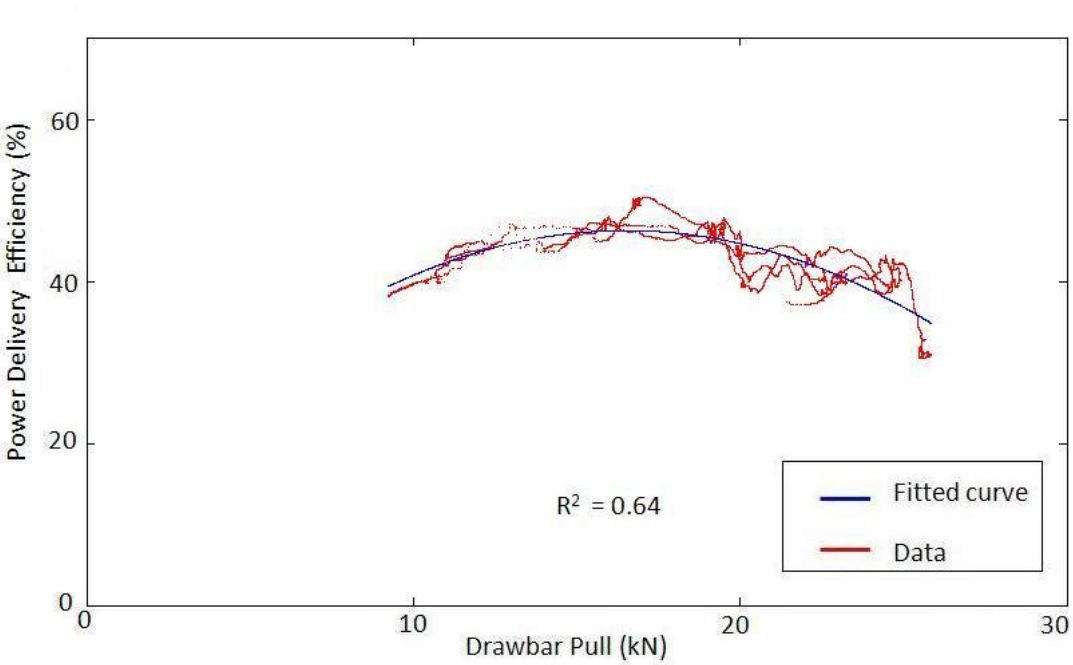

The relationship between power delivery efficiency and drawbar pull,
operating uphill on sand at +10% lead

4.13.5 Power delivery efficiency versus drawbar pull downhill on sand

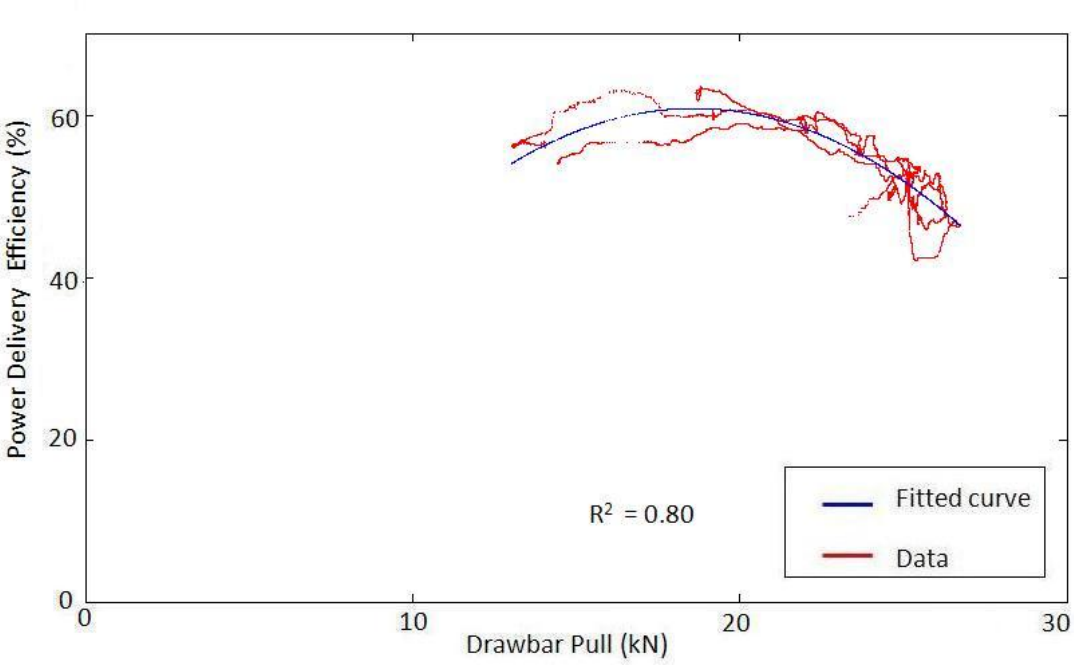

The relationship between power delivery efficiency and drawbar pull, operating downhill on sand at -4% lead

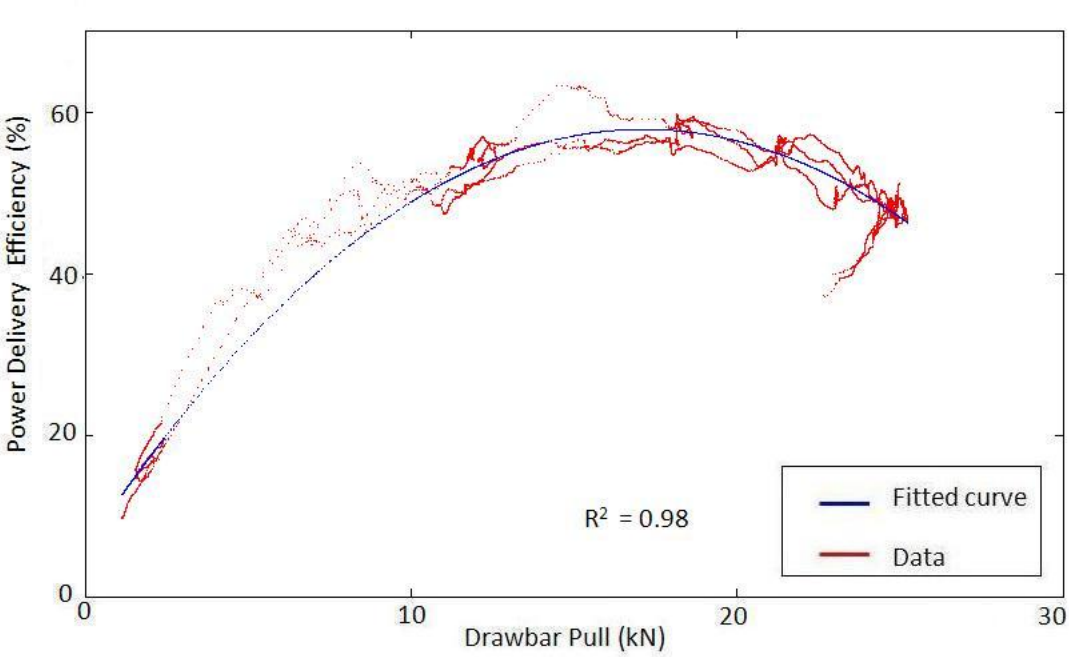

The relationship between power delivery efficiency and drawbar pull, operating downhill on sand at +2% lead

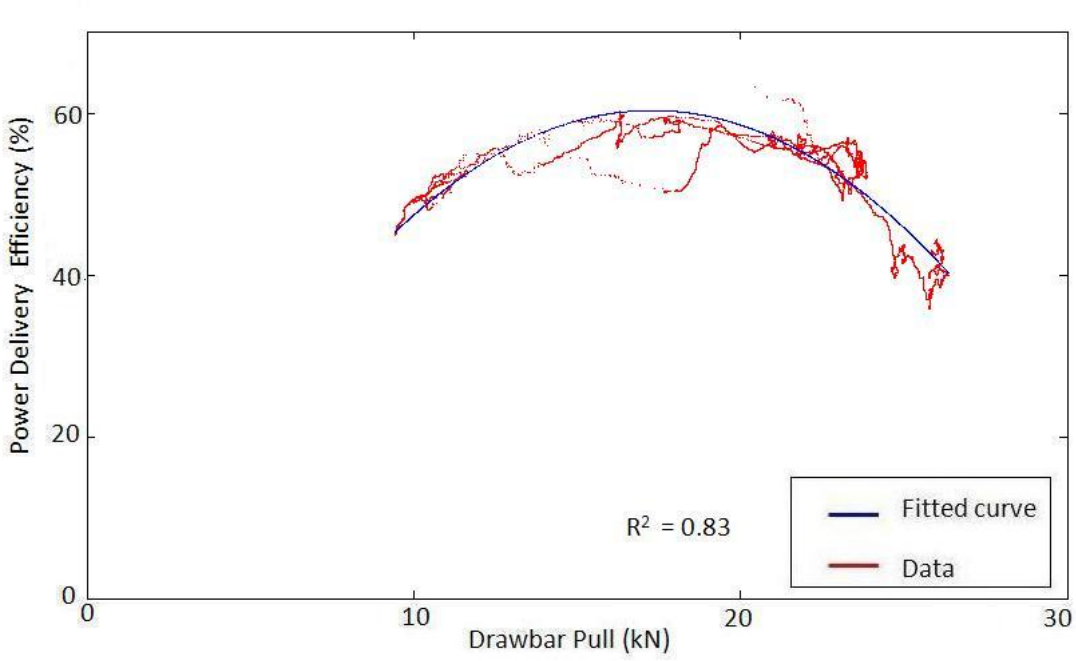

The relationship between power delivery efficiency and drawbar pull, operating downhill on sand at +10% lead

4.13.6 Power delivery efficiency versus drawbar pull on clay

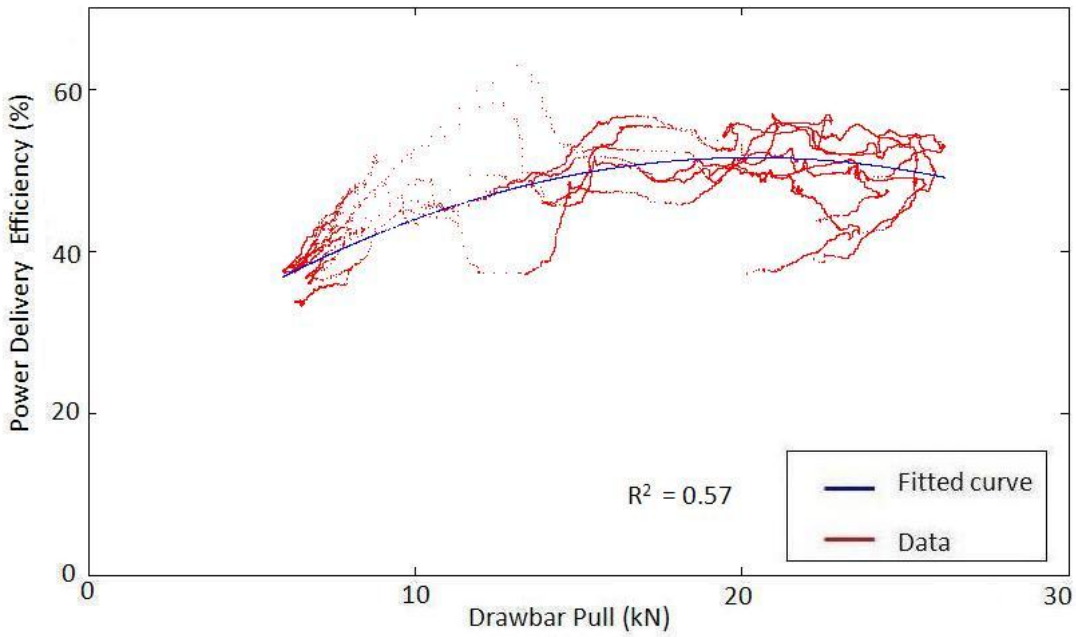

The relationship between power delivery efficiency and drawbar pull, operating on clay at -4% lead

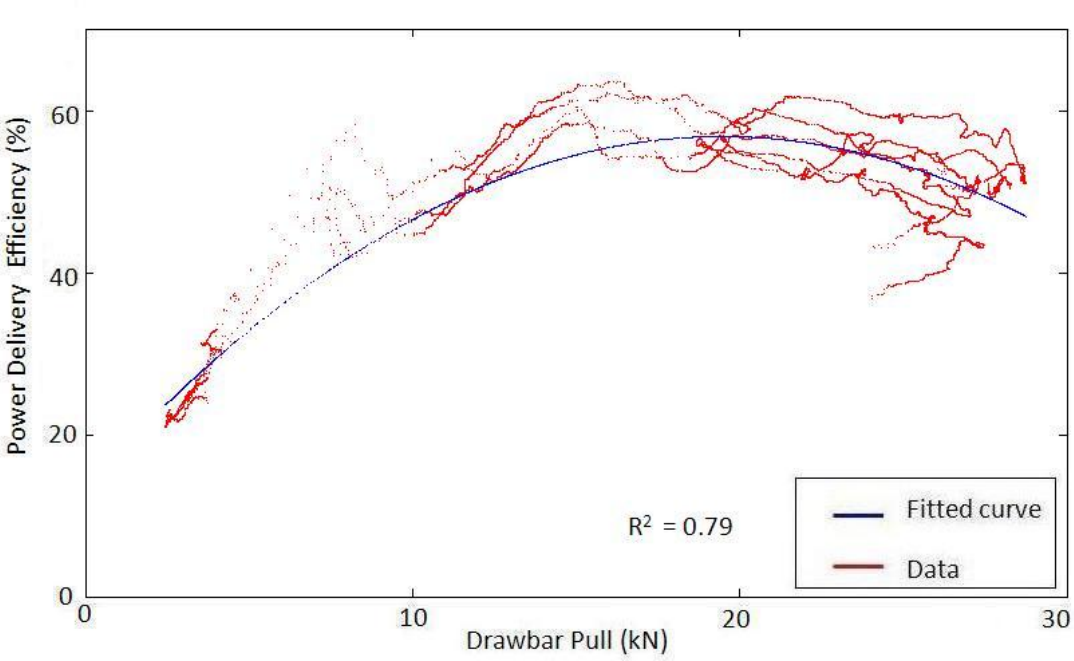

The relationship between power delivery efficiency and drawbar pull, operating on clay at +2% lead

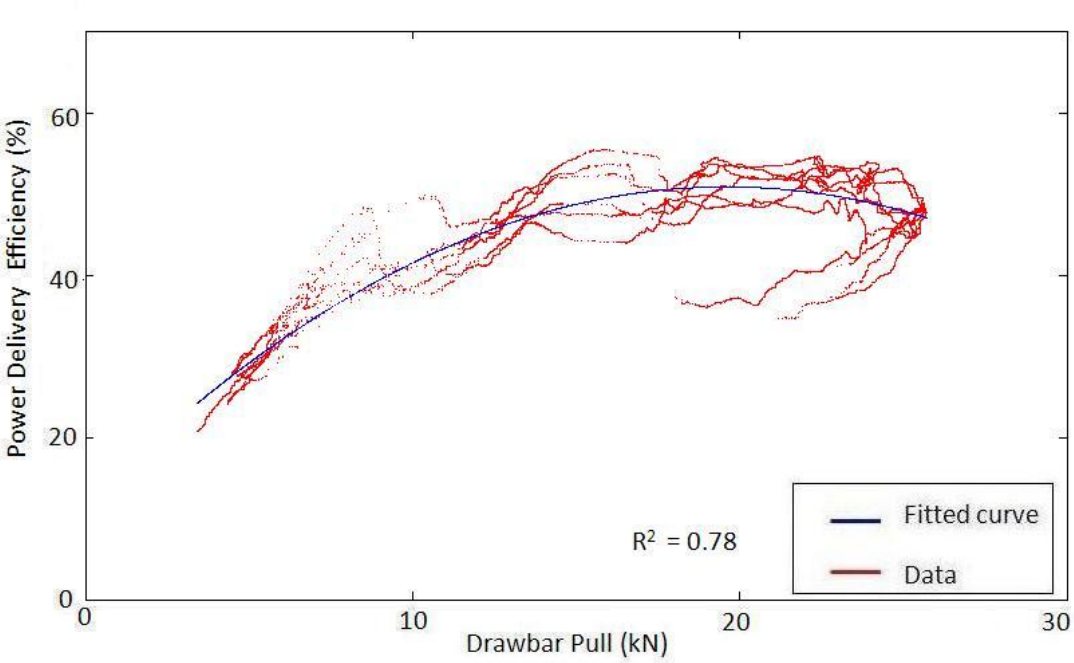

The relationship between power delivery efficiency and drawbar pull, operating on clay at +10% lead

4.13.7 Power delivery efficiency versus rear wheel slip uphill on sand

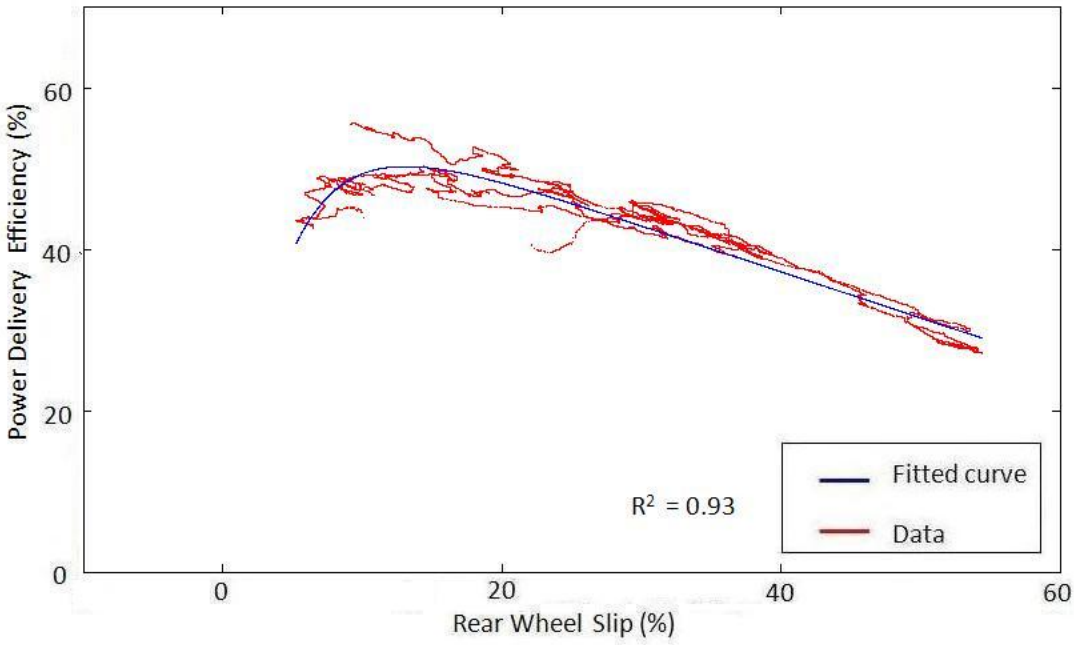

The relationship between power delivery efficiency and rear wheel slip, operating uphill on sand at -4% lead

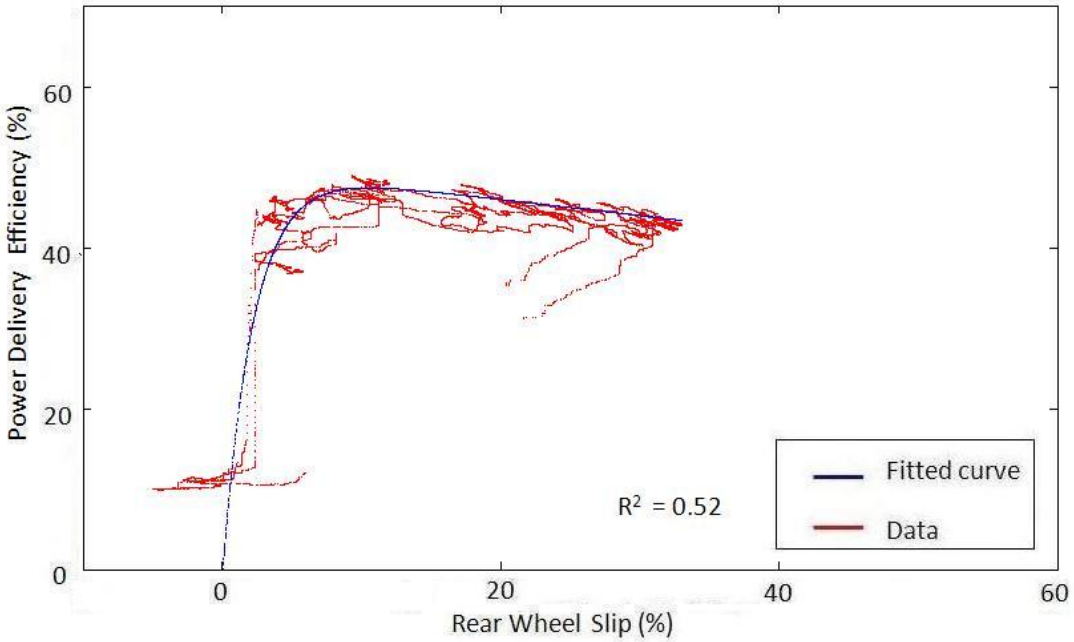

The relationship between power delivery efficiency and rear wheel slip, operating uphill on sand at +2% lead

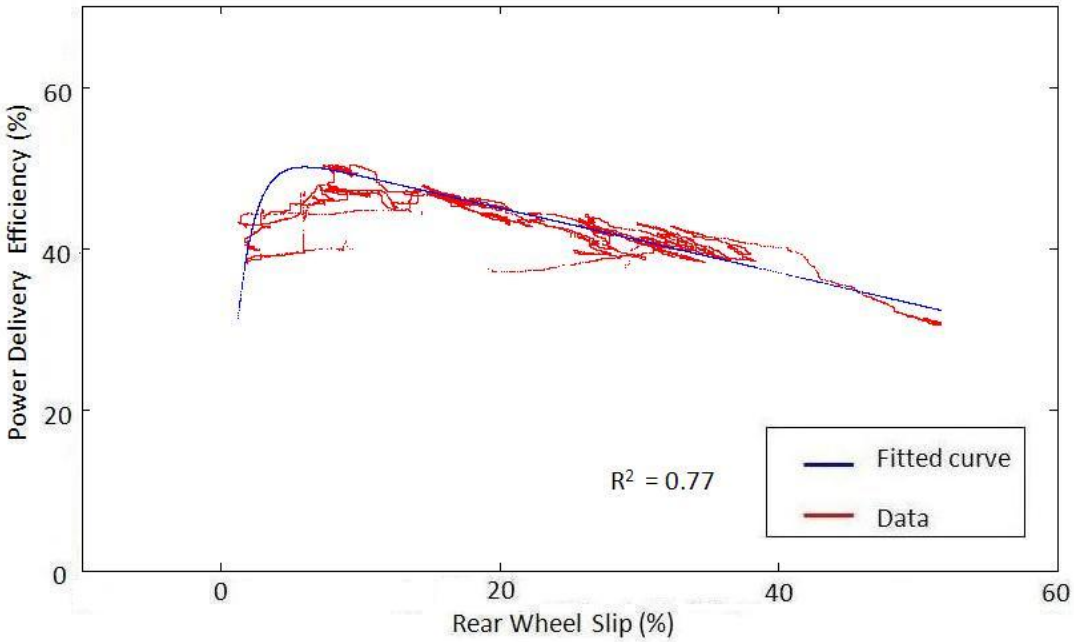

The relationship between power delivery efficiency and rear wheel slip, operating uphill on sand at +10% lead

4.13.8 Power delivery efficiency versus rear wheel slip downhill on sand

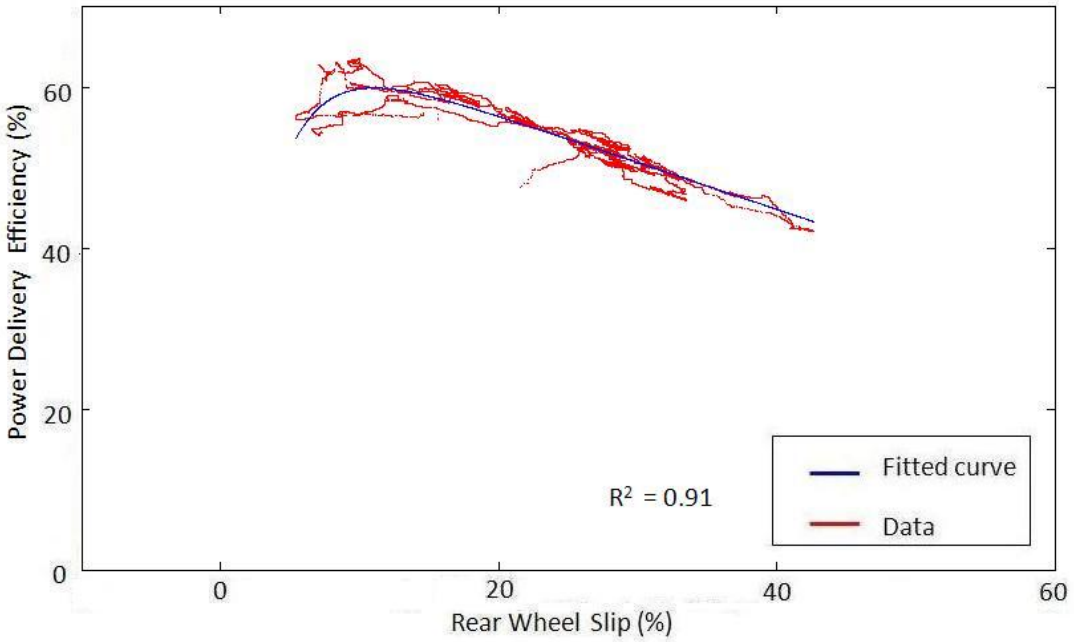

The relationship between power delivery efficiency and rear wheel slip, operating downhill on sand at -4% lead

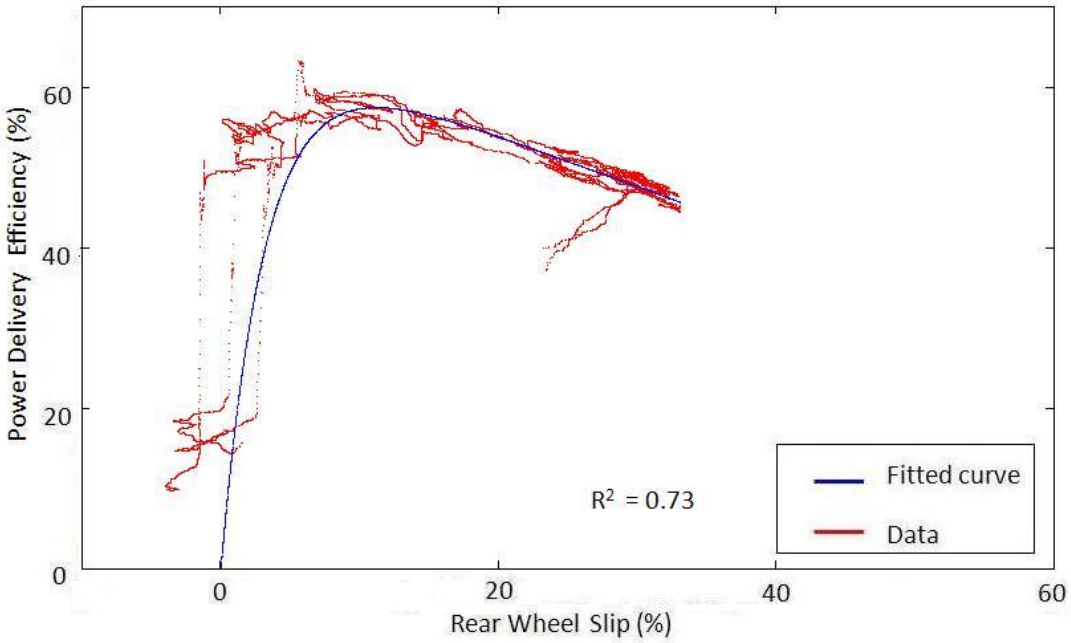

The relationship between power delivery efficiency and rear wheel slip, operating downhill on sand at +2% lead

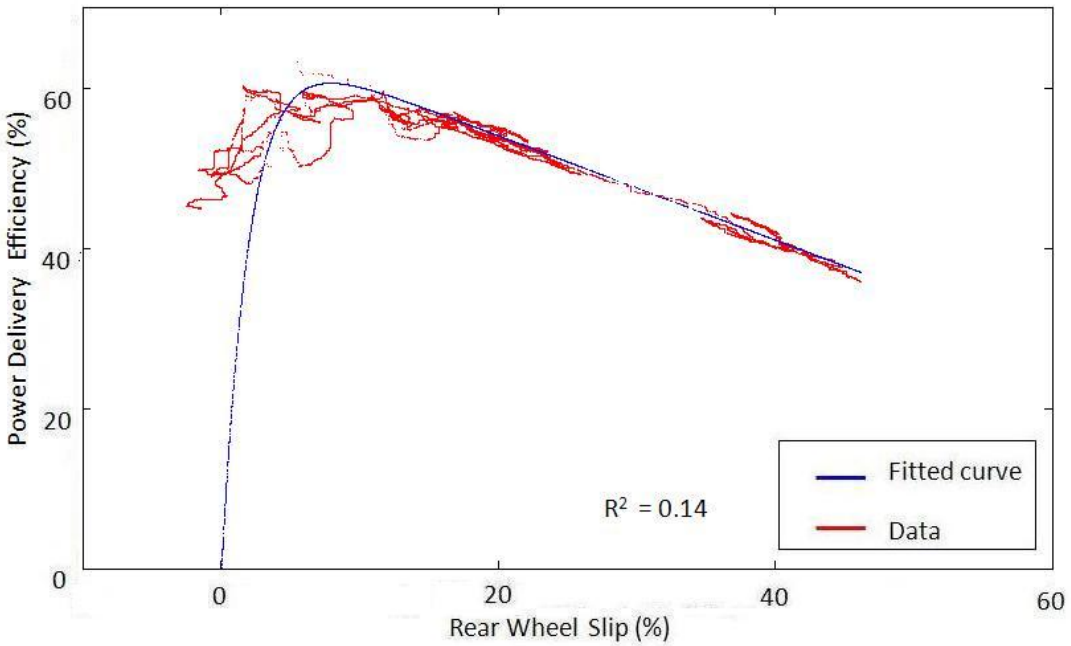

The relationship between power delivery efficiency and rear wheel slip, operating downhill on sand at +10% lead

4.13.9 Power delivery efficiency versus rear wheel slip on clay

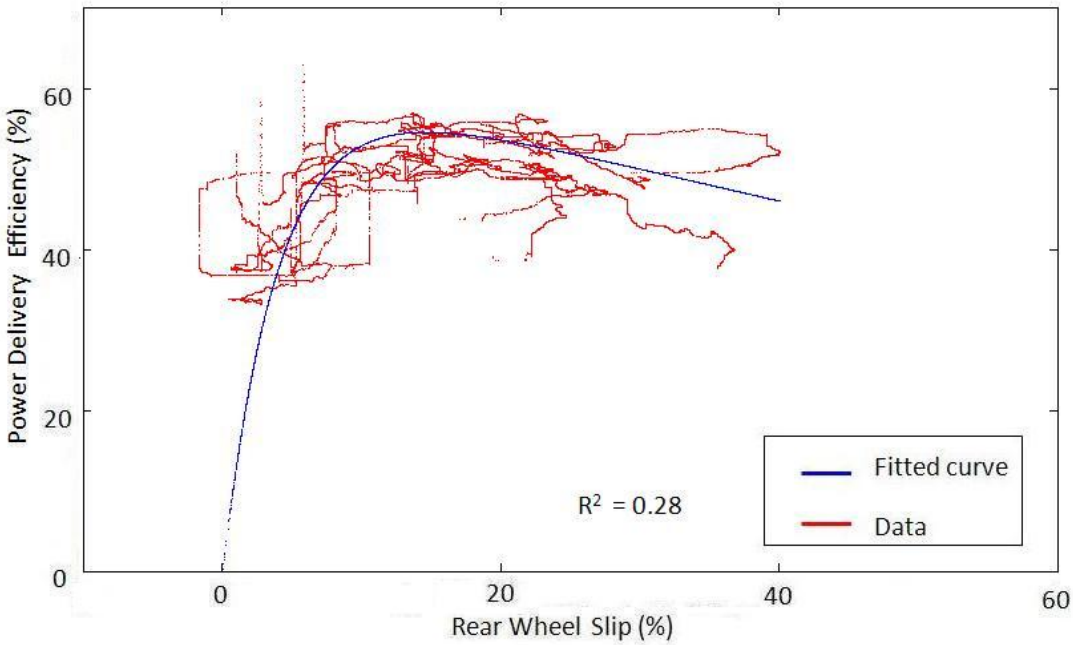

The relationship between power delivery efficiency and rear wheel slip, operating on clay at -4% lead

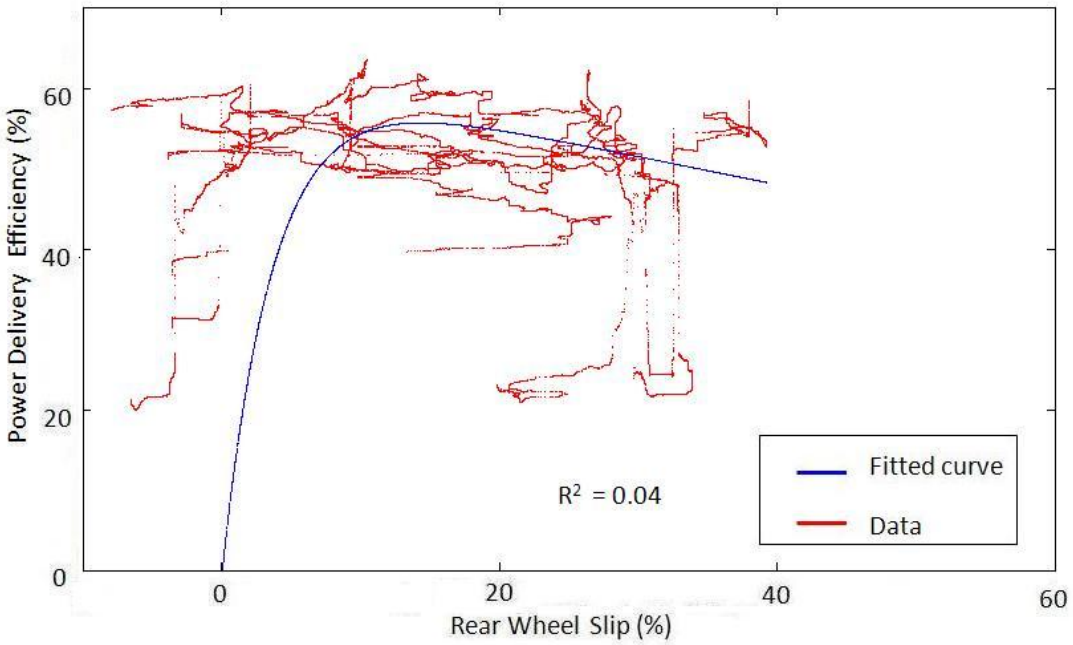

The relationship between power delivery efficiency and rear wheel slip, operating on clay at +2% lead

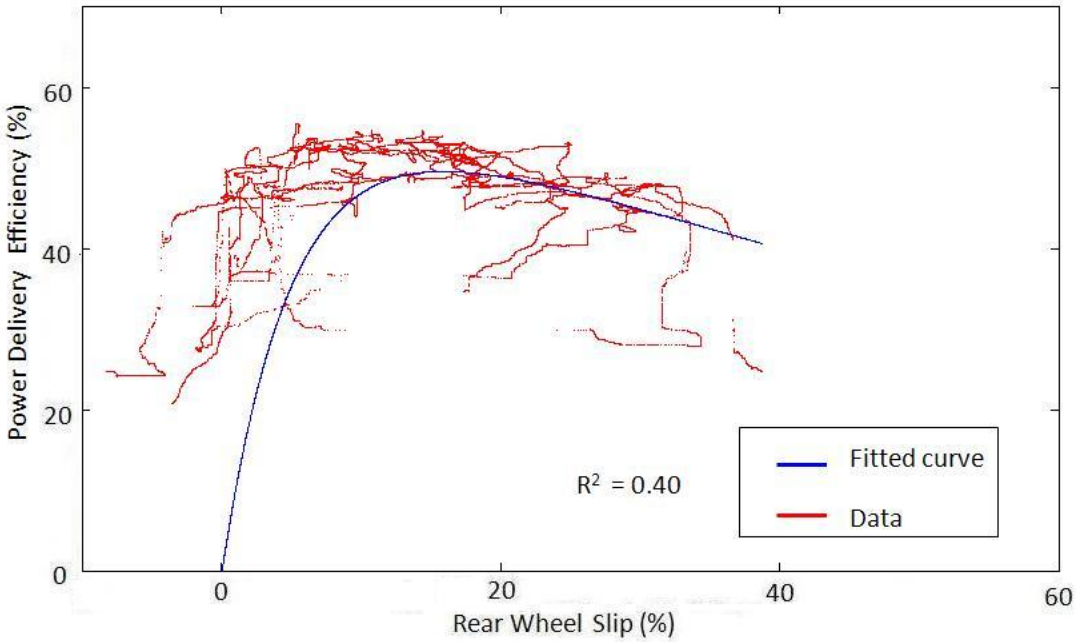

The relationship between power delivery efficiency and rear wheel slip, operating on clay at +10% lead

4.13.10 Axle torque versus drawbar pull uphill on sand

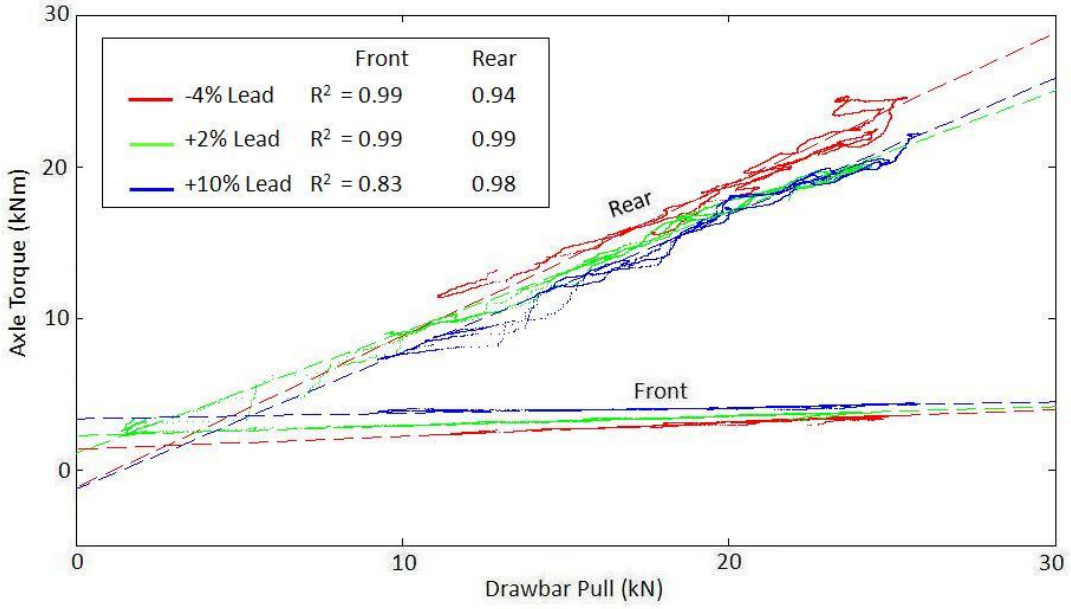

The relationship between axle torque and drawbar pull, operating uphill on sand, showing the raw data collected in the field and fitted lines with the form y = mx + c. The fitted lines are shown as broken lines.

4.13.11 Axle torque versus drawbar pull downhill on sand

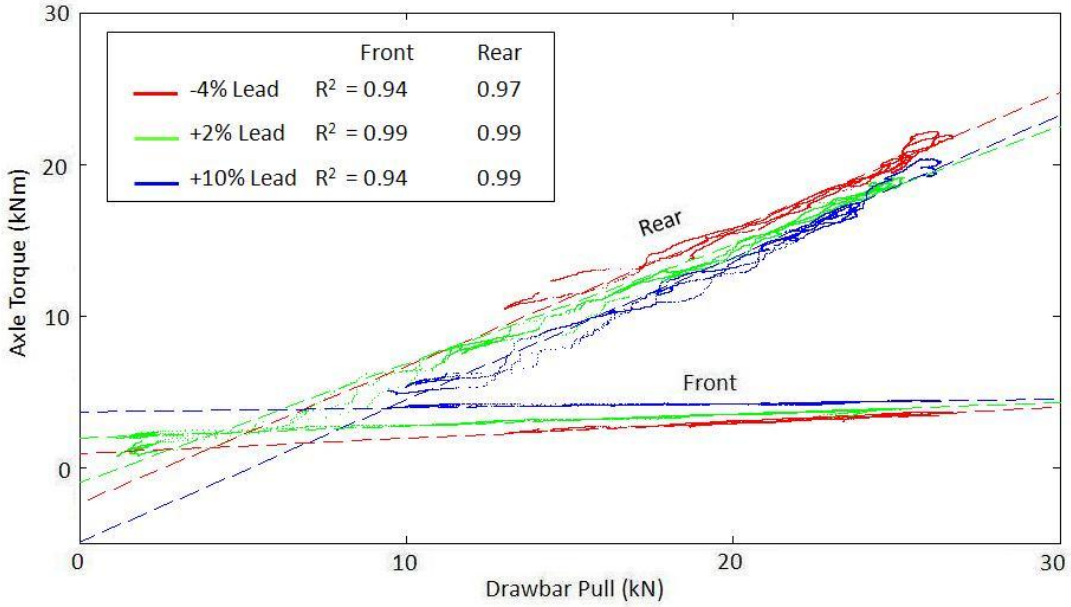

The relationship between axle torque and drawbar pull, operating downhill on sand, showing the raw data collected in the field and fitted lines with the form y = mx + c. The fitted lines are shown as broken lines.

4.13.12 Axle torque versus drawbar pull on clay

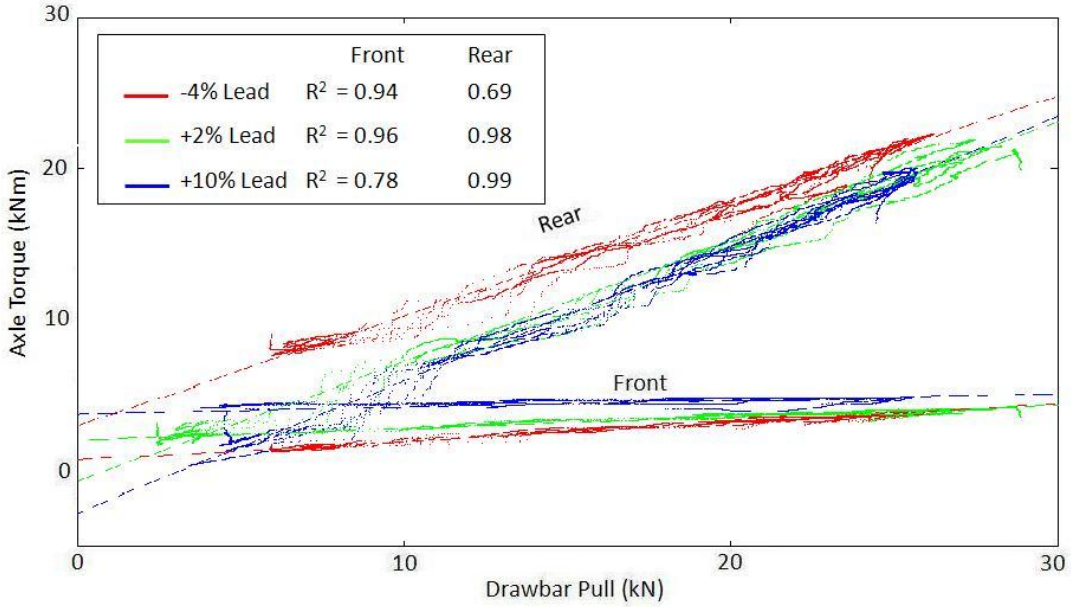

The relationship between axle torque and drawbar pull, operating on clay, showing the raw data collected in the field and fitted lines with the form y = mx + c. The fitted lines are shown as broken lines.

4.13.13 Engine power and drawbar power versus drawbar pull uphill on sand

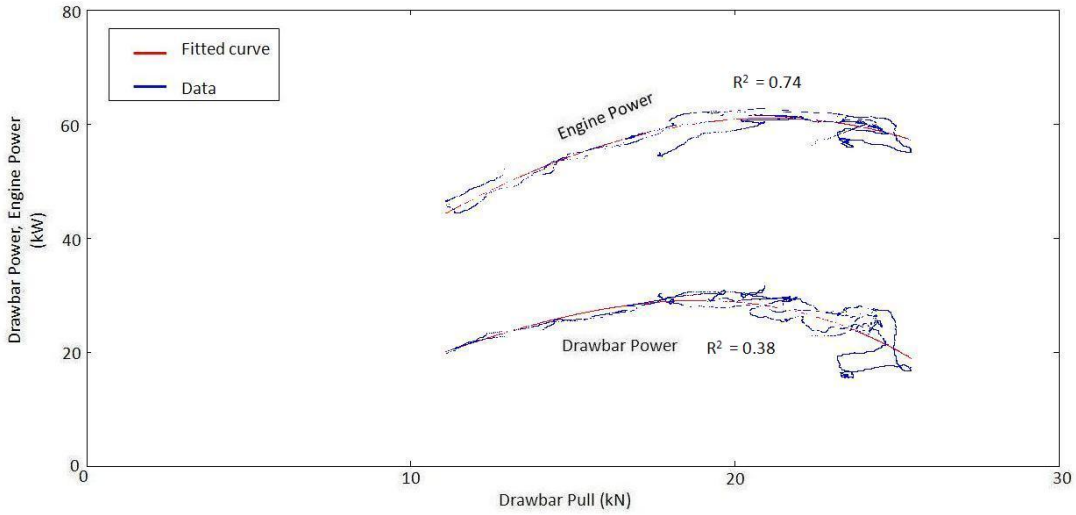

The relationship between engine power, drawbar power and drawbar pull operating uphill on sand at -4% lead, showing both the raw data and third order polynomial curves fitted to them.

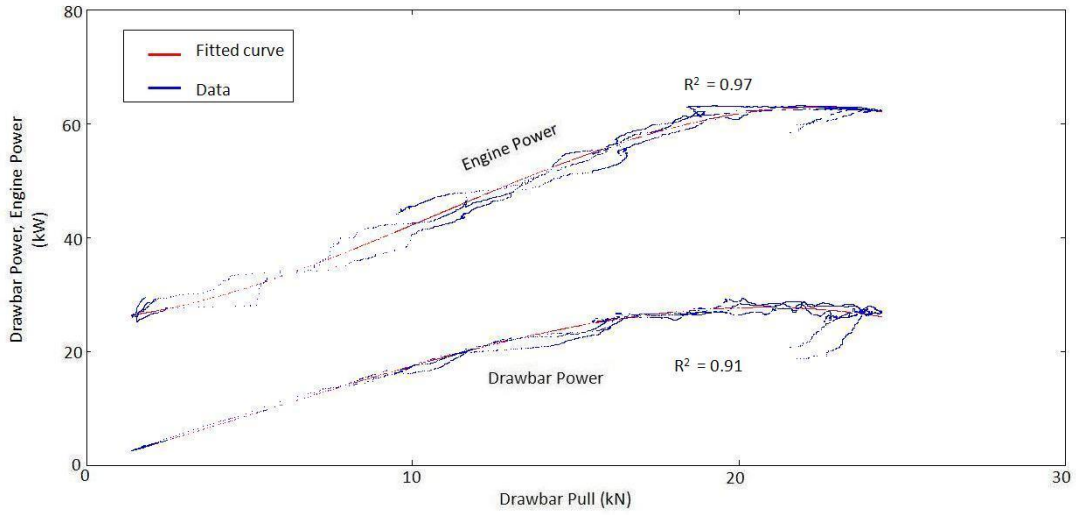

The relationship between engine power, drawbar power and drawbar pull operating uphill on sand at +2% lead, showing both the raw data and third order polynomial curves fitted to them.

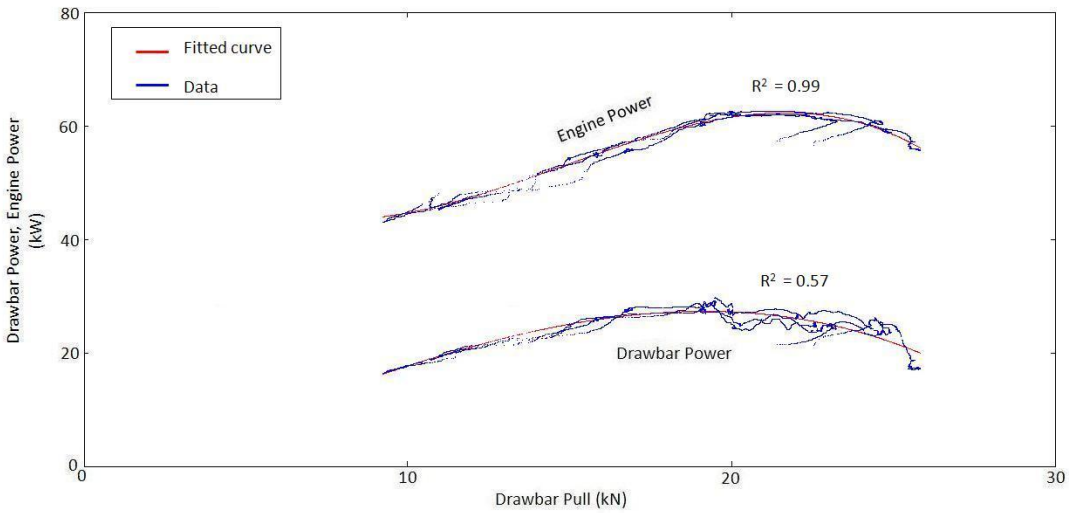

The relationship between engine power, drawbar power and drawbar pull operating uphill on sand at +10% lead, showing both the raw data and third order polynomial curves fitted to them.

4.13.14 Engine power and drawbar power versus drawbar pull downhill on sand

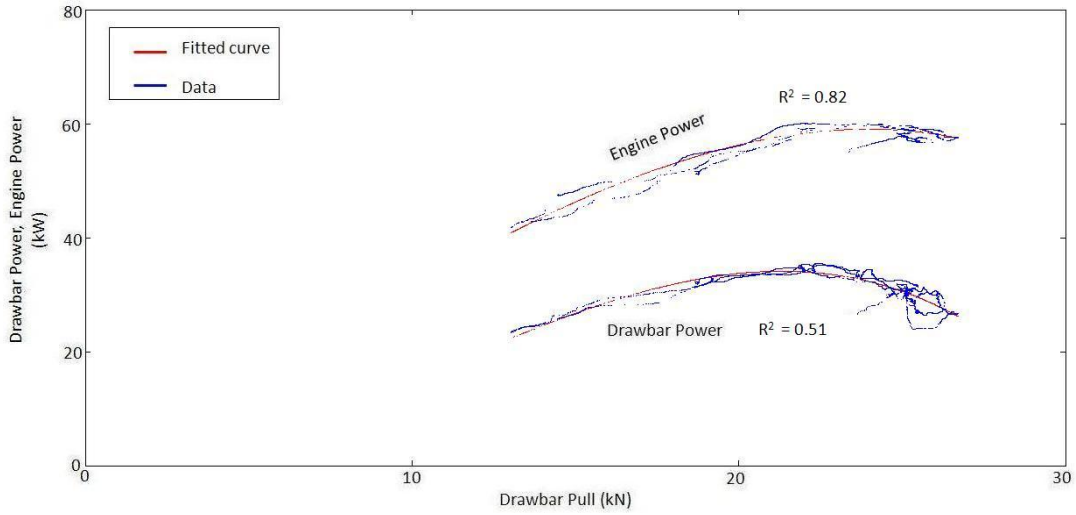

The relationship between engine power, drawbar power and drawbar pull operating downhill on sand at -4% lead, showing both the raw data and third order polynomial curves fitted to them.

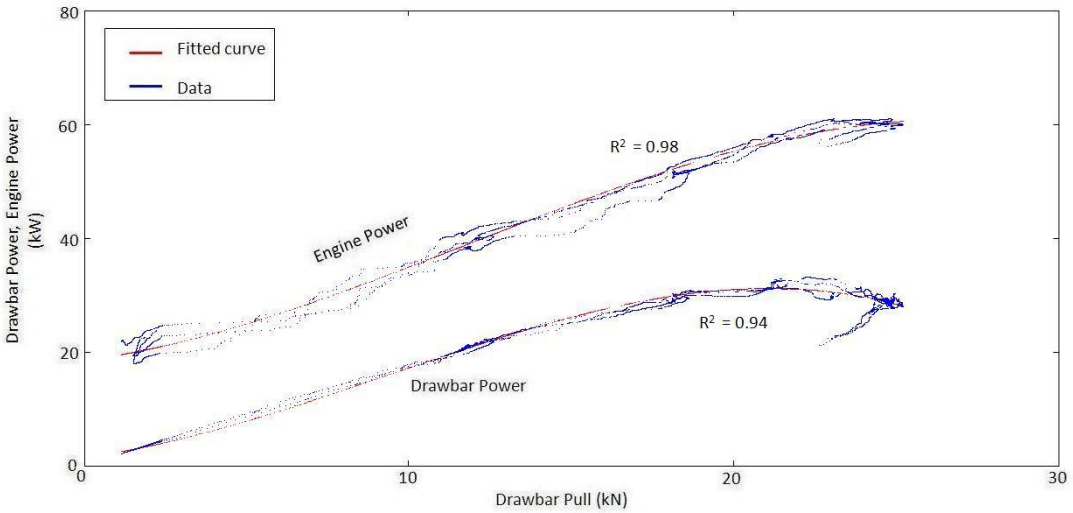

The relationship between engine power, drawbar power and drawbar pull operating downhill on sand at +2% lead, showing both the raw data and third order polynomial curves fitted to them.

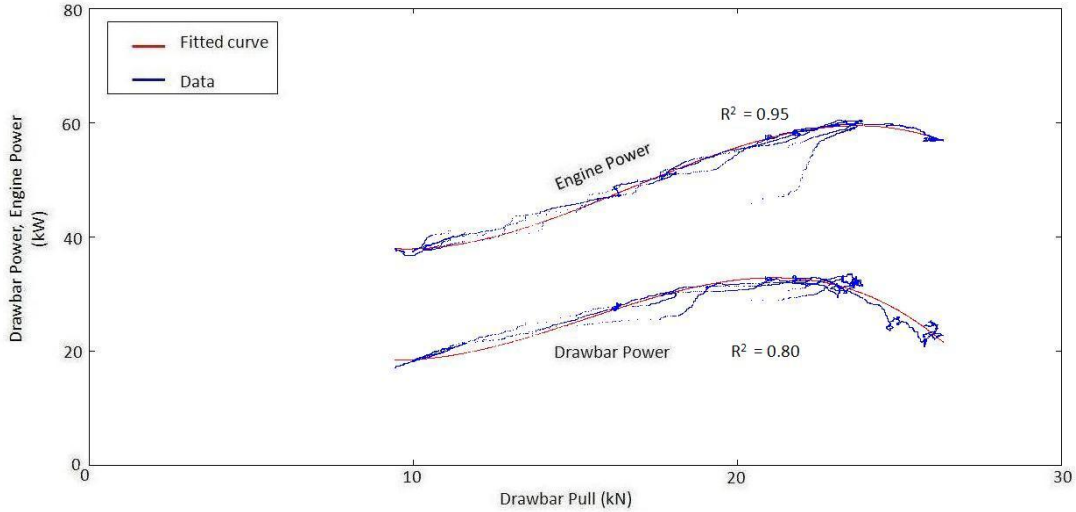

The relationship between engine power, drawbar power and drawbar pull operating downhill on sand at +10% lead, showing both the raw data and third order polynomial curves fitted to them.

4.13.15 Engine power and drawbar power versus drawbar pull on clay

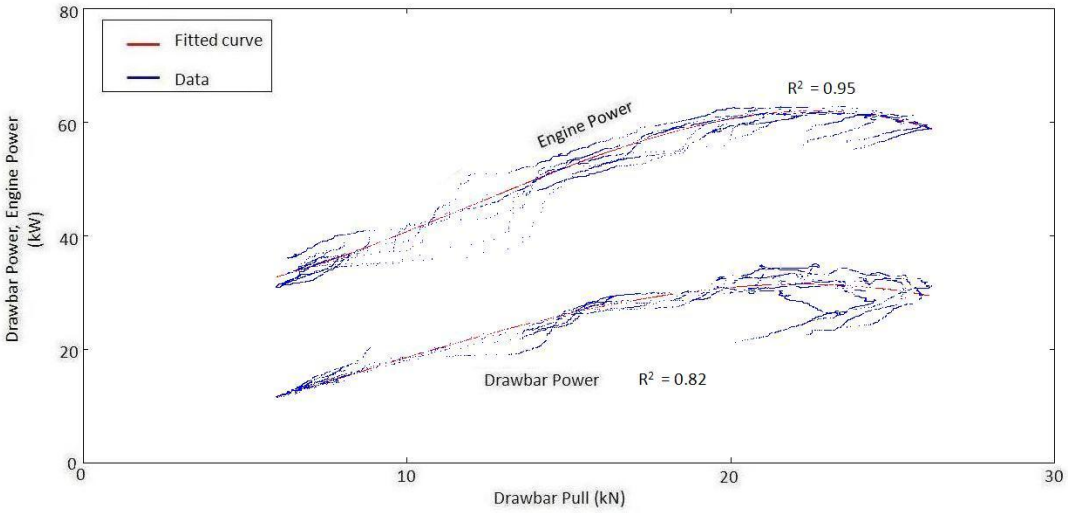

The relationship between engine power, drawbar power and drawbar pull operating on clay at -4% lead, showing both the raw data and third order polynomial curves fitted to them

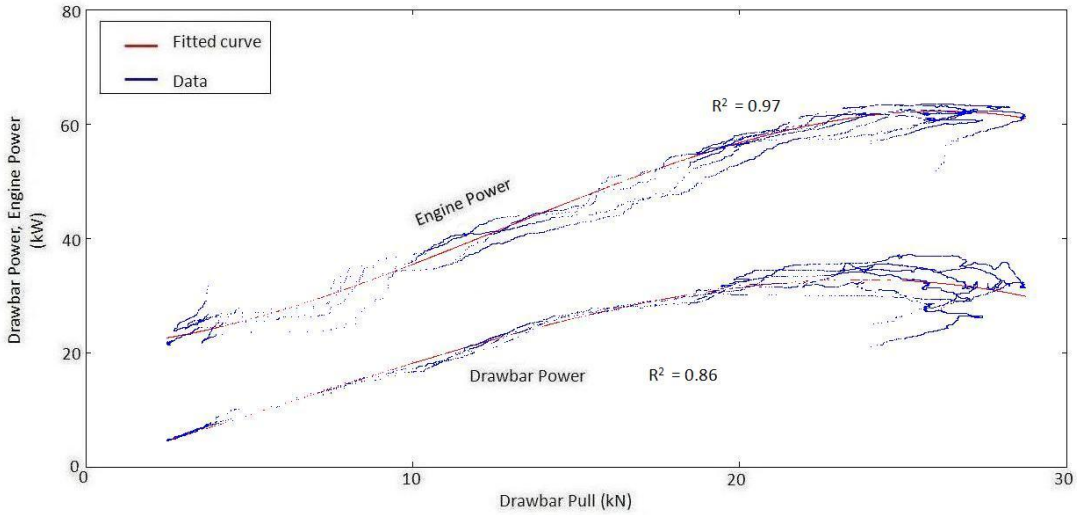

The relationship between engine power, drawbar power and drawbar pull operating on clay at +2% lead, showing both the raw data and third order polynomial curves fitted to them

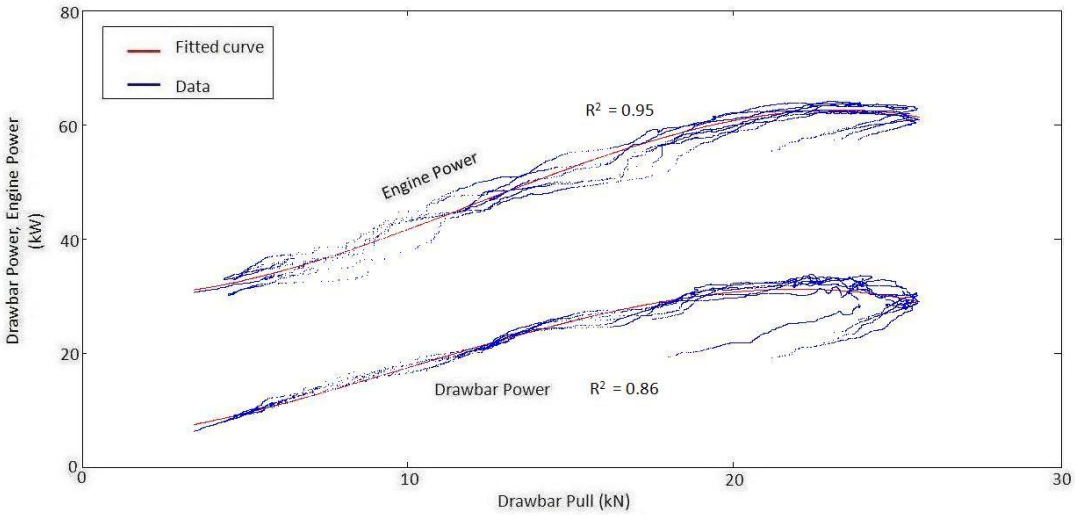

The relationship between engine power, drawbar power and drawbar pull operating on clay at +10% lead, showing both the raw data and third order polynomial curves fitted to them

4.13.16 Forward speed versus drawbar pull uphill on sand

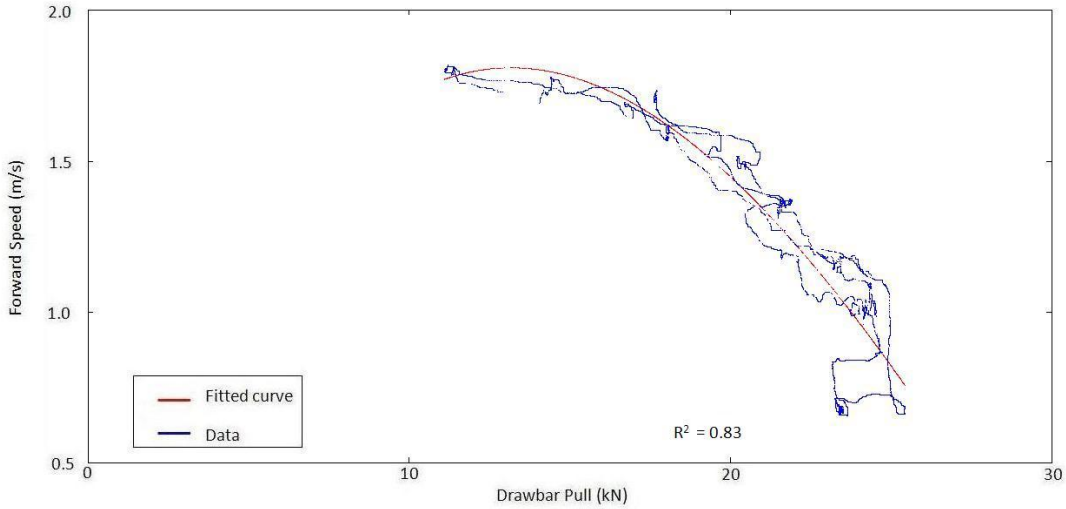

The relationship between forward speed and drawbar pull, operating uphill on sand at -4% lead, showing both the raw data and the third order polynomial curve fitted to them

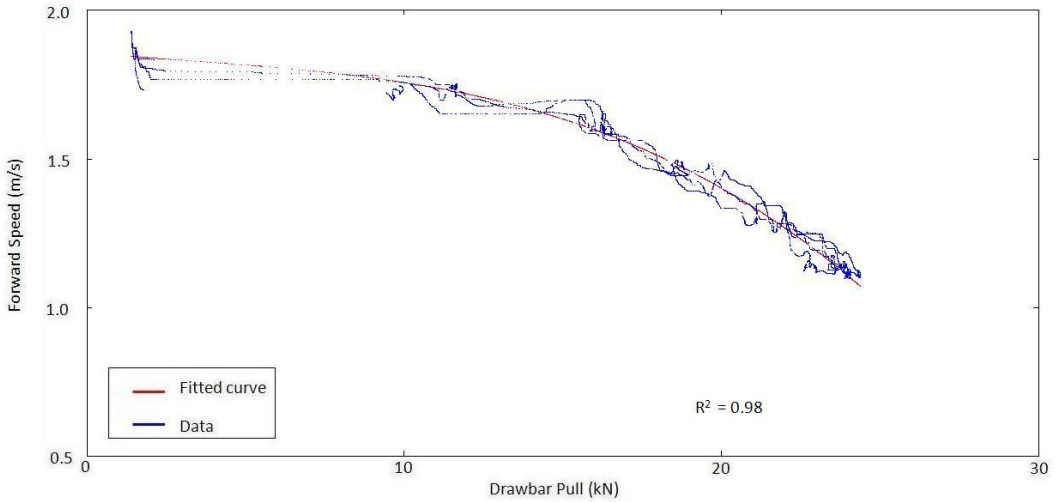

The relationship between forward speed and drawbar pull, operating uphill on sand at +2% lead, showing both the raw data and the third order polynomial curve fitted to them

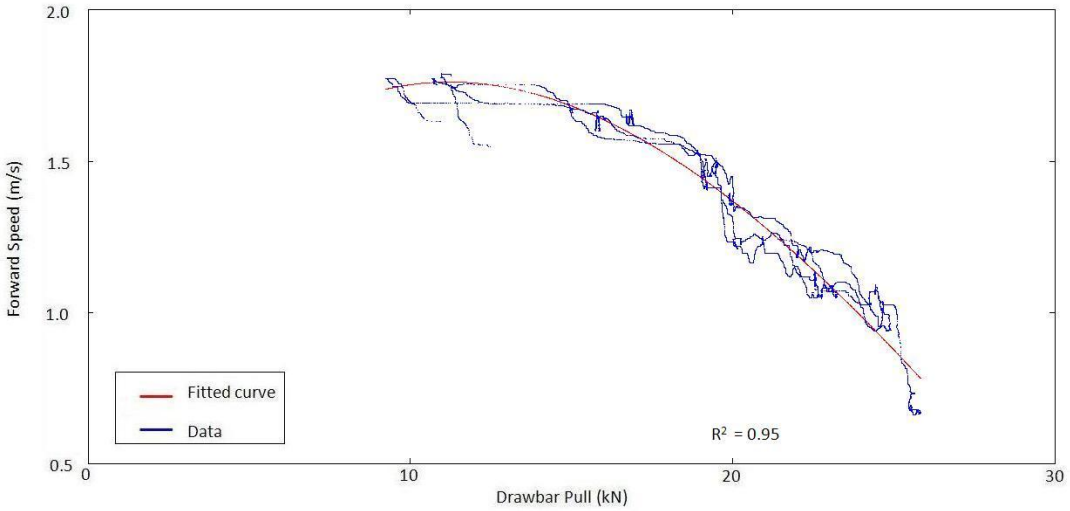

The relationship between forward speed and drawbar pull, operating uphill on sand at +10% lead, showing both the raw data and the third order polynomial curve fitted to them

4.13.17 Forward speed versus drawbar pull downhill on sand

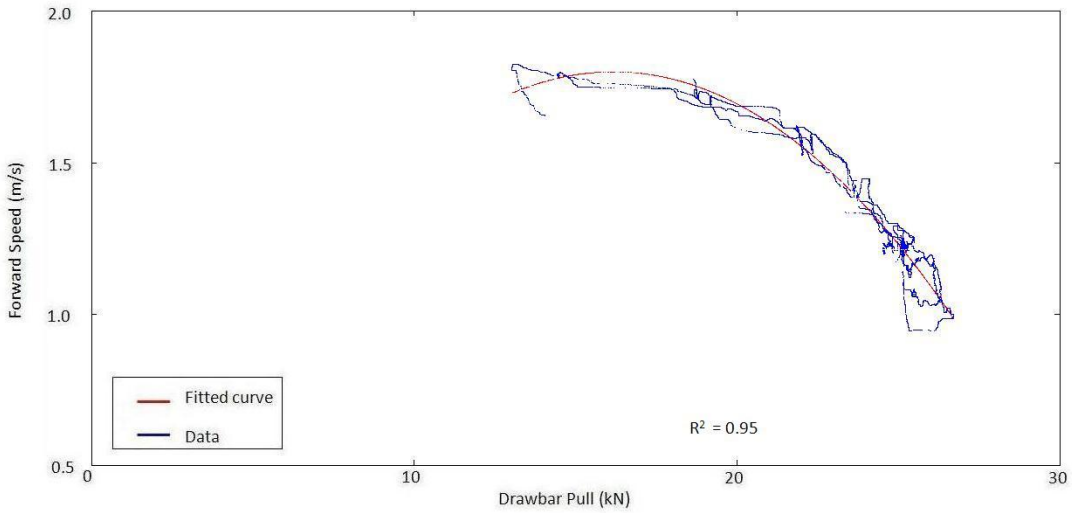

The relationship between forward speed and drawbar pull, operating downhill on sand at -4% lead, showing both the raw data and the third order polynomial curve fitted to them

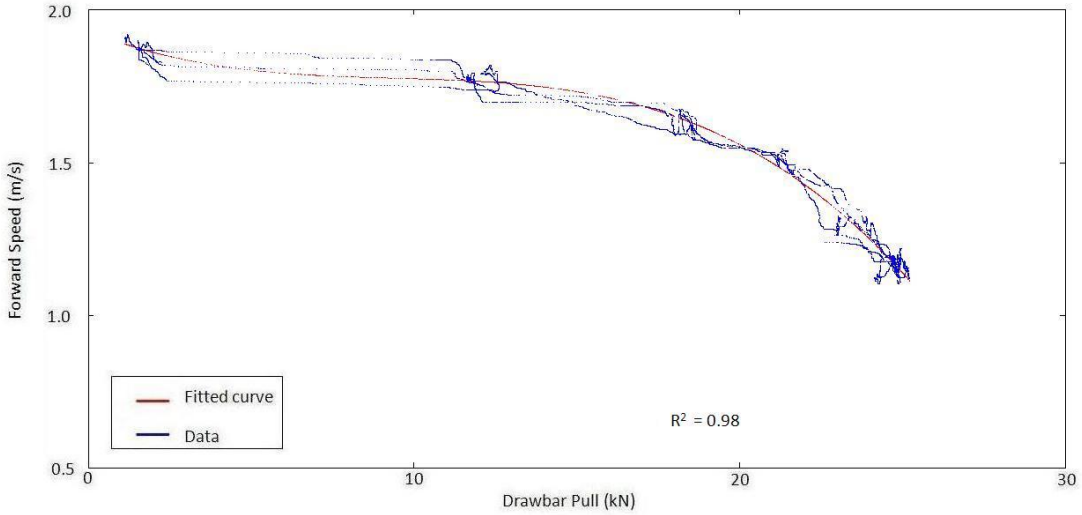

The relationship between forward speed and drawbar pull, operating downhill on sand at +2% lead, showing both the raw data and the third order polynomial curve fitted to them

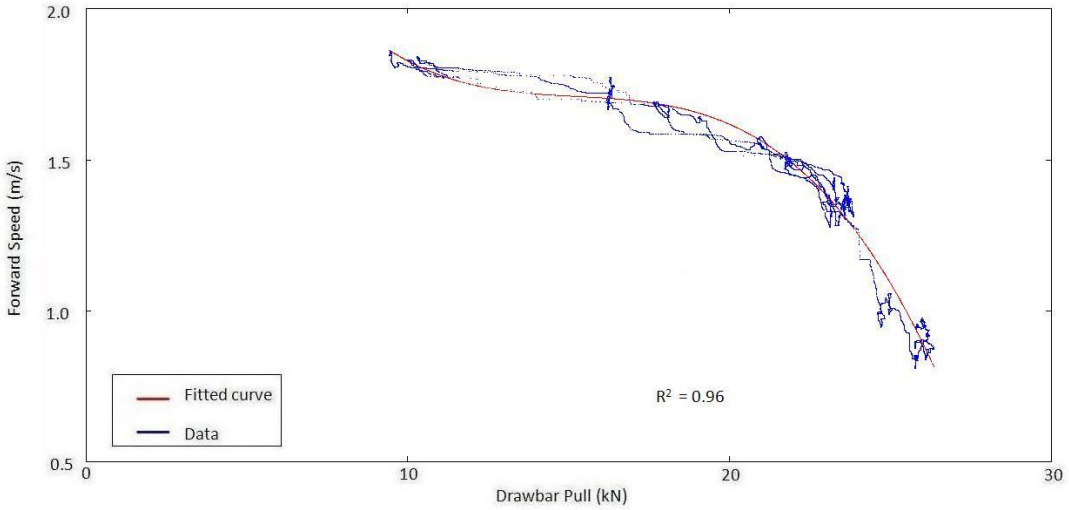

The relationship between forward speed and drawbar pull, operating downhill on sand at +10% lead, showing both the raw data and the third order polynomial curve fitted to them

4.13.18 Forward speed versus drawbar pull on clay

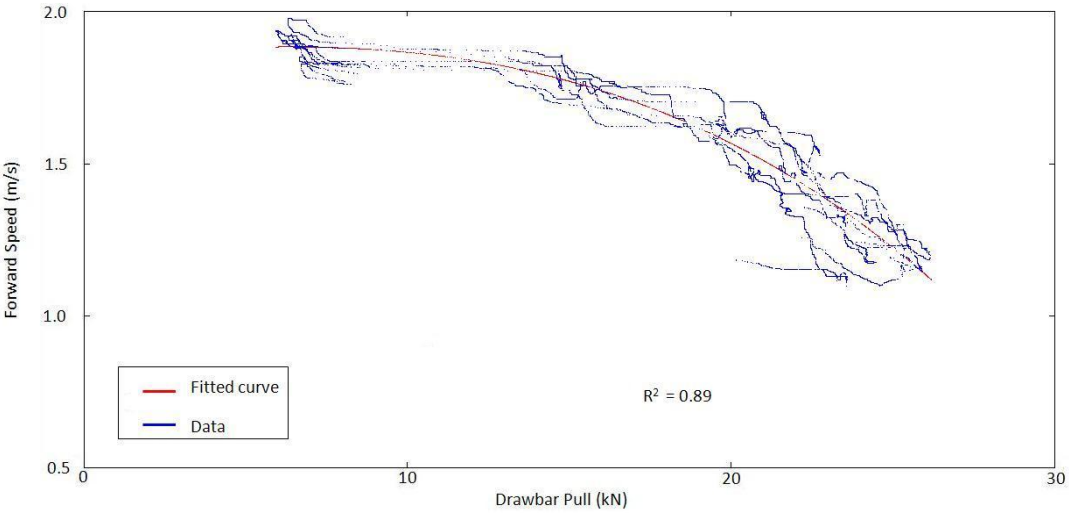

The relationship between forward speed and drawbar pull, operating on clay at -4% lead, showing both the raw data and the third order polynomial curve fitted to them

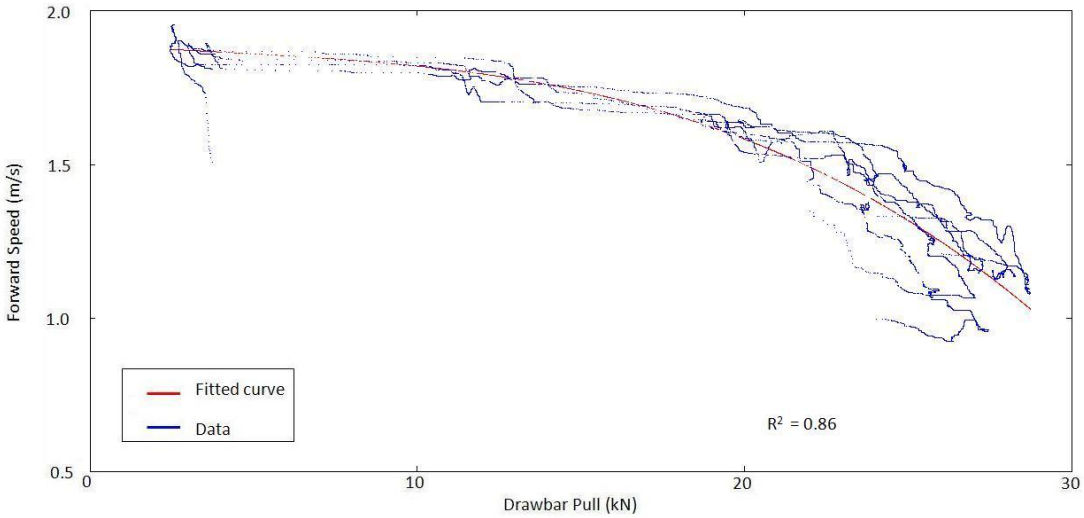

The relationship between forward speed and drawbar pull, operating on clay at +2% lead, showing both the raw data and the third order polynomial curve fitted to them

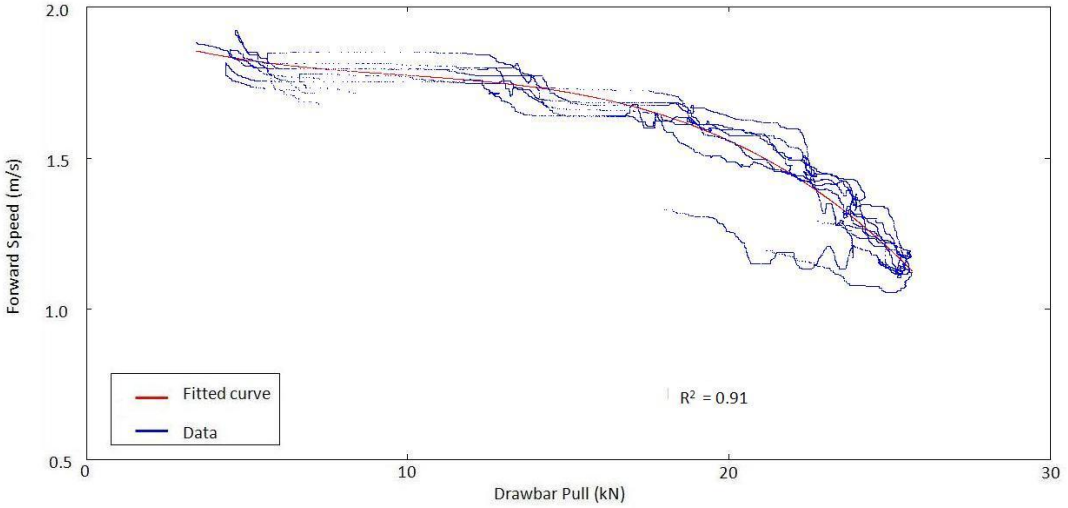

The relationship between forward speed and drawbar pull, operating on clay at +10% lead, showing both the raw data and the third order polynomial curve fitted to them

4.13.19 Shaft power versus drawbar pull uphill on sand

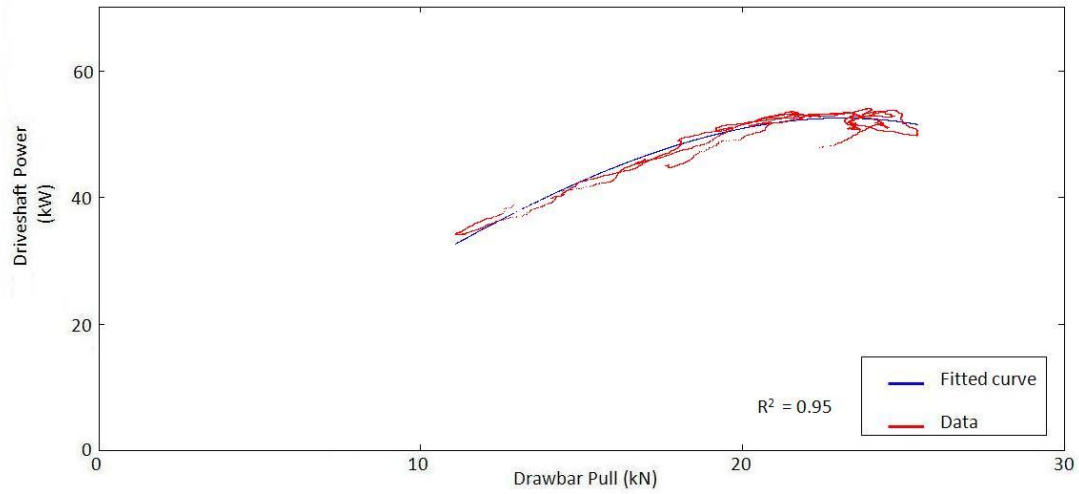

The relationship between the combined power transmitted by the front and rear driveshafts and drawbar pull, operating uphill on sand at -4% lead, showing both the raw data and the third order polynomial curve fitted to them

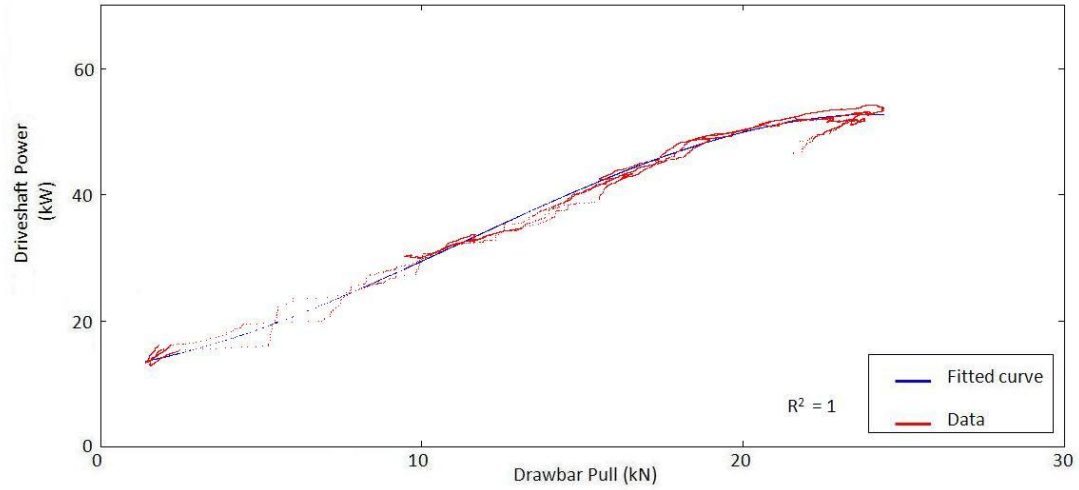

The relationship between the combined power transmitted by the front and rear driveshafts and drawbar pull, operating uphill on sand at +2% lead, showing both the raw data and the third order polynomial curve fitted to them

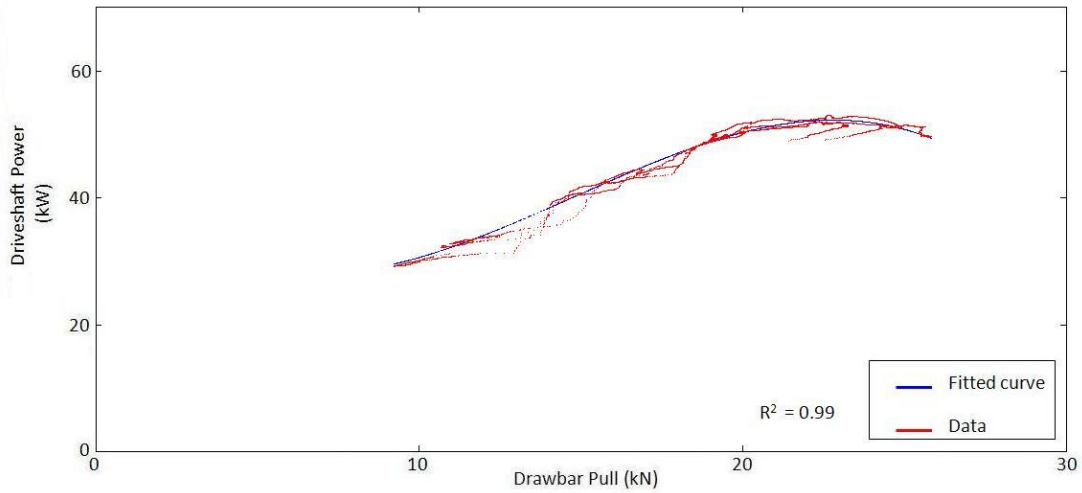

The relationship between the combined power transmitted by the front and rear driveshafts and drawbar pull, operating uphill on sand at +10% lead, showing both the raw data and the third order polynomial curve fitted to them

4.13.20 Shaft power versus drawbar pull downhill on sand

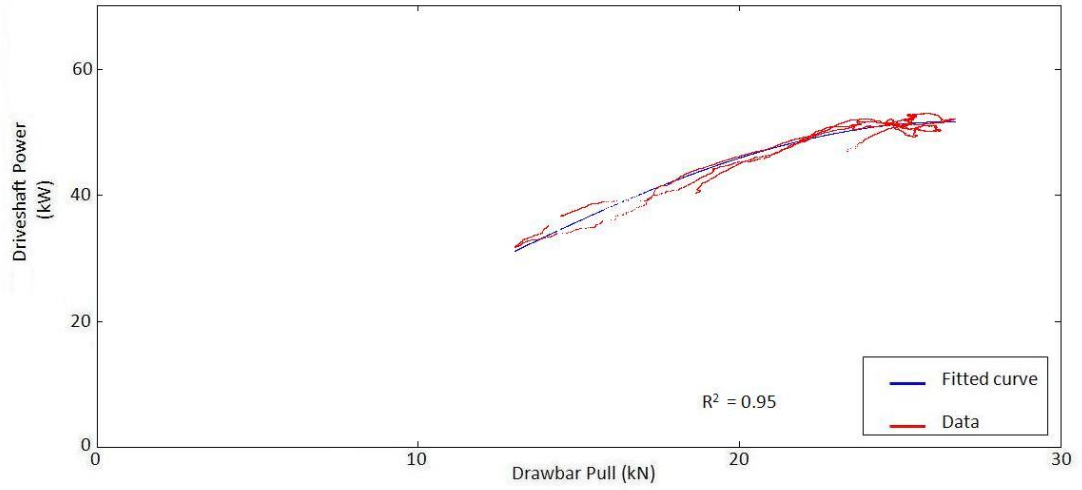

The relationship between the combined power transmitted by the front and rear driveshafts and drawbar pull, operating downhill on sand at -4% lead, showing both the raw data and the third order polynomial curve fitted to them

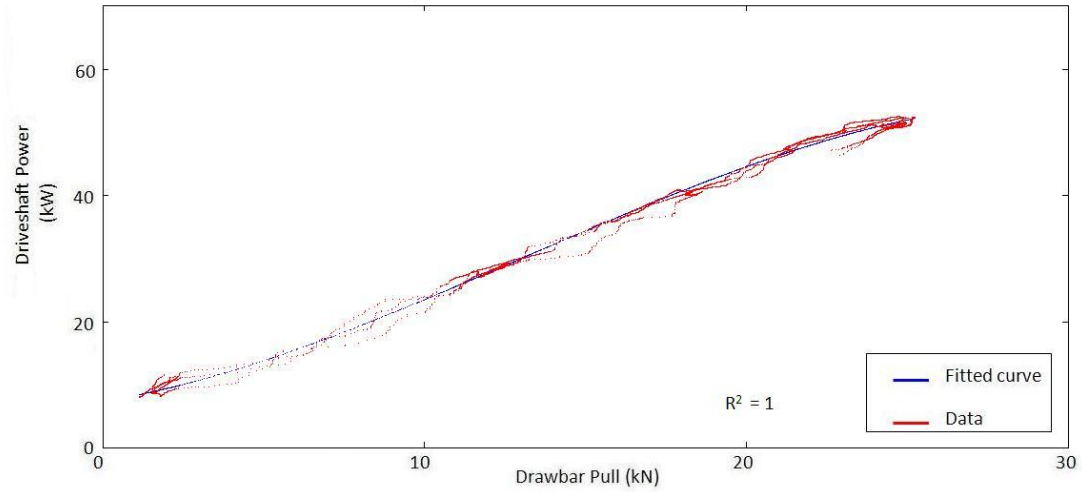

The relationship between the combined power transmitted by the front and rear driveshafts and drawbar pull, operating downhill on sand at +2% lead, showing both the raw data and the third order polynomial curve fitted to them

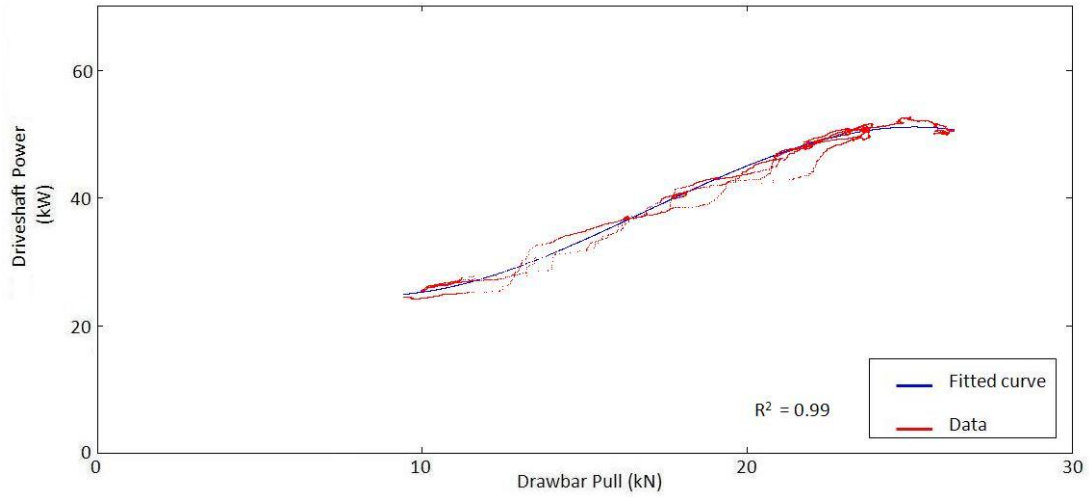

The relationship between the combined power transmitted by the front and rear driveshafts and drawbar pull, operating downhill on sand at +10% lead, showing both the raw data and the third order polynomial curve fitted to them

4.13.21 Shaft power versus drawbar pull on clay

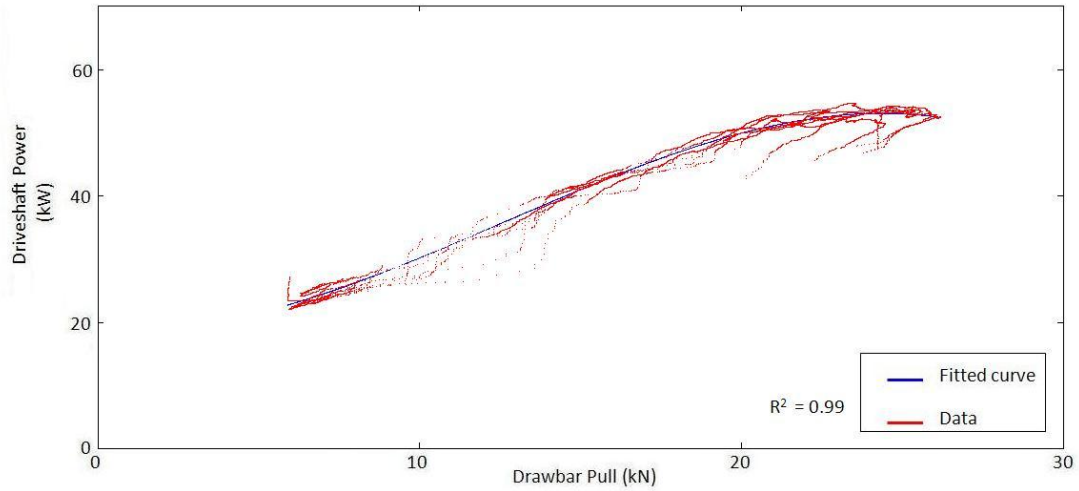

The relationship between the combined power transmitted by the front and rear driveshafts and drawbar pull, operating on clay at -4% lead, showing both the raw data and the third order polynomial curve fitted to them

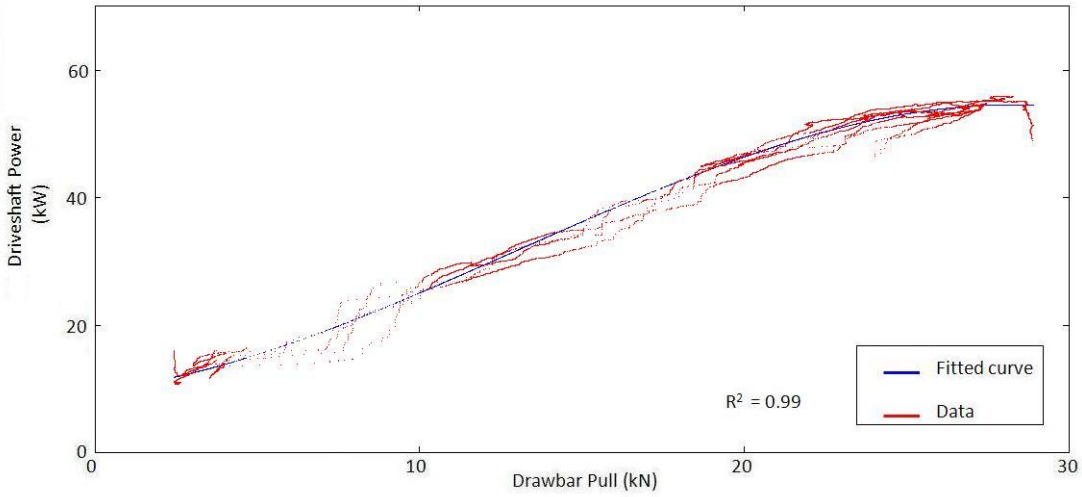

The relationship between the combined power transmitted by the front and rear driveshafts and drawbar pull, operating on clay at +2% lead, showing both the raw data and the third order polynomial curve fitted to them

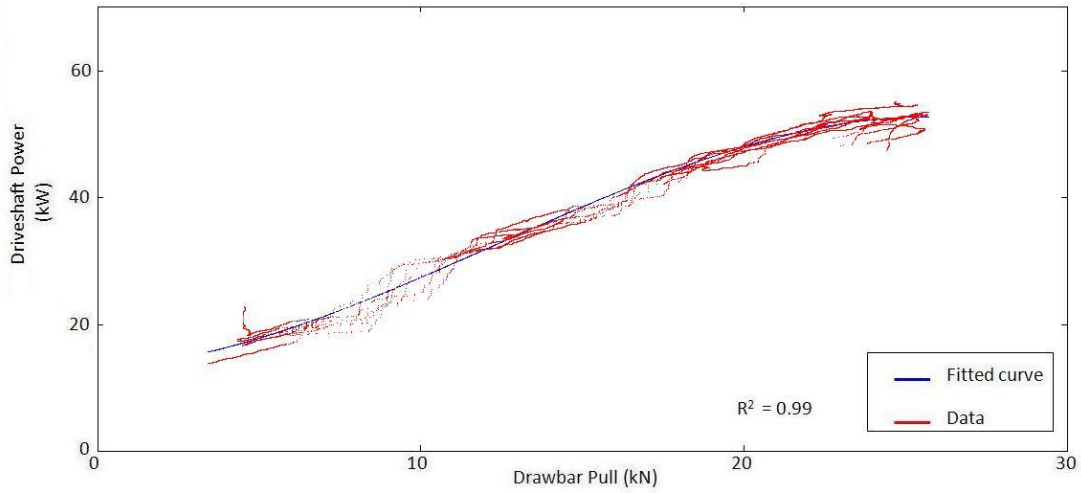

The relationship between the combined power transmitted by the front and rear driveshafts and drawbar pull, operating on clay at +10% lead, showing both the raw data and the third order polynomial curve fitted to them

Appendix to chapter 5

5.1 Easy 5 engine map

Engine RPM	Torque (Nm) Throttle Closed	Torque (Nm) Throttle Open
0	0	50
500	0	75
750	-26	200
1000	-40	250
1250	-54	325
1500	-83	310
1750	-111	300
2000	-126	275
2250	-140	200
2500	-160	-160

5.2 Easy 5 Main gearbox ratios

Gear	Ratio
1	4.5:1
2	2.7:1
3	1.3:1
4	1:1

5.3 Easy 5 Vehicle mass and dimensions

Parameter	Value	Source
Vehicle Mass	4600.0 kg	Measured
Position of C.O.M. from Rear Axle	1.0 m	Calculated
Position of C.O.M. from Ground	0.5 m	Estimated
Position of Front Axle from Rear Axle	2.4 m	Measured
Position of Drawbar Load from Ground	0.6 m	Measured

5.4 Easy 5 component equations

5.4.1 Tractive force developed by the simple tire (Ricardo, 2005a)

FT_VehConn_ST = MUX_ST x NF_VehConn_ST x

MVS_ST(|SLP_ST|)sgn(SLP_ST)

Where:

FT_VehConn_ST = Tractive force acting on the simple tire (N)

MUX_ST = Maximum friction coefficient

NF_VehConn_ST = The normal force on the simple tire (N)

MVS_ST = Table of normalized effective friction coefficients versus slip

5.4.2 Rolling resistance torque developed by the simple tire (Ricardo, 2005a)

FR2_ST = CR_ST + CRR_ST x |VE_VehConn_ST|

Where:

FR2_ST = Rolling resistance torque (Nm)

CR_ST = Constant term in rolling resistance equation (Nm)

CRR_ST = Vehicle velocity dependent rolling resistance term (Ns)

VE_VehConn_ST = Vehicle velocity (m/s)

5.4.3 Rolling radius of the off highway tire (Ricardo, 2005b)

$$r \equiv \frac{2.5 \times RU\_OT \times RL\_OT}{1.5 \times RU\_OT + RL\_OT}$$

Where:

r = Tyre rolling radius (m)

RU_OT = Overall unloaded tyre radius (m)

RL_OT = Loaded tyre radius (m)

5.4.4 Loaded tyre deflection of the off highway tire (Ricardo, 2005b)

$$\delta \equiv RU\_OT - RL\_OT$$

Where:

ð = Loaded tyre deflection (m)

5.4.5 Tire section height of off highway tire (Ricardo, 2005b)

$$h \equiv RU\_OT - 0.53 \times NRD\_OT$$

Where:

NRD_OT = Nominal rim diameter (m)

5.4.6 Wheel numeric of off highway tire (Ricardo, 2005b)

$$C_N \equiv \frac{2 \times r \times CI\_OT \times B\_OT}{NF\_VehConn\_OT}$$

Where:

CI_OT = Soil cone index (N/m^2)

B_OT = Tyre section width (m)

5.4.7 Mobility number of off highway tyre (Ricardo, 2005b)

$$BN\_OT \equiv C_N \frac{1 + 5.0 \times \frac{\delta}{h}}{1 + 1.5 \times \frac{B\_OT}{r}}$$

Where:

BN_OT = Mobility number

5.4.8 Wheel-tread slip of off highway tire (Ricardo, 2005b)

$$SLP\_OT \equiv 1 - \frac{VE\_VehConn\_OT}{RL\_OT \times VTR\_OT}$$

Where:

VE_VehConn_OT = Vehicle velocity (m/s)

VTR_OT = Tread velocity (rad/s)

5.4.9 Torque ratio of off highway tire (Ricardo, 2005b)

$$TR\_OT = 0.88 \times (1 - e^{-0.1 \times BN\_OT}) \times (1 - e^{-7.5 \times SLP\_OT}) + 0.04$$

Where:

TR_OT = Torque ratio

5.4.10 Rolling resistance ratio of off highway tire (Ricardo, 2005b)

$$RRR\_OT = \frac{1}{BN\_OT} + 0.004 + \frac{SLP\_OT}{2 \times \sqrt{BN\_OT}}$$

Where:

RRR_OT = Rolling resistance ratio

5.4.11 Pull ratio of off highway tire (Ricardo, 2005b)

$$PR\_OT = TR\_OT - RRR\_OT$$

Where:

PR_OT = Pull ratio

5.4.12 Tractive force developed by off highway tire (Ricardo, 2005b)

$$FT\_VehConn\_OT = PR\_OT \times NF\_VehConn\_OT$$

Where:

FT_VehConn_OT = Tractive force developed by tyre (N)

NF_VehConn_OT = Normal force on tyre (N)

5.4.13 Rolling resistance force developed by off highway tire (Ricardo, 2005b)

$$FR2\_OT = RRR\_OT \times NF\_VehConn\_OT$$

Where:

FR2_OT = Rolling resistance force on off highway tyre (N)

5.4.14 Tyre carcass torque in off highway tire (Ricardo, 2005b)

$$TWT\_OT = (FT\_VehConn\_OT - FR2\_OT) \times RL\_OT$$

Where:

TWT_OT = Tyre carcass torque (Nm)

5.4.15 Transmission of tyre carcass torque via tyre carcass stiffness and damping in off highway tire (Ricardo, 2005b)

Combining equations 5.4.12, 5.4.13 and 5.4.14 gives:

$$-(\boldsymbol{KT\_OT} \times \boldsymbol{DWT\_OT} + \boldsymbol{CT\_OT} \times \boldsymbol{VWT\_OT}) = (\boldsymbol{FT\_VehConn\_OT} - \boldsymbol{FR\_VehConn\_OT}) \times \boldsymbol{RL\_OT}$$

Where:

KT_OT = Tyre carcass stiffness (N.m/rad)

DWT_OT = Wheel-tread relative displacement (m)

CT_OT = Tyre carcass damping (N.m.s/rad)

VWT_OT = Wheel-tread relative velocity (rad/s)

FR_VehConn_OT = Rolling resistance force on off highway tyre (N)